

**Microglial TRPM2 Channel Activation and Its Relationship
to Neurodegenerative Diseases**

Sharifah Alawieyah Binti Syed Mortadza

Submitted in accordance with the requirements for the degree of
Doctor of Philosophy

The University of Leeds

School of Biomedical Science
Institute of Membrane and System Biology

September, 2017

The candidate confirms that the work submitted is her own, and that appropriate credit has been given where reference has been made to the work of others.

This copy has been supplied on the understanding that it is copyright material and that no quotation from the thesis may be published without proper acknowledgement.

© 2017 The University of Leeds and Sharifah Alawieyah Binti Syed Mortadza

The right of Sharifah Alawieyah Binti Syed Mortadza to be identified as Author of this work has been asserted by her in accordance with the Copyright, Designs and Patents Act 1988.

Acknowledgement

I would like to express my biggest gratitude to my main supervisor, Dr Lin Hua Jiang who has been the most helpful mentor for me throughout the PhD years. Firstly, thank you for giving me the opportunity to work in your lab and also for your countless time, attention and efforts in the journey of my research. You have provided me with the unwavering guidance and moral supports which keep me positive all the times.

I would also like to thank my secondary supervisor Dr Martin Stacey and my internal examiner Professor Rao Asipu Sivaprasadarao for their advice. My appreciation also goes to Dr S. Ponnambalam and Dr John D. Lippiat for their help and encouragement. I would like to acknowledge the University Putra Malaysia and Ministry of Higher Education Malaysia, who funded my PhD.

Many thanks to the members of my lab group including; Fatma Mousawi, Yunjie Hao, Madiha Khalid, Emily Caseley and Tim Munsey for their unconditional guidance and moral support. They have not only provided helps in term of the research, but also the friendships they offered were way much important in making my PhD years thoroughly enjoyable.

I will be forever grateful to the family and friends who have helped me over the past four years. I would like to thank my Mum and Dad (Syed Mortadza and Sharifah Fadzlon), who are thoroughly brilliant and couldn't have been more supportive if they tried. I am also thankful for Kakwa, Abang, Ajah, Alok, Aman, Shadia and Mariam, my siblings, for their dua'a, encouragement and support throughout my PhD. Special thanks to Shazana Hilda Shamsuddin (my officemate from Paul Millner group), who has been the best supporter, keeping me positive and being a good listener all the way throughout the last 3 years.

Last but not least, the biggest thank you to my husband, Syed Ahmad Saifullah, for being the best person in my life; who has been always trust in my intelligence even if I haven't, who has been there whenever I experienced difficulties, and who have tolerated my constant complaining. I couldn't have done this without you and I love you all very much.

Abstract

Microglial cell plays a key role in neuroinflammation induced by diverse danger associated molecular patterns (DAMP) molecules, such as Zn²⁺, Aβ₄₂ and TNF-α, and strongly implicated in neurodegenerative diseases. The molecular mechanisms for neuroinflammation are however not fully defined. Reactive oxygen species (ROS) production is critical in DAMP-induced microglial cell activation and cytokine production. Studies presented in this thesis aimed to investigate, using immunocytochemistry, single cell imaging, cell death and ELISA assays in combination with genetic and pharmacological interventions, the role of ROS-sensitive TRPM2 channel in cell death, cell activation and production of TNF-α in primary microglial cells in response to Zn²⁺, Aβ₄₂ and TNF-α as well as H₂O₂.

H₂O₂ (10-300 μM) and Zn²⁺ (10-300 μM) induced concentration-dependent increases in the intracellular Ca²⁺ concentration ([Ca²⁺]_i) via Ca²⁺ influx, which were prevented by TRPM2 knockout (TRPM2-KO) or treatment with TRPM2 inhibitor 2-APB or PARP inhibitor PJ34. Pathological concentrations of H₂O₂ (100-300 μM) and Zn²⁺ (100-300 μM) induced substantial cell death that was ablated by TRPM2-KO and treatment with 2-APB or PJ34. Zn²⁺ also induced ROS production and PARP-1 activation. All these Zn²⁺-induced effects were suppressed by treatment with PKC inhibitor chelerythrine, NOX inhibitors DPI, GKT137831 or Phox-I2. Zn²⁺-induced PARP-1 stimulation, increase in the [Ca²⁺]_i and cell death were also inhibited by PYK2 inhibitor PF431396 or MEK/ERK inhibitor U0126.

Exposure to Aβ₄₂ (30-300 nM) and TNF-α (10-100 ng/ml) resulted in concentration-dependent TRPM2-mediated Ca²⁺ influx and increases in the [Ca²⁺]_i, microglial cell activation and TNF-α production. Aβ₄₂ and TNF-α stimulated ROS production and PARP-1 activation. These effects induced by Aβ₄₂ or TNF-α were suppressed by inhibiting PKC and NOX. Moreover, Aβ₄₂/TNF-α induced PARP-1 activation, increase in the [Ca²⁺]_i, microglial cell activation and TNF-α production were attenuated by inhibiting PYK2 and MEK/ERK.

In summary, studies provide strong evidence to reveal a critical role for the TRPM2 channel in Ca²⁺ signalling in microglial cells induced by Zn²⁺, Aβ₄₂ and TNF-α. TRPM2 channel activation by Zn²⁺, Aβ₄₂ and TNF-α depends on PKC/NOX-mediated ROS production and PARP-1 activation and is additionally enhanced by the PYK2-MEK-ERK signalling pathway. Such mechanisms are critically involved in cell

death in response to Zn^{2+} , or microglial cell activation and TNF- α production in response to $A\beta_{42}$ and TNF- α . These findings provide novel insights into the role of microglial cells in neuroinflammation and in the pathogenesis of neurodegenerative diseases.

Table of Contents

ACKNOWLEDGEMENT.....	iii
ABSTRACT	iv
TABLE OF CONTENTS	vi
LIST OF TABLES	xi
LIST OF FIGURES	xii
LIST OF ABBREVIATIONS	xvi
AMINO ACID ABBREVIATIONS.....	xxiv
CHAPTER 1 GENERAL INTRODUCTION	1
1.1 Mammalian TRP Channels	2
1.1.1 Discovery and classification	2
1.1.2 Structural properties	2
1.1.3 Activation, expression and function.....	5
1.1.3.1 TRPC.....	6
1.1.3.2 TRPV	8
1.1.3.3 TRPM.....	9
1.1.3.4 TRPA	11
1.1.3.5 TRPP	12
1.1.3.6 TRPML	13
1.2 TRPM2 Channels.....	14
1.2.1 Genes.....	14
1.2.2 Structural and biophysical properties.....	14
1.2.3 Alternative splicing isoforms	15
1.2.4 Activation.....	15
1.2.4.1 ADPR.....	17
1.2.4.2 OAADPR	17
1.2.4.3 NAD	18
1.2.4.4 cADPR	18
1.2.4.5 NAADP.....	19
1.2.4.6 Ca^{2+}	19
1.2.4.7 Temperature	20
1.3 ROS-Induced Activation of TRPM2 Channels.....	20
1.3.1 Reactive oxygen species (ROS)	20

1.3.2 Mitochondrial ROS generation	21
1.3.3 NOX-mediated ROS generation	25
1.3.4 TRPM2 channel activation by ROS.....	30
1.4 TRPM2 Channel Inhibitors	31
1.4.1 AMP	31
1.4.2 8-Br-cADPR	31
1.4.3 2-APB	34
1.4.4 ACA	34
1.4.5 FFA	34
1.4.6 Azoles	35
1.4.7 Curcumin.....	35
1.4.8 PARP inhibitors.....	35
1.5 Expression of TRPM2 Channels.....	35
1.6 Physiological Roles of TRPM2 Channels.....	36
1.6.1 Generation of IL-1 β and IL-18	36
1.6.2 Production of other cytokines and chemokines	40
1.6.3 Regulation of heme-oxygenase-1 expression	41
1.6.4 Secretion of insulin	42
1.6.5 Cell maturation and chemotaxis.....	42
1.6.6 Protection against ischemia/reperfusion-induced heart damage	43
1.7 Pathological Roles Of TRPM2 Channels	44
1.7.1 ROS-induced cell death	45
1.7.2 Alzheimer's Disease	45
1.7.3 Parkinson's Disease	47
1.7.4 Ischemia/reperfusion-induced damages in brain and heart.....	47
1.7.5 Neuropathic pain	48
1.7.6 Cancer	49
1.7.7 Acetaminophen overdosing-induced liver damage.....	50
1.7.8 Endothelial barrier permeability	50
1.8 Microglial Cell Activation and Neuroinflammation.....	51
1.8.1 Microglial cell activation	52
1.8.2 Neuroinflammation	5454
1.8.3 Role of TRPM2 channel in microglial activation and neuroinflammation?..	56

1.9 Aims and Objectives	56
CHAPTER 2 MATERIALS AND METHODS.....	58
2.1 Materials	59
2.1.1 Chemicals.....	59
2.1.2 Solutions	59
2.1.3 Antibodies, fluorescence indicators and ELISA kits	59
2.1.4 Cell culture media	59
2.1.5 Animal and genotyping of TRPM2-KO mice.....	59
2.2 Methods.....	64
2.2.1 Preparation of microglial cell culture	64
2.2.1.1 Preparations of PLL-coated culture flasks	64
2.2.1.2 Isolation of microglial cells	64
2.2.1.3 Treatment of microglial cells.....	65
2.2.2 Immunofluorescence imaging.....	65
2.2.3 Single cell calcium imaging.....	67
2.2.4 Cell death assay.....	67
2.2.5 Characterization of microglial cell morphology	68
2.2.6 Measurement of ROS production	68
2.2.7 Enzyme-linked immunosorbent assay (ELISA)	69
2.3 Statistical Analysis.....	69
CHAPTER 3 A ROLE OF TRPM2 IN DAMP-INDUCED MICROGLIAL CELL DEATH AND CELL ACTIVATION	70
3.1 Introduction.....	71
3.2 Results.....	72
3.2.1 TRPM2 channel expression and its role in H ₂ O ₂ -induced Ca ²⁺ responses	72
3.2.2 TRPM2 channel in mediating H ₂ O ₂ -induced microglial cell death	72
3.2.3 TRPM2 channel in H ₂ O ₂ -induced microglial cell activation.....	77
3.2.4 TRPM2 channel in DAMP-induced Ca ²⁺ responses.....	79
3.2.5 TRPM2 channel in Zn ²⁺ -induced microglial cell death	79
3.2.6 TRPM2 channel in DAMP-induced cell activation	888
3.3 Discussion	933
CHAPTER 4 SIGNALLING MECHANISMS FOR H₂O₂- AND ZN²⁺-INDUCED TRPM2-MEDIATED MICROGLIAL CELL DEATH	966
4.1 Introduction.....	97

4.2 Results.....	98
4.2.1 TRPM2 channel in H ₂ O ₂ -induced Ca ²⁺ influx in microglial cells	98
4.2.2 Effects of TRPM2 channel inhibitors on H ₂ O ₂ -induced microglial cell death	98
4.2.3 PARP-1 in H ₂ O ₂ -induced microglial cell death	98
4.2.4 Effects of PKC/NOX inhibitors on H ₂ O ₂ -induced cell death.....	101
4.2.5 Effects of PYK2 and MEK/ERK inhibitors on H ₂ O ₂ -induced cell death ...	104
4.2.6 TRPM2 channel in Zn ²⁺ -induced Ca ²⁺ influx in microglial cells	104
4.2.7 Effects of TRPM2 channel inhibitors on Zn ²⁺ -induced microglial cell death	107
4.2.8 PARP-1 in Zn ²⁺ -induced TRPM2 channel activation and microglial cell death	107
4.2.9 Effects of PKC and NOX inhibitors in Zn ²⁺ -induced ROS production, PARP-1 activity, TRPM2 channel activation and cell death in microglial cells.....	107
4.2.10 Effects of PYK2 and MEK/ERK inhibitors on PARP-1 activity, TRPM2 channel activation and cell death in microglial cells.....	110
4.3 Discussion	122
CHAPETR 5 SIGNALLING MECHANISMS FOR A_β₄₂-INDUCED TRPM2-MEDIATED MICROGLIAL ACTIVATION AND TNF-α GENERATION.....	125
5.1 Introduction.....	126
5.2 RESULTS	127
5.2.1 TRPM2 channel role in A _β ₄₂ -induced Ca ²⁺ influx.....	127
5.2.2 Effects of TRPM2 channel inhibitor on A _β ₄₂ -induced microglial cell activation	127
5.2.3 A _β ₄₂ -induced TNF-α production is TRPM2-dependent	127
5.2.4 PARP-1 in A _β ₄₂ -induced TRPM2 channel activation, cell activation and TNF-α production in microglial cells.....	130
5.2.5 PKC and NOX in A _β ₄₂ -induced ROS production, activation of PARP-1 and TRPM2 and TNF-α production in microglial cells	136
5.2.6 PYK2 and MEK/ERK in A _β ₄₂ -induced activation of PARP-1 and TRPM2-activation and TNF-α production in microglial cells	136
5.3 Discussion	146
CHAPTER 6 TNF-α AUTOCRINE/PARACRINE SIGNALLING MECHANISMS VIA TRPM2 CHANNEL IN MICROGLIAL CELLS	149
6.1 Introduction.....	150

6.2 Results.....	151
6.2.1 TRPM2 channel in TNF- α -induced Ca^{2+} influx and microglial cell activation	151
6.2.2 TRPM2 channel in TNF- α induced TNF- α production in microglial cells	151
6.2.3 PARP-1 is required in TNF- α -induced TRPM2 channel activation and TNF- α generation in microglial cells	154
6.2.4 PKC and NOX in TNF- α -induced ROS production, activation of PARP-1 and TRPM2 channel, and TNF- α generation in microglial cells	160
6.2.5 PYK2-MEK/ERK signalling as a positive feedback in TNF- α -induced microglial cell activation and TNF- α generation	160
6.3 Discussion	170
CHAPTER 7 GENERAL DISCUSSION AND CONCLUSIONS.....	174
7.1 General Discussion and Conclusions.....	175
LIST OF REFERENCES	180

List of Tables

Table 1.1 NOX inhibitors, their selectivity and potentiation	29
Table 1.2 A summary of the major functional roles of the TRPM2 channel expression in different cell types	37
Table 2.1 Stock solutions	61
Table 2.2 Solutions.....	62
Table 2.3 Antibodies	63
Table 2.4 Stock solutions of fluorescence indicators	63
Table 2.5 Dissection tools used for microglia cells isolation.....	66
Table 2.6 Preparations of microglial cells.....	66
Table 3.1 Summary of the TRPM2 channel in microglial cell responses against various DAMP molecules	95

List of Figures

Figure 1.1 The mammalian TRP superfamily	3
Figure 1.2 Membrane topology and structural features of the TRP proteins	4
Figure 1.3 TRPM2 channel activators structure	16
Figure 1.4 Electron transfer and ROS generation in mitochondrial electron transport chain	23
Figure 1.5 NADPH oxidase activation	26
Figure 1.6 The TRPM2 channel and PARP inhibitors	33
Figure 3.1 TRPM2 expression and H ₂ O ₂ -induced increase in the [Ca ²⁺] _i in microglial cells	73
Figure 3.2 A critical role of the TRPM2 channel in H ₂ O ₂ -induced increase in [Ca ²⁺] _i in microglial cells	74
Figure 3.3 H ₂ O ₂ induces TRPM2 channel-dependent microglial cell death.....	76
Figure 3.4 A critical role of the TRPM2 channel in H ₂ O ₂ -induced change in microglial cell morphology	78
Figure 3.5 Zn ²⁺ induces TRPM2 channel-dependent increase in the [Ca ²⁺] _i in microglial cells	80
Figure 3.6 Aβ ₄₂ induces TRPM2 channel-dependent increase in the [Ca ²⁺] _i in microglial cells	82
Figure 3.7 TNF-α induces TRPM2 channel-dependent increase in the [Ca ²⁺] _i in microglial cells	84
Figure 3.8 TRPM2 channel is involved in Zn ²⁺ -induced microglial cell death	86
Figure 3.9 Exposure to Aβ ₄₂ and TNF-α induces no microglial cell death	87
Figure 3.10 TRPM2 channel is required for Zn ²⁺ -induced microglial activation.....	89
Figure 3.11 TRPM2 channel is required for Aβ ₄₂ -induced microglial activation.....	90
Figure 3.12 TRPM2 channel is required for TNF-α-induced microglial cell activation	92
Figure 4.1 TRPM2 channel is required for H ₂ O ₂ -induced Ca ²⁺ signalling in microglial cells	99

Figure 4.2 TRPM2 channel-mediated calcium signalling in H ₂ O ₂ -induced microglial cell death	100
Figure 4.3 PARP-1 activation is critical in H ₂ O ₂ -induced microglial cell death	102
Figure 4.4 PKC and NOX are not involved in H ₂ O ₂ -induced PARP-1 activation and microglial cell death	103
Figure 4.5 PYK2/MEK signalling is not involved in H ₂ O ₂ -induced PARP-1 activation and microglial cell death	105
Figure 4.6 Ca ²⁺ influx and PARP activation in Zn ²⁺ -induced Ca ²⁺ signalling	106
Figure 4.7 A role of TRPM2 channel in Zn ²⁺ -induced microglial cell death.....	108
Figure 4.8 Zn ²⁺ -induced PARP-1 activation in microglial cells	109
Figure 4.9 PKC in Zn ²⁺ -induced ROS generation, PARP-1 activation increase in the [Ca ²⁺] _i and cell death in microglial cells.....	112
Figure 4.10 NOX in Zn ²⁺ -induced ROS generation, PARP-1 activation increase in the [Ca ²⁺] _i and cell death in microglial cells.....	114
Figure 4.11 PYK2/MEK/ERK in Zn ²⁺ -induced PARP-1 activation, increase in the [Ca ²⁺] _i and microglial cell death	116
Figure 4.12 PKC/NOX is required for, and the PYK2/MEK signalling pathway depends on, Zn ²⁺ -induced PARP-1 activation	119
Figure 4.13 PKC/NOX is required for, and the PYK2/MEK signalling pathway depends on, Zn ²⁺ -induced TRPM2 channel activation	120
Figure 4.14 Summary of the signalling mechanisms mediating Zn ²⁺ -induced TRPM2 channel activation and cell death in microglial cells	121
Figure 5.1 A β ₄₂ induces Ca ²⁺ influx through the TRPM2 channel in microglial cells	128
Figure 5.2 A role of TRPM2 channel in A β ₄₂ -induced microglial cell activation.....	129
Figure 5.3 A β ₄₂ induces TNF- α production in microglial cells.....	131
Figure 5.4 TRPM2 is required for A β ₄₂ -induced TNF- α production by microglial cells	132
Figure 5.5 A role of PARP in A β ₄₂ -induced cell activation and TNF- α production in microglial cells	134

Figure 5.6 A β ₄₂ induces PARP-1 activation in microglial cells.....	135
Figure 5.7 A role for PKC and NOX in A β ₄₂ -induced ROS production in microglial cells	137
Figure 5.8 PKC and NOX in A β ₄₂ -induced PARP-1 activation and TRPM2 channel activation in microglial cells	138
Figure 5.9 PKC and NOX in A β ₄₂ -induced microglial activation and TNF- α production	140
Figure 5.10 PYK2/MEK/ERK in A β ₄₂ -induced PARP-1 activation and TRPM2 channel activation in microglial cells	142
Figure 5.11 PYK2/MEK/ERK in A β ₄₂ -induced microglial cell activation and TNF- α production	143
Figure 5.12 PKC/NOX activation is required for, and PYK2/MEK activation depends on, A β ₄₂ -induced TRPM2 channel activation	145
Figure 5.13 Schematic summary of the signalling mechanisms mediating A β ₄₂ -induced TRPM2 channel activation, microglial activation and TNF- α generation.....	148
Figure 6.1 TNF- α induces Ca ²⁺ influx through the TRPM2 channel in microglial cells	152
Figure 6.2 Activation of TRPM2 channel is required for TNF- α -induced microglial cell activation.....	153
Figure 6.3 TNF- α induces autocrine/paracrine action by producing TNF- α in microglial cells	155
Figure 6.4 TRPM2 channel is required for TNF- α -induced TNF- α production by microglial cells.....	156
Figure 6.5 Activation of PARP is required for TNF- α -induced microglial cell activation	158
Figure 6.6 TNF- α induces PARP-1 activation in microglial cells	159
Figure 6.7 A role of PKC and NOX in TNF- α -induced ROS production in microglial cells	161

Figure 6.8 PKC and NOX in TNF- α -induced PARP-1 activation and TRPM2 channel activation in microglial cells.....	162
Figure 6.9 PKC/NOX is critical in TNF- α -induced microglial activation and TNF- α production	164
Figure 6.10 PYK2/MEK/ERK is involved in TNF- α -induced microglial cell activation and TNF- α production	166
Figure 6.11 PYK2/MEK/ERK is involved in TNF- α -induced PARP-1 activation and TRPM2 channel activation in microglial cells	167
Figure 6.12 PKC/NOX activation is required for, and PYK2/MEK activation depends on, TNF- α -induced TRPM2 channel activation	169
Figure 6.13 Schematic summary of the TNF- α -induced autocrine/paracrine signalling mechanisms via TRPM2 channel in microglia.....	173
Figure 7.1 Schematic summary of the signalling mechanisms mediating Zn ²⁺ , A β ₄₂ - and TNF- α -induced TRPM2 channel activation, microglial activation and TNF- α generation	Error! Bookmark not defined.

List of Abbreviations

μg	Microgram
μl	Microlitre
μM	Micromolar
μm	Micrometer
2-APB	2-aminoethoxydiphenyl borate
3-AB	3-aminobenzamide
3-CF_3	Trifluoromethyl
3-MFA	2-(3-methylphenyl) aminobenzoic acid
8-Br-cADPR	8-bromo-cADPR
ACA	N-(p-amylocinnamoyl) anthranilic acid
AD	Alzheimer disease
ADPR	Adenosine diphosphate ribose
AMP	Adenine monophosphate
ASC	Apoptosis-associated speck-like protein containing a CARD
ATP	Adenosine triphosphate
$\text{A}\beta$	Amyloid beta
BSA	Bovine serum albumin
Ca^{2+}	Calcium ion
CaM	Calmodulin
cAMP	Cyclic adenosine monophosphate
CD38	Cluster differentiation 38
CLP	Cecal ligation and puncture
CNS	Central nervous system
CO_2	Carbon dioxide

CoQ	Coenzyme Q
CoQH ₂	Reduced CoQ
CTC	Chelerythrine chloride
CXCL	C-X-C motif ligand
CXCR	C-X-C motif receptor
cyt <i>b</i> _H	Cytochrome <i>b</i> high
cyt <i>b</i> _L	Cytochrome <i>b</i> low
cyt <i>c</i>	Cytochrome <i>c</i>
DA	Dopamine
DAG	Diacylglycerol
DAMP	Danger-associated molecular patterns
DAPI	4',6-diamidino-2-phenylindole
DCFH-DA	Dichloro-dihydro-fluorescein diacetate
DMEM	Dulbecco's modified Eagle's medium
DMEM/F12	Dulbecco's modified Eagle's medium-F12
DMSO	Dimethylsulphoxide
DNA	Deoxyribonucleic acid
DPI	Diphenyleneiodonium
DPQ	3, 4-dihydro-5-[4-(1-piperidinyl)butoxy]-1(2H)-isoquinolinone
DSS	Dextran sulphate sodium
DUOX	Dual oxidase
EC ₅₀	Half of the maximal response
EDTA	Ethylene diamine tetraacetic acid
EGTA	Ethylene glycol tetraacetic acid
ELISA	Enzyme-linked immunosorbent assay

ER	Endoplasmic reticulum
FAD	Flavin adenine dinucleotide
FBS	Foetal bovine serum
FeS	Iron-sulphur
FET	Forward electron transport
FFA	Flufenamic acid
FITC	Fluorescein isothiocyanate
Fluo4/AM	Fluo4-acetoxymethyl ester
fMLP	Formyl-methionyl-leucyl-phenylalanine
FMN	Flavin mononucleotide
FOXO	Forkhead box transcription factors
GPx	Glutathione peroxidase
GSH	Glutathione
H ₂ O ₂	Hydrogen peroxide
HBSS	Hank's Balanced Salt Solution
HIF-1 α	Hypoxia-inducible factors
HNO	Nitroxyl
HNO ₂	Nitrous acid
HO-1	Heme oxygenase-1
HOCl	Hypochlorous acid
HPLC	High performance liquid chromatography
hr	hour
I/R	Ischemia and reperfusion
IC ₅₀	Half of the maximal inhibition
IFN γ	Interferon gamma

IL-1 β	Interleukin-1 beta
IP ₃	Inositol 1,4,5-triphosphate
I-V	Current-voltage
K ⁺	Potassium
kb	Kilobase
kDa	Kilodalton
KO	Knockout
Lm	Listeria monocytogenes
LPS	Lipopolysaccharide
MAPK	Mitogen-activated protein kinase
Mg ²⁺	Magnesium
MHD	TRPM2 homology domain
min	Minute
ml	Mililitre
mM	Milimolar
MPP ⁺	1-methyl-4-phenylpyridinium ions
MPTP	1-methyl-4-phenyl-1,2,3,6-tetrahydropyridine
mRNA	Messenger RNA
N ₂ O ₃	Dinitrogen trioxide
Na ⁺	Sodium
NAADP	Nicotinic acid adenine dinucleotide phosphate
NAD	Nicotinamide adenine dinucleotide
NAPQI	N-acetyl-parabenzo-quinoneimine
NF- κ B	Nuclear factor-kappa of activated B cell
NLRP3	Nucleotide binding domain 3-leucine-rich repeat

nM	Nanomolar
NO [·]	Nitric oxide
NOX	Nicotine adenine dinucleotide phosphate (NADPH) oxidase
NUDT-9	Nucleoside diphosphate-linked moiety X-type motif 9
NUDT9-H	NUDT-9 homology
O ₂	Singlet oxygen
O ₂ ^{·-}	Superoxide
O ₂ ⁻²	Peroxide
O ₃	Ozone
OAADPR	2'- <i>O</i> -acetyl-ADPR
OH [·]	Hydroxyl
ONOO ⁻	Peroxynitrite
p	T-test critical significance level
PA	Pluronic acid
PAK	p21-activated kinase
PAMP	Pathogen-associated molecular patterns
PARG	Poly (ADPR) glycohydrolases
PARP-1	Poly (ADPR) polymerase-1
PBS	Phosphate buffer saline
PC12	Pheochromocytoma cells
PD	Parkinson disease
PFA	Paraformaldehyde
Phox	Phox-I2
PI	Propidium iodide
PIP ₂	Phosphatidylinositol 4,5-biphosphate

PJ34	<i>N</i> -(6-oxo-5,6-dihydro-phenanthridin-2-yl)- <i>N,N</i> -dimethylacetamide
PKA	Protein kinase A
PKC	Protein kinase C
PLC	Phospholipase C
PLL	Poly-L-lysine
PRR	Pattern recognition receptor
pS	Picosiemens
pSNL	Peripheral sciatic nerve ligation
Q	Ubiquinone-reduction centre
Q _o	Ubiquinone-oxidation centre
RACK1	Receptor for activated C kinase 1
RET	Reverse electron transport
RNA	Ribonucleic acid
RNS	Reactive nitrogen species
RO·	Alkoxy
RO ₂ ·	Peroxy
ROS	Reactive oxygen species
rpm	Rotations per minutes
RT	Room temperature
RT-PCR	Reverse transcriptase polymerase chain reaction
SBS	Standard bath solution
SDH	Succinate dehydrogenase
SEM	Standard error of the mean
shRNA	Short hairpin RNA

siRNA	Small interference RNA
SM	Sulphur mustard
SN	Substantia nigra
SNT	Spinal nerve transection
SOD	Superoxide dismutase
SPH	D-erythro-sphingosine
SSF	Striatum short protein
TACE	TNF- α converting enzyme
TLC	Thin layer chromatography
TM	Transmembrane
TNF- α	Tumor necrosis factor alpha
TNFR1/2	TNF- α receptor 1 or 2
TRP	Transient receptor potential
TRPA	TRP ankyrin
TRPC	TRP canonical or classic
TrpL	Trp-like
TRPM	TRP melastatin
TRPM2-S	TRPM2-short
TRPM2-TE	Tumor-enriched TRPM2
TRPML	TRP mucolipin
TRPP	TRP polycystin
TRPV	TRP vanilloid
Trp γ	Trp gamma
TRX	Thioredoxin
WT	Wild-type

Zn^{2+}

Zinc

ΔE

Difference in the redox potential

Δp

Proton motive force

Amino Acid Abbreviations

A	Alanine	Ala
C	Cysteine	Cys
D	Aspartic acid	Asp
E	Glutamic acid	Glu
F	Phenylalanine	Phe
G	Glycine	Gly
H	Histidine	His
I	Isoleucine	Ile
K	Lysine	Lys
L	Leucine	Leu
M	Methionine	Met
N	Asparagine	Asp
P	Proline	Pro
Q	Glutamine	Gln
R	Arginine	Arg
S	Serine	Ser
T	Threonine	Thr
V	Valine	Val
W	Tryptophan	Trp
Y	Tyrosine	Tyr

CHAPTER 1

GENERAL INTRODUCTION

1.1 MAMMALIAN TRP CHANNELS

1.1.1 Discovery and classification

The transient receptor potential (TRP) protein was initially discovered in genetic studies of the photo-transduction signalling mechanism in the fruit fly *Drosophila Melanogaster*. Stimulation of the photoreceptor cells with continuous bright light evoked a sustained receptor potential in wild-type (WT) flies, but only a transient receptor potential in a mutant fly (Cosens and Manning, 1969; Minke et al., 1975). These led to the discovery of the gene responsible, *Trp*, which encodes a membrane protein located in the rhabdomeric membrane of photoreceptor cells (Montell and Rubin, 1989). Years later, patch-clamp recording showed that the Trp protein and its homologues, Trp-like (TrpL) and Trp γ , form Ca^{2+} -permeable cation channels (Hardie and Minke, 1992; Phillips et al., 1992; Xu et al., 1997; Xu et al., 2000).

Twenty-eight mammalian homologues of the *Drosophila* Trp proteins were later identified, forming the TRP superfamily (Wes et al., 1995; Ramsey et al., 2006; Nilius, 2007; Venkatachalam and Montell, 2007). The mammalian TRP family can be grouped into six subfamilies based on amino acid sequence relatedness; TRPC (canonical or classic), TRPV (vanilloid), TRPM (melastatin), TRPA (ankyrin), TRPP (polycystin) and TRPML (mucolipin) (Pedersen et al., 2005; Sumoza-Toledo and Penner, 2011) (Fig. 1.1). Alternatively, the mammalian TRP proteins can be divided into two groups according to sequence similarity to the *Drosophila* Trp proteins; group 1 includes TRPC, TRPV, TRPM and TRPA which exhibit strong homology, with the TRPC proteins being greatest, whereas group 2 contains TRPP and TRPML which show less similarity (Venkatachalam and Montell, 2007).

1.1.2 Structural properties

All mammalian TRP proteins have a common membrane topology, comprising six α -transmembrane segments (S1-S6) and N- and C-termini both facing towards the cytoplasm (Montell, 2005; Ramsey et al., 2006; Pedersen et al., 2005; Venkatachalam and Montell, 2007; Nilius, 2007) (Fig. 1.2). As shown in atomic structures of the TRPV1 (Liao et al., 2013) and TRPV2 channels (Huynh et al., 2016; Zubcevic et al., 2016) recently determined using electron cryo-microscopy, TRP channels are tetrameric, made of four identical subunits (homomeric channels) or four different subunits (heteromeric channels). From each of the four subunits, the fifth and sixth transmembrane segments

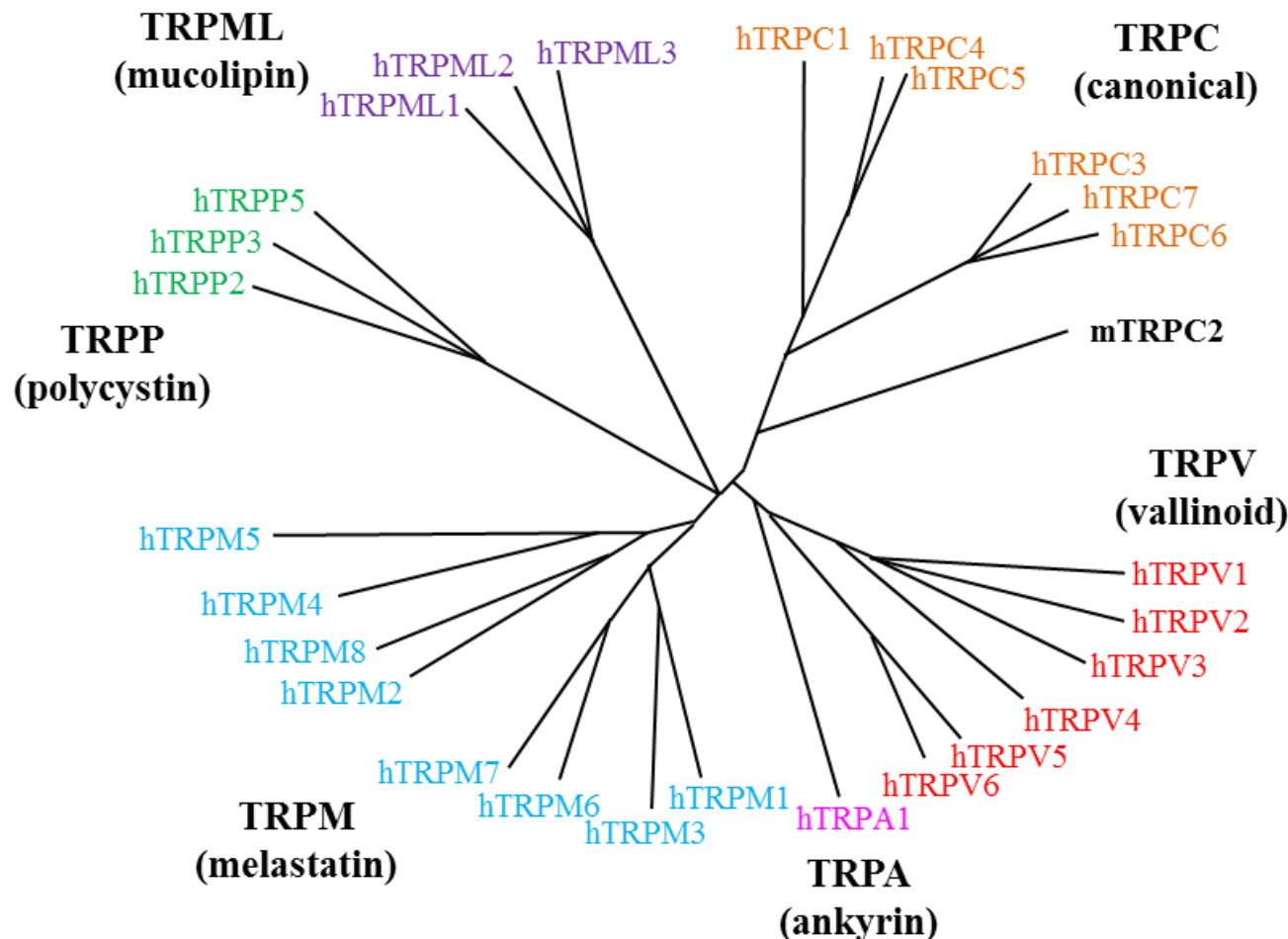


Fig. 1.1 The mammalian TRP superfamily.

The diagram shows the amino acid sequence relatedness of the human TRP protein superfamily, which comprise of the TRPC, TRPM, TRPV, TRPA, TRPP and TRPML subfamilies, except mouse TRPC2, which is a pseudogene in humans (Nilius et al., 2007).

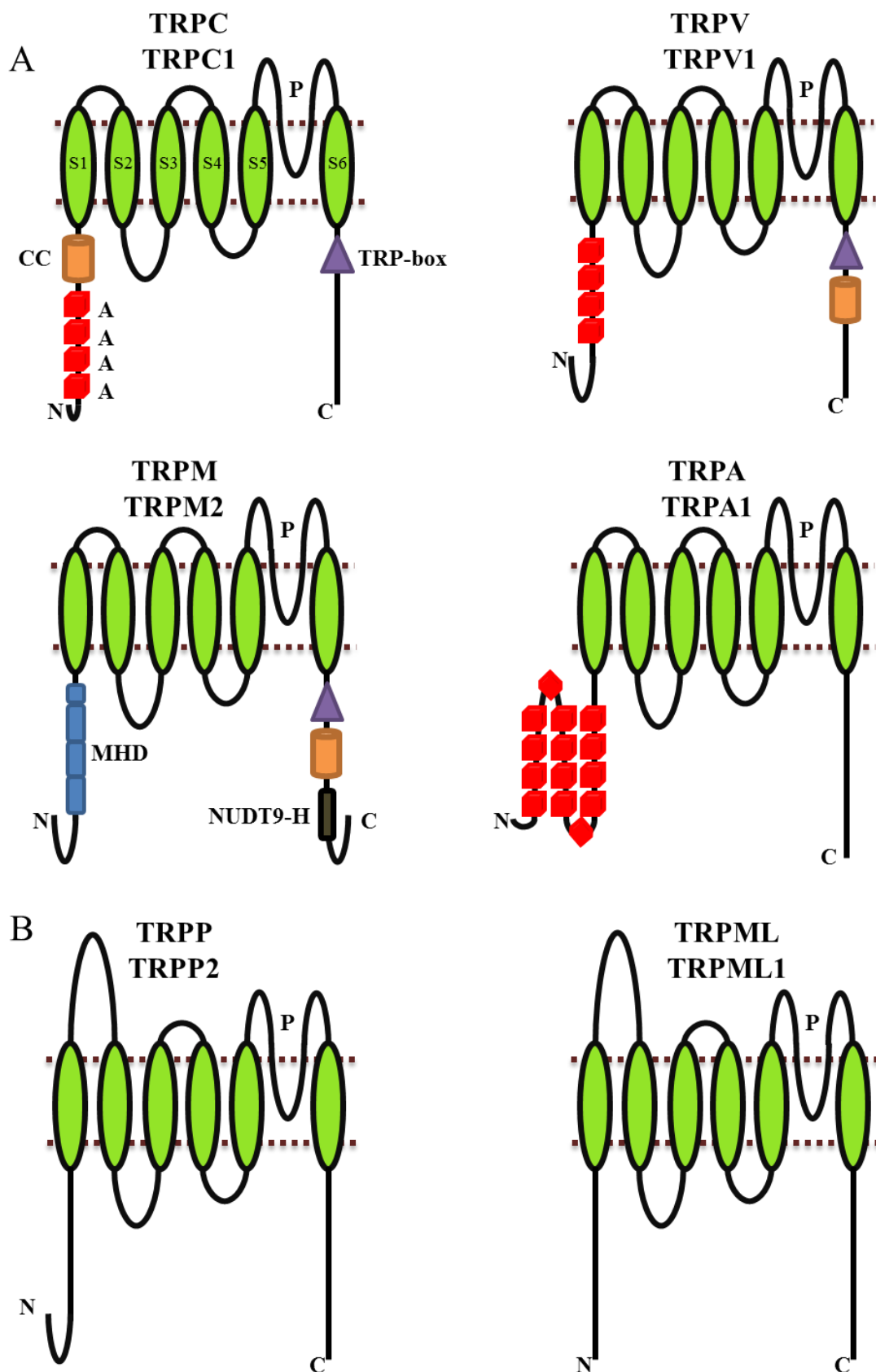


Fig. 1.2 Membrane topology and structural features of the TRP proteins.

Diagrams showing example TRP proteins in group 1 (A) and group 2 (B). Six transmembrane segments (S1-S6) are indicated by vertical oval columns; P, pore loop; CC, coiled-coil domain; A, ankyrin repeat; TRP-box; MHD, TRPM homology domains; NUDT9-H, NUDT9 homology domain.

and the re-entrant pore loop (P loop; Fig. 1.2) between them form an aqueous ion-conducting canal that allows the flux of cations into or out of the cell.

The mammalian TRP proteins in group 1 manifest several distinct structural features in the N- and C-termini, as illustrated in Fig. 1.2A. The N-terminus of the TRPC, TRPV and TRPA protein contain ankyrin repeats, each composed of approximately 33 amino acid residues which are important in forming helix-turn-helix structures (Montell et al., 2002; Chang et al., 2004; Clapham, 2003 p. 2; Owsianik et al., 2006; Hellwig et al., 2005; Phelps et al., 2008). With the exception of the TRPA protein, the TRPC, TRPV and TRPM proteins have a stretch of 23-25 highly conserved amino acid residues in the proximal C-terminus immediately after the transmembrane domain. This is known as TRP signature box. Furthermore, coiled-coil motifs, which are known to mediate protein-protein interactions, are present in the N- or C-termini of the TRPC, TRPM and TRPV proteins. The C-terminal coiled-coil motif in the proteins has been shown to be critical in mediating TRPM channel formation (Mei et al., 2006; Lepage et al., 2006; Erler et al., 2006; Jiang et al., 2010) (Fig. 1.2A). Finally, the TRPM2, TRPM6 and TRPM7 proteins are unique in that they possess an enzymatic domain in the distal C-terminus. This part of the TRPM2 protein exhibits significant homology to NUDT-9, an ADP-ribose (ADPR) pyrophosphatase, and is thus referred to the NUDT9-H domain (Fig. 1.2) (Perraud et al., 2001; Fleig and Penner, 2004a; Jiang et al., 2010; Sumoza-Toledo and Penner, 2011). The distal C-terminus in the TRPM6 and TRPM7 proteins is an α -kinase domain (Ryazanova et al., 2004; Matsushita et al., 2005).

The TRP proteins in group 2, TRPP and TRPML, have an exceptionally large loop between the first and second transmembrane segments (Fig. 1.2B), making their membrane topology distinct from that of the TRP proteins in group 1.

1.1.3 Activation, expression and function

While some TRP channels are constitutively active, many others are activated by a variety of stimuli through multiple signalling mechanisms. These channels are expressed in many cell types and play a major role in numerous physiological and pathological functions (Ramsey et al., 2006; Nilius, 2007; Venkatachalam and Montell, 2007; Dong et al., 2010). Below is a brief introduction of the activation, expression and function of the TRP channels, except the TRPM2 channel, which will be discussed in detail in a later section.

1.1.3.1 TRPC

TRPC proteins were identified as the first mammalian homologues of the *Drosophila* TRP proteins (Wes et al., 1995; Zhu et al., 1995). There are seven TRPC proteins (TRPC1-TRPC7) that can form non-selective Ca^{2+} -permeable cation channels. This family of proteins can be further divided into four subsets, based on sequence homology and functional similarities; TRPC1, TRPC2, TRPC3/6/7 and TRPC4/5 (Montell et al., 2002; Pedersen et al., 2005; Venkatachalam and Montell, 2007).

All TRPC channels have been shown to be activated through the G protein-coupled receptor-dependent phospholipase C (PLC) signalling pathway. Activation of various G protein-coupled receptors leads to PLC activation, which catalyses the cleavage of the membrane lipid phosphatidylinositol 4,5-biphosphate (PIP_2) into inositol 1,4,5-triphosphate (IP_3) and diacylglycerol (DAG). IP_3 binds to and activates the IP_3 receptor (IP_3R) on the endoplasmic reticulum (ER), resulting in Ca^{2+} release from the ER. With the exception of the TRPC2 and TRPC6 channels, all TRPC channels are activated by the depletion of ER Ca^{2+} (Philipp et al., 1998; Vannier et al., 1999; Warnat et al., 1999; Ma et al., 2002; Lockwich et al., 2001; Venkatachalam et al., 2002). The TRPC2, TRPC3, TRPC6 and TRPC7 channels can be activated by DAG (Hofmann et al., 1999; Liman et al., 1999; Lucas et al., 2003; Lievremont et al., 2005; Soboloff et al., 2005). Uniquely, the TRPC1 channel has been shown to be activated by mechanical stretch (Maroto et al., 2005; Patel et al., 2010).

TRPC1 is expressed in neurons (Kim et al., 2003), smooth muscle cells (Sweeney et al., 2002; Flemming et al., 2003), endothelial cells (Nilius and Droogmans, 2001; Ahmmmed et al., 2004) and lymphocytes (Mori et al., 2002). TRPC1 channel-mediated Ca^{2+} entry has been proposed to be required for the generation of postsynaptic potential in neurons (Kim et al., 2003) and smooth muscle cell proliferation (Sweeney et al., 2002). Besides that, the TRPC1 channel is suggested to mediate store-operated Ca^{2+} entry in endothelial cells (Ahmmmed et al., 2004).

TRPC2 expression has been documented in neurons (Lucas et al., 2003; Stowers et al., 2002) and sperm cells (Vannier et al., 1999; Jungnickel et al., 2001). The TRPC2 channel has been shown to be involved in the pheromone transduction signalling mechanism (Lucas et al., 2003), which is reflective of its expression in sensory neurons. There is evidence showing that the TRPC2 channel is critical in the regulation of sexual behaviour (Stowers et al., 2002). Furthermore, the TRPC2 channel is also suggested to

be important in mediating Ca^{2+} entry into sperm cells upon stimulation by an egg (Jungnickel et al., 2001).

TRPC3 is expressed in neurons (Hartmann et al., 2008; Amaral and Pozzo-Miller, 2007), lymphocytes (Philipp et al., 2003) and cardiomyocytes (Onohara et al., 2006). It has been proposed that the TRPC3 channel has a role in a broad spectrum of physiological and pathological functions, including neuronal dendritic spine formation (Amaral and Pozzo-Miller, 2007), lymphocyte activation (Philipp et al., 2003) and angiotensin II-induced cardiac hypertrophy (Onohara et al., 2006).

TRPC4 is expressed in endothelial cells (Freichel et al., 2001; Tiruppathi et al., 2002; Ahmed and Malik, 2005), neurons (Munsch et al., 2003) and interstitial cells (Torihashi et al., 2002; Walker et al., 2002). The TRPC4 channel has been shown to be important in increasing endothelial cell permeability (Tiruppathi et al., 2002). This channel is also implicated in mediating neurotransmitter release from neuronal dendrites (Munsch et al., 2003). The expression of the TRPC4 channel in the interstitial cells has led to the discovery of its role in mediating pacemaker currents in the small intestine (Torihashi et al., 2002; Walker et al., 2002).

TRPC5 expression has been documented in neurons (Bezzerides et al., 2004; Greka et al., 2003) and smooth muscle cells (Xu et al., 2006). The TRPC5 channel in neurons has been linked to a role in neuronal cell migration (Greka et al., 2003) and neuronal remodelling (Bezzerides et al., 2004). Additionally, this channel is involved in mediating Ca^{2+} entry which is essential for smooth muscle cell contraction (Xu et al., 2006).

TRPC6 expression has been identified in smooth muscle cells (Jung et al., 2002; Weissmann et al., 2006), neurons (Inoue et al., 2001), thrombocytes (Hassock et al., 2002) and white blood cells (Heiner et al., 2003). Studies using transgenic TRPC6 knockout mice have shown the importance of this channel in hypoxia-induced pulmonary hemodynamics (Weissmann et al., 2006). Furthermore, TRPC6 channel-mediated Ca^{2+} entry is suggested to have a role in vasopressin-induced smooth muscle cell contraction (Jung et al., 2002) and sympathetic nerve activity (Inoue et al., 2001). The TRPC6 channel in thrombocytes plays a role in the formation of the store-operated Ca^{2+} channels (Hassock et al., 2002).

Finally, TRPC7 expression has been found in endothelial cells (Yip et al., 2004), neurons (Ben-Mabrouk and Tryba, 2010) and myometrial cells (Dalrymple et al., 2004). TRPC7, on its own, is involved in relatively few physiological functions. However, TRPC7 can interact with TRPC3 and TRPC6 to form heteromeric channels (Yip et al.,

2004; Dalrymple et al., 2004; Lièvremont et al., 2004; Zagranichnaya et al., 2005). There is evidence to suggest the heteromeric channels made of TRPC7 and TRPC3 or TRPC6 are involved in mediating the Ca^{2+} entry which influences women's pregnancy and labour (Dalrymple et al., 2004) as well as respiratory rhythm activity (Ben-Mabrouk and Tryba, 2010). Moreover, studies have shown that TRPC7 is implicated in the formation of store-operated Ca^{2+} -channels (Zagranichnaya et al., 2005).

1.1.3.2 TRPV

Of all the mammalian TRP subfamilies, TRPV proteins are most related to the TRPC proteins, due to their similarities on highly conserved residues in the fifth and sixth transmembrane segments (Montell, 2005; Venkatachalam and Montell, 2007). Mammalian cells express six genes encoding six different TRPV proteins, TRPV1-TRPV6 (Gunthorpe et al., 2002; Pedersen et al., 2005). The TRPV channels exhibit significant variation in their selective Ca^{2+} permeability, with the TRPV1-TRPV4 channels functioning as nonselective Ca^{2+} permeable channels and the TRPV5 and TRPV6 channels being highly selective for Ca^{2+} . All the TRPV channels except TRPV5 and TRPV6 are sensitive to activation by temperature, each with a different temperature threshold (TRPV1: $\geq 43^\circ\text{C}$; TRPV2: $> 52^\circ\text{C}$, TRPV3: 33-39°C, TRPV4: 27-42°C) (Smith et al., 2002; Xu et al., 2002; Guler et al., 2002; Ahluwalia et al., 2002; Pedersen et al., 2005). The TRPV1-TRPV3 channels can be activated by 2-aminoethoxydiphenyl borate (2-APB), with the TRPV1 and TRPV2 channels having the lower sensitivity to 2-APB than the TRPV3 channel (Chung et al., 2004; Hu et al., 2004). The TRPV1-TRPV4 channels are also activated by various other stimuli, including vanilloid compounds (TRPV1) (Caterina et al., 2000; Pedersen et al., 2005; Valente et al., 2008), nicotine (TRPV1) (Liu et al., 2004), growth factor (TRPV2) (Kanzaki, 1999), camphor (TRPV3) (Moqrich et al., 2005) and osmotic pressure (TRPV4) (Nilius, Prenen, et al., 2003). The TRPV5 and TRPV6 channels are also activated by low intracellular Ca^{2+} concentrations (30-50 nM) (Bödding et al., 2002; Lee et al., 2005).

TRPV1 is mainly expressed in neurons, and this has led to studies that have shown its critical role in the detection of heat and painful stimuli (Caterina et al., 2000; Hazan et al., 2015). Also, the TRPV1 channel has been shown to be important in feeding behaviour and body weight regulation (Ahern, 2003; Wang et al., 2005). There is also evidence to suggest that the TRPV1 channel is expressed in the pancreas and is critical in mediating the release of substance P (Nathan et al., 2001).

TRPV2 expression has been documented in smooth muscle cells (Kanzaki, 1999; Kanzaki et al., 1999; Beech et al., 2004), cardiomyocytes (Muraki et al., 2003; Iwata et al., 2003; Katanosaka et al., 2014), pancreatic β cells (Aoyagi et al., 2010), interstitial cells (Kashiba et al., 2004) and neurons (Shimosato et al., 2005). The TRPV2 channel is involved in cardiac shortening (Katanosaka et al., 2014) and glucose-induced insulin secretion (Aoyagi et al., 2010). Furthermore, there is evidence to show that the TRPV2 channel can act as an osmotic-sensitive cation channel in cardiomyocytes (Muraki et al., 2003).

TRPV3 is expressed in keratinocytes (Peier, Reeve, et al., 2002; Smith et al., 2002; Chung et al., 2005; Pedersen et al., 2005), smooth muscle cells (Xu et al., 2002; Murphy et al., 2016) and neurons. The expression of the TRPV3 channel in these cells has led to the discovery of its roles in skin sensitisation (Moqrich et al., 2005) and blood vessel vasodilation (Murphy et al., 2016). Additionally, it has been reported that TRPV3 can form a hetero-oligomeric channel with TRPV1 (Hellwig et al., 2005).

TRPV4 expression has been found in neurons (Alessandri-Haber et al., 2003; Delany et al., 2001), hair cells (Liedtke et al., 2000; Strotmann et al., 2000), endothelial cells (Nilius, et al., 2003b) and epithelial cells (Andrade et al., 2005; Strotmann et al., 2000). The TRPV4 channel is additionally involved in hypotonicity-induced nociceptive responses (Alessandri-Haber et al., 2003; Delany et al., 2001; Liedtke et al., 2000). This channel has also been reported to play a role in thermosensing (Guler et al., 2002) or mechanosensing (Fernandes et al., 2008; Lorenzo et al., 2008; Strotmann et al., 2000).

There is highly restricted TRPV5 expression in epithelial cells (Nijenhuis et al., 2003; de Groot et al., 2008). This directly links to its role in mediating Ca^{2+} reabsorption in the kidney and intestine.

Similarly to TRPV5, TRPV6 expression has been documented in epithelial (Nijenhuis et al., 2003; Nijenhuis et al., 2005) and interstitial cells (van de Graaf et al., 2006). The TRPV6 channel has been proposed to be critical in maintaining the Ca^{2+} homeostasis in the kidney and intestine.

1.1.3.3 TRPM

The TRPM subfamily was named after melastatin (TRPM1), the first member, and is comprised of eight members (TRPM1-TRPM8). The TRPM proteins can be further divided into four pairs based on sequence homology; TRPM1/TRPM3, TRPM6/TRPM7, TRPM4/TRPM5 and TRPM2/TRPM8 (Fleig and Penner, 2004a;

Fleig and Penner, 2004b; Eisfeld and Luckhoff, 2007). All TRPM proteins contain four stretches of highly conserved amino acid residues in the N-terminus, named TRPM homology domains (MHD) I-IV (Fig 1.2A) (Eisfeld and Luckhoff, 2007). These domains, however, have not been assigned with specific channel function.

All TRPM proteins can form functional channels, which exhibit significant variation in their ion permeability to divalent cations such as Ca^{2+} . The TRPM1, TRPM3, TRPM6 and TRPM7 channels are relatively more permeable to divalent cations (Xu et al., 2001; Oberwinkler et al., 2005; Voets et al., 2004; Li et al., 2006). Conversely, the TRPM4 and TRPM5 channels are highly permeable to monovalent cations (Hofmann et al., 2003; Liu and Liman, 2003; Launay et al., 2002). The TRPM2 and TRPM8 channels show an intermediate permeability to divalent cations (Sano et al., 2001; Perraud et al., 2001; Kuhn et al., 2007; Peier, Moqrich, et al., 2002).

The TRPM1 channel is constitutively active. The TRPM3 channel can be activated by osmotic pressure (Grimm et al., 2003), steroid compounds such as pregnenolone sulphate (Wagner et al., 2008) and d-erythro-sphingosine (SPH), a lipophilic substance (Grimm et al., 2005). There is evidence to suggest that both the TRPM4 and TRPM5 channels are directly activated by intracellular Ca^{2+} (Launay et al., 2002; Hofmann et al., 2003; Nilius, Prenen, et al., 2003). In addition, the TRPM5 channel is activated by PIP_2 (Ueda et al., 2003; Liu and Liman, 2003). The TRPM7 channel can be activated by Mg-ATP (Hermosura et al., 2002), cyclic adenosine monophosphate (cAMP) (Takezawa et al., 2004)(McKemy, 2005; Peier, Moqrich, et al., 2002; Behrendt et al., 2004) and PIP_2 (Runnels et al., 2001). The TRPM8 channel is activated by cold temperature and cooling agents such as menthol and icilin (McKemy, 2005; Peier, Moqrich, et al., 2002; Behrendt et al., 2004).

TRPM1 was first identified in melanocytes, playing role in melanin trafficking (Duncan et al., 1998; Miller, 2004; Oancea et al., 2009). Recent studies have shown that the TRPM1 channel is expressed in retinal bipolar cells and is important in determining cell viability (Koike et al., 2010; Shen et al., 2009).

TRPM3 expression has been documented in smooth muscle cells (Naylor et al., 2010), neurons (Vriens et al., 2011; Vandewauw et al., 2013) and pancreatic β cells (Wagner et al., 2008; Wagner et al., 2010). The TRPM3 channel has been shown to play a functional role in smooth muscle cell contraction and proliferation (Naylor et al., 2010). Furthermore, TRPM3 channel expression in neurons has led to the discovery of its role in chemosensing and thermosensing (Vriens et al., 2011; Straub et al., 2013).

Evidence also exists to suggest that the TRPM3 channel is involved in glucose-induced insulin secretion (Wagner et al., 2008; Wagner et al., 2010).

TRPM4 is expressed in dendritic cells (Barbet et al., 2008), smooth muscle cells (Isogai et al., 2016) and sperm cells (Kumar et al., 2016). The TRPM4 channel has been shown to be important in cell migration (Barbet et al., 2008; Holzmann et al., 2015), smooth muscle cell contraction (Isogai et al., 2016) and sperm fertilisation (Kumar et al., 2016).

TRPM5 channel expression has been described in taste receptor cells, leading to the discovery of its significant involvement in the taste transduction mechanism (Talavera et al., 2005; Ueda et al., 2003; Liu and Liman, 2003; Liman, 2007). The TRPM5 channel is also expressed in intestinal cells, where it plays a role in post-ingestive chemosensation (Pérez et al., 2002). In pancreatic β cells, the TRPM5 channel is involved in insulin secretion (Liman, 2010; Brixel et al., 2010).

TRPM6 is mainly found in epithelial cells and plays a vital role in mediating in Mg^{2+} reabsorption in the kidney and intestine (Runnels et al., 2001; Hermosura et al., 2002; Voets et al., 2004; Nijenhuis et al., 2006).

TRPM7 expression has been documented in neuroblastoma cells (Clark et al., 2006; Su et al., 2006), neurons (Aarts et al., 2003; Nicotera and Bano, 2003) and pheochromocytoma cells (PC12) (Brauchi et al., 2008). The TRPM7 channel is shown to have a role in cell adhesion, cell viability and hormone secretion, respectively. Furthermore, a study shows a function for the TRPM7 channel in the cell proliferation implicated in carcinogenesis (Yee et al., 2011).

TRPM8 expression is found in epithelial cells (Patapoutian et al., 2003; Zhang and Barritt, 2004), neurons (Clapham, 2003; McKemy et al., 2002; McKemy, 2005), endothelial cells (Genova et al., 2017) and smooth muscle cells (Mukerji et al., 2006). The most remarkable role for the TRPM8 channel is sensing cold temperature (Patapoutian et al., 2003; Mukerji et al., 2006). There is evidence to show that the TRPM8 channel plays a role in prostate and pancreatic carcinogenesis (Tsavaler et al., 2001; Liu et al., 2016; Yee, 2015). In addition, the TRPM8 channel is involved in endothelial cell migration (Genova et al., 2017) and smooth muscle cell contraction (Mukerji et al., 2006).

1.1.3.4 TRPA

The TRPA subfamily consists only one member, TRPA1. The TRPA1 protein can form a Ca^{2+} -permeable cation channel which is activated by intracellular Ca^{2+}

(Nagata et al., 2005; Zurborg et al., 2007; Doerner et al., 2007). The TRPA1 channel is potently activated by proalgesic compounds such as bradykinin, allicin and horseradish, and environmental irritants like vehicle exhaust and tear gas (Story et al., 2003; Bandell et al., 2004; Macpherson et al., 2005; McKemy, 2005; Bautista et al., 2006). Additionally, TRPA1 channel activation can be stimulated by mechanical pressure (Corey et al., 2004) and noxious cold temperature (Story et al., 2003; Sawada et al., 2007).

Restricted TRPA1 expression is seen in hair cells (Corey et al., 2004; Nagata et al., 2005; Wu et al., 2016) and neurons (Story et al., 2003; Bautista et al., 2006). There is evidence to suggest that the TRPA1 channel plays a key role in auditory signal transduction mechanisms or hearing (Corey et al., 2004; Nagata et al., 2005; Wu et al., 2016). Besides that, the TRPA1 channel has been proposed to mediate pain perception (Voets et al., 2005) and heat sensation (McKemy, 2005; Bautista et al., 2006).

1.1.3.5 TRPP

There are three TRPP proteins; TRPP2, TRPP3 and TRPP5 (or TRPP2-like), which are structurally similar to other TRP proteins in that they have six α -transmembrane segments (Fig. 1.2B). They can form Ca^{2+} -permeable cation channels (Inoue et al., 2006). The TRPP2 and TRPP3 channels are activated by intracellular Ca^{2+} (Koulen et al., 2002; Chen et al., 1999; Li et al., 2002). Additionally, the TRPP2 channel can be activated by mechanical stimuli (Delmas, 2004; Delmas, 2005), whereas the TRPP3 channel activation can be stimulated by voltage, pH and mechanical stress (Shimizu et al., 2009). Molecular cloning has identified TRPP1 and related proteins (TRPP1-like) that consist of 11 putative transmembrane segments (Hughes et al., 1995), and are therefore not part of the TRP superfamily.

TRPP2 was first discovered in search for the gene responsible for autosomal dominant polycystic kidney disease (AD-PKD) (Mochizuki et al., 1996; Pedersen et al., 2005; Venkatachalam and Montell, 2007). Subsequent studies showed TRPP2 expression in renal epithelial cells and its role in the mechanotransduction signalling in kidneys (Yoder et al., 2002; Bai et al., 2008; Nauli et al., 2003; Kottgen, 2007; Delmas, 2004). TRPP2 channel expression has also been documented in cardiomyocytes, smooth muscle cells, endothelial cells (Ong, 2000) and sperm cells (Kottgen et al., 2011), where it is proposed to be involved in determining cell viability (Kottgen, 2007), cell proliferation (Aguiari et al., 2004), asymmetric cell polarization (Pennekamp et al., 2002) and sperm fertilization (Kottgen et al., 2011). Additionally, studies have reported

that the TRPP2 protein can co-assemble with TRPP1-like protein to form a functional Ca^{2+} -permeable channel mediating mechanotransduction signalling (Delmas, 2004; Hanaoka et al., 2000).

TRPP3 expression has been documented in neurons (Huang et al., 2006; Djenoune et al., 2014; Orts-Del'Immagine et al., 2014), retinal cells (Keller et al., 1994) and hair cells (Nomura et al., 1998). Studies by genetic deletion or pharmacological inhibition of the TRPP3 channel have shown its role in taste sensation (Huang et al., 2006; Ishimaru et al., 2006; LopezJimenez et al., 2006). The TRPP3 channel has also been implicated in cell growth (Keller et al., 1994; Nomura et al., 1998) and hedgehog signalling mechanisms (DeCaen et al., 2013; Delling et al., 2013).

TRPP5 expression is primarily found in sperm cells, where it plays a role in spermatogenesis (Guo et al., 2000; Chen et al., 2008; Xiao et al., 2010). The TRPP5 channel has also been identified in epithelial cells (Xiao et al., 2010) and cardiomyocytes (Volk et al., 2003), where it has been suggested to be involved in cell proliferation and cell viability.

1.1.3.6 TRPML

The TRPML subfamily includes three proteins, TRPML1-TRPML3. TRPML1 and TRPML2 proteins are localised in the lysosomal membrane (Dong et al., 2008; Karacsonyi et al., 2007), whereas the TRPML3 protein is present in the plasma membrane (Kim et al., 2007). All TRPML proteins have been shown to be able to form nonselective cation-permeable channels (Dong et al., 2010).

The TRPML1 channel is activated by nicotinic acid adenine dinucleotide phosphate (NAADP) (Zhang and Li, 2007). In addition, evidence suggests that the TRPML1 and TRPML2 channels can be activated by voltage and low pH (Xu et al., 2007; Dong et al., 2008), whereas TRPML3 channel activation can be induced by extracellular Na^+ (Kim et al., 2007; Kim et al., 2008).

TRPML1 is expressed in smooth muscle cells (Zeevi et al., 2007), hepatocytes (Zhang and Li, 2007) and melanocytes (Xu et al., 2007). Studies have shown the importance of this channel in the pathogenesis of lysosomal storage disorder mucolipidosis type IV, which is characterised by mental retardation, motor defects and retinal degeneration (Sun et al., 2000; Bach, 2001; Bach, 2005). The TRPML1 channel is also critical in lysosomal formation and recycling (Piper and Luzio, 2004; Qian and Noben-Trauth, 2005).

TRPML2 expression has been shown in hepatocytes, endothelial cells and smooth muscle cells (Samie et al., 2009). Similarly to the TRPML1 channel, the TRPML2 channel is suggested to have a significant role in lysosomal formation (Di Palma et al., 2002).

TRPML3 is expressed in hair cells (Di Palma et al., 2002; Nagata et al., 2008), melanocytes (Xu et al., 2007) and epithelial cells (Kim et al., 2009). Studies using TRPML3 knockout mice have demonstrated the importance of this channel in hair cell maturation and melanocyte cell death (Di Palma et al., 2002; Nagata et al., 2008; Xu et al., 2007). In addition, there is evidence that suggests the TRPML3 channel is involved in deafness, pigmentation defects and perinatal lethality (Di Palma et al., 2002).

1.2 TRPM2 CHANNELS

1.2.1 Genes

TRPM2 genes have been cloned in humans (Nagamine et al., 1998), mice (Uemura et al., 2005) and rats (Wong et al., 1993). The human TRPM2 gene is located on chromosome 21q22.3, consisting of 32 exons spanning approximately 90 kb. The full-length human TRPM2 protein comprises of 1503 amino acid residues and has a predicted molecular weight of approximately 171 kDa (Nagamine et al., 1998). The full-length rat and mouse TRPM2 proteins are 1507 amino acid residues in length. A recent study has characterised the TRPM2 orthologue from the sea anemone *Nematostella vectensis* (Kuhn et al., 2015). This protein contains 1553 amino acid residues and exhibits 31% sequence identity with the human TRPM2 protein. In addition to the full-length isoform, several short alternative splicing variants of human TRPM2 have been reported (Jiang et al., 2010), which will be discussed in detail later.

1.2.2 Structural and biophysical properties

The TRPM2 channel has the same overall structure that is described in section 1.1.2 (Fig. 1.2A). The TRPM2 channel is distinguished from other TRP channels in that its intracellular C-terminus contains the NUDT9-H domain as briefly mentioned above. This domain, consisting of approximately 300 amino acid residues, displays sequence homology with the human NUDT9 ADPR pyrophosphatase, a mitochondrial hydrolase that degrades ADPR into adenine monophosphate (AMP) and ribose 5'-phosphate (Perraud et al., 2001; Fleig and Penner, 2004b; Shen et al., 2003). An early study

showed that the NUDT9-H domain, when expressed on its own, exhibited low but detectable ADPR hydrolase activity (Perraud et al., 2001), which has however been refuted in a recent study (Iordanov et al., 2016). The binding of intracellular ADPR to the NUDT9-H domain causes the TRPM2 channel to open its ion-permeating pore across the membrane, allowing the permeation of cations, including Ca^{2+} , Mg^{2+} , K^+ and Na^+ (Perraud et al., 2001; Sano et al., 2001; Mederos y Schnitzler et al., 2008; Xia et al., 2008). The TRPM2 channel currents display a linear current-voltage (I-V) relationship with zero reversal potential, consistent with the fact that it is non-selective cation channel. The single channel conductance is approximately 60 pS (Perraud et al., 2001).

1.2.3 Alternative splicing isoforms

Several alternative splicing isoforms have been reported for the TRPM2 protein. TRPM2- ΔN and TRPM2- ΔC were identified in monocytes and neutrophils (Wehage et al., 2002; Kuhn et al., 2009). The TRPM2- ΔN isoform has a deletion of 20 amino acid residues (538-557 according to the full-length human TRPM2) in the N-terminus. The TRPM2- ΔC lacks 34 amino acid residues in the C-terminus. The deletion in TRPM2- ΔC includes the ADPR-binding domain, but this mutant can still form a channel (Zhang et al., 2003; Wehage et al., 2002; Du et al., 2009). Later studies discovered two further alternative splicing isoforms, TRPM2-short (TRPM2-S) and striatum short protein (SSF)-TRPM2. The TRPM2-S protein contains only the N-terminus and the first two transmembrane segments. This truncated isoform is generated by a stop codon between exons 16 and 17 and has been reported to act as a dominant negative inhibitor when co-expressed with the full-length TRPM2 protein (Zhang et al., 2003). The SSF-TRPM2 isoform does not contain the first 214 amino acid residues in the N-terminus and has been shown to form a functional TRPM2 channel, although the channel activity is reduced compared to the full-length TRPM channel (Uemura et al., 2005). More recently, studies on melanoma and breast cancer cells have identified the tumour-enriched TRPM2 (TRPM2-TE) isoform, which lacks part of exon 26 and the entire exon 27 (Orfanelli et al., 2008). The deletion in TRPM2-TE includes 34 amino acid residues in the NUDT9-H domain; however TRPM2-TE is still able to demonstrate the enzymatic activity of TRPM2 channel (Orfanelli et al., 2008).

1.2.4 Channel Activation

ADPR and several structure- or metabolism-related compounds, including 2'-*O*-acetyl-ADPR (OAADPR), nicotinamide adenine dinucleotide (NAD), cyclic ADP-

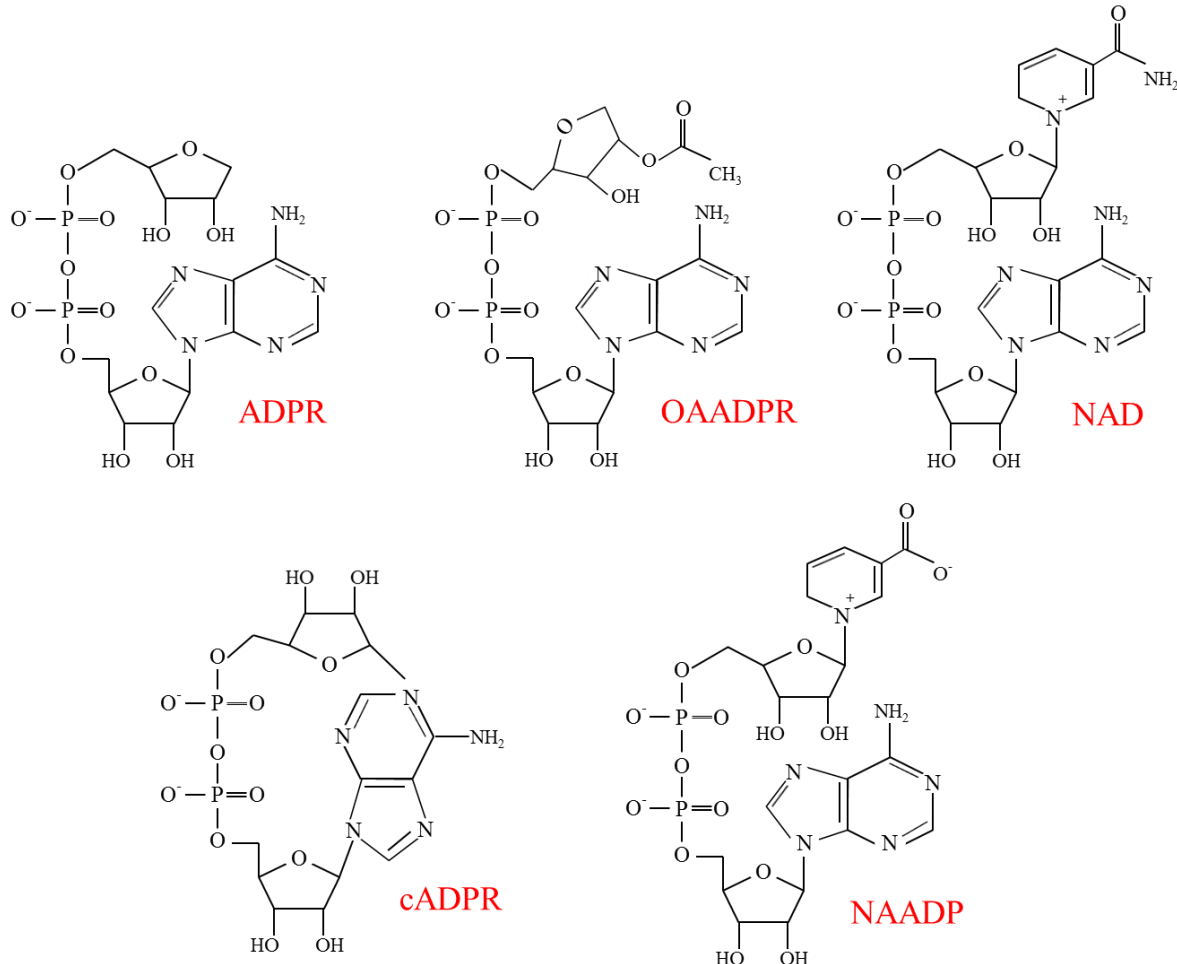


Fig. 1.3 TRPM2 channel activator structures.
 Diagrams showing the chemical structures of ADPR, OAADPR, NAD, cADPR and NAADP

ribose (cADPR) and nicotinic acid adenine dinucleotide phosphate (NAADP) have been shown to activate TRPM2 channels in submillimolar to millimolar concentrations (Jiang et al., 2010; Sumoza-Toledo and Penner, 2011). Figure 1.3 illustrates the structures of the TRPM2 channel activators described in this section.

1.2.4.1 ADPR

ADPR is the most potent agonist of the TRPM2 channel (Fig. 1.3), with the concentration inducing half of the maximal response (EC_{50}) varying from 1 to 90 μ M, depending on the cell types and the methods used to measure the channel activity (Perraud et al., 2001; Sano et al., 2001; Wehage et al., 2002; Beck et al., 2006; Lange et al., 2008). Site-directed mutagenesis studies suggest that two residues in the NUDT9-H domain, Ile¹⁴⁰⁵ and Lue¹⁴⁰⁶, are critical for TRPM2 channel activation by ADPR (Perraud et al., 2003; Kuhn and Luckhoff, 2004).

ADPR can be generated extracellularly by the hydrolysis of NAD⁺ catalysed by membrane-bound CD38 ectoenzyme (Lund et al., 1995; Malavasi et al., 2006; Lund, 2006). Studies using neutrophils from CD38-KO mice showed a decrease in the $[Ca^{2+}]_i$ induced by formyl-methionyl-leucyl-phenylalanine (fMLP) when compared to WT neutrophils (Partida-Sánchez et al., 2003). Interestingly, similar results were reported in TRPM2-KO neutrophils (Yamamoto et al., 2008). These findings consistently suggest that CD38 may play a role in generating the ADPR required for TRPM2 channel activation. However, it is still a matter of debate as to how extracellular ADPR produced by CD38 reaches the cytosolic NUDT9-H domain of the TRPM2 channel. In addition to the ectoenzyme CD38, NAD⁺ hydrolysis resulting in ADPR generation can also be induced in the nucleus and mitochondria in response to oxidative stress, which will be discussed later.

1.2.4.2 OAADPR

NAD-dependent deacetylase sirtuin-2 catalyses the deacetylation of acetylated substrates by removing the acetyl groups and transferring them to NAD⁺, producing OAADPR (Fig 1.3). Studies using patch-clamp recording and binding assays have revealed that OAADPR can activate the TRPM2 channel by binding to the NUDT9-H domain (Grubisha et al., 2006; Tong and Denu, 2010). OAADPR shows a similar binding affinity to ADPR, suggesting that OAADPR can directly gate the TRPM2 channel.

1.2.4.3 NAD

NAD serves as the precursor for the production of ADPR. Earlier studies reported that NAD can gate the TRPM2 channel, although high concentrations of NAD are required with, EC₅₀ values of 1-1.8 mM (Hara et al., 2002; Sano et al., 2001; Naziroğlu and Lückhoff, 2008). Furthermore, NAD displayed significant synergy with ADPR, each increasing channel sensitivity to the other (Beck et al., 2006). Additional studies showed that NAD-induced TRPM2 channel currents were significantly smaller compared to those induced by ADPR (Heiner et al., 2003; Kraft et al., 2004).

However, later studies have shown that purified NAD fails to activate the TRPM2 channel, therefore refuting the notion that NAD is a TRPM2 channel activator (Beck et al., 2006; Toth and Csanady, 2010; Megnone et al., 2012; Toth et al., 2015). These suggest that the NAD-induced TRPM2 channel activation observed in early studies is likely due to ADPR contamination. Indeed, thin layer chromatography (TLC) analysis showed substantial ADPR contamination in commercially available NAD (Toth and Csanady, 2010). In addition, Toth *et al.* have recently shown using inside-out patch-clamp recording that purified NAD was ineffective in inducing TRPM2 channel activation (Toth et al., 2015). They have further demonstrated that the purified NAD does not compete with ADPR for binding to the TRPM2 channel. Altogether, these findings have clarified the earlier contradiction by confirming that NAD-induced TRPM2 channel activation was due to the presence of ADPR and also that NAD on its own cannot act as a direct activator of the TRPM2 channel.

1.2.4.4 cADPR

cADPR can be synthesized from NAD by ectoenzyme CD38. When applied intracellularly, cADPR at concentrations of above 100 µM can activate the TRPM2 channel with an EC₅₀ value of 0.4-0.7 mM, which is far less effective than ADPR (Kolisek et al., 2005; Beck et al., 2006; Heiner et al., 2006; Lange et al., 2008). cADPR at lower micromolar concentrations (10 µM) shows a strong synergy with ADPR, causing an increase in the TRPM2 channel sensitivity to each other (Kolisek et al., 2005).

High performance liquid chromatography (HPLC) analysis has found a considerable amount of ADPR in commercial cADPR (Heiner et al., 2006). Additionally, Beck and her colleagues showed that adenosine diphosphate (AMP) potently suppresses the TRPM2 channel activation induced by ADPR but not cADPR

(Beck et al., 2006; Lange et al., 2008). More recently, a study using patch-clamp recording showed that AMP strongly abolished cADPR-induced TRPM2 currents (Toth et al., 2014), supporting the notion that cADPR-induced TRPM2 channel activation is due to ADPR.

1.2.4.5 NAADP

NAADP has been shown to activate the TRPM2 channel with an EC₅₀ value of 0.73-1 mM (Beck et al., 2006; Lange et al., 2008). There is evidence to show that NAADP is capable of directly binding and activating the TRPM2 channel, albeit with a very low binding affinity (Toth and Csanady, 2010). The concentration of NAADP required for TRPM2 channel activation is much higher than its physiological concentration and it has therefore been suggested that NAADP does not act as an agonist of the TRPM2 channel *in vivo*. Nonetheless, NAADP at low micromolar concentrations shows synergy with ADPR in activating the TRPM2 channel (Lange et al., 2008).

1.2.4.6 Ca²⁺

TRPM2 channel is a Ca²⁺-permeable channel and thus the elevation in [Ca²⁺]_i is an early downstream event following channel activation. Intracellular Ca²⁺ itself is critical for full activation of the TRPM2 channel. In the absence of Ca²⁺, ADPR is very efficient in inducing TRPM2 channel activation (Starkus et al., 2007; Carter et al., 2006; Lange et al., 2008). Intracellular Ca²⁺ potentiates ADPR-induced TRPM2 channel activation by increasing the sensitivity of the channel to ADPR, with a concentration of 0.3 μM producing half maximal potentiation (Lange et al., 2008; Starkus et al., 2007; McHugh et al., 2003). There is evidence to suggest that the minimum intracellular Ca²⁺ concentration of 30 nM is required to facilitate ADPR-induced TRPM2 channel activation (Starkus et al., 2007). In addition, it is suggested that intracellular Ca²⁺ on its own can activate the TRPM2 channel in a concentration-dependent manner, with an EC₅₀ value of 17 μM (McHugh et al., 2003; Starkus et al., 2007; Du et al., 2009). Ca²⁺-induced activation of the TRPM2 channel or facilitation of the TRPM2 channel activation by other agonists has been shown to result from calmodulin (CaM)-dependent interaction of Ca²⁺ and the TRPM2 channel via the N-terminal IQ-like CaM-binding motif (Du et al., 2009).

1.2.4.7 Temperature

Several studies support temperature dependence of the TRPM2 channel activation, but there is some discrepancy in terms of the temperature threshold and how temperature activates the TRPM2 channel. An early study reported that warm temperature ($>35^{\circ}\text{C}$) strongly synergises with ADPR, NAD and cADPR in activating the TRPM2 channel (Togashi et al., 2006). Further studies showed that heat and cADPR evoked the TRPM2 channel activity which is critical in mediating glucose-induced insulin secretion in pancreatic β cells (Togashi et al., 2006). Body temperature has been reported to enhance H_2O_2 -induced TRPM2 channel activation in microglial cells (Mortadza et al., 2017). However, recent studies report that body temperature can activate the TRPM2 channel in the absence of agonist (Tan and McNaughton, 2016; Song et al., 2016). The mechanism underlying temperature-dependent TRPM2 channel activation is still remain to be elucidated.

1.3 ROS-INDUCED ACTIVATION OF TRPM2 CHANNELS

1.3.1 Reactive oxygen species (ROS)

Molecular oxygen contains two unpaired electrons in its outer electron shell; this physiochemical property makes it readily available to generate a group of highly reactive chemicals called reactive oxygen species (ROS). These molecules can be categorized into two different groups; oxygen radical and oxygen non-radical molecules. Oxygen radicals, including superoxide (O_2^-), hydroxyl (OH^\cdot), peroxide ($\text{O}_2^{\cdot-2}$), alkoxyl (RO^\cdot) and peroxy (RO₂·), contain one or two free unpaired electrons, whereas non-radical oxygen molecules, such as hydrogen peroxide (H_2O_2), hypochlorous acid (HOCl), singlet oxygen (O_2) and ozone (O_3), have electrons in a pair. Another group of molecules called reactive nitrogen species (RNS), including nitric oxide (NO^\cdot), dinitrogen trioxide (N_2O_3), nitroxyl (HNO), peroxynitrite (ONOO⁻), and nitrous acid (HNO_2) have similar biologically reactive properties (Martinez and Andriantsitohaina, 2009).

Mitochondria and nicotine adenine dinucleotide phosphate (NADPH) oxidase (NOX) are the primary sources of ROS as discussed below. ROS generation also occurs in the ER, in which superoxide is produced as a result of electron leakage from cytochrome p450 reductase (Cross & Jones 1991). Other sources of ROS include the

peroxisome, xanthine oxidase, lipoxygenase and cyclooxygenase (Kamata and Hirata, 1999).

ROS is known to have roles in both physiological and pathological functions via the activation of intracellular signalling cascades (Allen and Tresini, 2000; Bedard and Krause, 2007). Under physiological conditions, ROS maintain cellular processes by mediating cytokine production, hormone secretion, neuromodulation and ion transportation. However, excessive ROS can result in an increase in the production of inflammatory mediators and induction of apoptotic gene expression, leading to inflammation and subsequent cell death and disease progression (Allen and Tresini, 2000; Bedard and Krause, 2007).

ROS impair or modify cellular functions mainly via oxidation of a number of molecules including lipids, protein, carbohydrates and DNA. For example, ROS, particularly OH[·], oxidizes fatty acids in the plasma membranes, leading to the production of aldehydes that causes the loss of structural integrity of the plasma membrane (Sohal et al., 2002; Radak et al., 2011). In addition, ROS interact with DNA bases, with guanine being most sensitive to ROS, leading to DNA damage (Hirano et al., 1996; Hirota et al., 2010). Furthermore, ROS are able to damage proteins by oxidizing amino acids, especially sulphur-containing amino acid, resulting in the loss of protein functions (Schieber and Chandel, 2014).

To counteract the overproduction of intracellular ROS, cells are equipped with various antioxidant defence mechanisms using enzymatic and non-enzymatic molecules, including superoxide dismutase (SOD), catalase, glutathione peroxidase (GPx), glutathione and thioredoxin (TRX). For example, SOD converts O₂^{·-} into H₂O₂ and water. Catalase, and GPx in conjunction with glutathione, convert H₂O₂ into water (Kamata and Hirata, 1999).

1.3.2 Mitochondrial ROS generation

Mitochondria have been recognized as the main source of ROS production, where ROS is generated as a by-product of the ATP synthesis metabolism. Studies using isolated mitochondria were the first to demonstrate the production of H₂O₂ within this organelle (Loschen et al., 1974; Boveris and Chance, 1973) and later studies verified that H₂O₂ was generated from O₂^{·-} (Loschen et al., 1974; Forman and Kennedy, 1974). These

findings were supported by the discovery of mitochondrial SOD (Weisiger and Fridovich, 1973). Energy metabolism processes occur in the mitochondria, depending on four complexes, complex I (NADH-ubiquinone oxidoreductase), complex II (succinate dehydrogenase (SDH)), complex III (cytochrome *c* reductase) and complex IV (cytochrome *c* oxidase) (Fig. 1.4). Complex I receives two electrons from the electron carrier, nicotinamide adenine dinucleotide (NADH), and transfers them to complex III and subsequently to complex IV by coenzyme Q (CoQ), also known as ubiquinone, and cytochrome *c*, respectively (Fig. 1.4). Each of these electron transfer processes is accompanied by translocation of one proton from the mitochondrial matrix into the intermembrane space. Additional electrons from a different carrier, flavin adenine dinucleotide (FAD), is delivered to CoQ involving complex II as the electron transporter (Fig. 1.4). However, unlike the complex I, III and IV, complex II does pump protons. Complex IV finally transfers electrons to oxygen, which reacts with protons to produce water.

The main sites of ROS production are complex I (Kudin et al., 2004) and complex III (Chen et al., 2003). Complex I is an intermembrane-bound multiprotein complex which is exposed to both matrix and intermembrane space (Fig 1.4). Studies have proposed that there are two mechanisms which attribute to ROS generation by complex I, conventional forward electron transport (FET) and reverse electron transport (RET), with RET contributing to a larger amount of superoxide production. FET-associated ROS production involves the normal process of mitochondrial electron transport chain, in which NADH sequentially passes electrons to different redox centres, including flavin mononucleotide (FMN), iron-sulphur (FeS) clusters and CoQ (Hirst et al., 2003; Sazanov, 2007) (Fig 1.4). The electron carriers are arranged in order of increasing redox potential. The process of electron transfer creates a membrane potential which produces energy for the movement of protons across the inner membrane to generate and maintain the proton motive force (Δp). However, several factors, such as Ca^{2+} overload and mitochondrial rupture as well as inhibitors like rotenone, can result in an imbalance of the membrane potential that inhibits electron transfer and increases the NADH/NAD^+ ratio to promote superoxide generation (Kalogeris et al., 2014; Kudin et al., 2004; Kussmaul and Hirst, 2006; Kushnareva et al., 2002). RET occurs when an electron is forced backwards from reduced coenzyme Q (CoQH_2) to NAD^+ instead of oxygen (Fig 1.4). Normally, the difference in the redox potential (ΔE) of the electron carriers in complex I has to be greater than the energy required to pump protons against the Δp . However, when the Δp is higher than the ΔE ,

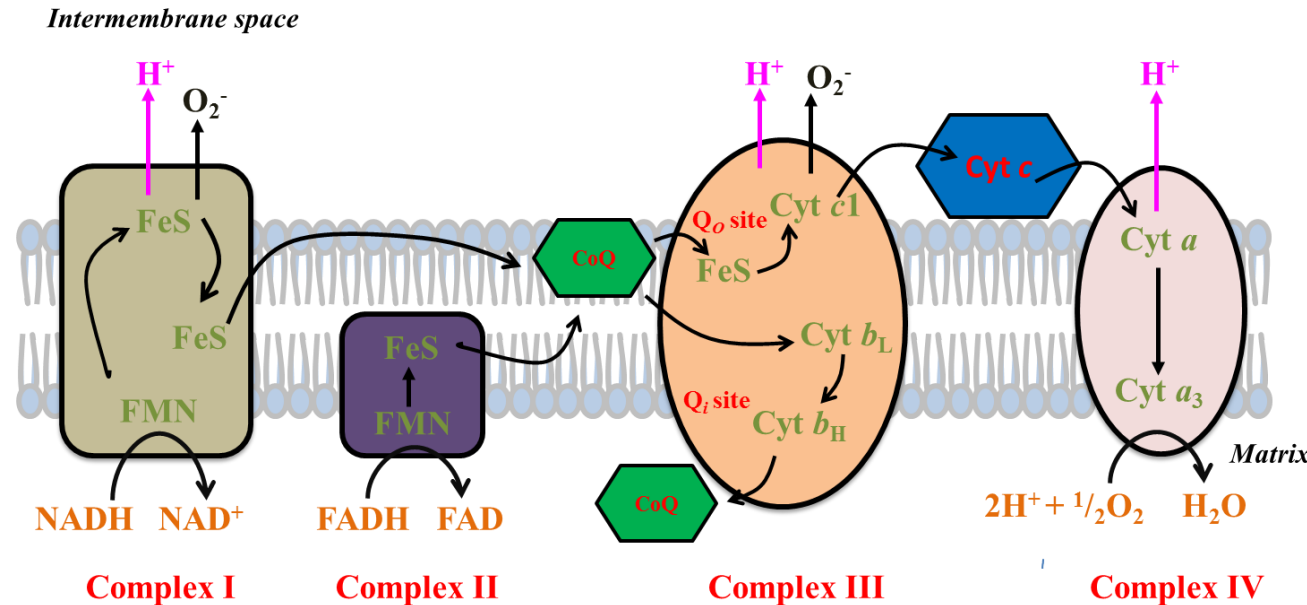


Fig. 1.4 Electron transfer and ROS generation in mitochondrial electron transport chain.

The mitochondrial electron transport chain (mETC) involves a series of redox reactions by transferring electrons (e^-) to and from different molecules, generating a transmembrane proton gradient. Complex I oxidizes nicotinamide adenine dinucleotide (NADH) and serially passes e^- to flavin mononucleotide (FMN), iron-sulphur (FeS) clusters and finally coenzyme Q (CoQ). Complex II transfers e^- from flavin adenine dinucleotide (FADH) to CoQ. Reduced CoQ ($CoQH_2$) act as the substrates of complex III in which it transfers its e^- to FeS cluster and subsequently to cytochrome c_1 (cyt c_1) in the Q_o redox centre. Cyt c accepts e^- from complex III and translocates it to complex IV, where oxygen acts as the final e^- acceptor and reacts with hydrogen to produce water. Each of the electron transfer processes occurs in complex I, III and IV is accompanied by a proton translocation from the matrix into the intermembrane space. Complex I can generate ROS from two different pathways which are forward electron transport (FET) and reverse electron transport (RET) processes. In FET, e^- are transferred as described above, however, the increase ratio of $NADH/NAD^+$ induced by mETC inhibitors can lead to ROS production. In RET, e^- is transferred against the redox membrane potential gradient, from CoQ to NAD^+ instead of oxygen, causing the accumulation of unstable CoQ^- . In complex III, ROS is generated in Q_i redox centre through the low reduction potential pathway, comprising cyt b_L and cyt b_H . This mechanism can also cause the accumulation of CoQ^- which is readily converted into superoxide, leading to the generation of ROS. Black lines with arrow resemble e^- transfer processes.

this can disrupt the membrane potential to cause electrons to flow backwards into complex I, where NAD⁺ is reduced to NADH (Turrens, 2003; Murphy, 2009; Chouchani et al., 2016). This process also leads to the accumulation of unstable CoQ[·], which are readily converted into superoxide.

Complex III is capable of generating a large amount of superoxide (Boveris et al., 1976; Turrens and Boveris, 1980; Grigolava et al., 1980). In complex III, electrons are transferred from CoQ to cytochrome *c* (cyt *c*), involving multiple redox reactions, which are collectively termed as ‘Q cycle’ (Cramer et al., 2011). Complex III contains two redox centres, ubiquinone-oxidation centre (Q_o site) and ubiquinone-reduction centre (Q_i site) (Fig. 1.4). The Q cycle begins with the oxidation of CoQH₂; in which the first electron in CoQH₂ is sequentially transferred to FeS, cyt *c1* and cyt *c*, leaving an unstable semi-ubiquinone (CoQ[·]) in the Q_o site. CoQ[·] transfers its remaining electron to another CoQ in the Q_i site, producing another CoQ[·] through the low reduction potential pathway that comprises of cyt *bL* and cyt *bH* (Osyczka et al., 2005; Zhang et al., 2007). In order to provide another electron and completely reduce the CoQ[·] in the Q_i site, the Q cycle is repeated (Bleier and Dröse, 2013). The superoxide production in complex III has been proposed to result from the CoQ[·] generated at the Q_o site (Turrens et al., 1985; Cape et al., 2007). The unstable CoQ[·] is converted into superoxide upon the loss of cyt *c* or imbalance in the mitochondrial redox homeostasis (Murphy, 2009). There are three specific inhibitors of complex III, antimycin A, myxothiazol and stigmatellin. Antimycin A suppresses the delivery of the second electron to the Q_i site and therefore causes the accumulation of unstable CoQ[·]. Myxothiazol prevents the binding of CoQH₂ at the Q_o site. Finally, stigmatellin inhibits the transfer of the first electron to FeS. Studies using these inhibitors have provided evidence to suggest that complex III acts as the source of ROS production (Crofts et al., 1999; Turrens, 2003; Konstantinov et al., 1987; Korshunov et al., 1997; Raha and Robinson, 2000; Starkov and Fiskum, 2001).

In addition to complex 1 and complex III discussed above, complex II (Rustin and Rötig, 2002; Miwa et al., 2003), α-ketoglutarate dehydrogenase complex (Starkov et al., 2004; Chinta et al., 2009), succinate dehydrogenase (McLennan and Degli Esposti, 2000) and monoamine oxidases (Kudin et al., 2004; Maurel et al., 2003; Kumar et al., 2003), albeit to a lesser extent, can contribute in generating ROS.

1.3.3 NOX-mediated ROS generation

NOX is a multi-subunit enzyme that transfers electrons across the plasma membrane to produce superoxide through the oxidation of NADPH to NADP and proton H⁺ (Fig 1.5). Unlike other sources, NOX does not produce ROS as a by-product, but ROS generation is its primary function. Respiratory burst in phagocytes results in the increase of H₂O₂ production, which was the first evidence leading to the discovery of the NOX protein (Iyer et al., 1961; Someya et al., 1999; Mander and Brown, 2005). Later studies identified NADPH to be the primary substrate and superoxide the initial product in the oxidative-burst generating enzyme system, referring to the NOX enzyme system (Rossi and Zatti, 1964; Babior et al., 1973).

Six NOX2 homologues have been identified, including NOX1, NOX3, NOX4, NOX5, DUOX1 and DUOX2 (Suh et al., 1999; Cheng et al., 2001; Geiszt and Leto, 2004; Shiose et al., 2001; Cheng et al., 2001; Banfi et al., 2001; De Deken et al., 2002; Dupuy et al., 1999). All NOX proteins are closely related with highly conserved structural features, as illustrated for NOX2 (gp91^{phox}) in Fig 1.5A, comprising six transmembrane segments (I-VI), four haeme binding sites with two sites located in the third and the fifth transmembrane segments, a flavin adenine dinucleotide (FAD)-binding site in the proximal C-terminus, and an NADPH binding site in the distal C-terminus (Cheng et al., 2001). However, NOX5, DUOX1 and DUOX2 are distinguished from NOX1-NOX4 in that NOX5 has a long intracellular N-terminus carrying an Ca²⁺-binding EF-hand domain, whereas DUOX1 and DUOX2 consist of an EF-hand domain and additional or seventh transmembrane domain at the N-terminus (Banfi et al., 2001; De Deken et al., 2002).

NOXs are reported to be activated by a broad spectrum of stimuli or activators, including inflammatory mediators such as tumour necrosis factor alpha (TNF- α) and interleukin 1-beta (IL-1 β) (Kamizato et al., 2009; Li et al., 2005), heavy metals such as lead, zinc and cadmium (Ni et al., 2004; Yeh et al., 2007; Pourrut et al., 2008), organic solvents such as ethyl and butyl alcohol (Hasegawa et al., 2002), ionising radiation (Tateishi et al., 2008), acidic pH (Abramov et al., 2005) and osmotic pressure (Martins et al., 2008). The activation mechanism of NOX1-NOX3 is similar, involving complex formation with the cytosolic regulatory subunits, as shown in Fig. 1.5. NOX4 has been proposed to be constitutively active (Ellmark et al., 2005). NOX5, DUOX1 and DUOX2 are distinct from other NOX in that they are activated by Ca²⁺ instead of by complex formation with the cytosolic subunits (Banfi et al., 2001; Cheng et al., 2001).

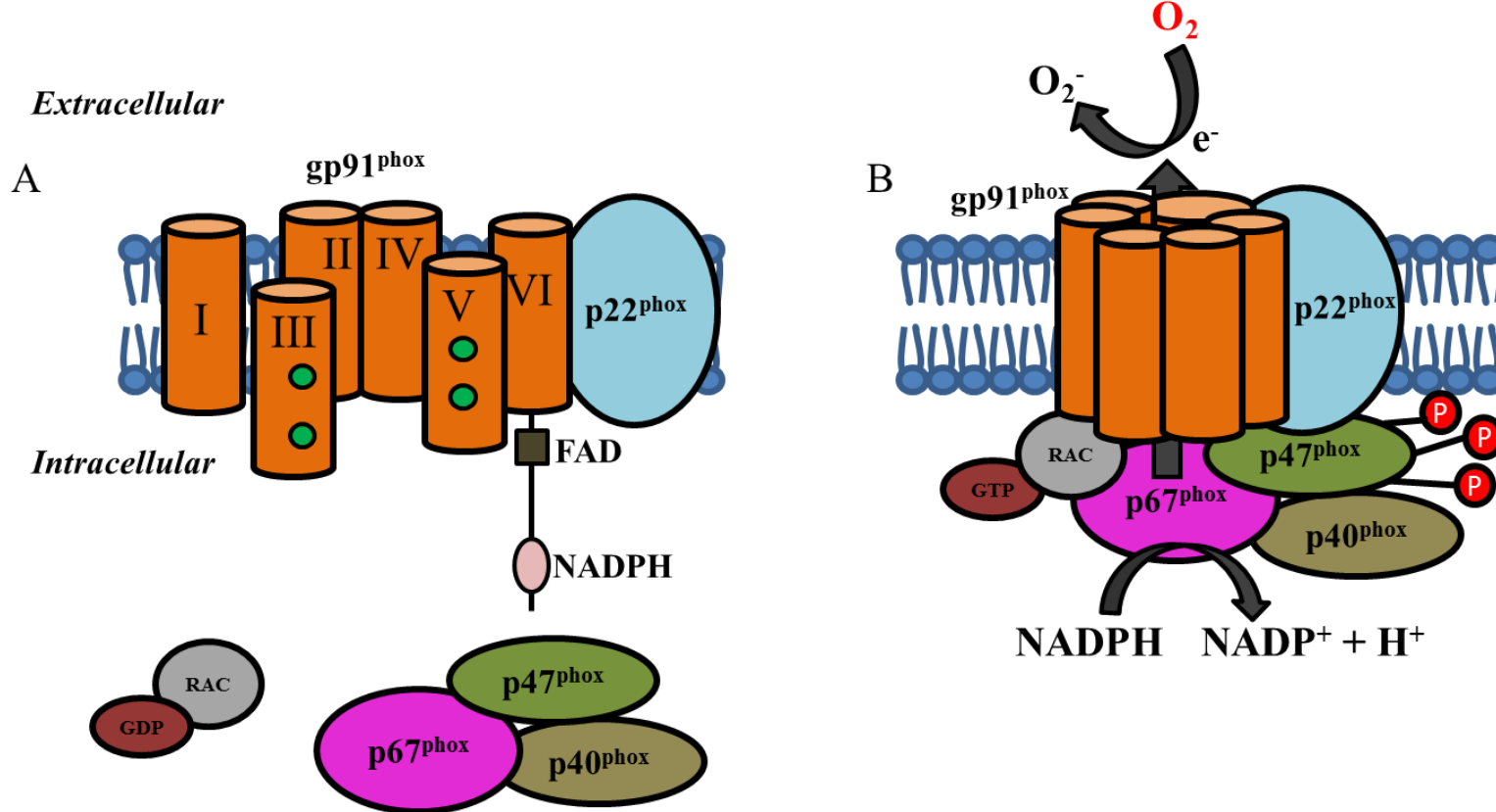


Fig. 1.5 NADPH oxidase activation.

The gp91^{phox} and p22^{phox} subunits are primarily localised at the plasma membrane and are separated from the cytosolic subunits, p47^{phox}-p67^{phox}-p40^{phox} trimeric complex and RAC in the resting condition (A). Upon activation (B), p47^{phox} is phosphorylated, leading to conformational changes that promote the translocation of p47^{phox}-p67^{phox}-p40^{phox} to p22^{phox}. GDP on RAC is changed into GTP, causing the activation of the RAC protein. GTP-bound RAC allows its interaction with gp91^{phox} and subsequently with p67^{phox}. Once assembled, the complex is activated and can transfer electrons from NADPH in the cytosol to oxygen in the extracellular space. The small green dots in panel A represent the haeme groups.

NOX2 is the prototype NOX that has been subjected to extensive investigation. Therefore, the activation mechanisms of NOX2 are best understood. NOX2 is composed of membrane-bound and cytosolic subunits, and the activation of NOX2 occurs through a complex series of protein-proteins interactions (Fig. 1.5). The membrane-bound subunits, gp91^{phox} and p22^{phox}, constitute the main catalytic domain of the enzyme. These subunits form heterodimeric flavocytochrome *b*₅₅₈ (cyt *b*₅₅₈), which enables electron transfer across the plasma membrane (Segal et al., 1992). FAD and haeme groups of the gp91^{phox} subunit play a role as intermediate electron carriers (Sheppard et al., 2005). The cytosolic subunits, including p47^{phox}, p67^{phox} and p40^{phox}, and the small protein Rac GTPase are required for the full NOX2 activation (Sheppard et al., 2005). In a resting state, p47^{phox}, p67^{phox} and p40^{phox} subunits form a trimeric complex in auto-inhibitory conformation. Amongst all of the cytosolic subunits, p47^{phox} has the most crucial role as it controls and facilitates the translocation of the cytosolic trimeric complex to the plasma membrane and accurately positions the complex with respect to the cyt *b*₅₅₈. In response to stimuli, p47^{phox} is phosphorylated, resulting in conformational changes in the p47^{phox}-p67^{phox}-p40^{phox} trimeric complex and subsequent localisation of the complex to the plasma membrane. The interactions between cytosolic and membrane domains are mediated by the Src homology 3 (SH3) domains of p47^{phox} and the cytoplasmic tail of p22^{phox} (Shiose and Sumimoto, 2000; de Mendez et al., 1997; Leto et al., 1994). Once at the membrane, p47^{phox} facilitates positioning p67^{phox} and further induces the conformational changes in the complex allowing interaction of p67^{phox} with gp91^{phox} (DeLeo et al., 1995; Paclet et al., 2000). GDP-bound Rac, upon phosphorylation, is converted into GTP-bound Rac, promoting its interaction with gp91^{phox} and subsequently with p67^{phox} (Diebold and Bokoch, 2001; Koga et al., 1999; Lapouge et al., 2000). Once assembled, the NOX2 enzyme is activated and able to transfer electrons from NADPH in the cytosol to oxygen bound to gp91^{phox} in the extracellular space (Nisimoto et al., 1999; Cross and Segal, 2004).

The activation of NOX is regulated by multiple signalling mechanisms, including protein phosphorylation, lipid-protein interaction, and Ca²⁺-binding mechanisms. All NOX subunits, particularly p47^{phox}, are phosphorylated during the activation process. It is proposed that protein kinase C (PKC) phosphorylates p47^{phox}, and such a mechanism is required for the translocation of the cytosolic p47^{phox}-p67^{phox}-p40^{phox} trimeric complex to the plasma membrane (El-Benna et al., 2005; El-Benna et al., 2009). There is also evidence to suggest that PKC is able to phosphorylate gp91^{phox}.

and p22^{phox}, facilitating the interaction of these proteins with p47^{phox} at the plasma membrane (Raad et al., 2009; Lewis et al., 2010). In addition to PKC, p-38 mitogen-activated protein kinase (MAPK)(El Benna, Han, et al., 1996; El Benna, Faust, et al., 1996; Dewas et al., 2000), p21-activated kinase (PAK) (Knaus et al., 1995), and protein B/AKT (Hoyal et al., 2003) have been reported to phosphorylate the 47^{phox} protein. Studies also have shown that p47^{phox} and p40^{phox} proteins interact with membrane phospholipids through their lipids-binding sites, facilitating interactions between the cytosolic and membrane subunits (Ago et al., 2001; Karathanassis et al., 2002; Zhan et al., 2002; Stahelin et al., 2003). Furthermore, Ca²⁺ binding to NOX5 is important in facilitating the interaction of the N- and C-termini of gp91^{phox}, leading to NOX5 activation (Banfi et al., 2004). Conversely, Ca²⁺ has been demonstrated to inhibit DUOX1 and DUOX2 (Wong et al., 2004; Song et al., 2007).

NOXs play diverse functions depending on the cell types expressing them. NOX, particularly NOX2, plays a crucial role in the respiratory burst of phagocytes which is critical in host defence (Babior, 2000). Additionally, NOX1 is highly expressed in epithelial cells and implicated in cell migration and proliferation (Banfi et al., 2003; Suh et al., 1999; Szanto et al., 2005). NOX3 has been documented to be expressed in splenocytes and endothelial cells and is important in determining cell viability (Kikuchi et al., 2000; Banfi et al., 2004; Cheng et al., 2001). NOX4 is highly expressed in vascular smooth muscle cells and plays a role in focal adhesion and cell contraction (Hilenski et al., 2004). NOX5 is present in sperm cells and smooth muscle cells and is involved in cell migration and proliferation (Banfi et al., 2001; Jay et al., 2008). DUOX1 and DUOX2 are expressed in fibroblast cells, where they are critical in host defence mechanisms (Katsuyama, 2010). NOX1, NOX2 and NOX4 have also been reported to be expressed in microglial cells, astrocytes and neurons in the CNS. NOX1 and NOX2 are known to play critical roles in oxidative stress-induced pro-inflammatory cytokine production (Infanger et al., 2006; Cheret et al., 2008), whereas NOX4 has been implicated in glutamate-induced neuronal toxicity (Ha et al., 2010; Harrigan et al., 2008; Ambasta et al., 2004).

Several NOX inhibitors have been identified, with some exhibiting specificity. Table 1.1 lists the common NOX inhibitors and their respective concentrations evoking 50% inhibition (IC_{50}). These include generic diphenyleneiodonium (DPI) and apocynin, NOX1/4-specific GKT 137831, and NOX2-specific Phox-I2 which are used in my studies.

Table 1.1 NOX inhibitors and their specificity, mode of action and potency (IC₅₀).

Inhibitors	NOX	Mode of inhibition	IC ₅₀ (μM)	Reference
DPI	Generic	Removing an electron from the electron transporter	0.003-1	Ellmark et al., 2005; Stuehr et al., 1991; Stolk et al., 1994
Apocynin	Generic	Inhibiting complex assembly	10	O'Donnell et al., 1993; Unger and Patil, 2009; Ahmad et al., 2010; Castor et al., 2010
GKT 137831	NOX1/4	Scavenging ROS	0.1-0.15	Suh et al., 2007; Gray et al., 2013; Zhao et al., 2015
VAS3947	NOX1/2/4	Inhibiting complex assembly	1-13	Wind, Beuerlein, Armitage, et al., 2010
VAS2870	NOX2/4/5	Inhibiting complex assembly	1-10	Niethammer et al., 2009; Stielow et al., 2006; Wind, Beuerlein, Eucker, et al., 2010
AEBSF	Generic	Disrupting the association of p47 ^{phox} subunit to the plasma membrane	300-1000	Citron et al., 1996; Nakabo and Pabst, 1996; Diatchuk et al., 1997
Phox-I2	NOX2	Disrupting GTPRAC binding to p67 ^{phox} subunit at the plasma membrane	1-6	Bosco et al., 2012
ML171	NOX1	Scavenging ROS	0.1-5	Gianni et al., 2010

Abbreviations: DPI; diphenyleneiodonium; AEBSF, benzo-sulphonyl fluoride; ML171, 2-acetylphenothiazine

1.3.4 TRPM2 channel activation by ROS

TRPM2 channels are activated by ROS and thus act as a molecular sensor for oxidative stress (Wehage et al., 2002; Hara et al., 2002; Kraft et al., 2004; Kolisek et al., 2005; Buelow et al., 2008; Kashio et al., 2012; Zhong et al., 2013). However, the mechanisms of TRPM2 channel activation by H₂O₂ remain controversial and not fully understood. An early study showed that the TRPM2-ΔC isoform, with a C-terminal deletion in the NUDT9-H domain, is sensitive to activation by H₂O₂ but not ADPR, indicating H₂O₂ can activate the TRPM2 channel independently of ADPR (Wehage et al., 2002). However, this finding was not confirmed in a subsequent study (Kuhn and Luckhoff, 2004). In addition, H₂O₂-induced TRPM2 channel activation kinetics is slow, suggesting that H₂O₂ does not activate the TRPM2 channel directly. Indeed, accumulating evidence shows that TRPM2 channel activation by H₂O₂ is dependent on ADPR generation.

As discussed above, several signalling pathways generate ADPR, including ROS-induced activation of poly (ADPR) polymerase-1 (PARP-1) in the DNA damage repair process (Fonfria et al., 2004; Buelow et al., 2008; Zou et al., 2013). Studies have shown that PARP inhibitors, including SB750139-B, (*N*-(6-oxo-5,6-dihydrophenanthridin-2-yl)-*N,N*-dimethylacetamide) (PJ34) and 3, 4-dihydro-5-[4-(1-piperidinyl)butoxy]-1(2H)-isoquinolinone (DPQ), are effective in inhibiting H₂O₂-induced TRPM2 channel activation (Fonfria et al., 2004; Zou et al., 2013). H₂O₂-induced TRPM2 channel-dependent Ca²⁺ and current responses were not observed in DT40 B lymphocytes deficient in PARP expression (Buelow et al., 2008). These findings strongly suggest that H₂O₂ induces TRPM2 channel activation primarily via PARP, particularly PARP-1. In the nucleus, PARP-1 and poly (ADPR) glycohydrolases (PARG) play a critical role in repairing DNA damage in response to oxidative stress. PARP-1 binds to the damaged DNA and catalyses NAD⁺ hydrolysis, leading to the production of poly-ADPR (PAR). Once the repair is completed, PAR is degraded by PARG into ADPR. There is evidence to suggest that ADPR is generated by PARP/PARG enzymes in response to the DNA damage triggered by H₂O₂ (Caiafa et al., 2009; Fauzee et al., 2010). PARP activation has also been shown to be important in the TRPM2 channel activation induced by Aβ₄₂ and TNF-α (Hara et al., 2002; Fonfria et al., 2005; W. Zhang et al., 2006). In a separate study, overexpression of the cytosolic NUDT9-H domain ablated H₂O₂-induced TRPM2 channel activation and more ADPR was required to induce TRPM2 channel activation (Perraud et al., 2005). Furthermore,

specific overexpression of the NUDT9-H domain in mitochondria inhibited the ability of H₂O₂, but not ADPR, to induce TRPM2 channel activation. These results lead to the notion that mitochondrial ADPR production is also involved in H₂O₂-induced TRPM2 channel activation (Perraud et al., 2005). Collectively, these studies suggest that H₂O₂-induced TRPM2 channel activation depends primarily on ADPR-generating mechanisms in nucleus or in mitochondria.

1.4 TRPM2 CHANNEL INHIBITORS

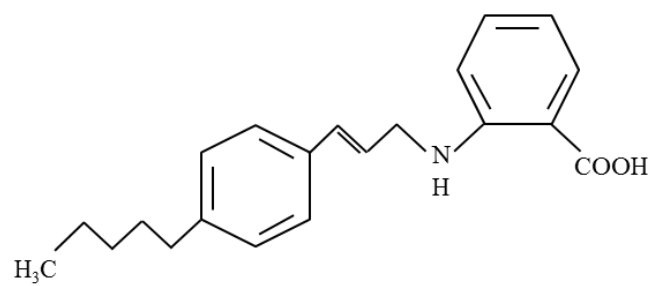
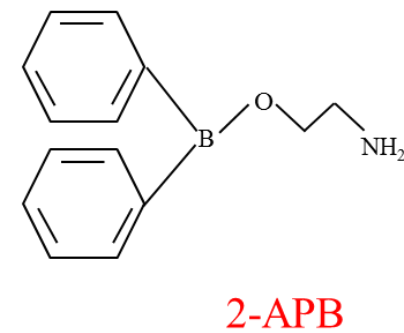
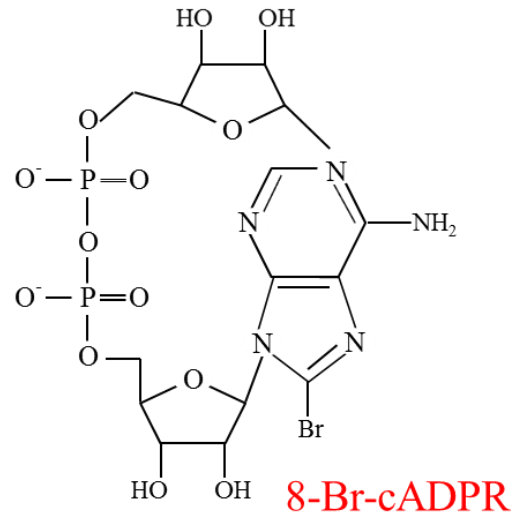
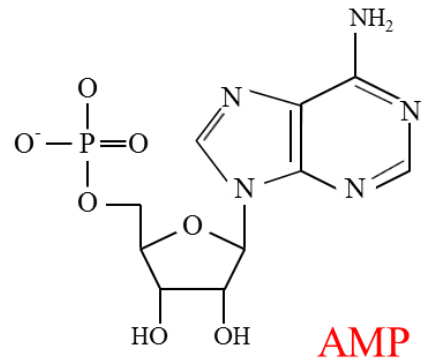
Several structurally different inhibitors that block the TRPM2 channel have been identified over the past few years. These inhibitors include AMP, 8-Br-cADPR, 2-APB, N-(p-amylcinnamoyl) anthranilic acid (ACA), flufenamic acid (FFA), azole compounds and curcumin. However, not all of them are TRPM2-specific as they can inhibit other proteins including ion channels. Potent and selective TRPM2 channel inhibitors are extremely useful in the study of the physiological and pathological functions of TRPM2 channels, particularly the human TRPM2 channel. The structures of the TRPM2 channel inhibitors described in this section are shown in Figure 1.6.

1.4.1 AMP

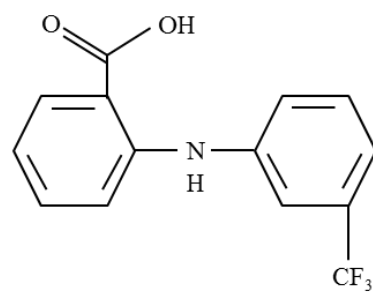
As mentioned above, AMP is a metabolite of ADPR (Perraud et al., 2001; Shen et al., 2003) (Fig. 1.6). AMP inhibits ADPR-induced recombinant TRPM2 channel activation with an IC₅₀ value of approximately 76 μM (Kolisek et al., 2005). AMP is also able to antagonise the activation of the endogenously expressed TRPM2 channels by ADPR (Lange et al., 2008). A previous study using a binding assay suggested that AMP inhibits the TRPM2 channel by binding to the ADPR-binding site in the NUDT9-H domain, with a relatively lower binding affinity than ADPR (Grubisha et al., 2006).

1.4.2 8-Br-cADPR

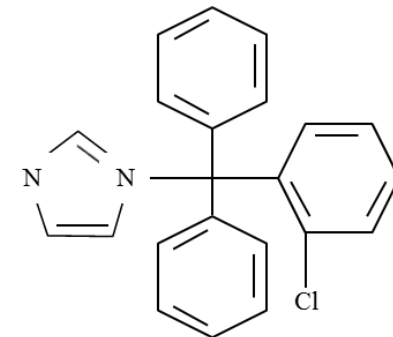
8-Br-cADPR at concentrations >100 μM can inhibit or delay the TRPM2 channel activation by NAD, cADPR, NAADP and H₂O₂ (Kolisek et al., 2005; Beck et al., 2006; Lange et al., 2008). Interestingly, 8-Br-cADPR shows a synergy with ADPR, increasing the sensitivity of the TRPM2 channel to ADPR (Kolisek et al., 2005). These findings suggest that 8-Br-cADPR to have a dual mode of action.



ACA



FFA



Clotrimazole

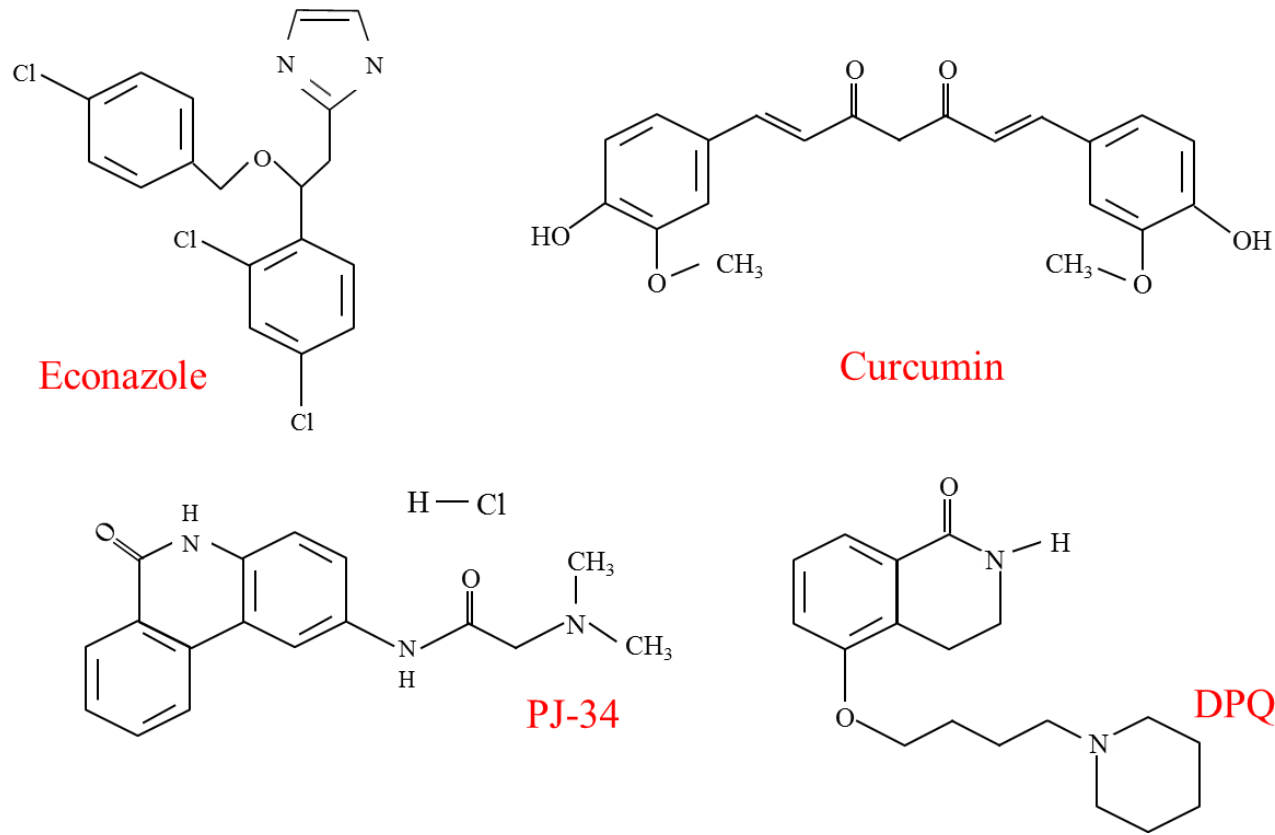


Fig. 1.6 TRPM2 channel and PARP inhibitors.

Diagrams showing the chemical structures of compounds that are known to inhibit the TRPM2 channel activity or ROS-induced TRPM2 channel activation via inhibiting PARP (PJ34 and DPQ).

1.4.3 2-APB

2-APB was initially identified as a membrane-permeable IP₃R inhibitor (Hagenston et al., 2009). It is now known that 2-APB can inhibit a wide range of ion channels, including TRPM2, TRPC5, TRPM7 and TRPM8 (Chung et al., 2004; Hu et al., 2004; Hill, McNulty, et al., 2004; Xu et al., 2005; Togashi et al., 2008; Zholos, 2010). 2-APB inhibits ADPR-induced activation of the TRPM2 channel expressed in various cell types (Ishii, Shimizu, Hagiwara, et al., 2006; Togashi et al., 2008; Naziroglu et al., 2011; Zou et al., 2013; Kashio et al., 2012; Chen et al., 2012). 2-APB blocks the TRPM2 channel more potently than other ion channels, with an IC₅₀ value of 1.2 µM (Togashi et al., 2008). The inhibition is reversible and voltage-independent (Togashi et al., 2008). There is evidence to suggest that 2-APB inhibits the TRPM2 channel extracellularly (Togashi et al., 2008). 2-APB has been used to show the role of the TRPM2 channel in mediating ROS-induced cell death, glucose-induced insulin secretion, and oxidative stress-induced production of proinflammatory cytokines (Zou et al., 2013; Togashi et al., 2008; Naziroglu et al., 2011).

1.4.4 ACA

ACA was known as an inhibitor of phospholipase A₂ (Konrad et al., 1992; Harteneck et al., 2007). This compound inhibits ADPR- and H₂O₂-induced TRPM2 channel activation, with an IC₅₀ value of approximately 1.7 µM (Kraft et al., 2006; Bari et al., 2009; Olah et al., 2009). ACA is also capable of blocking the TRPM2 channel currents evoked by cADPR and heat (Togashi et al., 2008).

1.4.5 FFA

FFA is derived from N-phenyl-substituted anthranilic acid and was initially identified as a non-steroidal anti-inflammatory drug. FFA can inhibit the TRPM2 channel, with an IC₅₀ value of 155 µM (Hill, Benham, et al., 2004; Kraft et al., 2006; Naziroglu et al., 2007; Guinamard et al., 2013; Klose et al., 2011; Olah et al., 2009; Naziroglu et al., 2011). FFA can only inhibit the TRPM2 channel when it is in the open state (Hill, Benham, et al., 2004).

FFA has had its structure modified in order to develop potent and specific TRPM2 channel inhibitors. 2-(3-methylphenyl) aminobenzoic acid (3-MFA) is a structural analogue of FFA produced by substituting the trifluoromethyl (3-CF₃) group (Fig 1.6) with meta-methyl (3-CH₃). 3-MFA has a higher selectivity towards, and

greater potency in inhibiting, the TRPM2 channel, with IC₅₀ value of 76 µM (Chen et al., 2012).

1.4.6 Azoles

Azole compounds, which include clotrimazole and econazole, are known as antifungal drugs. Clotrimazole and econazole inhibit TRPM2 channels at concentrations of 3-30 µM (Hill, McNulty, et al., 2004; Togashi et al., 2008; Chen et al., 2012). This inhibition is concentration-dependent (Hill, McNulty, et al., 2004). Similarly to FFA, clotrimazole and econazole only block TRPM2 in the open state (Hill, McNulty, et al., 2004). The mechanisms of inhibition are still not well-defined.

1.4.7 Curcumin

Curcumin ((1E,6E)-1,7-bis(4-hydroxy-3-methoxyphenyl)-1,6-heptadiene-3,5-dione) is a polyphenol, the main curcuminoid of turmeric (*Curcuma longa*), and has been used as a traditional remedy for oxidative stress-induced liver damage (Esatbeyoglu et al., 2012). Recently, curcumin has been shown to be effective in suppressing ADPR-induced TRPM2 channel activation with an IC₅₀ of approximately 50 nM (Kheradpezhouh et al., 2016).

1.4.8 PARP inhibitors

As discussed above, activation of PARP, particularly PARP-1 in the nucleus, results in ROS-induced TRPM2 channel activation via ADPR production. Several PARP inhibitors, including PJ34, DPQ, SB750139-B (Lubisch et al., 2001) and 3-aminobenzamide (3-AB), have been shown to inhibit H₂O₂-induced TRPM2 channel activation, with IC₅₀ values of approximately 7.5 µM, 6.7 µM and 4.8 µM, for PJ34, DPQ and SB750139-B, respectively (Fonfria et al., 2004). However, PJ34, DPQ and SB750139-B show no inhibition of ADPR-evoked TRPM2 channel activation (Fonfria et al., 2004).

1.5 EXPRESSION OF TRPM2 CHANNELS

TRPM2 is expressed in various tissues, including the brain, heart, kidney, liver, lung, pituitary, stomach, intestine, bone marrow, placenta, adipose, pancreas and spleen (Ishii, Shimizu, Hara, et al., 2006; Ishii, Shimizu, Hagiwara, et al., 2006; Togashi et al., 2006; Lange et al., 2009; Uchida and Tominaga, 2011; Fonfria et al., 2005). As summarised in Table 1.2, the TRPM2 channel has been documented in a variety of cell

types and plays a role in diverse physiological and pathological processes as discussed in the following sections.

The TRPM2 channel is found on the cell surface in the majority of cell types examined, except for dendritic cells and pancreatic β -cells. In dendritic cells, the TRPM2 channel is exclusively located in the membranes of lysosomes and functions as an intracellular Ca^{2+} -release channel (Sumoza-Toledo et al., 2011). In pancreatic β -cells, the TRPM2 channel is present in both the plasma and lysosomal membranes (Lange et al., 2009). The expression of the TRPM2 in different cell types is listed in Table 1.2 with the channel major functional roles, which are discussed in the next sections (sections 1.6 and 1.7).

1.6 PHYSIOLOGICAL ROLES OF TRPM2 CHANNELS

Extensive research efforts over the past few years have revealed important roles for the TRPM2 channel in multiple physiological functions, including the production of cytokines from immune cells, glucose-stimulated insulin secretion from pancreatic β -cells, antitumor activity, cell maturation and chemotaxis, and protection against ischemia-induced heart damage (Table 1.2). In addition to the pharmacological tools, the transgenic TRPM2 deficient or TRPM2-KO mice has been effectively utilised in numerous studies to provide evidence for the involvement of the TRPM2 channel in physiological as well as pathological states. The TRPM2-KO mice express mutated alleles without exons 17 and 18 of the *trpm2* gene (Zou et al. 2013). The remaining sequence of the TRPM2-KO gene, however, can form an open reading frame that encodes an internally deleted TRPM2 protein lacking the $\text{Leu}^{843}\text{-Met}^{931}$, resulting in no expression of functional TRPM2 channel. The TRPM2-KO mice showed no difference in terms of their phenotype compared with the WT mice and therefore, are valuable to evolve a full understanding of the TRPM2 channel roles.

1.6.1 Generation of IL-1 β and IL-1 α

The immune system recognises diverse pathogen-associated molecular patterns (PAMPs) molecules derived from microorganisms and bacteria, by expressing the pattern recognition receptor (PRR) on the immune cell surface. Immune cells also express PRRs for danger-associated molecular patterns (DAMPs) molecules, such as Zn^{2+} , $\text{A}\beta$, TNF- α , and ATP released by injured or dying cells as ‘danger signals’. The innate immune response represents the first line of cellular defence against PAMPs and DAMPs. Such responses are supposed to eliminate the PAMPs or DAMPs to heal

Table 1.2 A summary of the major functional roles of the TRPM2 channel expression in different cell types.

Cell type	Associated cell functions	References
Macrophage	<ul style="list-style-type: none"> Activation of the NLRP3 inflammasome and IL-1β maturation in response to charged lipids, silica and alum <i>in vitro</i> Zymosan-induced production of CXCL2, G-CSF and IL-1α <i>in vitro</i> Up-regulated HO-1 expression induced by LPS <i>in vitro</i> and CLP <i>in vivo</i> H₂O₂-induced cell death <i>in vitro</i> Ischemia brain-induced cell migration into ischemic brain tissues Production of CXCL2 and NO in response to carrageenan-induced inflammation or nerve injury <i>in vivo</i> 	Zhong et al., 2013 Kashio et al., 2012 Qian et al., 2014 Zou et al., 2013 Gelderblom et al., 2014 Haraguchi et al., 2012
Monocyte	<ul style="list-style-type: none"> LPS-induced production of IL-6, IL-8, IL-10 and TNF-α <i>in vitro</i> TNF-α-induced cell death Production of CXCL2/CXCL8 induced by H₂O₂ <i>in vitro</i> and CXCL2 <i>in vitro</i> in response to dextran sodium sulphate-induced colon inflammation 	Wehrhahn et al., 2010 W. Zhang et al., 2006 Yamamoto et al., 2008
Neutrophil	<ul style="list-style-type: none"> Sulphur mustard-induced priming and production of IL-6, IL-8 and TNF-α <i>in vitro</i> Ischemia brain-induced migration into ischemic brain tissues 	Ham et al., 2012 Gelderblom et al., 2014
Spleenocyte	<ul style="list-style-type: none"> Production of IL-12 and IFNγ in response to <i>Listeria monocytogenes</i> (<i>Lm</i>)-induced infection 	Knowles et al., 2011
Dendritic cell	<ul style="list-style-type: none"> Production of IL-12 in response to <i>Lm</i>-induced infection Chemokine-induced cell maturation and migration <i>in vitro</i> and chemotaxis to <i>E. coli</i>-induced infection <i>in vivo</i> 	Knowles et al., 2011 Sumoza-Toledo et al., 2011
Microglial cell	<ul style="list-style-type: none"> Production of CXCL2 in response to nerve injury <i>in vitro</i> and in response to LPS/IFN-γ <i>in vitro</i> LPS/IFN-γ-induced release of NO <i>in vitro</i> Microglial cell activation in the APP/PS1 AD mouse brain 	Haraguchi et al., 2012 Miyake et al., 2014 Ostapchenko et al., 2015

Pancreatic β cell	<ul style="list-style-type: none"> Temperature-dependent insulin secretion <i>in vitro</i> Glucose-induced insulin secretion <i>in vitro</i> 	Kashio and Tominaga, 2015 Uchida and Tominaga, 2011
Cardiomyocyte	<ul style="list-style-type: none"> Increase the expression of HIF-1α, FOXOs and SODs H_2O_2-induced cell death <i>in vitro</i> Contractility dysfunction following I/R injury <i>in vivo</i> 	Miller et al., 2013 Yang et al., 2006 Hiroi et al., 2013
Neurons	<ul style="list-style-type: none"> Aβ-induced cell death striatal neurons <i>in vitro</i> Aβ-induced endothelial and neurovascular dysfunctions H_2O_2-induced death of the DA neurons <i>in vitro</i> Burst firing induced in GABAergic neurons Transient ischemia-induced infarction and neurological deficits <i>in vivo</i> 	Fonfria et al., 2005 Park et al., 2014 Sun et al., 2016 Lee et al., 2013 Alim et al., 2013; Ye et al., 2014
Hepatocyte	<ul style="list-style-type: none"> H_2O_2- and acetaminophen-induced Ca^{2+} influx <i>in vitro</i> and acetaminophen overdosing-induced liver injury <i>in vivo</i> 	Kheradpezhoh et al., 2014
Endothelial cells	<ul style="list-style-type: none"> H_2O_2-induced endothelial barrier dysfunction 	Hecquet et al., 2008
Cancer cells	<ul style="list-style-type: none"> Prostate cancer cell proliferation <i>in vitro</i> H_2O_2-induced prostate cancer cell migration <i>in vitro</i> H_2O_2-induced squamous cancer cell migration and viability <i>in vitro</i> 	Zeng et al., 2010 Li et al., 2016 Zhao et al., 2016

Abbreviations: CXCL, C-X-C ligand; LPS, lipopolysaccharide; ROS, reactive oxygen species; NADPH oxidase, nicotinamide adenine dinucleotide phosphate oxidase; IFN γ , interferon γ ; IL, interleukin; TNF- α , tumour necrosis factor- α ; G-CSF, granulocyte colony stimulating factor; HO-1, hem oxygenase-1; CLP, cecal ligation and puncture; NO, nitric oxide; HIF-1 α , hypoxia-inducible factors; FOXOs, forkhead box transcription factors; SODs, superoxide dismutase; DA, dopamine; GABAergic, gamma-aminobutyric acid-containing neurons; I/R, ischemia/reperfusion.

injuries but, when they are not resolved in time and become prolonged or persistent, can lead to several diseases such as Alzheimer's disease (AD) (Frederickson et al., 2005; Kauppinen et al., 2011), Parkinson's disease (PD) (Tanaka et al., 2006) and ischemia-induced brain injury (Clausen et al., 2008).

IL-1 β is a key inflammatory cytokine that is generated in response to PAMPs and DAMPs. The generation of the leaderless IL-1 β by immune cells commonly requires two signals, termed the priming and activation signals. The priming signal activates a Toll-like receptor (TLR) such as TLR4 by lipopolysaccharide (LPS) or other receptors to stimulate signalling mechanisms leading to the production of biologically inactive pro-IL-1 β . The activation signal, on the other hand, activates the nucleotide binding domain 3-leucine-rich repeat (NLRP3) inflammasome, which is critical in converting pro-IL-1 β into biologically active IL-1 β . The NLRP3 inflammasome is a multiple-protein complex composed of the NLRP3 receptor, apoptosis-associated speck-like protein containing a CARD domain (ASC), and pro-caspase-1 cysteine protease. The NLRP3 receptor is predominantly expressed in immune cells, such as microglial cells, macrophages and lymphocytes. Upon sensing PAMPs or DAMPs, the NLRP3 receptor interacts with ASC and pro-caspase-1 to assemble the NLRP3 inflammasome complex. NLRP3 inflammasome activation induces proteolytic cleavage of pro-caspase-1 to generate active caspase-1, which in turn converts pro-IL-1 β to IL-1 β .

Recent studies have discovered that production of ROS is required for the activation of the NLRP3 inflammasome by structurally diverse activators (Bauer et al., 2010; Cruz et al., 2007; Dostert et al., 2008). The mechanisms by which ROS activates the NLRP3 inflammasome are still a matter of extensive investigation. There is evidence to suggest that ROS generation occurs upstream of the NLRP3 inflammasome activation (Cassel et al., 2008). In a recent study, Zhong *et al.* examined the role of the TRPM2 channel in NLRP3 inflammasome activation and the maturation of IL-1 β in macrophage cells treated with crystals such as silica, alum or charged lipids (Zhong et al., 2013). This study demonstrated that the IL-1 β secretion in response to the treatment with silica, alum or charged lipids was significantly reduced in the TRPM2-KO macrophage cells. Furthermore, the removal of the extracellular Ca²⁺ from the culture media significantly impaired the aforementioned particulate-induced IL-1 β release in macrophage cells, suggesting the critical role for the TRPM2 channel-mediated Ca²⁺ influx in IL-1 β release. In addition, the deficiency of TRPM2 in macrophage cells

resulted in the reduced production of mature caspase-1 and activation of NLRP3 inflammasome in response to silica, alum and charged lipids. Together, these findings suggest that the TRPM2 channel is critical in coupling ROS to Ca^{2+} influx and the subsequent activation of the NLRP3 inflammasome, leading to the production of IL-1 β (Zhong et al., 2013).

1.6.2 Production of other cytokines and chemokines

Proinflammatory cytokines other than IL-1 β are also released by monocytes and macrophages as part of the innate immune response to infection and tissue inflammation. A recent study shows that LPS stimulates the production of proinflammatory cytokines, including IL-6, IL-8, IL-10, and TNF- α , in THP1 monocytic cells (Wehrhahn et al., 2010). These effects were significantly reduced by knocking down the TRPM2 expression using short hairpin RNA (shRNA). Furthermore, LPS-induced Ca^{2+} influx and generation of TNF- α were diminished upon removal of extracellular Ca^{2+} using EGTA, a Ca^{2+} chelator. Treatment with TRPM2 shRNA resulted in concomitant decreases in LPS-induced Ca^{2+} influx and TNF- α generation, consistent with the notion that TRPM2 channel-mediated Ca^{2+} influx is crucial in the production of these cytokines. Sulphur mustard (SM), an alkylating agent employed in chemical warfare, can destroy immune and other cell types by disrupting intracellular organelles and causing DNA damage, thereby inducing the inflammatory responses characterised by the infiltration of leukocytes in the site of injury. One study showed that SM-induced production of TNF- α , IL-6 and IL-8 in human neutrophils requires TRPM2 channel-mediated Ca^{2+} influx that results in activation of the p38-MAPK signalling pathways and subsequent nuclear transcription of NF- κ B (Ham et al., 2012). It has also been shown that zymosan-induced generation of granulocyte colony-stimulating factor (G-CSF) and IL-1 α from macrophage cells was significantly inhibited by TRPM2-KO (Kashio et al., 2012).

Another recent study has examined the importance of the TRPM2 channel in the innate immune response to infection by *Listeria monocytogenes* (*Lm*) in a mouse model of listeriosis (Knowles et al., 2011). The *Lm*-infected TRPM2-KO mice survived at a reduced rate compared to the *Lm*-infected WT mice. Infection with *Lm* *in vitro* of cells isolated from the spleen or splenocytes in WT mice induced robust production of IL-12 and interferon gamma (IFN γ), which was significantly attenuated in the splenocytes from TRPM2-KO mice. Consistently, the serum levels of IL-12 and IFN γ present in

TRPM2-KO mice following *Lm* infection were significantly reduced. Further analysis suggests that activation of the TRPM2 channel is required for the *Lm* infection-induced production of the early inflammatory cytokine IL-12 by dendritic cells and other innate immune cells, which elicits IFN γ -mediated innate immune responses. Similarly, the production of IL-12 and IFN γ was strongly increased in dextran sulphate sodium (DSS)-induced colon inflammation, which was significantly decreased in TRPM2-KO mice (Yamamoto et al., 2008). However, there was no difference in the production of IL-6 by splenocytes and the serum level of IL-6 between the WT and TRPM2-KO mice after *Lm* infection (Knowles et al., 2011), in contrast with the observation that LPS-induced production of IL-6 in THP1 monocytic cells strongly depends on TRPM2 expression (Wehrhahn et al., 2010). In addition, there was no significant change in the production of CXCL2 and the recruitment of neutrophils during *Lm* infection (Knowles et al., 2011), which noticeably differs from the TRPM2-dependent production of CXCL2 by monocytes and recruitment of neutrophils in response to DSS-induced colon inflammation (Yamamoto et al., 2008). Currently, the reasons for these discrepancies remain unknown.

1.6.3 Regulation of heme-oxygenase-1 expression

Heme oxygenase-1 (HO-1) plays a role in limiting oxidative stress-induced tissue damage during inflammation and sepsis (Angus and van der Poll, 2013; Motterlini and Foresti, 2014). A recent study has investigated the role of the TRPM2 channel in regulating HO-1 expression in sepsis using cecal ligation and puncture (CLP)-induced models (Qian et al., 2014). The expression of HO-1 in mouse macrophages was enhanced by treatment with LPS *in vitro* and CLP *in vivo*. Both LPS-induced increase in the $[Ca^{2+}]_i$ and the HO-1 expression were diminished by removing extracellular Ca^{2+} and in macrophages from TRPM2-KO mice. CLP-induced increase in HO-1 expression was also reduced in TRPM2-KO mice. Furthermore, the TRPM2-KO mice exhibited significantly lower survival rate, accompanied with increased bacterial burden, tissue injury and inflammation. Taken together, these results support the idea that TRPM2 channel-mediated Ca^{2+} influx is important in up-regulating the HO-1 expression and enhancing bacterial clearance during sepsis.

1.6.4 Secretion of insulin

The expression of oxidative stress-sensitive cationic channels has been well documented in insulin-secreting cells (Herson et al., 1997; Herson and Ashford, 1999; Togashi et al., 2006; Inamura et al., 2003; Hill, McNulty, et al., 2004). In pancreatic β cells and insulin-secreting cell lines, an increase in the $[Ca^{2+}]_i$ induced by body temperature in synergy with cADPR has been reported to stimulate insulin secretion (Togashi et al., 2006). Such a mechanism was strongly suppressed by treatment with TRPM2-specific small interference RNA (siRNA). Consistently, a more recent study has shown a substantial decrease in temperature-dependent insulin secretion from pancreatic β cells from TRPM2-KO mice (Kashio and Tominaga, 2015). In a separate study, Uchida *et al.* revealed that the blood glucose level was higher in TRPM2-KO mice than that seen in WT mice (Uchida and Tominaga, 2011). Additionally, they showed that the increase in the $[Ca^{2+}]_i$ and insulin secretion in response to a high concentration of glucose was lower in pancreatic β cells isolated from TRPM2-KO cells than in those from WT mice (Uchida and Tominaga, 2011). Collectively, these findings provide compelling evidence to suggest a fundamental role for the TRPM2 channel in glucose-induced insulin secretion from pancreatic β cells. The mechanisms by which TRPM2 channel activation leads to glucose-induced insulin secretion is still a matter of investigation. It was initially proposed that glucose-induced TRPM2 channel-mediated insulin secretion involved the classical ATP-sensitive potassium channel (K_{ATP}) mechanism (Leech et al., 2010). Recent investigations suggest that glucose-induced TRPM2-dependent insulin secretion may engage the activation of glucagon-like peptide 1 receptor to stimulate cAMP-dependent protein kinase A (PKA) and phosphorylation by PKA of the TRPM2 channel or its associated protein (Togashi et al., 2006; Yosida et al., 2014; Kurashina et al., 2015).

1.6.5 Cell maturation and chemotaxis

The TRPM2 channel was originally found in the plasma membrane. Thus, it was surprising to find that the TRPM2 channel is exclusively present in the membrane of endolysosomal compartments as a Ca^{2+} release channels in bone marrow-derived dendritic cells (BMDCs) (Sumoza-Toledo et al., 2011). It has been further shown that the exposure of dendritic cells to chemokines, including CXCL12, CXCL21 and CXCL7 increased the $[Ca^{2+}]_i$ (Partida-Sanchez et al., 2007; Barbet et al., 2008). However, genetic depletion of the TRPM2 channel expression significantly reduced

chemokine-induced Ca^{2+} responses in BMDCs and resulted in impaired cell maturation (Sumoza-Toledo et al., 2011). Furthermore, the chemokine receptors, including CXCR4, CXCR5 and CXCR7, were not up-regulated in BMDCs deficient in TRPM2 expression, resulting in an impairment in the migration of BMDCs to the site of infection induced by subcutaneous injection of *E.coli* (Sumoza-Toledo et al., 2011).

1.6.6 Protection against ischemia/reperfusion-induced heart damage

Ischemia can reduce or prevent the oxygen and glucose supply to tissues. Reperfusion following ischemia is an inflammatory response essential for healing tissues but it can cause substantial injury. The mechanisms for ischemia/reperfusion (I/R) injury still remain incompletely understood. Studies have proposed that oxidative stress-induced intracellular Ca^{2+} overload and inflammatory processes are critical in the early phase of reperfusion (Vinten-Johansen, 2004; Frangogiannis, 2014). There is evidence that suggests that the TRPM2 channel is involved in protective mechanisms against I/R-induced myocardial injuries (Miller et al., 2013; Hoffman et al., 2015). Following I/R, hearts isolated from TRPM2-KO mice displayed decreased ventricular shortening and contractility compared to hearts isolated from WT mice (Miller et al., 2013). In cardiomyocytes subjected to hypoxia followed by re-oxygenation, TRPM2-KO resulted in significant reduction in the $[\text{Ca}^{2+}]_i$ low expression of hypoxia-inducible factors (HIF-1 α), forkhead box transcription factors (FOXOs) and SODs leading to a higher level of ROS. A more recent study has shown that I/R-induced TRPM2 channel-dependent Ca^{2+} influx is required for maintaining mitochondrial function and promoting the expression of cell survival proteins such as the receptor for activated C kinase 1 (RACK1) (Hoffman et al., 2015). Taken together, these studies support a role for the TRPM2 channel in the protective mechanisms against I/R-induced cardiomyocyte injuries.

1.6.7 Protection against bipolar disorder

Bipolar disorder (BD) is a psychiatric disease that causes states of depression and elevated mood. Genomic analyses have identified the susceptible locus of this disease, 21q22.3; which consist of the *trpm2* gene (Xu et al., 2006 and 2009). Comparative analyses of genomic DNA from BD patients suggest TRPM2 is a promising candidate contributing to the vulnerability to BD (Xu et al., 2006; Xu et al., 2009). In addition, studies have shown the impairment of Ca^{2+} signalling transduction in mononuclear leukocytes and platelets from BD patients (Cipriani et al., 2016). The

TRPM2 mRNA levels were significantly reduced in B-lymphoblast (BL) from BD patients with increased $[Ca^{2+}]_c$ compared with healthy subjects (Yoon et al., 2001), suggesting a role of TRPM2 channel for the disturbance of Ca^{2+} homeostasis. TRPM2 channel-mediated Ca^{2+} influx in BL isolated from BD patients was remarkably reduced by prolonged oxidative stress. This result indicates that oxidative stress alters TRPM2 channel function during BD (Roedding et al., 2012; Roedding et al., 2013).

Recent study using anxiety- and depression-related behavioral tests including, maze and light/dark transition tasks, showed that TRPM2-KO mice exhibited increased anxiety and impaired social behavior (Jang et al., 2015), providing evidence that suggest the important role of TRPM2 channel in the pathophysiology of BD. In the same study, the authors found a single mutation at position 543 (Asp-543-Glu), which is located in the N-terminus of the TRPM2 channel in BD patients. Such a mutation results in loss of TRPM2 channel function and phosphorylation of glycogen synthase kinase (GSK)-3. The abnormal GSK-3 activity is closely related to BD. Lithium ions (Li^+), the first drug of choice for treating BD, inhibit GSK-3 activity by increasing the phosphorylation of the inhibitory serine residues in GSK-3 (Freeland and Beaulieu, 2012). The treatment of Li^+ significantly reduced met-amphetamine-induced hyperactivity in WT mice, but not in the TRPM2-KO mice (Jang et al., 2015). Additionally, an increase in the phosphorylation of the inhibitory serine residues in GSK-3 was observed in the TRPM2-KO mice, but not in the WT mice. Overexpression of loss-of-function mutant Asp-543-Glu significantly augmented the phosphorylation of GSK-3 (Jang et al., 2015). Altogether, these findings suggest that TRPM2 deficiency results in the uncontrolled phosphorylation of GSK-3, which may contribute to the pathogenesis of BD.

1.7 PATHOLOGICAL ROLES OF TRPM2 CHANNELS

In addition to the physiological roles discussed above, studies over the past few years provide substantial evidence to reveal a critical role for the TRPM2 channel in ROS-induced cell death. Such a mechanism contributes to the pathogenesis of various diseases, exemplified by Alzheimer's disease, Parkinson's disease, I/R-induced damage to heart and brain, neuropathic pain, paracetamol overdosing-induced liver damage and endothelial barrier permeability.

1.7.1 ROS-induced cell death

There is evidence to suggest that ROS and a variety of oxidative stress-inducing stimuli induce cell death via activating the TRPM2 channel (Sumoza-Toledo and Penner, 2011; Jiang et al., 2010; Eisfeld and Luckhoff, 2007). This has been shown in different cell types, including neurons, macrophages, monocytes and cardiomyocytes (Zou et al., 2013 p. 201; Yang et al., 2006; Kaneko et al., 2006; Fonfria et al., 2005; Bai and Lipski, 2010; Sun et al., 2016).

Apoptosis and necrosis are the two major forms of cell death. Apoptosis is programmed cell death characterised by specific changes, including nuclear condensation and fragmentation, cell shrinkage, and membrane blebbing (Ouyang et al., 2012). Necrosis is, on the other hand, a form of cell injury leading to premature cell death, and is characterised by the loss of plasma membrane integrity, resulting in the leakage of intracellular contents into the extracellular space (Vanden Berghe et al., 2014). An early study showed that oxidative stress-induced cardiomyocyte cell death was due to the excessive accumulation of intracellular Ca^{2+} , leading to loss of mitochondrial membrane potential, release of cytochrome c and apoptotic cell death (Yang et al., 2006). As has been published recently (Mortadza et al., 2017) and described in detail in chapter 4, my studies have shown that TRPM2 channel-mediated increase in the $[\text{Ca}^{2+}]_i$ plays a pivotal role in microglial cell death through necrosis induced by H_2O_2 and Zn^{2+} . Therefore, H_2O_2 -induced TRPM2 channel-mediated cell death can occur via apoptosis or necrosis.

1.7.2 Alzheimer's Disease

Alzheimer's disease (AD) is a neurodegenerative disease representing the most common cause of dementia (Hardy, 2006; Scheltens et al., 2016). Accruing evidence from preclinical and clinical studies support the notion that an imbalance between the generation and removal of A β peptides is an early and initiating factor in AD (Mucke and Selkoe, 2012; Hong et al., 2016 p. 201; Selkoe and Hardy, 2016). A β is a major component of the neuritic and cerebrovascular amyloid plaque. A β is derived from the cleavage of amyloid precursor protein (APP) by membrane-bound secretases into A β species 39-43 amino acids in length, including A β_{1-39} , A β_{1-40} , A β_{1-42} , A β_{1-43} and A β_{1-46} . While A β_{1-40} is the most abundant species in a healthy brain, A β_{1-42} shows a higher level toxicity and has been shown to be the predominant species deposited in an AD brain (Murphy and LeVine, 2010; Lista et al., 2015). A β - and oxidative stress-induced

neuroinflammation have been considered to be a major part in the pathogenesis and progression of AD (Heneka et al., 2015; Heppner et al., 2015; Alam et al., 2016; Colonna and Wang, 2016; Tönnies and Trushina, 2017). Studies have shown that the elevation in A β peptide levels can lead to the production of neurotoxicity mediators, such as ROS, cytokines and chemokines, which increase the susceptibility of neurons to oxidative stress-induced neuroinflammation and apoptosis (Yamamoto et al., 2007; Bezprozvanny and Mattson, 2008).

Early studies showed that treatment of primary rat cortical neurons with A β ₄₀ caused an increase in the intracellular H₂O₂ level, leading to cortical neuronal cell death (Behl et al., 1994). A separate study found that H₂O₂ as well as A β ₄₂ induced substantial striatal neuronal cell death (Fonfria et al., 2005). Further investigation showed that overexpression of TRPM2-S, the dominant negative inhibitor of the TRPM2 channel, or inhibition of the TRPM2 channel by ACA, suppressed both H₂O₂- and A β ₄₂-induced striatal neuronal cell death (Fonfria et al., 2005). These findings provide initial evidence to suggest a potential role of the TRPM2 channel in the pathogenesis of AD.

The Tg2576 transgenic mouse carrying an APP (K670N, M671L) double mutation (Iadecola et al., 1999) and the APPswe/PS1dE9 (APP/PS1) transgenic mouse (Jankowsky et al., 2003) are the two most commonly used mouse models of AD. A recent study using the Tg2576 transgenic mouse model has shown that TRPM2 deficiency prevents A β -induced brain endothelial cell damage and cerebrovascular dysfunction (Park et al., 2014), suggesting a critical role for the endothelial TRPM2 channel in mediating A β -induced disruption of the cerebrovascular regulation leading to AD. Another recent study using the APP/PS1 mouse model has shown that TRPM2-KO prevents synapse loss and reduces age-dependent cognitive impairment (Ostapchenko et al., 2015). An early study showed that genetic disruption of the NLRP3 inflammasome activation in APP/PS1 transgenic mice impaired the ability of microglial cells to produce mature IL-1 β , leading to the enhancement of A β clearance (Heneka et al., 2013). In this recent study, it has been shown that genetic ablation of TRPM2 expression in the APP/PS1 mice strongly suppresses microglial cell activation (Ostapchenko et al., 2015). As described in detail in chapter 5, my studies have shown that the TRPM2 channel is important in mediating A β ₄₂-induced microglial cell activation and TNF- α production. Taken together, these findings support a critical role of the TRPM2 channel in the pathogenesis of AD and suggest that TRPM2 channel is a promising therapeutic target.

1.7.3 Parkinson's Disease

Parkinson's disease (PD) is another prominent neurodegenerative disorder resulting from the degeneration of dopaminergic (DA) neurons in the substantia nigra pars compacta (SNpc). PD is typically manifested by a loss of autonomic movements, impaired posture and balance, and mood disturbance (Rodriguez-Oroz et al., 2009; Blesa and Przedborski, 2014). Earlier studies show that the activity of mitochondrial complex I is reduced in the substantia nigra region of the PD brain (Mizuno et al., 1989; Schapira et al., 1989; Keeney et al., 2006). MPTP (1-methyl-4-phenyl-1,2,3,6-tetrahydropyridine) and its metabolite, MPP⁺ (1-methyl-4-phenylpyridinium ions), are neurotoxins that selectively destroy the DA neurons and are commonly used to induce PD-like syndromes in rodent models (George et al., 2009; van den Berge et al., 2011; Tian et al., 2012; Blesa and Przedborski, 2014). ROS production has been reported to be increased in cultured DA neurons following treatment with MPP⁺ (Sun et al., 2016). Overall, it is well recognized that the overproduction of ROS is a major contributing factor leading to the degeneration of DA neurons (Zhou et al., 2008; Uttara et al., 2009; Boll et al., 2011; Bollimuntha et al., 2011; Sun et al., 2016). The TRPM2 channel is expressed in DA neurons in the SN region of human and rat brains (Uemura et al., 2005; Chung et al., 2011). In a recent study, the TRPM2 expression in the SN has been shown to be up-regulated in the post-mortem brain tissues of PD patients and MPTP-injected mice (Sun et al., 2016). Furthermore, DA neuronal cell death induced by H₂O₂ and MPTP is reduced by inhibition of the TRPM2 channel with clotrimazole or using siRNA-mediated knockdown of the TRPM2 channel expression (Sun et al., 2016), suggesting a potential role for the TRPM2 channel in the pathogenesis of PD.

1.7.4 Ischemia/reperfusion-induced damage in the brain and heart

While reperfusion is essential in preventing brain damage induced by ischemic stroke, it is well known that reperfusion results in excessive ROS production and brain damage. In the case of ischemia/reperfusion (I/R), free H₂O₂ concentration in the brain can reach approximately 100 μM (Hyslop et al., 1995), at which H₂O₂ exhibits neurotoxic effects and induces striatal and cortical neuronal death (Hyslop et al., 1995; Whittemore et al., 1994). Recent studies show that the TRPM2 channel mediates neuronal death induced by transient cerebral ischemia (Alim et al., 2013) and transient global ischemia followed by reperfusion (Ye et al., 2014), suggesting a role for the TRPM2 channel in I/R-induced brain damage. Furthermore, TRPM2-KO mice exhibit

reduced infarct volumes compared with WT mice after transient ischemia, but not in the absence of reperfusion (Alim et al., 2013). In addition, TRPM2-KO prevents cognitive impairment due to transient global ischemia and reperfusion (Ye et al., 2014). These findings suggest a critical role for the TRPM2 channel in I/R-induced brain injuries.

Emerging evidence also suggests the involvement of immune cells in I/R brain injury. The infiltration of neutrophils and macrophages into the ischemic brain was noticeably reduced in TRPM2-KO mice, suggesting a critical role for the TRPM2 channel in determining the migration of neutrophils and macrophages into ischemic brain tissues (Gelderblom et al., 2014). Furthermore, TRPM2 deficiency in microglia and macrophage improved the neurological deficits induced by cerebral ischemia/reperfusion injury (Shirakawa et al., 2014). These studies are consistent in supporting a role for post-ischemia activation of the TRPM2 channel in mediating the inflammation that contributes to reperfusion-induced brain damages after transient ischemia.

The role of the TRPM2 channel in I/R-induced heart damage has been a matter of debate. As discussed above, the TRPM2 channel provides a protective mechanism in I/R-induced cardiomyocyte injuries. However, there is also evidence to suggest a role for the TRPM2 channel in mediating I/R-induced cardiomyocyte injuries. A study by Hiroi et al. showed that TRPM2-KO reduced myocardial infarct and improved cardiac contractile functions after I/R, but not ischemia alone (Hiroi et al., 2013). Neutrophil activation and migration to the myocardium have been shown to be involved in I/R-induced heart damage. Neutrophils lacking TRPM2 expression induce the same infarct size in both WT and TRPM2-KO hearts (Hiroi et al., 2013), indicating that the TRPM2 channel in neutrophils is responsible for I/R-induced myocardial injuries. The discrepancies in the findings reported by different studies with respect to the role of the TRPM2 channels in I/R-induced heart damage have been thought to, at least in part, be due to the difference in the age of the animals used, the duration of ischemia and reperfusion, and the anaesthesia approaches (Zhan et al., 2016).

1.7.5 Neuropathic pain

Neuropathic pain is a pathological condition that is associated with peripheral nerve injuries. Accruing evidence supports a role of neuron-immune interactions in pathological pain (Nieto et al., 2016). As a result of peripheral nerve injuries, peripheral immune cells are activated and release inflammatory mediators, a process termed

peripheral sensitisation. Extensive evidence has supported a critical role for ROS in the development of neuropathic pain induced by nerve injuries (Gao et al., 2007; Z.Q. Wang et al., 2004; Park et al., 2006; Kim et al., 2004; Yowtak et al., 2011; Munoz et al., 2017).

Haraghuci and colleagues studied the role of the TRPM2 channel in pain, using mouse models of inflammatory pain induced by injection of carrageenan and neuropathic pain induced by peripheral sciatic nerve ligation (pSNL) and spinal nerve transection (SNT) (Haraguchi et al., 2012). Carrageenan and pSNL induced significant inflammation and paw swelling in WT mice, which were reduced in TRPM2-KO. Carrageenan and pSNL induced an increase in the TRPM2 mRNA expression level, dominantly due to the TRPM2 expression in macrophage and neutrophils. The mechanical allodynia in WT mice induced by injection of LPS-primed TRPM2-KO macrophages was weaker than that caused by injection of LPS-primed WT macrophages in WT mice, suggesting the TRPM2 expression in macrophage contributes to the generation of mechanical allodynia. Microglial cells in the spinal cord also receive signals from injured peripheral neurons and become activated, resulting in the excitation of nociceptive dorsal horn neurons, a process known as central sensitization (Gao and Ji, 2010). Microglial cell activation in the spinal cord induced by pSNL was significantly suppressed in TRPM2-KO mice (Haraguchi et al., 2012). Additionally, SNT-induced microglia cell activation in the spinal cord and mechanical allodynia were attenuated in TRPM2-KO mice. These observations suggest the TRPM2 channel in microglia cells plays a critical role in neuropathic pain. Another recent study using mouse models of osteoarthritis and diabetic neuropathy pain has shown that the mechanical allodynia was significantly reduced by TRPM2-KO (So et al., 2015). These studies support a critical role of the TRPM2 channel in a broad spectrum of inflammatory and neuropathic pain pathologies.

1.7.6 Cancer

An increased level of intracellular ROS has been detected in many types of cancer cells (Liou and Storz, 2010). There is an increasing interest in the role of the TRPM2 channel in cancer cells. TRPM2 expression has been reported in cells of prostate cancer, breast cancer, skin cancer, and tongue and oral squamous cancers and, in addition, the expression level in cancer cells is significantly higher than in non-cancerous cells (Nilius et al., 2005; Bodding, 2007; Orfanelli et al., 2008; Orfanelli et

al., 2015; Rah et al., 2015; Zhao et al., 2016). Studies so far demonstrate different functional roles for the TRPM2 channel in different types of cancer cells. The TRPM2 channel has been shown to promote proliferation and migration in cancer cells (Zeng et al., 2010; Zhao et al., 2016). For example, siRNA-based knockdown of TRPM2 channel expression in PC-3 and DU-145 prostatic cancer cells inhibited cell proliferation (Zeng et al., 2010 p. 201). Additionally, knockdown of TRPM2 channel expression by shRNA suppressed squamous cancer cell migration (Zhao et al., 2016). Li *et al.* have recently shown a critical role for the TRPM2 channel in H₂O₂-induced PC-3 cell migration (Li et al., 2016).

There is evidence that suggests the TRPM2 channel mediates H₂O₂-induced cancer cells survival. Knockdown of the TRPM2 channel expression using shRNA in squamous cancerous cells attenuated H₂O₂-induced cell death (Zhao et al., 2016). Collectively, these findings suggest that the TRPM2 channel is important in mediating ROS-induced cell migration and cell survival, which may contribute to cancer development and progression.

1.7.7 Acetaminophen overdosing-induced liver damage

Acetaminophen, also known as paracetamol, has been widely used as an analgesic drug. Acetaminophen overdosing is well known to induce hepatocellular damage, even fatal liver failure (Davidson and Eastham, 1966; Mitchell et al., 1973; Larson et al., 2005). In the liver, acetaminophen is mainly converted into non-toxic metabolites by glucuronidation and sulfation, but a small amount of acetaminophen is metabolised by cytochrome P450 into toxic N-acetyl-parabeno-quinoneimine (NAPQI) and then into non-toxic substances through conjugation by glutathione (GSH). However, acetaminophen overdosing can cause accumulation of NAPQI and depletion of cellular GSH, leading to the generation of excessive ROS (Kheradpezhouh et al., 2014). Early studies reported that treatment of hepatocytes with a toxic dose of acetaminophen resulted in an increase in the concentrations of intracellular H₂O₂ and ADPR as well as activation of PARP-1 (Lores Arnaiz et al., 1995; Cover et al., 2005; Cover et al., 2006). A recent study has shown that the TRPM2 channel mediates H₂O₂- and acetaminophen-induced increase in the [Ca²⁺]_i in hepatocytes (Kheradpezhouh et al., 2014). Furthermore, the study has demonstrated that acetaminophen-induced liver injury was significantly attenuated in TRPM2-KO mice. Altogether, these findings strongly support an important role of the TRPM2 channel in mediating acetaminophen-induced hepatocyte toxicity and liver damage.

1.7.8 Endothelial barrier permeability

In the cardiovascular system, the endothelium provides a physical barrier between the blood vessel and interstitium. Endothelial cells are one of the main sources of ROS during pathological conditions, particularly during ischemia (Lounsbury et al., 2000; Papaharalambus and Griendling, 2007). ROS-induced Ca^{2+} influx into endothelial cells results in the formation of inter-endothelial cell junction leading to an increase of the endothelial permeability or endothelial barrier dysfunction (Hecquet et al., 2008; Hecquet and Malik, 2009; Kwan et al., 2007; Boueiz and Hassoun, 2009). Hacquet *et al.* showed that the TRPM2 channel is functionally expressed in endothelial cells from the human pulmonary arteries and that exposure to H_2O_2 at $\geq 300 \mu\text{M}$ increased endothelial barrier permeability. Reduction in TRPM2 channel expression using siRNA, or inhibition of the TRPM2 channel using an anti-TRPM2 blocking antibody or overexpression of the TRPM2-S isoform, attenuated H_2O_2 -induced endothelial barrier dysfunction as well as H_2O_2 -induced increase in the $[\text{Ca}^{2+}]_i$ and currents in endothelial cells. Altogether, these results provide strong evidence to indicate a significant role for the TRPM2 channel in mediating ROS-induced endothelial barrier dysfunction.

1.8 MICROGLIAL CELL ACTIVATION AND NEUROINFLAMMATION

Microglial cells, first described by Pio Del Rio-Hortega in 1932 (Del Rio-Hortega et al., 1932), represent the major population of cells in the CNS. Microglial cells are considered to be functionally similar to macrophage cells in the systemic immune system and are thus often termed the resident macrophage cells in the brain. Studies using direct RNA sequencing has examined the transcriptome profiles of microglial and macrophage cells in adult mice and found that there is a significant number of shared transcript between the cells (Hickman et al., 2013). These include *CD11b*, *CD68*, *TLR2* and *TLR4*. Furthermore, both microglial and macrophage cells share several functions which contribute to the physiological and pathological processes. For example, both are involved in sensing exogenous or endogenous signals (Miron et al., 2013), migration to the lesion area (Rolls et al., 2008; Shechter et al. 2009; Saederup et al. 2010), producing reactive oxygen species and promoting the secretion of multitude factors including cytokines, chemokines as well as growth factor (Miron et al., 2013). There is a significant overlap between microglial and macrophages sources, which can be distinguished through the expression patterns of CD45 or C-C chemokine receptor 2 (CCR2) (low-to-intermediate CD45 and CCR2⁻ vs. CCR2⁺ and

high CD45 for microglial vs. macrophage cells respectively) (Hickman et al., 2013; Miron et al., 2013).

Microglial cells originate from the mesoderm and migrate into the CNS and distribute throughout the brain parenchyma. The colonisation of microglial cells in the CNS takes place during the embryonic development stage in rodents (Rezaie, 2003).

1.8.1 Microglial cell activation

Microglial cells in a healthy brain remain at the stage of ramification, characterised by a small cell body with elongated and branched processes. During CNS pathologies, diverse DAMPs can trigger microglial cell activation. The activated microglial cells are manifested by changes in the cell morphology; microglial cells undergo body enlargement and retract their branching processes. Microglial cells in the activated state are able to proliferate, migrate, possess phagocytic properties and release pro-inflammatory mediators.

ROS as well as Zn^{2+} , $A\beta$ and TNF- α are DAMPs that can trigger microglial cell activation (Kauppinen et al., 2008; Jekabsone et al., 2006; Mander et al., 2006; Kauppinen et al., 2011; Diestel et al., 2003). There is evidence to suggest that ROS can induce changes in microglial cell morphology (Qin et al., 2004). In the brain, Zn^{2+} is mostly concentrated within presynaptic vesicles at the glutamatergic terminal (Beaulieu et al., 1992) and is released following neuronal stimulation. Vesicular Zn^{2+} release into the extracellular space has been identified as a trigger for the changes in microglial cells morphology (Assaf and Chung, 1984; Howell et al., 1984). In addition, the changes in microglial cells morphology can be induced following the exposure to extracellular Zn^{2+} (Monsonego and Weiner, 2003; Tai et al., 2007; Kauppinen et al., 2008). $A\beta$ induces the changes in microglial cell morphology and cell proliferation as well as TNF- α and IL-1 β production (Ostapchenko et al., 2015; Jekabsone et al., 2006; Hanisch, 2002; Xiang et al., 2006). While TNF- α can be produced by activated microglial cells following stimulation by PAMPs, TNF- α itself can act as an autocrine or paracrine signalling molecule to induce microglial cell activation (Jekabsone et al., 2006; Mander et al., 2006). Exposure of microglial cells to TNF- α is known to stimulate changes in the cell morphology and cell proliferation (Kauppinen and Swanson, 2005; Jekabsone et al., 2006). Furthermore, exposure to TNF- α induces migration of microglial cells to injury sites in the CNS (Angelov et al., 1998).

The underlying signalling mechanisms involved in microglial cell activation induced by DAMPs are not fully understood. However, extensive evidence shows that ROS production as well as NOX and PARP-1 activation is critical in microglial cell activation (Kauppinen et al., 2008; Mander et al., 2006; Diestel et al., 2003; Jekabsone et al., 2006). For example, an increase in the intracellular ROS level has been reported to be critical in Zn^{2+} -induced microglial cell activation (Kauppinen et al., 2008; Abid et al., 2000; Heinloth et al., 2000). It has been proposed that TNF- α stimulates microglial cell activation by inducing ROS production (Radeke et al., 1990; Meier et al., 1989). It has been shown that the change in cell morphology accompanying microglial cell activation triggered by extracellular Zn^{2+} is dependent on NOX (Kauppinen et al., 2008). In addition, microglial cell proliferation is triggered by ROS from NOX following stimulation by TNF- α (Mander et al., 2006). These findings suggest that NOX-dependent ROS production is involved in mediating microglial cell activation. Furthermore, genetic ablation of PARP-1 inhibited the change in microglial cell morphology induced by Zn^{2+} (Kauppinen et al., 2008), A β (Kauppinen et al., 2011) and TNF- α (Kauppinen and Swanson, 2005), suggesting engagement of PARP-1 in microglial cell activation.

The activated microglial cells exhibit diverse functions in the brain under normal conditions. For instance, they induce immune responses upon sensing CNS injuries in the healthy brain (Nimmerjahn et al., 2005), scavenging cellular debris by phagocytosis (Marin-Teva et al., 2004) and eliminating synapses during normal synaptic development (Paolicelli et al., 2011; Schafer et al., 2012). Yet, microglial cell activation is also well-recognised to be involved in many neuropathological processes that can result in CNS disorders. Activated microglial cells are present in a large number of CNS tissues from patients with AD, PD and ischemic stroke (Perry et al., 2007; Ostapchenko et al., 2015; Wang et al., 2007; Kauppinen et al., 2008). Early studies using transgenic mouse models of AD showed an increased number of activated microglial cells near the A β plaque (Irizarry et al., 1997; Frautschy et al., 1998). Further investigations revealed that microglial cells migrate to the A β plaque and become activated, leading to an increase in the production of pro-inflammatory cytokines (Sasaki et al., 1997; Hardy and Selkoe, 2002; Rogers et al., 2002). These studies provide strong evidence to support the notion that microglial cell activation is critically involved in AD. Microglial cell activation has also been observed in the brain of PD patients (Chouchani et al., 2016; Gerhard et al., 2006). Administration of MPTP in mice can induce morphological changes in microglial cells (Czlonkowska et al., 1996;

Kurkowska-Jastrzebska et al., 1999). In addition, microglial cell activation was found in the brain of MPTP-injected monkeys (Hurley et al., 2003; Barcia et al., 2004). There is evidence to suggest that DA neuronal loss is accompanied by microglial cell activation in PD mouse models (Lee et al., 2009; Qian et al., 2010). These results suggest that microglial cell activation acts as an important factor in the pathogenesis of PD. Moreover, *in vivo* studies have demonstrated microglial cell activation following transient cerebral I/R (Kauppinen et al., 2008). Altogether, these findings imply that microglial cell activation is involved in a broad spectrum of neurodegenerative diseases.

1.8.2 Neuroinflammation

As discussed above, microglial cells play a significant role in initiating immune responses to brain damage. Prolonged or persistent activation of microglial cells can cause excessive generation of a number of pro-inflammatory mediators including cytokines, chemokines, ROS and NO, resulting in neuroinflammation (Liu and Hong, 2003; Block et al., 2007; Colonna and Butovsky, 2017; Regen et al., 2017; Wolf et al., 2017; Weinstein et al., 2010). Microglial cells are the major source of pro-inflammatory cytokines in the CNS (Hanisch, 2002; Welser-Alves and Milner, 2013). Pro-inflammatory cytokines, including TNF- α and IL-1 β , are crucial mediators of neuroinflammation. High levels of these pro-inflammatory cytokines are associated with a variety of neurodegenerative diseases including AD, PD, and I/R induced brain injuries (Block et al., 2007; Alam et al., 2016; Colonna and Butovsky, 2017; Regen et al., 2017; Wolf et al., 2017)

TNF- α is one of the major pro-inflammatory cytokines generated by microglial cells and is well-known for its neurotoxicity (Liu and Hong, 2003; Block et al., 2007; Alam et al., 2016; Krabbe et al., 2017). TNF- α is first synthesised as a transmembrane protein, which is then cleaved by TNF- α converting enzyme (TACE) to produce soluble TNF- α . TNF- α binds to two different receptors, TNF- α receptor 1 (TNFR1) and TNF- α receptor 2 (TNFR2). Such mechanisms lead to a wide variety of physiological or pathological functions in cells expressing these receptors (MacEwan, 2002; Kuno et al., 2005). TNF- α has been shown to have a critical role in neuroinflammatory responses resulting in neurodegenerative diseases. Studies have reported high generation and co-localisation of TNF- α with A β plaques in the brains of AD mice and patients (Wyss-Coray and Rogers, 2012; Montgomery et al., 2013). It is also suggested that an increase in the TNF- α generation occurred earlier than the development of histopathological

hallmarks in AD mice and long-term TNF- α expression leading to neuronal death in these mice (Liu and Hong, 2003; Kauppinen et al., 2011; Montgomery et al., 2011; Wyss-Coray and Rogers, 2012; Montgomery et al., 2013). These findings strongly suggest that TNF- α production is critically involved in A β -induced neuroinflammation in AD pathogenesis. In addition, there is evidence showing the role of TNF- α in PD. TNF- α was found to be localised to activated microglial cells in the SN of PD patients (Mogi et al., 1994; McGeer, 2008; Nagatsu and Sawada, 2007). Besides, MPTP induces an increase in TNF- α production in the mouse brain, leading to DA neuronal death (Sriram et al., 2002; McCoy and Tansey, 2008). Further investigation showed that DA neuronal death is significantly reduced in mice lacking TNFR1 expression (Sriram et al., 2002), suggesting that TNF- α serves as crucial trigger in DA neurotoxicity associated with PD. The increase in TNF- α production has also been documented in I/R-induced brain injuries. Microglial cell activation induced by cerebral ischemia and reperfusion resulted in an increase in the production of TNF- α (Clausen et al., 2008). In a separate study, inhibition of TNFR1 and TNFR2 or TACE can protect neuronal injuries induced by cerebral ischemia and reperfusion (Nawashiro et al., 1997; X. Wang et al., 2004). Inclusively, these results support the notion that TNF- α production following microglial cell activation plays a major role in I/R-induced brain injuries.

Besides TNF- α , high levels of IL-1 β , IL-18 and IL-6 are also observed in the neurodegenerative diseases (Brodacki et al., 2008; Clausen et al., 2008; Lambertsen et al., 2012; Block et al., 2007 p. 200; Wolf et al., 2017). A β -induced microglial cell activation has been shown to result in an increase in the level of IL-1 β , IL-18 and IL-6, which subsequently causes neuronal cell death (von Bernhardi et al., 2010). In addition, an increase in IL-1 β production by LPS-stimulated microglial cells induces deficits in learning and memory (Tanaka et al., 2006). Furthermore, *in vivo* studies showed that microglial cell activation induced by cerebral ischemia and reperfusion results in a high level of IL-1 β in the mouse brains (Clausen et al., 2008). Previous studies also showed that the change in microglial cell morphology leads to an increase in the production of IL-1 β and IL-6 following chronic stress-induced brain injuries (Tynan et al., 2010; Hinwood et al., 2012; Wohleb et al., 2011). Taken together, the findings suggest that IL-1 β , IL-18 and IL-6 production by microglial cell activation play a crucial role in neurodegenerative diseases.

Collectively, there is extensive evidence to support the idea that the production of pro-inflammatory cytokines, particularly TNF- α , by microglial cell activation is one

of the major causative factors in the pathogenesis of multiple neurodegenerative diseases. Investigations into the signalling mechanisms responsible for microglial cell activation and generation of pro-inflammatory cytokines may offer a promising therapeutic target for the prevention of neurological dysfunction in a variety of CNS pathologies.

1.8.3 Role of TRPM2 channel in microglial activation and neuroinflammation?

As discussed above (section 1.7), there is an increasing interest in the TRPM2 channel in the pathogenesis of multiple neurodegenerative diseases, but the role of the TRPM2 channel in microglial cells still remains to be elucidated. Nonetheless, recent studies have shown a role for the TRPM2 channel in LPS/IFN γ -induced increase in the $[Ca^{2+}]_i$ and production of NO in WT microglial cells as well as LPS/IFN γ -induced production of chemokine CXCL2 and NO by microglial cells (Haraguchi et al., 2012; Miyake et al., 2014). Furthermore, the TRPM2 channel is also involved in oxidative stress-induced production of TNF- α and IL-6 in microglial cells (Lee et al., 2010). A more recent study has found that genetic deletion of TRPM2 expression strongly attenuates the morphological changes in microglial cells in the brain of APP/PS1 mouse model of AD (Ostapchenko et al., 2015). Taken together, these results suggest that the TRPM2 channel is highly involved in microglial cell activation and neuroinflammation.

Further studies are required to elucidate the signalling mechanism of TRPM2 channel activation in microglial cells, which is crucial in providing mechanistic insights into the pathogenesis of neurodegenerative diseases.

1.9 AIMS AND OBJECTIVES

As discussed above, the expression of the TRPM2 channel in microglial cells has been well established, but its functional role remains yet to be fully understood. Hence, this project aimed to investigate the role of the TRPM2 channel and the signalling mechanisms in microglial cell functions, using a multidisciplinary approach including primary microglial isolation, single cell calcium imaging, immunocytochemistry, confocal microscopy, computer-aided analysis of cell morphology and cell death and ELISA assays.

I started with using primary microglial cells isolated from WT mice to determine whether ROS, Zn $^{2+}$, A β_{42} and TNF- α induced Ca $^{2+}$ signalling, cell death and cell

activation. This was followed by experiments using primary microglial cells from TRPM2-KO mice to determine the role of the TRPM2 channel in Ca^{2+} signalling, cell death and microglial cell activation in response to these stimuli. These results are presented in chapter 3.

Following the findings in chapter 3 that H_2O_2 and Zn^{2+} induced TRPM2 channel-mediated microglial cell death, I investigated the signalling mechanisms underlying H_2O_2 - and Zn^{2+} -induced TRPM2 channel activation and cell death in primary microglial cells from WT mice. These results are presented in chapter 4.

Finally, I investigated the role of TRPM2 in $\text{A}\beta_{42}$ - and TNF- α -induced microglial cell activation and the production of TNF- α using primary microglial cells from WT and TRPM2-KO mice. This was followed by experiments exploring the signalling mechanisms involved in TRPM2 channel-mediated microglial cells activation and TNF- α production induced by $\text{A}\beta_{42}$ and TNF- α . These results are presented in chapter 5 and chapter 6 for $\text{A}\beta_{42}$ and TNF- α , respectively.

CHAPTER 2

MATERIALS AND METHODS

2.1 MATERIALS

2.1.1 Chemicals

General chemicals were purchased at the appropriate grade from Sigma-Aldrich, unless otherwise stated. The stock solutions prepared and used are described in Table 2.1.

2.1.2 Solutions

All solutions were prepared with Milli-Q deionised water (summarized in Table 2.2). All solutions used in cell culture were sterilised by autoclaving or syringe filtering.

2.1.3 Antibodies, fluorescence indicators and ELISA kits

Antibodies and fluorescence indicators were sourced as indicated in Table 2.3 and Table 2.4, respectively. Mouse tumor necrosis factor- α (TNF- α) ELISA kits were purchased from Peprotech.

2.1.4 Cell culture media

Hank's Balanced Salt Solution (HBSS), Dulbecco's Phosphate Buffer Saline (dPBS), 0.5% Trypsin-EDTA, Dulbecco's Modified Eagle Medium (DMEM), foetal bovine serum (FBS) and penicillin/streptomycin were purchased from Invitrogen (Table 2.2).

2.1.5 Animal and genotyping of TRPM2-KO mice

C57BL/6 (WT) and TRPM2-KO mice were obtained from and maintained by the Central Biomedical Service (CBS), University of Leeds. The TRPM2-KO mice express trpm2 gene lacking exons 17 and 18 resulting in no expression of functional TRPM2 channel (Zou et al. 2013). The genotyping of the TRPM2 transgenic mice was performed using both male and female mice, as described previously by Zou *et al.* (Zou et al. 2013). Briefly, the total genomic DNA was isolated from tissue sample obtained by 2 mm ear clip. The tissue samples were digested using phenol: chloroform: isoamyl alcohol. PCR was conducted using *Taq* polymerase, forward primer (For1: 5'-CCC TGG

TCT GTG GGA GCC TAG or For2: 5'-GCA GAG GCT GAG GTG GTA CC) and reverse primer (Rev: 5'-CCC CCA CTA TCA CCC GGA TAC). The PCR was performed under the following conditions: 95°C for 5 min, 29 cycles of 95°C for 30 s, 60°C for 30 s and 72°C for 30 s and an additional step of 72°C for 5 min. The PCR products were analyzed by electrophoresis using 1% agarose gel and the deletion was confirmed by the expected size and sequencing of the PCR amplicons from genomic DNA. All experiments and experimental protocols involving mice were approved by the University of Leeds Ethical Review Committee and performed in accordance with the University of Leeds guidelines and procedure and conforming to the UK Home Office rules and regulations.

Table 2.1 Stock solutions

Compounds	Concentrations	Sources
H ₂ O ₂	10 M	Sigma
ZnSO ₄	0.3 M	Sigma
Aβ ₁₋₄₂	1 mg/ml in ammonium hydroxide (NH ₄ OH)	Eurogentec
Aβ ₄₂₋₁	1 mg/ml in DMSO	China Peptide
TNF-α	10 µg/ml in water	Cell Signalling Technology
BAPTA-AM	1 µg/ml in DMSO	Bio-Vision
PJ34	15 mM in water	Santa Cruz Biotechnology
2-APB	10 mM in DMSO	Sigma
DPQ	10 mM in DMSO	Calbiochem
CTC	10 mM in DMSO	Tocris
DPI	10 mM in DMSO	Sigma
GKT139396	5 mM in DMSO	Cayman Chemical
Phox-I2	10 mM in DMSO	Sigma
PF431396	1 mM in DMSO	Tocris
U0126	5 mM in DMSO	Cayman Chemical
IM-54	5 mM in DMSO	Sigma
Ac-DVED-CMK	10 mM in DMSO	Cayman Chemical
Necrostatin-1	10 mM in DMSO	Alfa Aesar

Table 2.2 Solutions

Primary microglial cell culture preparation	
Borate acid buffer	100 mM boric acid, 75 mM NaCl and 25 mM sodium in water, pH 8.5 with NaOH
Dulbecco's Phosphate Buffer Saline (dPBS)	2.7 mM KCl, 1.5 mM KH ₂ PO ₄ , 136.9 mM NaCl, 8.9 mM Na ₂ HPO ₄
Poly-L-lysine (PLL)	10 mg/ml stock prepared in DMSO and 0.1 mg/ml used by dissolving in borate acid buffer
10X Hank's Balanced Bath Solution (HBSS)	HBSS (1X) freshly prepared by diluting in water
Planting media	DMEM/F12 supplemented with 10 units/ml penicillin and 100 µg/ml streptomycin
10X Trypsin-EDTA	5 g/l trypsin, 2 g/l EDTA•4Na, 8.5 g/l NaCl resolved in phosphate buffered saline (PBS)
For immunofluorescence	
Phosphate Buffer Saline (PBS)	One PBS tablet dissolved in 200 ml water
Para-formaldehyde (PFA) fixative	4% (w/v) PFA dissolved in water
Permeabilization buffer	0.1% (v/v) Triton-X-100 diluted in PBS
Washing buffer (PBST)	0.5% (v/v) Tween-20 diluted in PBS
Blocking and antibody dilution buffer	5% (v/v) goat serum diluted in PBS
For live cell imaging	
Standard Bath Solution (SBS)	134 mM NaCl, 5 mM KCl, 0.6 mM MgCl ₂ , 8 mM glucose, 10 mM HEPES and 1.5 mM CaCl ₂ in water, pH 7.4 with NaOH
Ca ²⁺ -free SBS solution	134 mM NaCl; 5 mM KCl; 0.6 mM MgCl ₂ ; 8 mM glucose; 10 mM HEPES; 0.4 mM EGTA, in water, pH 7.4 with NaOH

Pluronic acid (PA) F-127	0.1 % (w/v) PA dissolved in DMSO
--------------------------	----------------------------------

Table 2.3 Antibodies

Antibodies	Sources	Dilutions
Primary antibodies		
Mouse anti-TRPM2	Bethyl	1:1000
Mouse anti-PAR	Enzo Life Science	1:500
Rabbit anti-TNF- α	Millipore	1:400
Secondary antibodies		
FITC-conjugated rabbit-anti mouse IgG	Sigma	1:1000
FITC-conjugated goat-anti rabbit IgG	Sigma	1:1000

Table 2.4 Stock solutions of fluorescence indicators

Fluorescence indicators	Sources	Live-cell imaging
Fluo4/AM	Thermo Fisher Scientific	1 mM in DMSO
DCFH-DA	Sigma	1 mM in DMSO
PI	Sigma	1 mg/ml in water
Hoechst 33342	Cell Signalling Technology	1 mg/ml in water

2.2 METHODS

2.2.1 Preparation of microglial cell culture

2.2.1.1 Preparations of PLL-coated culture flasks

A stock of 10 mg/ml of PLL was diluted to 0.1 mg/ml with borate acid buffer (Table 2.2), and 4 ml of 0.1 mg/ml PLL-coating solution was added into 75-cm² culture flask. The flask was tilted to ensure that the PLL-coating solution covered the whole surface. This was followed by incubating the flask for 1 hr at 37°C. The PLL-coating solution was removed by aspiration and the surface of the flask was rinsed thoroughly with dPBS (Table 2.2) for 3 times, using 6 ml each time. The PLL-coated flasks were left to dry in the tissue culture hood for 2 hr before they were covered with aluminium foil and kept at 4°C. Culture flasks were pre-coated with PLL in advance in order to improve the number of cells obtained at the end of the culturing period.

2.2.1.2 Isolation of microglial cells

Microglia cells were isolated from 1-5 day old mice. The dissecting tools (summarized in Table 2.5) was cleaned with ethanol and laid out in the dissecting hood prior of the isolation procedure. The brain was removed, after the mice was sacrificed, and transferred into a petri-dish containing pre-cooled dissecting HBSS on ice. The cerebral hemispheres were separated from the mid-brain before the meninges layers were removed under a dissecting microscope using tweezers. It is important to remove the meninges layers completely from the brain tissues as this can improve the quality of the cell culture and therefore increase the number of microglia cells. Following the removal of the meninges layer, the brain tissues were collected into cold planting media prior to the incubation in 10 volumes of 0.5% trypsin-EDTA solution for 20 min at 37°C. After the trypsin-EDTA solution was removed by extensive aspiration, the tissues were further dissociated in 4 ml of planting media by triturating using a pipette before subsequently filtered into a 50 ml-falcon tube using a 70-µm cell strainer. Cells were collected by centrifugation at 1300 rpm for 5 min, and the pellet was re-suspended in 2 ml of DMEM/F12 supplemented with 10% FBS, 10 units/ml penicillin and 100 µg/ml streptomycin. The cell suspension from 2 brains was added to a PLL-coated 75-cm² flask in total 15 ml of the same culture media.

Cells were maintained at 37°C in a humidified atmosphere of 5% CO₂. Following 4 days of incubation, one half of the culture media was collected and

centrifuged for 5 min at 1300 rpm and the supernatant was added back into the culture flask, while the other half of the culture media was replaced with fresh DMEM/F12 supplemented with 10% FBS, 10 units/ml penicillin and 100 µg/ml streptomycin. The purpose of this step is to reduce the debris and also provide nutrients supplemented by the fresh media to the cells. Cells were incubated further for 5-8 days.

After 12-14 days in culture, the microglial cells were loosely attached and separated from the rest of cell culture by shaking the flasks in a rotary platform in a tissue culture incubator at 37°C at 180 rpm for 90 min. The culture media containing microglia cells were collected by centrifuging at 1300 rpm for 5 min, re-suspended in fresh culture medium and seeded in different cell culture microplates depending on the experiment purposes. The type of culture plates, the number of cells and the amount of medium used are described in Table 2.6.

2.2.1.3 Treatment of microglial cells

Microglial cells were routinely incubated for 72 hr before use to ensure the cells were in a resting state. Primary microglial cells were treated directly without (Control) or with H₂O₂, Zn²⁺, Aβ₄₂ or TNF-α alone at indicated concentrations as detailed in the Result chapters. In experiments studying an inhibitor, cells were pre-treated with the solvent control DMSO or the indicated inhibitor at 37°C, 30 min before and during exposure to H₂O₂, Zn²⁺, Aβ₄₂ or TNF-α. Table 2.3 provides a list of the compounds used and also the solvent controls. All compounds were prepared to the final concentration (as described in the Result chapters) using fresh media and were directly added into the culture plate for the indicated experiment duration.

2.2.2 Immunofluorescence imaging

Microglial cells were seeded onto 13-mm coverslips with 50,000-65,000 cells per slip (Table 2.6), and incubated for 72 hr prior to use. Following the treatments as detailed in the Results chapters, cells were fixed with 250 µl of 4% (w/v) paraformaldehyde (PFA) for 15 min at -20°C. Cells were permeabilized 3 times, with each time using 300 µl PBS containing 0.1% Triton X-100 which was added, left for 5 min at room temperature (RT), and removed. Following rinsing twice with 300 µl of PBST wash buffer (Table 2.2), cells were incubated in 400 µl of blocking solution (Table 2.2) for 2 hr at RT. Primary rabbit anti-TRPM2 antibody, mouse anti-PAR antibody, or rabbit anti-TNF-α antibody was added into the blocking solution at the dilution described in Table 2.3, and cells were incubated overnight at RT. Cells were

extensively washed with 300 µl of PBST wash buffer for 3 times, as described in the permeabilization step. Cells were then incubated with 400 µl of blocking solution containing secondary fluorescein isothiocyanate (FITC)-conjugated rabbit anti-mouse or goat anti-rabbit antibody (dilutions summarized in Table 2.3) in the dark for 2 hr at RT. After rinsing with PBST wash buffer for 3 times as described above, the cover slips were mounted onto microscope slides with SlowFade Gold Antifade mounting reagent with 4',6-diamidino-2-phenylindole (DAPI) and stored at 4°C. Images were captured using an EVOS FL cell imaging system (Life Technologies). The FITC fluorescence intensities were quantified using ImageJ and at least 70 cells were examined from each coverslip.

Table 2.5 Dissection tools used for microglia cells isolation

Dissecting Tools	Size	Sources
Straight blunt dissecting scissor	165 mm	Thermo Scientific
Scalpel surgical blade handle	No. 3	Swann-Morton
Surgical scalpel blade	No. 10A	Swann-Morton
45° angled delicate forceps	90 mm	Fine Science Tools
Micro-dissecting forceps curved	4 inch	Sigma
Micro-dissecting forceps straight	4 inch	Sigma
Jewelers forceps, Dumont No. 5	4.25 inch	Sigma
Tweezers, No.5	110 mm	Sigma

Table 2.6 Preparations of microglial cells

Experiments	Culture plate	Number of cells/well	Amount of media (µl)
Single cell Ca ²⁺ imaging	96-well plate	25000	180
Immunofluorescent staining for TRPM2 and PAR	24-well plate	50000	300
Immunofluorescent staining for TNF-α	24-well plate	65000	300

Cell death assay	96-well plate	15000	180
Imaging of cell morphology	96-well plate	20000	180
Measurement of ROS	96-well plate	25000	180
TNF- α release by ELISA	96-well plate	45000	50

2.2.3 Single cell calcium imaging

Single cell calcium imaging was performed using Fluo4-acetoxymethyl ester (Fluo-4/AM). The measurement of intracellular Ca^{2+} concentrations was performed on cells seeded in 96-well plates at densities described in Table 2.6. Following 72 hr incubation, the media were removed and cells in each well were rinsed twice with 200 μl of SBS (Table 2.2), and incubated in 100 μl of SBS containing 5 μM Fluo-4/AM and 0.01% (v/v) pluronic acid at 37°C for 45 min. Cells were rinsed with SBS for 3 times, each time using 200 μl . Following washing, 200 μl of SBS or Ca^{2+} -free SBS containing either control DMSO or a stimulus (as detailed in the Results chapters) were added into each well. The plate was incubated for 2 or 8 hr (as described in Result chapters) at 37°C. In experiments examining the effect of an inhibitor, cells were pre-treated with the inhibitor for 30 min at 37°C prior to exposure to the stimulus. At the end of treatment with the stimulus, cells were counter-stained by Hoechst 33243 at a concentration of 5 $\mu\text{g}/\text{ml}$ by incubating for 15 min at 37°C. The fluorescent images were captured using an EVOS FL cell imaging system. The Fluo4 intensities in individual cells were quantified using ImageJ and at least 100 cells were examined in each well.

2.2.4 Cell death assay

Cells were seeded as described in Table 2.6 and incubated at 37°C for 72 hr prior to use. Solvent control DMSO or stimuli indicated at the concentrations shown in the Results chapters, were added to the culture media in each well. The plate was incubated at 37°C for 24 hr in a majority of experiments or 2, 4, 8 hr in a small number of experiments. PI and Hoechst 33243 were added to a final concentration of 2 $\mu\text{g}/\text{ml}$ and 5 $\mu\text{g}/\text{ml}$, respectively and the plate was incubated at 37°C in the dark for a further 30 min prior to imaging. In experiments studying an inhibitor, cells were pre-treated with the indicated inhibitor at 37°C, 30 min before and during exposure to the stimulus. Cells were imaged using an EVOS FL cell imaging system. The number of PI-stained dead cells and the total number of cells identified by Hoechst-staining in three randomly chosen areas in each image were counted using ImageJ, and at least 100 cells were

examined in each well. Cell death was presented by expressing PI-stained cells as percentage of Hoechst-stained cells.

2.2.5 Characterization of microglial cell morphology

Microglial cell morphology was examined on live cells. Cells were seeded as described in Table 2.6 and incubated at 37°C for 72 hr. Cells were treated with either solvent control DMSO or stimuli (described in the Results chapters) for 24 hr at 37°C. In experiments assessing the effect of an inhibitor, the inhibitor was added at indicated concentrations to the culture media 30 min before and during exposure to the stimulus. Images were captured using an Incucyte ZOOM imaging system (Essence Bioscience) with a 10x object lens or an EVOS FL cell imaging system with a 40x object lens. The change in cell morphology was characterized by computer-assisted analysis (ImageJ) of form factor and aspect ratio of individual cells as described in previous studies (Soltys et al., 2001; Zanier et al., 2015). The form factor was calculated using the formula of $4\pi \times \text{area}/\text{perimeter}^2$, with the highest value of 1.0 indicating a perfect circle and with value approaching 0 indicating an elongated shape. The aspect ratio is defined as the length-to-width ratio, with the minimal value of 1.0 indicating a perfect circle.

2.2.6 Measurement of ROS production

Cellular ROS production was assayed using 2',7'-dichlorodihydrofluorescein diacetate (DCFH-DA) as described recently (Shen et al., 2014). Briefly, cells were plated in 96 well plates, as described in Table 2.6, and incubated for 72 hr prior to use. Cells were treated with either solvent control DMSO or stimuli at indicated concentrations (described in the Results chapters) at 37°C for 2 or 8 hr. After the media was removed, cells were rinsed twice with 200 µl of SBS and incubated in 100 µl of SBS containing 20 µM DCFH-DA in the dark at 37°C for 45 min. Cells were washed 3 times, each time with 200 µl of SBS, and then maintained in 200 µl of SBS. Hoechst 33243 at a final concentration of 5 µg/ml was added in each well. Cells were incubated at 37°C for a further 30 min. In experiments studying the effect of an inhibitor, cells were treated with the inhibitor at 37°C 30 min before and during exposure to the stimulus. Images were captured using an EVOS FL cell imaging system. The fluorescence intensities in individual cells were quantified using ImageJ and at least 100 cells were examined in each well.

2.2.7 Enzyme-linked immunosorbent assay (ELISA)

Cells were plated as described in Table 2.6 and incubated at 37°C for 72 hr. After the culture media were removed, cells were rinsed twice with dPBS, and 50 µl fresh culture media containing either solvent control DMSO or stimuli at indicated concentrations (described in the Results chapters) were added to each well. Cells were incubated at 37°C for 72 hr. In experiments studying the effect of an inhibitor, the media were replaced with 50 µl of fresh culture media containing the inhibitor at indicated concentrations (described in the Result chapter) at 37°C, 30 min before and during exposure to stimuli. At the end of treatment with the stimulus, the culture media were collected. The TNF- α concentrations in the culture media were determined by a TNF- α ELISA kit (Peprotech) according to the manufacturer's instructions.

2.3 STATISTICAL ANALYSIS

Experiments were performed in at least triplicate and repeated using three different cell cultures prepared independently. All data are presented as mean \pm standard error of mean (SEM). Statistical analysis was made using Student's t-test for comparison of two groups and one-way ANOVA followed by post hoc Tukey's test for comparison among multiple groups with $p < 0.05$ being considered to be significant. Data was analysed and figures were prepared in Origin (version 9.1).

CHAPTER 3

**A ROLE OF TRPM2 IN DAMP-INDUCED MICROGLIAL CELL
DEATH AND CELL ACTIVATION**

3.1 INTRODUCTION

Microglial cells, as discussed in the Introduction chapter, represent the resident macrophage cells in the CNS (see section 1.8.1). It is widely recognized that microglia cell plays an important role in neurodegenerative diseases, including AD (Vincenti et al., 2016; Wes et al., 2016), PD (Ouchi et al., 2005; Gerhard et al., 2006) and ischemic-induced brain injury (Wang et al., 2016; Szalay et al., 2016). Microglial cell is a highly plastic cell in which it retracts its branched processes upon activation by structurally diverse molecules known as DAMPs, including Zn^{2+} (Kauppinen et al., 2008), $A\beta$ (Jekabsone et al., 2006) and TNF- α (Kauppinen and Swanson, 2005).

Elevation of Zn^{2+} , $A\beta$ and TNF- α in the brain has been implicated in a diversity of diseases conditions in the CNS, in which these molecules promote production of toxicity mediators, such as ROS (Yamamoto et al., 2007; Bezprozvanny and Mattson, 2008; Gloire et al., 2006). Additionally, evidence have suggested that $A\beta$ and TNF- α as well H_2O_2 induce an increase in the $[Ca^{2+}]_i$ (Kraft et al., 2004; Fonfria et al., 2005; W. Zhang et al., 2006) and cell death in neurons, macrophages and monocytes via activating the TRPM2 channel (Zou et al., 2013; Fonfria et al., 2005; Kaneko et al., 2006; Bai and Lipski, 2010; Sun et al., 2016). The high level of TRPM2 expression in microglial cells (Kraft et al., 2004; Fonfria et al., 2006; Miyake et al., 2014) raises the question of whether TRPM2 channel has a role in mediating cell death in response to H_2O_2 , Zn^{2+} , $A\beta$ and TNF- α .

ROS produced from NOX has been shown to induce change in microglial cell morphology (Qin et al., 2004). In addition, as mentioned in the Introduction chapter, zinc release from glutamatergic neurons as well as exogenous zinc can induce the change in microglial cell morphology (Assaf and Chung, 1984; Kauppinen et al., 2008). Also, evidence has suggested that $A\beta$ and TNF- α stimulate change in cell morphology and cell proliferation in microglial cells (Ostapchenko et al., 2015; Kauppinen and Swanson, 2005; Angelov et al., 1998). A recent study reported a critical function of TRPM2 channel in mediating $A\beta_{42}$ -induced microglial cell activation (Ostapchenko et al., 2015).

Therefore, the studies presented in this chapter aim to investigate the TRPM2 channel role in the Ca^{2+} signalling, cell death, and cell activation in microglial cells in response to H_2O_2 as well as Zn^{2+} , $A\beta_{42}$ and TNF- α . Such information is useful for a better understanding of microglial cells in oxidative stress-related pathologies.

3.2 RESULTS

3.2.1 TRPM2 channel expression and its role in H_2O_2 -induced Ca^{2+} responses

I started with confirming the TRPM2 expression in microglial cells using immunofluorescent confocal microscopy. Positive immunostaining was observed in primary microglial cells labelled with an anti-TRPM2 antibody, but not in control cells (Fig. 3.1a). Next, I examined the $[Ca^{2+}]_i$ in cells after exposure to different concentrations of H_2O_2 (10-300 μM) for 2 hr and 8 hr, using single cell calcium imaging. There was a significant increase in the $[Ca^{2+}]_i$ after exposure for 2 hr to 100-300 μM H_2O_2 (Fig. 3.1b-c), but not to 10-30 μM H_2O_2 . However, 10-30 μM H_2O_2 induced strong Ca^{2+} responses when the exposure duration was prolonged to 8 hr (Fig. 3.1d-e). These results show that H_2O_2 induces a concentration- and time-dependent increase in the $[Ca^{2+}]_i$. In striking contrast with the robust Ca^{2+} responses in WT microglial cells, exposure to 100-300 μM H_2O_2 for 2 hr (Fig. 3.2a) and 10-30 μM for 8 hr (Fig. 3.2b) induced very small increases in the $[Ca^{2+}]_i$ in TRPM2-KO microglial cells. Taken together, these results provide compelling evidence to support a role for the TRPM2 channel in mediating H_2O_2 -induced Ca^{2+} signalling in microglial cells.

3.2.2 TRPM2 channel in mediating H_2O_2 -induced microglial cell death

It has been shown that TRPM2 channel plays a crucial role in ROS-induced cell death in various cell types including macrophage cells (section 1.7.1). However, it was unclear whether the TRPM2 channel has a similar role in microglial cells. Therefore, I examined microglial cell death after exposure to 10-300 μM H_2O_2 for 2, 4, 8 and 24 hr, using PI staining. Exposure to 10-300 μM H_2O_2 for 24 hr evoked a concentration-dependent increase in cell death in WT microglial cells (Fig. 3.3a). H_2O_2 -induced cell death was also dependent of exposure duration. For example, cell death induced by 300 μM H_2O_2 , increased from $35.1 \pm 3.1\%$ to $68.9 \pm 0.5\%$, $79.3 \pm 01.1\%$ and $89.1 \pm 1.8\%$ as the exposure duration was extended from 2 hr to 4, 8 and 24 hr (Fig. 3.3b). However, under these experimental conditions, there was no or modest cell death in TRPM2-KO microglial cells (Fig. 3.3c-d). As a positive control, exposure to 3 mM H_2O_2 in parallel experiments caused massive cell death that was not different between WT and TRPM2-KO microglial cells (Fig. 3.3d). Therefore, these results support that H_2O_2 can induce

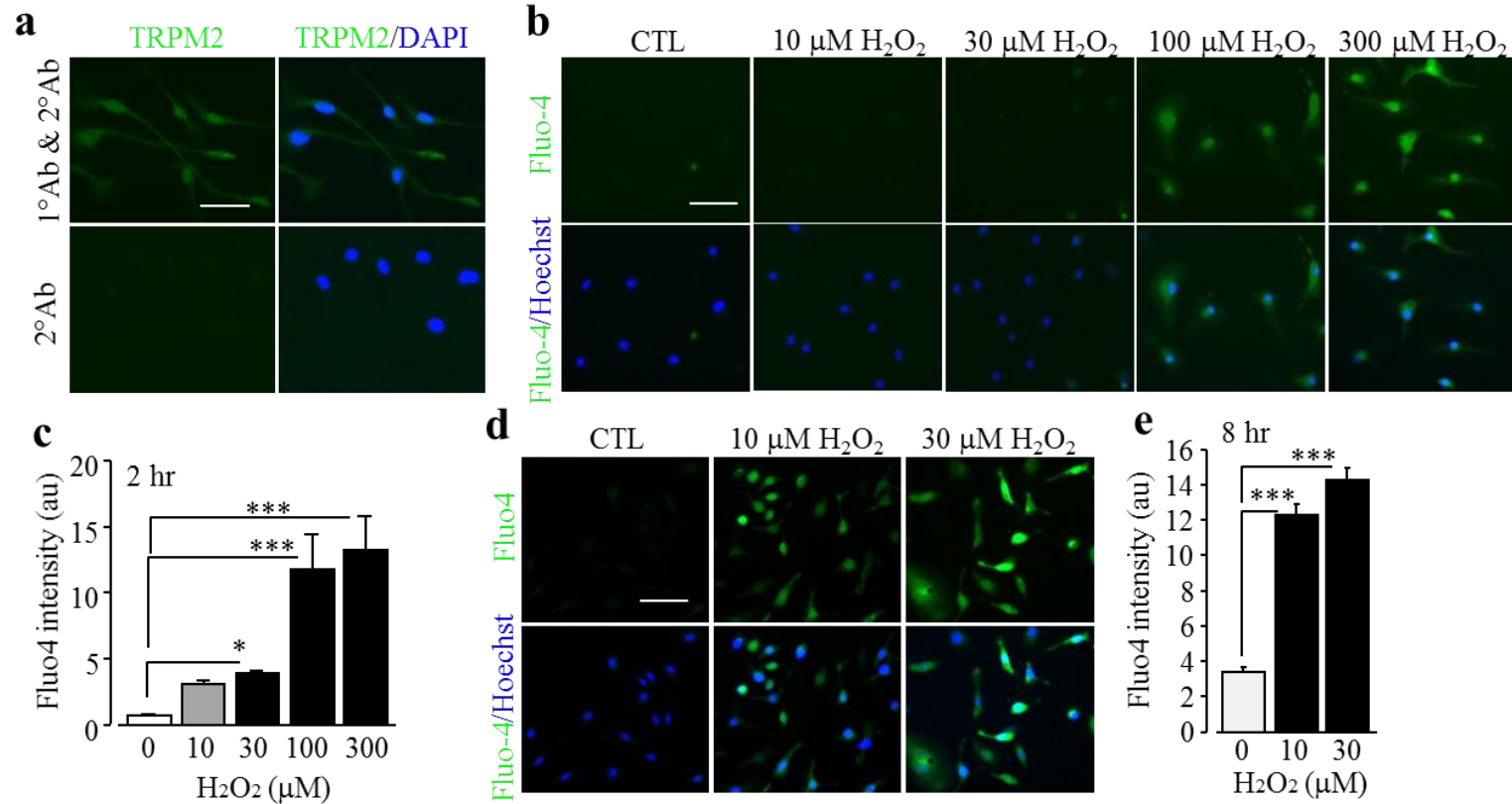


Fig. 3.1 TRPM2 expression and H₂O₂-induced increase in the [Ca²⁺]_i in microglial cells.

(a) Representative images showing TRPM2 immunoreactivity in microglial cells. Cells were counterstained with DAPI. Similar results were observed in three independent cell preparations. (b, d) Representative single cell images showing Ca²⁺ responses in microglial cells without (CTL) or with treatment of H₂O₂ at indicated concentrations for 2 hr (b) and 8 hr (d) (top row: Fluo-4 fluorescence; bottom row: counter staining with Hoechst). (c, e) Summary of the mean H₂O₂-induced Ca²⁺ responses under indicated conditions from 4 independent cell preparations using 3 wells of cells for each condition in each experiment. Scale bar, 40 µm. *, p < 0.01; ***, p < 0.005 compared to indicated control group.

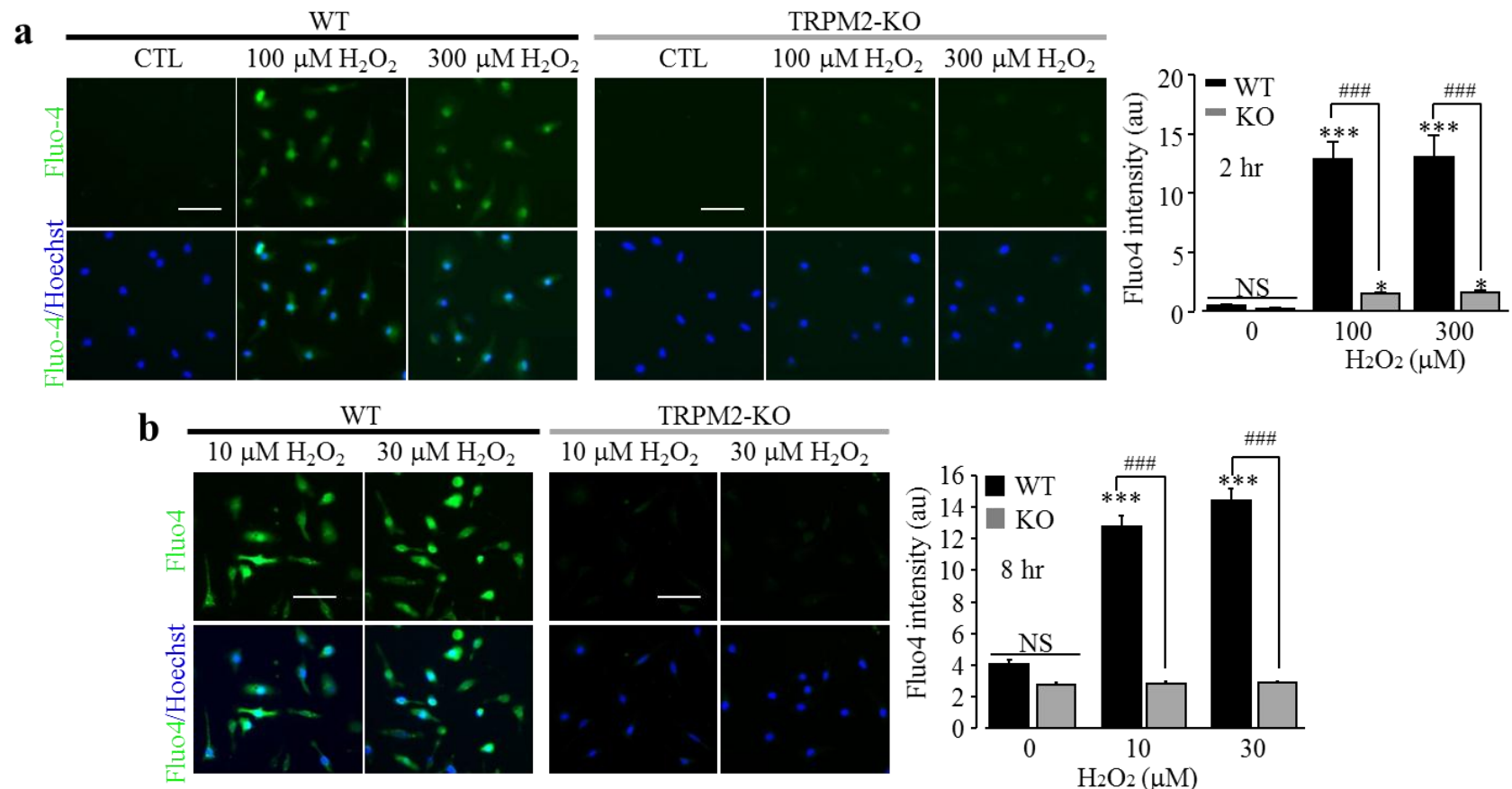
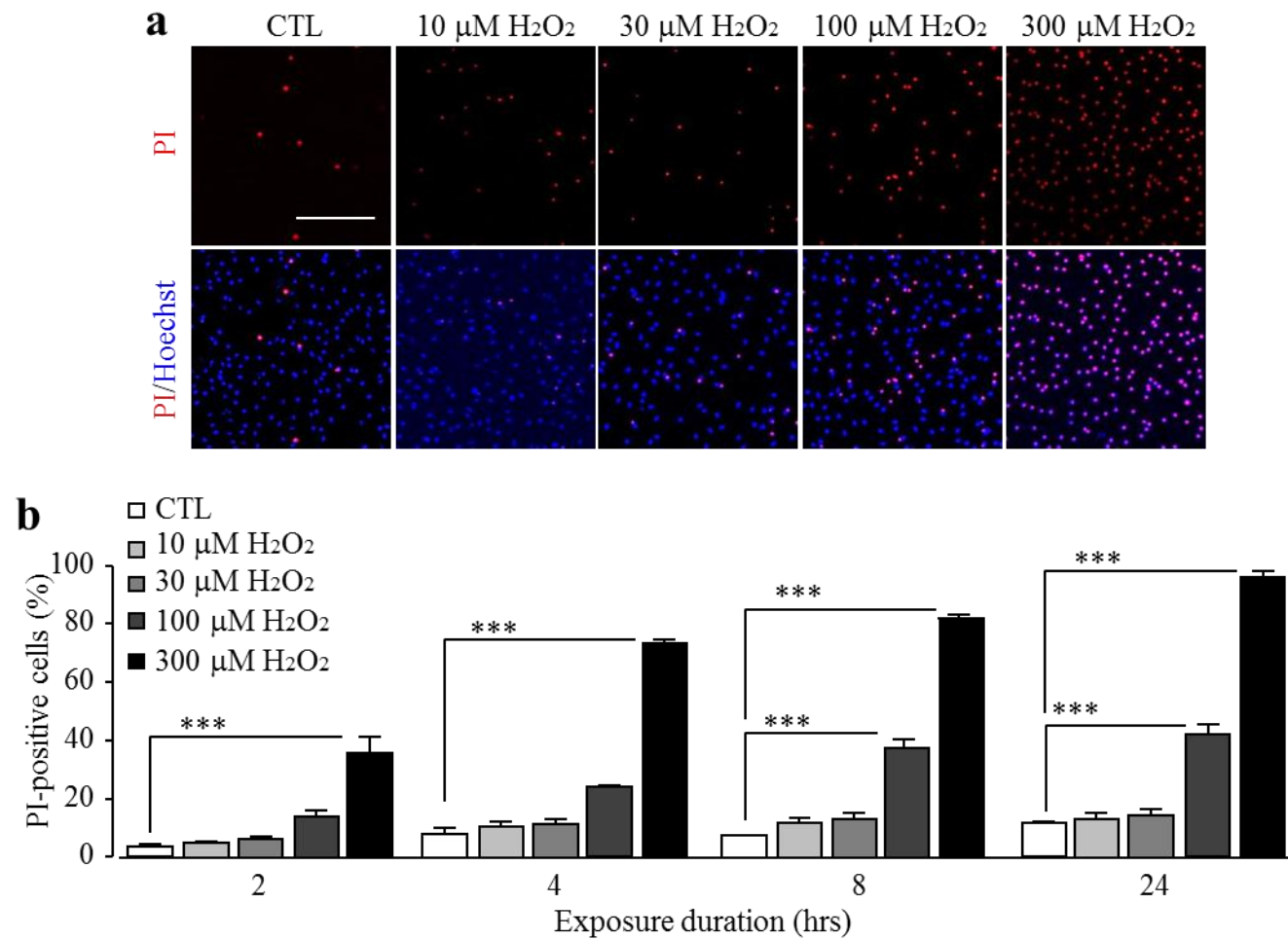


Fig. 3.2 A critical role of the TRPM2 channel in H_2O_2 -induced increase in $[\text{Ca}^{2+}]_i$ in microglial cells.

(a, b) Left, representative single cell images showing Ca^{2+} responses in microglial cells from WT and TRPM2-KO mice treated with 100 and 300 μM H_2O_2 for 2 hr (a), and 10 and 30 μM H_2O_2 for 8 hr (b) (top row: Fluo-4 fluorescence; bottom row: counter staining with Hoechst). Right, summary of the mean H_2O_2 -induced Ca^{2+} responses under indicated conditions from 4 independent cell preparations using 3 wells of cells for each condition in each experiment. Scale bar, 40 μm . ***, p < 0.005 compared to control group and, **#, p < 0.005 compared between WT and TRPM2-KO cells under the same treatment.



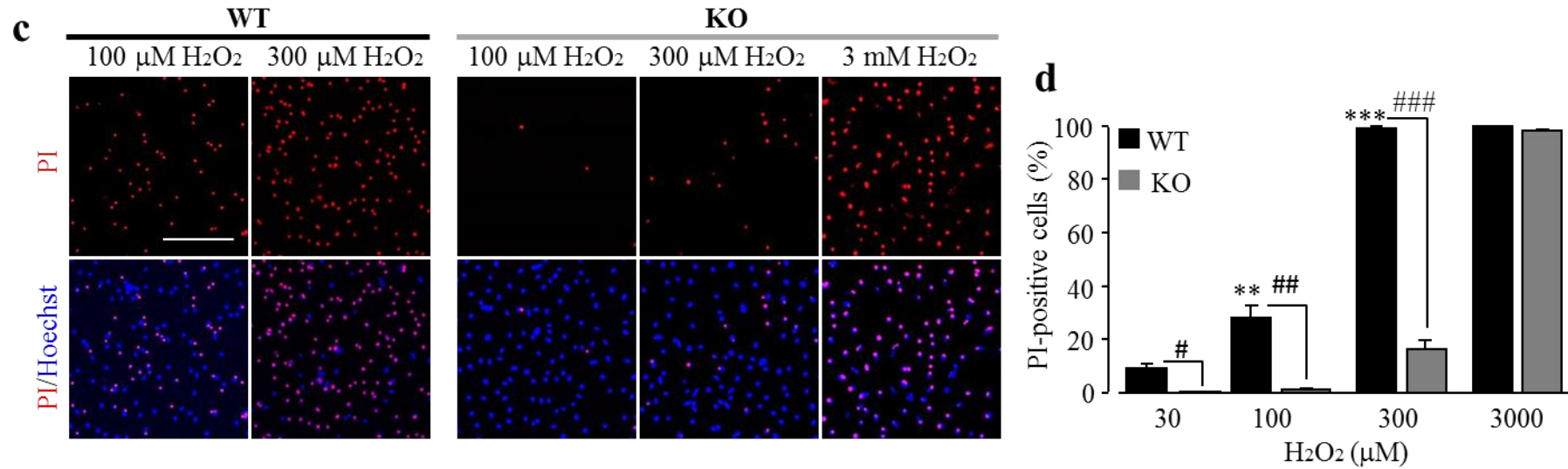


Fig. 3.3 H₂O₂ induces TRPM2 channel-dependent microglial cell death.

(a) Representative images showing microglial cell death upon exposure to H₂O₂ at indicated concentrations for 24 hr (top row: PI-stained dead cells; bottom row: all cells stained with Hoechst). (b) Summary of the mean cell death induced by exposure to H₂O₂ at indicated concentrations for 2, 4, 8 and 24 hr from 3 independent experiments, using 3 wells of cells for each condition in each experiment. (c) Representative images showing microglial cell death upon exposure to H₂O₂ at indicated concentrations for 24 hr in the WT and TRPM2-KO cells. (d) Summary of the mean H₂O₂-induced cell death under indicated conditions from 3 independent cell preparations using 3 wells of cells for each condition in each experiment. ***, p < 0.005 compared to indicated control group and, **#, p < 0.005 compared between the WT and TRPM2-KO cells under the same treatment.

microglial cell death and the TRPM2 channel plays an important role in mediating H₂O₂-induced microglial cell death.

3.2.3 TRPM2 channel in H₂O₂-induced microglial cell activation

As described in the introduction above, previous studies have provided evidence to suggest that ROS can induce changes in microglial cell morphology (Qin et al., 2004). However, it remained unclear whether TRPM2 channel plays a critical role in such a mechanism. Therefore, I firstly examined the cell morphology change in the WT microglial cells in response to H₂O₂. Under control culturing conditions, a majority of microglial cells displayed a ramified rod-like morphology and a small number of cells presented a more ramified morphology with thicker and more extensive processes (Fig 3.4a and b), indicative of resting or partially activated states. Exposure to 10-30 μM H₂O₂ for 24 hr caused microglial cells to retract their processes and develop amoeboid-like morphology, indicating that H₂O₂ induced microglial cells into a more activated state (Fig 3.4a, top). These changes induced by H₂O₂ were more observable in images captured using an EVOS microscope system with a 40X object lens (Fig 3.4b, top). Noticeably, H₂O₂-treated cells also displayed larger cell bodies compared to untreated cells (Fig 3.4a-b, top). To quantitatively evaluate such H₂O₂-induced effects, I performed computer-assisted analysis of the form factor (or circularity) and aspect ratio, as described in detail in section 2.2.5. Both parameters exhibited widespread distribution in microglial cells (Fig 3.4c, top), indicating heterogeneity in cell morphology. Nonetheless, it was evident that the mean value of form factor increased (Fig 3.4d, left), whereas the mean value of aspect ratio was progressively reduced, with the H₂O₂ concentration increasing (Fig 3.4d, right). These suggest that H₂O₂ can induce microglial cells to change from elongated with branched processes to circular shape and assume rounded morphology.

In contrast to the significant change in the morphology of WT microglial cells, exposure to 10-30 μM H₂O₂ induced no significant change in the morphology of TRPM2-KO microglial cells (Fig. 3.4 a-d). These results suggest an important role for the TRPM2 channel in determining H₂O₂-induced microglial cell activation.

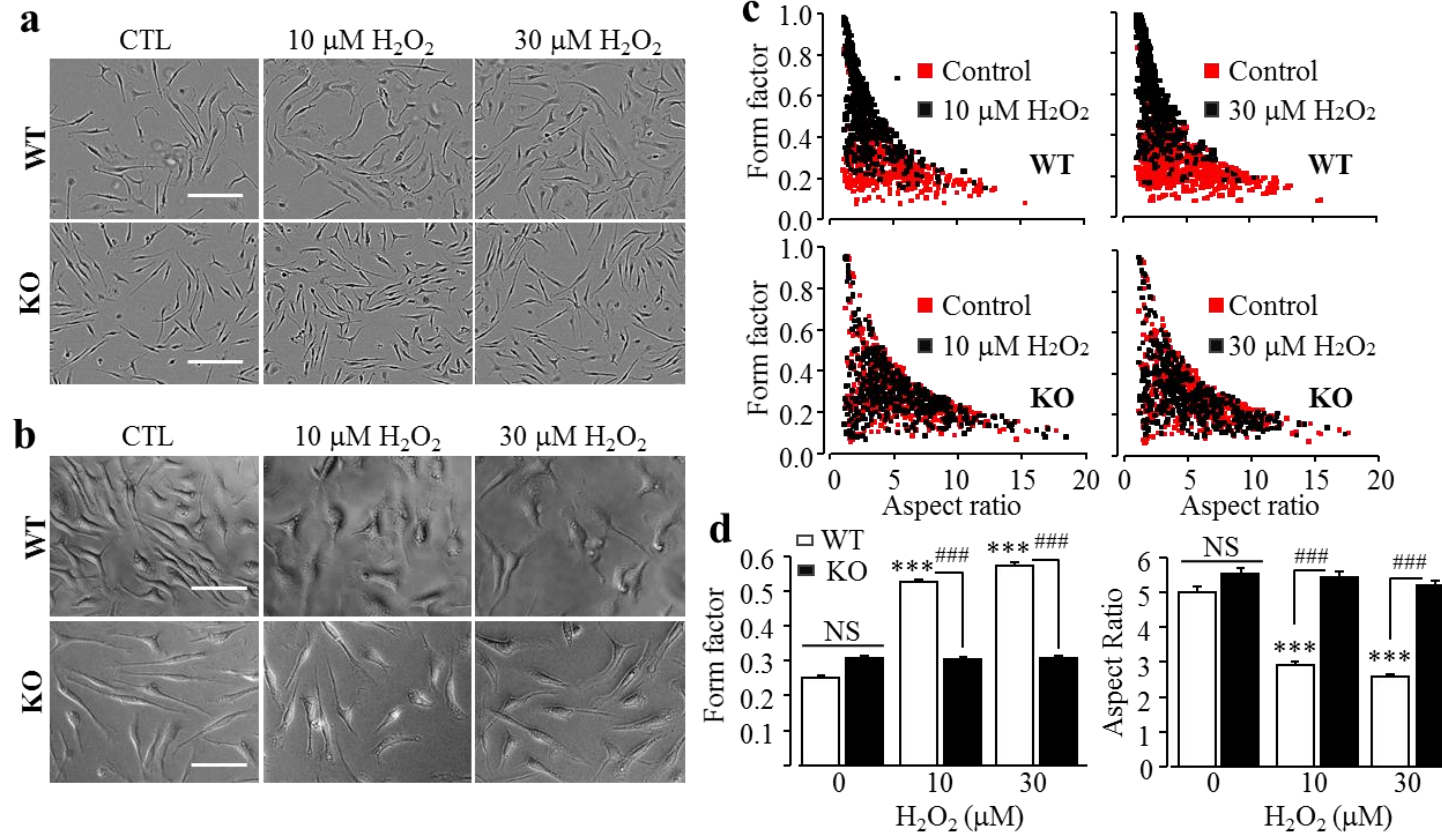


Fig. 3.4 A critical role of the TRPM2 channel in H_2O_2 -induced change in microglial cell morphology.

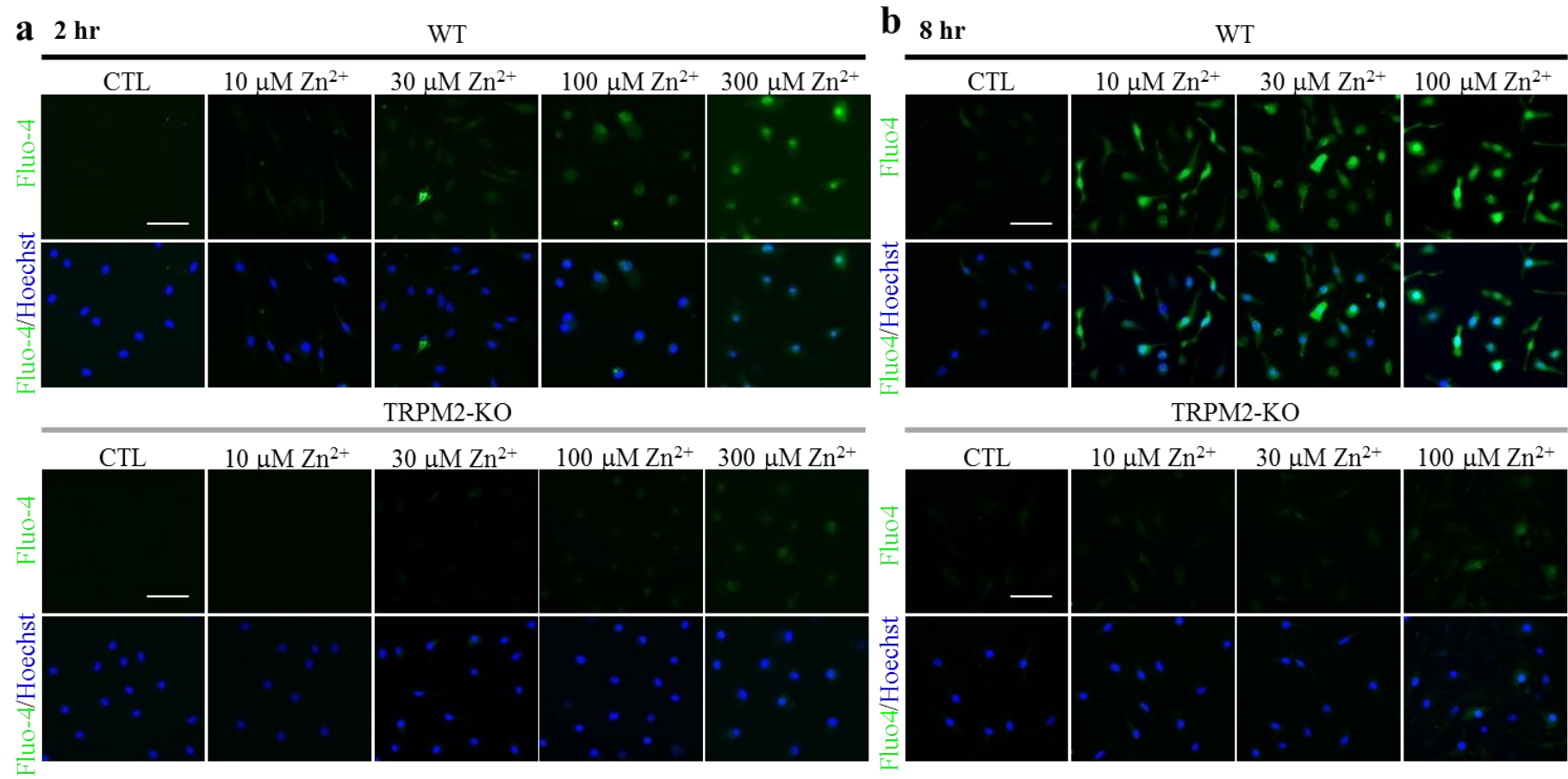
(a, b) Representative phase-contrast images showing cell morphology of WT and TRPM2-KO microglial cells without (CTL) or with exposure to H_2O_2 at indicated concentrations for 24 hr, using an Incucyte imaging system with a 10x object lens (a) and an EVOS microscope with a 40x object lens (b). (c, d) Scatter plot showing the distribution of form factor and aspect ratio values of individual cells (c), and the mean form factor (left) and aspect ratio (right) values under indicated conditions, from 4 independent cell preparations using 3 wells of cells for each condition in each experiment. Scale bar, 200 μm (a) and 50 μm (b). ***, p < 0.005 compared to control. ###, p < 0.005 compared between WT and TRPM2-KO cells under the same treatment.

3.2.4 TRPM2 channel in DAMP-induced Ca^{2+} responses

To demonstrate the role of the TRPM2 channel in microglial cell responses to Zn^{2+} , $\text{A}\beta$ and $\text{TNF-}\alpha$, I investigated whether such stimuli induce the TRPM2 channel activation by measuring the increase in the $[\text{Ca}^{2+}]_i$ in microglial cells after exposure to these stimuli, using single cell calcium imaging. Application of 10-300 μM Zn^{2+} for 2 hr resulted in a concentration-dependent increase in the $[\text{Ca}^{2+}]_i$ in WT microglial cells but failed to induce any significant increase in the $[\text{Ca}^{2+}]_i$ in TRPM2-KO microglial cells (Fig. 3.5a and c). A robust increase in the $[\text{Ca}^{2+}]_i$ induced by lower concentrations of Zn^{2+} (10-30 μM) was observed only following exposure for 8 hr and such Ca^{2+} responses were also abolished in TRPM2-KO microglial cells (Fig. 3.5b and d). Similarly to Zn^{2+} , exposure to 30-300 nM $\text{A}\beta_{42}$ for 8 hr led to a concentration-dependent increase in the $[\text{Ca}^{2+}]_i$ (Fig. 3.6a and c), which was absent in the TRPM2-KO microglial cells (Fig. 3.6a and c). Furthermore, exposure to 300 nM $\text{A}\beta_{42-1}$ elicited no Ca^{2+} response in WT microglial cells (Fig. 3.6b and d). In addition to Zn^{2+} and $\text{A}\beta_{42}$, exposure to 10-100 ng/ml $\text{TNF-}\alpha$ for 8 hr resulted in a significant increases in the $[\text{Ca}^{2+}]_i$ in WT microglial cells, but such Ca^{2+} responses were strongly attenuated in TRPM2-KO microglial cells (Fig. 3.7a-b). Taken together, these findings provide strong evidence to suggest that Zn^{2+} , $\text{A}\beta_{42}$ and $\text{TNF-}\alpha$ can activate the TRPM2 channel in microglial cells.

3.2.5 TRPM2 channel in Zn^{2+} -induced microglial cell death

As introduced above, excessive accumulation of Zn^{2+} is cytotoxic. I investigated whether microglial cell death occur after exposure to Zn^{2+} . Exposure of microglial cells to 10-300 μM Zn^{2+} for 24 hr resulted in significant and concentration-dependent cell death (Fig. 3.8a). Zn^{2+} -induced microglial cell death was strongly dependent of exposure duration which occurred at a significant level only after the duration was prolonged to 24 hr (Fig. 3.8b). Such 100-300 μM Zn^{2+} -induced cell death was largely abolished in TRPM2-KO microglial cells (Fig. 3.8c-d), demonstrating that the TRPM2 channel is critical in Zn^{2+} -induced microglial cell death. In contrast to Zn^{2+} , exposure of WT microglial cells to 30-300 nM $\text{A}\beta_{42}$ (Fig. 3.9a-b) and 10-100 ng/ml $\text{TNF-}\alpha$ (Fig. 3.9c-d) for 72 hr did not induce significant cell death.



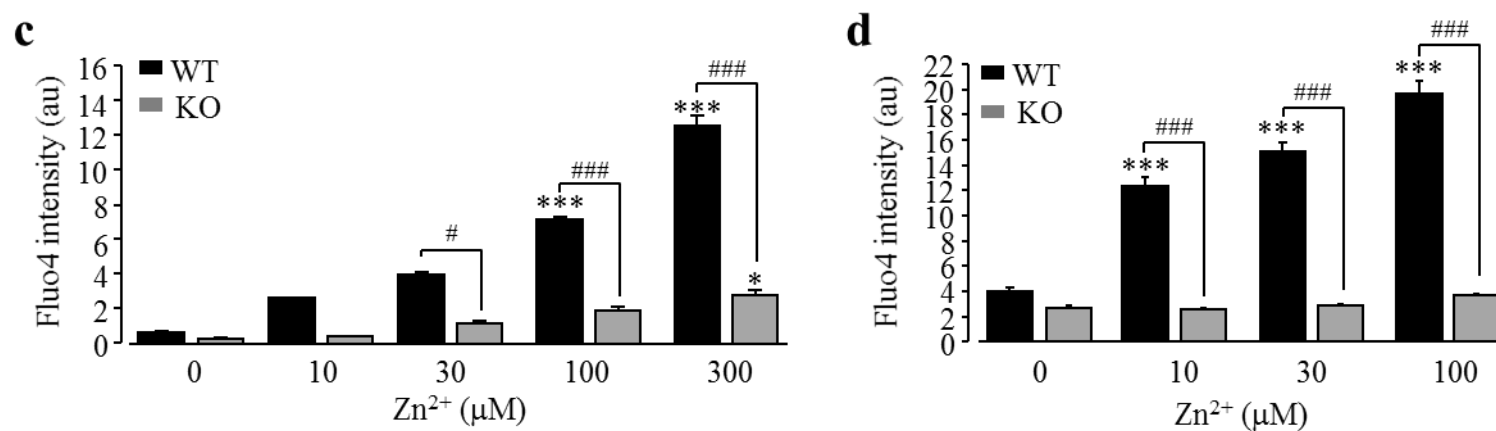
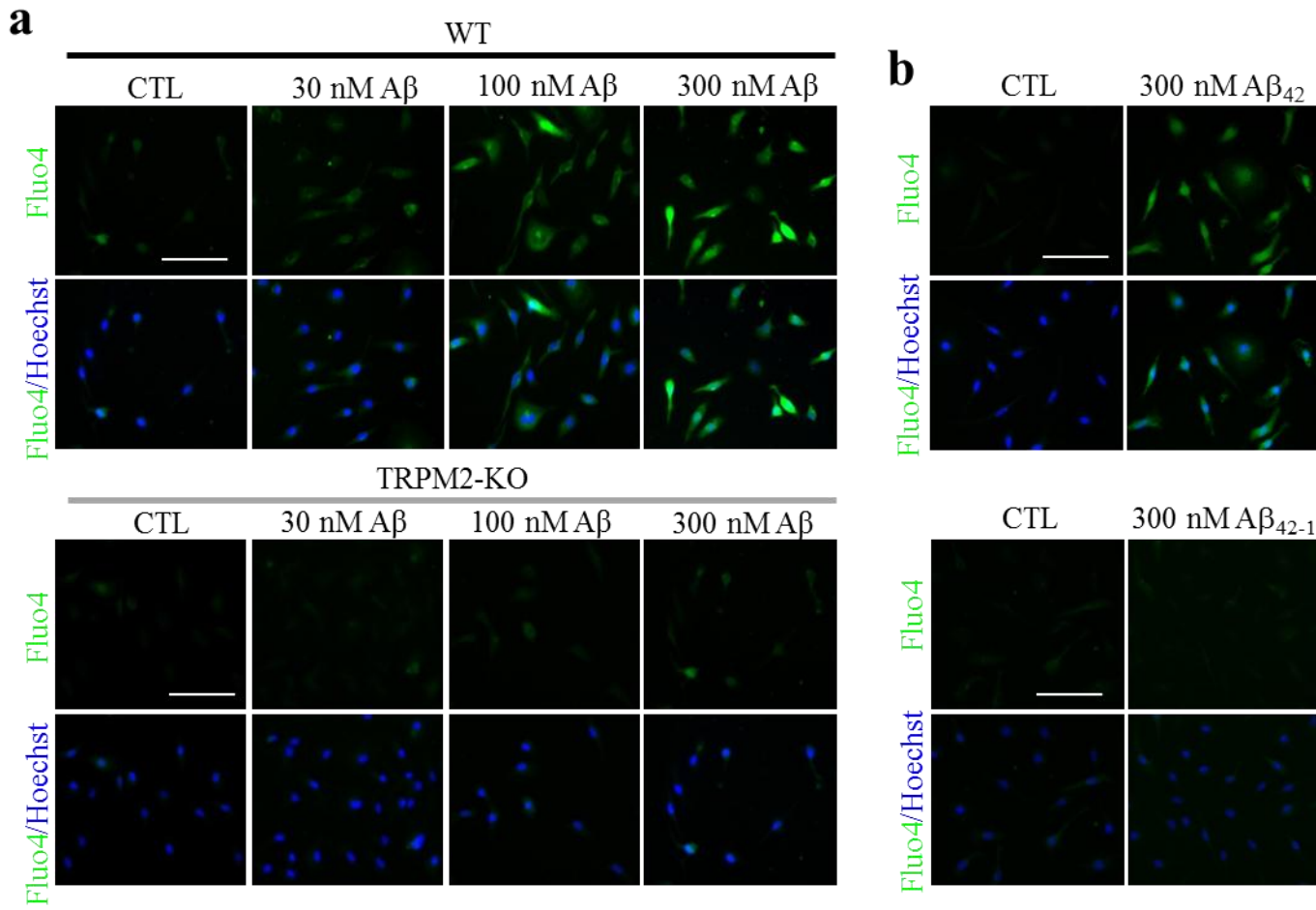


Fig. 3.5 Zn²⁺ induces TRPM2 channel-dependent increase in the [Ca²⁺]_i in microglial cells.

(a, b) Representative images showing the Ca²⁺ responses in WT and TRPM2-KO microglia cells treated with 10-300 μM Zn²⁺ for 2 hr (a) and 10-100 μM Zn²⁺ for 8 hr (b) (top row: Fluo-4 fluorescence; bottom row: counter staining with Hoechst). (c, d) Summary of the mean Ca²⁺ responses in microglial cells under indicate conditions, from 3 independent cell preparations using 3 wells of cells for each condition in each experiment. Scale bar, 40 μm. *, p < 0.01; **, p < 0.05; ***, p < 0.005 compared to control. #, p < 0.01; ###, p < 0.005 compared between WT and TRPM2-KO cells under the same treatment.



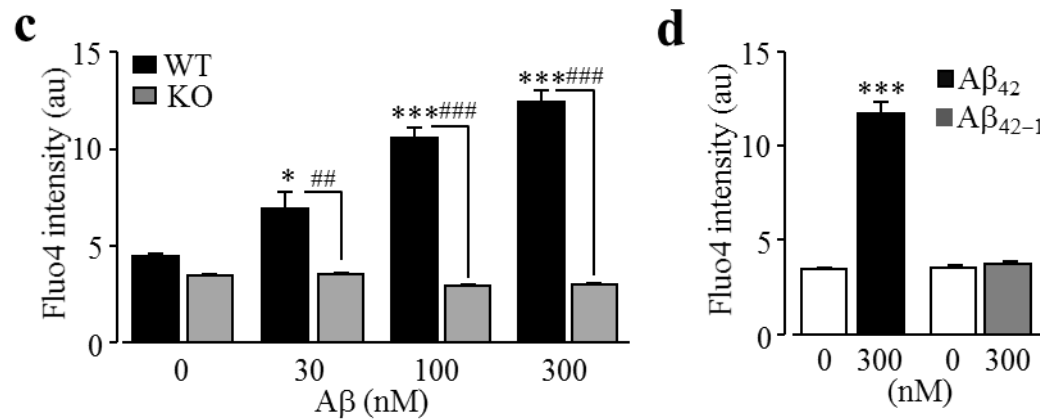


Fig. 3.6 A β_{42} induces TRPM2 channel-dependent increase in the [Ca $^{2+}$]_i in microglial cells.

(a) Representative single cell images showing intracellular Ca $^{2+}$ levels (top row: Fluo4 fluorescence; bottom row: counter staining with Hoechst) in WT and TRPM2-KO microglial cells without (CTL) and with exposure to A β_{42} at indicated concentrations for 8 hr. (b) Representative single cell images showing intracellular Ca $^{2+}$ levels in WT microglial cells (top row: Fluo-4 fluorescence; bottom row: counter staining with Hoechst) without (CTL) or with exposure for 8 hr to 300 nM A β_{42} (top) or 300 nM A β_{42-1} (bottom). (c, d) Mean intracellular Ca $^{2+}$ levels in microglial cells under the conditions indicated in (a and b), from 3 independent cell preparations using 3 wells of cells for each condition in each time. Scale bar: 40 μ m. *, p < 0.05; ***, p < 0.005 compared to control, and ##, p < 0.01; ###, p < 0.005 between WT and TRPM2-KO cells under the same treatment.

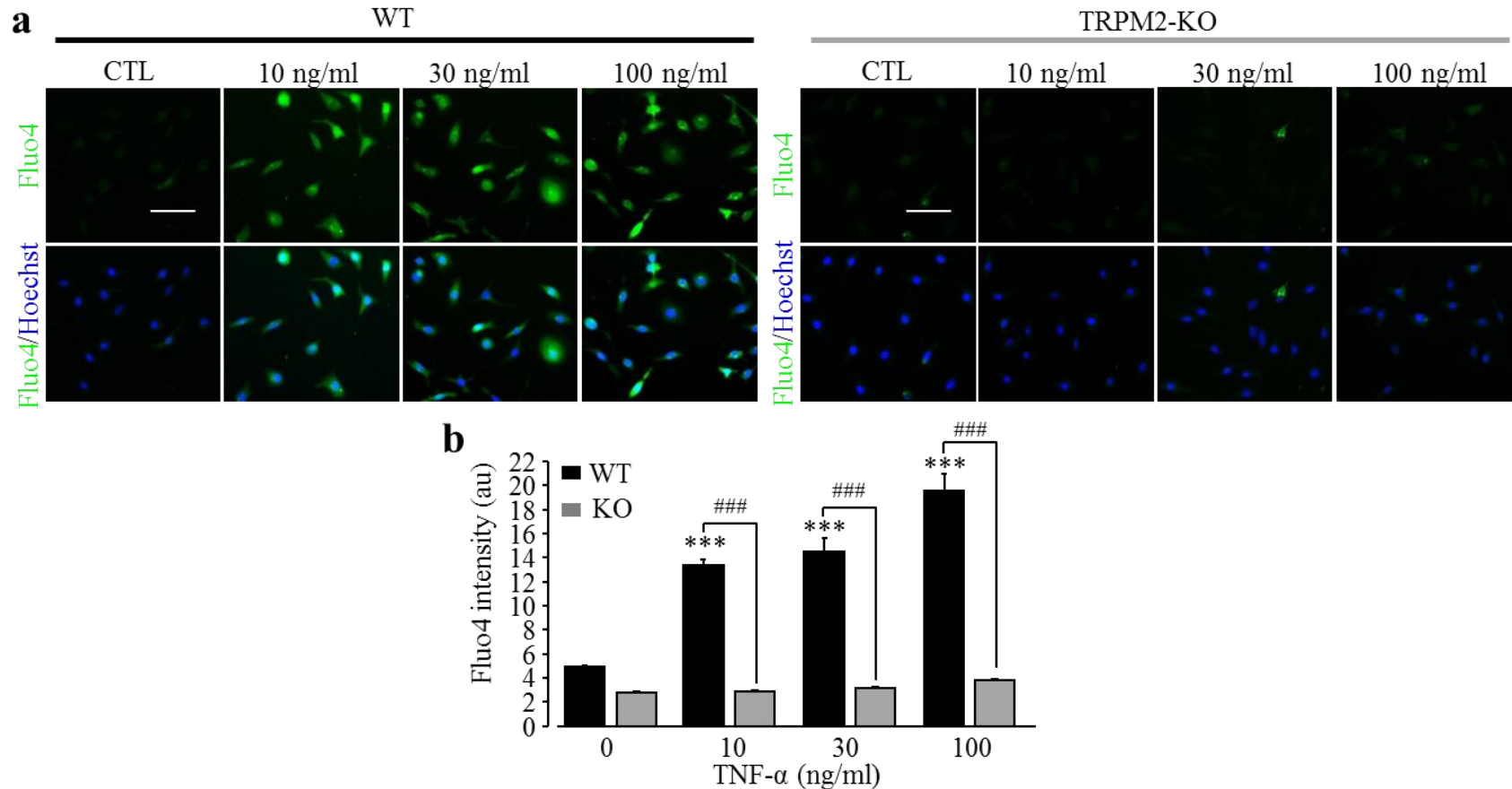
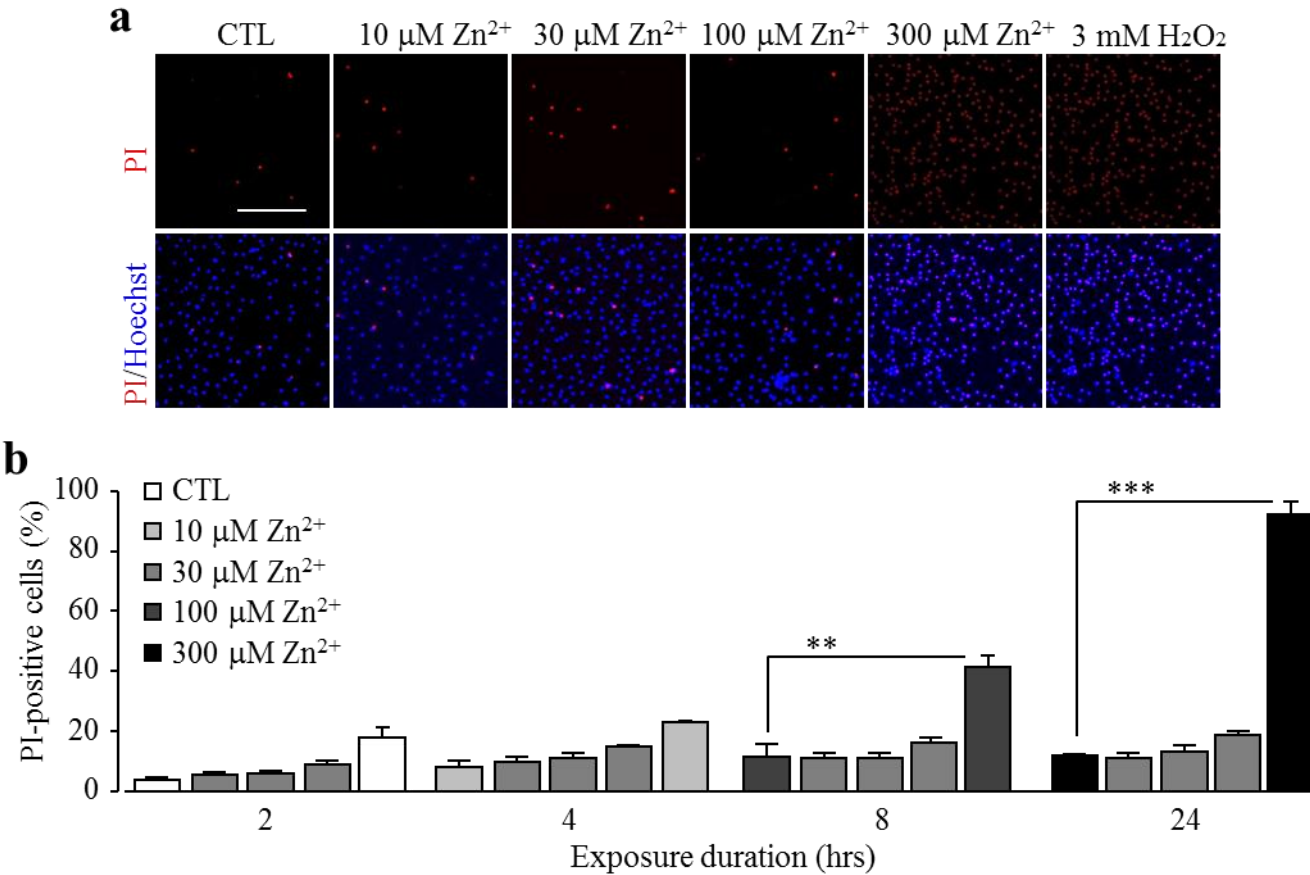


Fig. 3.7 TNF- α induces TRPM2 channel-dependent increase in the $[\text{Ca}^{2+}]_i$ in microglial cells.

(a) Representative single cell images showing intracellular Ca^{2+} levels (top row: Fluo4 fluorescence; bottom row: counter staining with Hoechst) in WT and TRPM2-KO microglial cells without (CTL) and with exposure to TNF- α at indicated concentrations for 8 hr. (b) Mean intracellular Ca^{2+} levels in microglial cells under the conditions indicated in (a), from 3 independent cell preparations using 3 wells of cells for each condition in each time. Scale bar, 40 μm . ***, p < 0.005 compared to control, and ###, p < 0.005 between WT and TRPM2-KO cells under the same treatment.



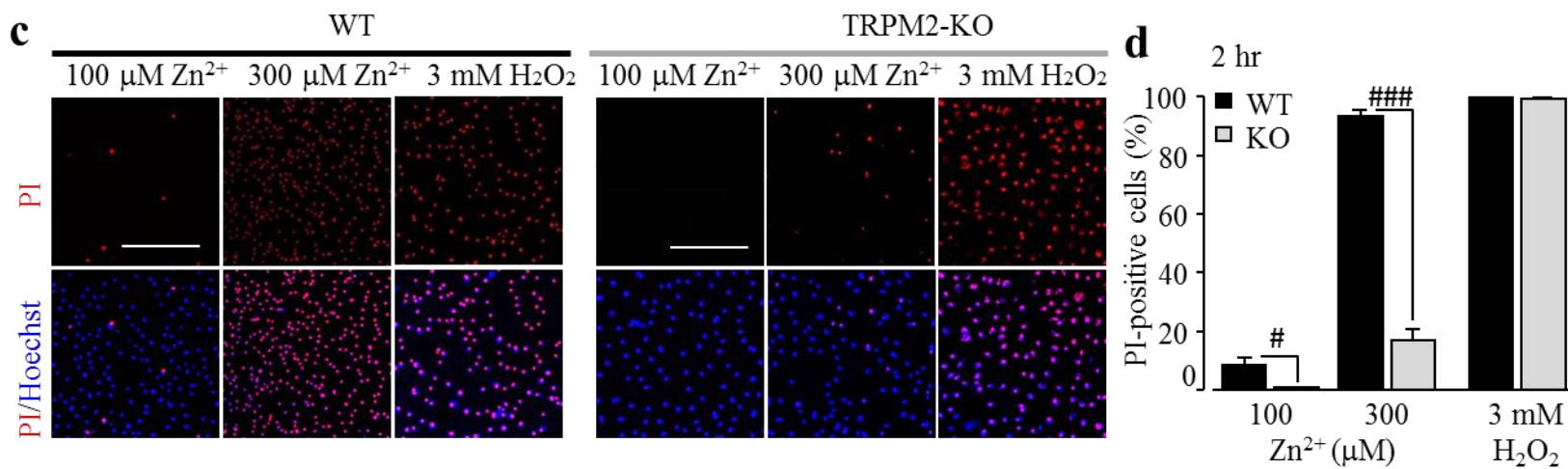


Fig. 3.8 TRPM2 channel is involved in Zn^{2+} -induced microglial cell death.

(a, c) Representative images showing microglial cell death (top row: PI-stained dead cells; bottom row: all cells stained with Hoechst) in WT cells upon exposure to 10 -300 μM Zn^{2+} (a) and in WT and KO cells upon exposure to 100 -300 μM Zn^{2+} (c). (b) Summary of the mean cell death under indicated conditions for 2, 4, 8, and 24 hr from 4 independent cell preparations using 3 wells of cells for each condition in each time. (d) Summary of the mean cell death under indicated conditions for 2 hr from 3 independent cell preparations using three wells of cells for each condition in each time. **, p < 0.05; ***, p < 0.005 compared to indicated control group and, ###, p < 0.005 compared between the WT and TRPM2-KO cells under the same treatment.

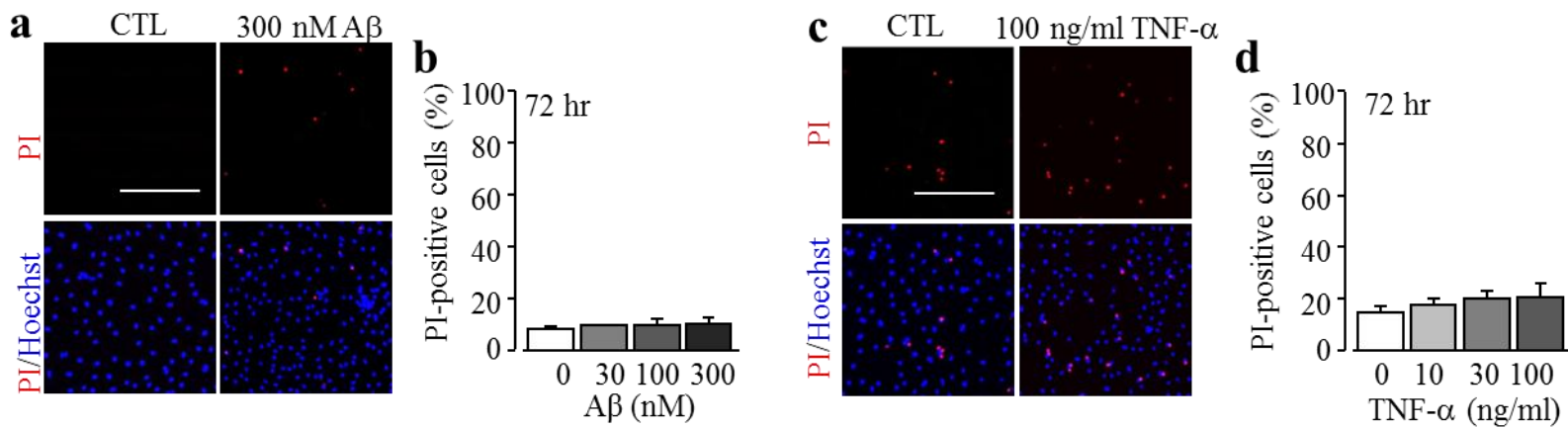


Fig. 3.9 Exposure to A β_{42} and TNF- α induces no microglial cell death.

(a, c) Representative images showing microglial cell death (top row: PI-stained dead cells; bottom row: all cells stained with Hoechst) in WT cells upon exposure for 72 hr to 300 nM A β_{42} (a) or 100 ng/ml TNF- α (c). (b, d) Summary of the mean cell death under indicated conditions from 3 independent cell preparations using 3 wells of cells for each condition in each time.

3.2.6 TRPM2 channel in DAMP-induced cell activation

Zn^{2+} , $A\beta_{42}$ and TNF- α , as mentioned above, can induce change in microglial cell morphology. However, whether the change in microglial cell morphology induced by these stimuli is mediated by the TRPM2 channel still remain unknown. Treatments with 10-30 μM Zn^{2+} for 24 hr caused significant change in the morphology of WT microglial cells, including process retraction and cell bodies enlargement that transform the cells into amoeboid-like shape (Fig. 3.10a). Consistent with the observations of the change in microglial cell morphology, the mean value of form factor increased, whereas the mean value of aspect ratio was progressively reduced, as the concentration of Zn^{2+} were elevated (Fig. 3.10b-c). Such changes were not observed in TRPM2-KO microglial cells (Fig. 3.10a-c). These findings suggest a critical role of the TRPM2 channel in Zn^{2+} -induced change in the morphology of microglial cells.

Exposure to $A\beta_{42}$ (100-300 nM) for 24 hr induces noticeable change in the morphology of WT microglial cells. The exposure to an increasing concentration of $A\beta_{42}$ induces more WT microglial cells to have a morphology with amoeboid-like shape (Fig. 3.11a). Therefore, the mean value of form factor increased, whereas the mean value of aspect ratio was progressively reduced, with the $A\beta_{42}$ concentration increasing (Figure 3.11b-c). In contrast with these remarkable change in the cell morphology induced by 300 nM $A\beta_{42}$, exposure to 300 nM $A\beta_{42-1}$ resulted in no noticeable change in the cell morphology (Fig 3.11d-e). $A\beta_{42}$ -induced changes in the cell morphology were not observed in TRPM2-KO microglial cells (Fig. 3.11a-c), suggesting that TRPM2 channel plays a crucial role in $A\beta_{42}$ -induced change in the morphology of microglial cells.

Like Zn^{2+} and $A\beta_{42}$, TNF- α at concentrations 10-30 ng/ml resulted in significant change in the morphology of WT microglial cells, with retracted processes and noticeably enlarged cell bodies (Fig 3.12a). TNF- α treated WT microglial cells exhibited rounded and larger cell bodies and short processes. On average, as the concentration of TNF- α were elevated, TNF- α induced progressive increase in the form factor whereas progressive reduction in the aspect ratio in WT microglial cells (Fig 3.12b-c). These changes were however not seen in TRPM2-KO cells (Fig 3.12a-c), consistent with the visual observation of the morphological change. These results suggest an important role of the TRPM2 channel in TNF- α -induced change in microglial cells morphology.

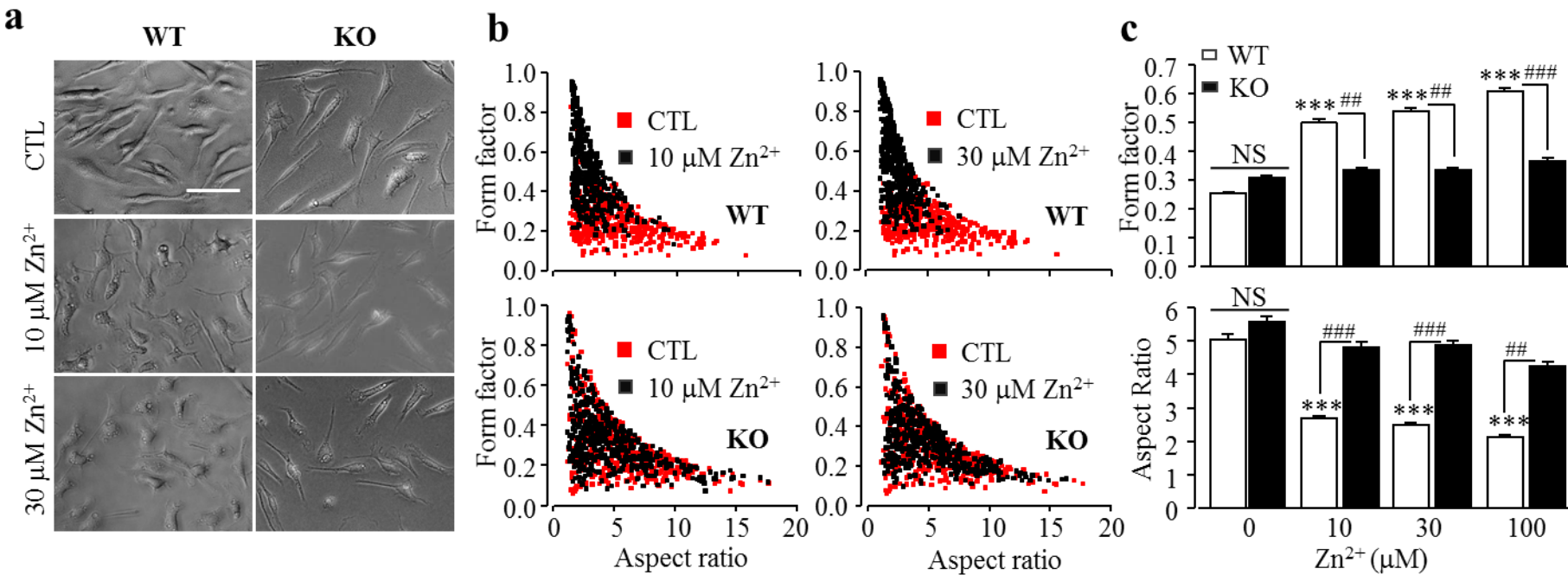
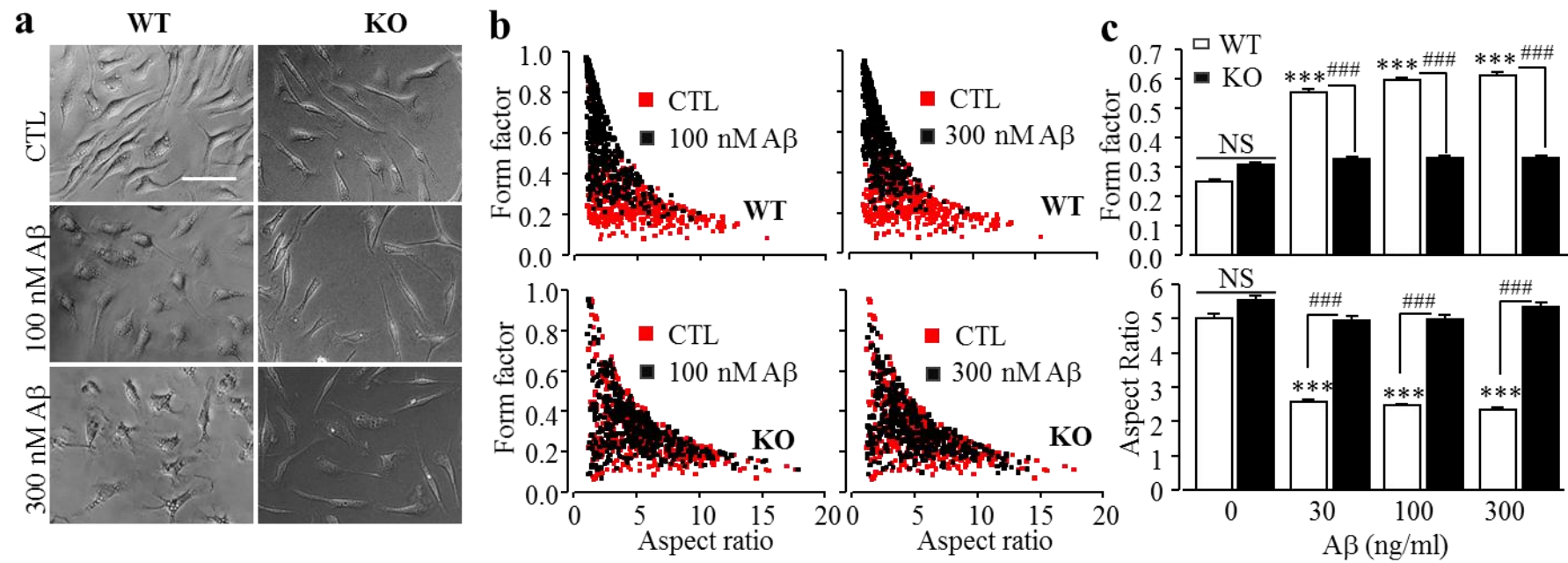


Fig. 3.10 TRPM2 channel is required for Zn²⁺-induced microglial activation.

(a) Representative phase-contrast images showing cell morphology of WT and TRPM2-KO microglial cells without (CTL) or with exposure to Zn²⁺ at indicated concentrations for 24 hr, captured using an EVOS microscope with a 40x object lens. (b, c) Scatter plot showing the distribution of form factor and aspect ratio values of individual microglial cells (b), and mean form factor (top) and aspect ratio (bottom) values for microglial cells under the conditions indicated in (a), from 3 independent cell preparations using 3 wells of cells for each condition in each experiment. Scale bar, 50 μ m. ***, p < 0.005 compared to control, and #, p < 0.01; ###, p < 0.005 compared between WT and TRPM2-KO cells under the same treatment.



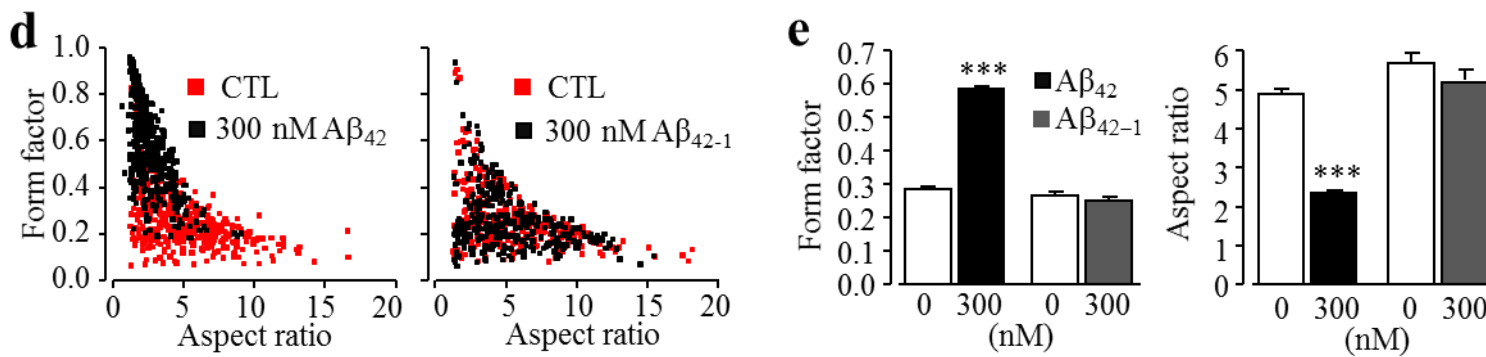


Fig. 3.11 TRPM2 channel is required for A β ₄₂-induced microglial activation.

(a) Representative phase-contrast images showing cell morphology of WT and TRPM2-KO microglial cells without (CTL) or with exposure to A β ₄₂ at indicated concentrations for 24 hr, captured using an EVOS microscope with a 40x object lens. (b, c) Scatter plot showing the distribution of form factor and aspect ratio values of individual microglial cells (b), and mean form factor (top) and aspect ratio (bottom) values for microglial cells under the conditions indicated in (a), from 3 independent cell preparations using 3 wells of cells for each condition in each experiment. (d, e) Scatter plot showing the distribution of form factor and aspect ratio values of individual microglial cells from WT mice without (CTL) or with exposure for 24 hr to 300 nM A β ₄₂ (left) or 300 nM A β ₄₂₋₁ (right), and mean form factor (left) and aspect ratio (right) values for microglial cells under indicated conditions from 3 independent cell preparations using 3 wells of cells for each condition in each experiment. Scale bar, 50 μ m. ***, p < 0.005 compared to control, and ###, p < 0.005 compared between WT and TRPM2-KO cells under the same treatment.

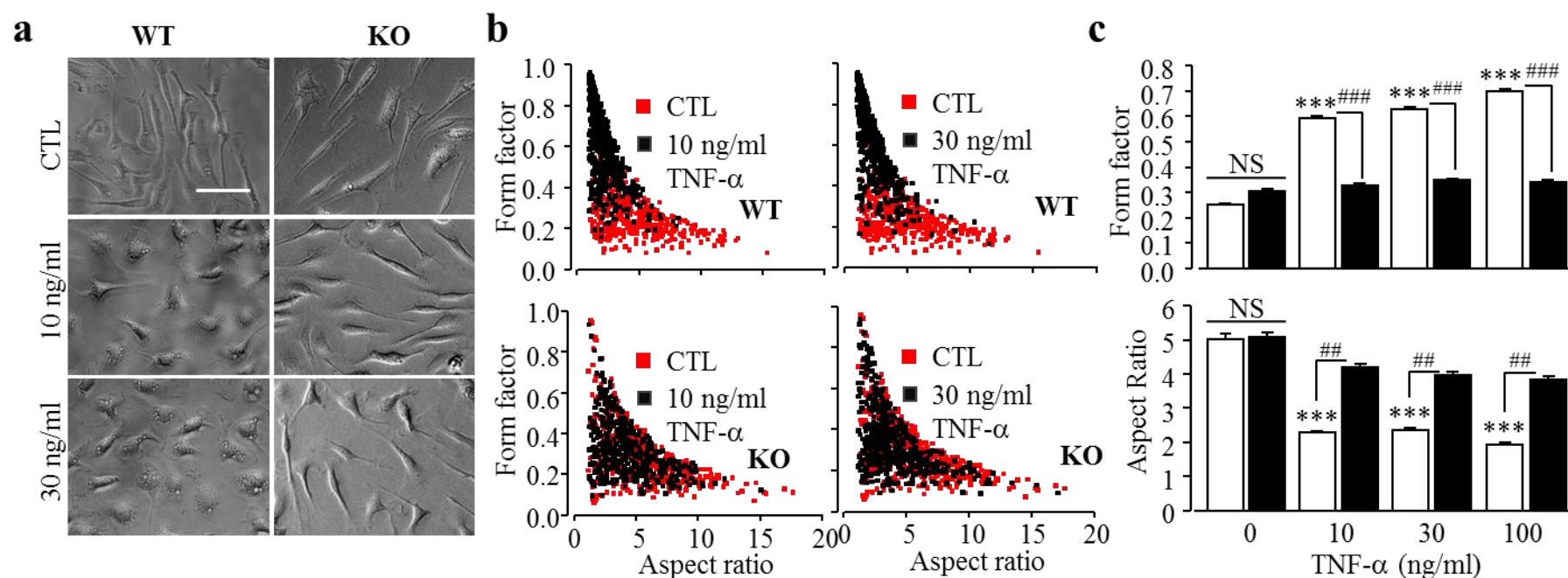


Fig. 3.12 TRPM2 channel is required for TNF- α -induced microglial cell activation.

(a) Representative phase-contrast images showing cell morphology of WT and TRPM2-KO microglial cells without (CTL) or with exposure to TNF- α at indicated concentrations for 24 hr, captured using an EVOS microscope with a 40x object lens. (b, c) Scatter plot showing the distribution of form factor and aspect ratio values of individual microglial cells (b), and mean form factor (top) and aspect ratio (bottom) values for microglial cells under the conditions indicated in (a), from 3 independent cell preparations using 3 wells of cells for each condition in each experiment. Scale bar, 50 μ m. ***, p < 0.005 compared to control, and ##, p < 0.01; ###, p < 0.005 compared between WT and TRPM2-KO cells under the same treatment.

3.3 DISCUSSION

In this chapter, studies examined the effects of TRPM2-KO on the increase in the $[Ca^{2+}]_i$, cell death and cell activation in microglial cells in response to Zn^{2+} , $A\beta_{42}$ and TNF- α as well as H_2O_2 . All these DAMP molecules induced concentration-dependently and time-dependently an increase in the $[Ca^{2+}]_i$ and cell activation. In addition, H_2O_2 and Zn^{2+} , at relatively high concentrations examined induced considerable microglial cell death (Table 3.1). Finally, all these effects were abolished or strongly inhibited by TRPM2-KO, providing evidence to suggest that the TRPM2 channel plays an important role in the Ca^{2+} signalling, cell death and cell activation in microglial cells in response to H_2O_2 , Zn^{2+} , $A\beta_{42}$ and TNF- α .

The expression of the TRPM2 channel in microglia cells has been well documented (Wehrhahn et al., 2010; Miyake et al., 2014; Kraft et al., 2004). In the present study, I confirmed the TRPM2 channel expression in microglial cells using immunofluorescent confocal microscopy (Fig. 3.1a). TRPM2 channel is a Ca^{2+} -permeable channel, and an early study reported that H_2O_2 induced an increase in the $[Ca^{2+}]_i$ in microglial cells (Kraft et al., 2004), but it was not clearly defined how important the TRPM2 channel was in such H_2O_2 -induced Ca^{2+} signalling. The present study also showed an increase in the $[Ca^{2+}]_i$ in microglial cells after exposure to 100-300 μM H_2O_2 for 2 hr (Fig. 3.1b-c). A significant increase in the $[Ca^{2+}]_i$ was induced by 10-30 μM H_2O_2 after exposure for 8 hr (Fig. 3.1d-e). Such H_2O_2 -induced time- and concentration-dependent increase in the $[Ca^{2+}]_i$ was almost completely lost in TRPM2-KO microglial cells (Fig. 3.2a-b). The findings provide strong evidence to support that the TRPM2 channel is functionally expressed and plays a major role in ROS-induced Ca^{2+} signalling in microglial cells.

There were significant increases in the $[Ca^{2+}]_i$ after exposure to 100-300 μM Zn^{2+} for 2 hr (Fig. 3.5a and c) and 10-30 μM Zn^{2+} for 8 hr (Fig. 3.5b and d). Such Zn^{2+} -induced time- and concentration-dependent increases in the $[Ca^{2+}]_i$ were abolished in TRPM2-KO microglial cells (Fig. 3.5a-d). These findings provide the first evidence to suggest that TRPM2 channel is important in mediating Zn^{2+} -induced Ca^{2+} signalling in microglial cells. Like Zn^{2+} , $A\beta_{42}$ induced strong and concentration-dependent increase in the $[Ca^{2+}]_i$ in microglial cells which was strongly dependent of TRPM2 channel expression (Fig. 3.6a and c). This finding is consistent with a previous study suggesting a critical role for the TRPM2 channel in mediating $A\beta_{42}$ induced increase in the $[Ca^{2+}]_i$ in striatal neurons (Fonfria et al., 2005). Consistently with a previous study showing

that TNF- α induces an increase in the $[Ca^{2+}]_i$ in monocytes by activating the TRPM2 channel (W. Zhang et al., 2006), TNF- α induced TRPM2-dependent increase in the $[Ca^{2+}]_i$ in microglial cells (Fig. 3.7a-b). Collectively, these results indicate a crucial role of TRPM2 channel in mediating the Ca^{2+} signalling induced by Zn^{2+} , $A\beta_{42}$ and TNF- α in microglial cells.

As introduced above, there is extensive evidence suggesting a crucial role for the TRPM2 channel in ROS-induced cell death in diverse cell types. In the present study, pathologically relevant concentrations of H_2O_2 (Coombes et al., 2011) caused considerable microglial cell death (Fig. 3.3a-b). Such detrimental effect was abolished by TRPM2-KO (Fig. 3.3c-d), indicating a critical role for the TRPM2 channel in mediating ROS-induced microglial cell death. It is well-known that excessive Zn^{2+} is highly cytotoxic, particularly to neuronal cells (Berry and Toms, 2006; Li et al., 2015; Hara et al., 2015). In the current study, Zn^{2+} at concentrations observed in I/R-induced brain damage and epilepsy (Sloviter, 1985; Koh et al., 1996), evoked significant microglial cell death (Fig. 3.8a-b). Such cell death was absent in TRPM2-KO microglial cells (Fig. 3.8c-d), supporting a critical role of the TRPM2 channel in Zn^{2+} -induced microglial cell death. An increase in the $[Ca^{2+}]_i$ in microglial cells was observed after exposure to Zn^{2+} for 2 hr but cell death occurred after exposure to Zn^{2+} for 24 hr, but not 2-8 hr (Fig. 3.8b). These findings suggest possible involvement of additional signalling pathways as positive feedback mechanisms that are responsible for such delayed cell death, which will be explored in the next chapter.

As discussed in the Introduction chapter, ROS production is one of the common events involved in mediating the change in morphology of microglial cells in response to the DAMPs molecules examined in this study. Consistently, the 10-30 μM H_2O_2 induced a significant change in the morphology of microglial cells (Fig. 3.4a-d). H_2O_2 -induced change in the cell morphology was prevented by TRPM2-KO (Fig. 3.4a-d), suggesting an important role of the TRPM2 channel in H_2O_2 -induced change in the morphology of microglial cells. Previous studies showed that exposure of microglial cells to Zn^{2+} , $A\beta$ and TNF- α induce change in the morphology of microglial cells (Kauppinen et al., 2008; Ostapchenko et al., 2015; Kauppinen and Swanson, 2005). Consistently, the studies presented in this chapter have shown that Zn^{2+} (10-30 μM), $A\beta_{42}$ (100-300 nM) and TNF- α (10-100 ng/ml) induced significant changes in the morphology of microglial cells. Furthermore, studies here show that such changes in the morphology of microglial cells were completely inhibited by TRPM2-KO (Figs. 3.9a-c,

3.10a-c, 3.11a-c). Collectively, these findings demonstrate that TRPM2 channel is crucial in mediating the change in morphology of microglial cells in response to Zn²⁺, Aβ₄₂ and TNF-α.

In conclusion, the study presented in this chapter provides genetic evidence to demonstrate a crucial role for the TRPM2 channel in mediating the Ca²⁺ signalling induced by Zn²⁺, Aβ₄₂ and TNF-α as well as H₂O₂. The present study has also revealed that the TRPM2 channel plays an important role in microglial cell death induced by H₂O₂ and Zn²⁺. Furthermore, the present study suggests that TRPM2 channel is critical in mediating microglial cell activation induced by H₂O₂, Zn²⁺, Aβ₄₂ and TNF-α. The next chapters will explore the signalling mechanisms underlying TRPM2 channel-mediated microglial cell death induced by H₂O₂ and Zn²⁺ (chapter 4) and TRPM2-mediated microglial cell activation in response to Aβ₄₂ and TNF-α in the context of neuroinflammation (chapters 5 and 6).

Table 3.1 Summary of the TRPM2 channel in microglial cell responses against various DAMP molecules.

DAMP molecules	Cell responses
H ₂ O ₂ (10-300 μM)	Increase in the [Ca ²⁺] _i (10-300 μM) Cell death at high concentration (100-300 μM) Change in cell morphology at low concentration (10-30 μM)
Zinc (10-300 μM)	Increase in the [Ca ²⁺] _i (10-300 μM) Cell death at high concentration (300 μM) Change in cell morphology at low concentration (10-30 μM)
Aβ ₄₂ (30-300 nM)	Increase in the [Ca ²⁺] _i (30-300 nM) Change in cell morphology (100-300 nM)
TNF-α (10-100 ng/ml)	Increase in the [Ca ²⁺] _i (10-100 ng/ml) Change in cell morphology (10-30 ng/ml)

CHAPTER 4

SIGNALLING MECHANISMS FOR H₂O₂- AND ZN²⁺-INDUCED

TRPM2-MEDIATED MICROGLIAL CELL DEATH

4.1 INTRODUCTION

Extensive research has reported on Zn^{2+} -induced neuronal toxicity. Studies presented in the previous chapter showed that Zn^{2+} as well as H_2O_2 induce microglial cell death and further suggest a critical role for the TRPM2 channel in Zn^{2+} - and H_2O_2 -induced microglial cell death. Nevertheless, the signalling mechanisms responsible for Zn^{2+} - and H_2O_2 -induced TRPM2 channel activation and subsequently cell death in microglial cell are still not fully elucidated. Previous studies have shown that Zn^{2+} can induce cytotoxicity via activation of multiple key players, including PKC, NOX, PARP and extracellular signal-regulated kinase (ERK) (Koh, 2001; Kim and Koh, 2002; Suh et al., 2007; Seo et al., 2001). As discussed in the Introduction chapter, PKC activates NOX by promoting translocation of the cytosolic subunits to the plasma membrane (Benna et al., 1997; Reeves et al., 1999; Min et al., 2004). Moreover, previous studies have provided evidence to show NOX as the main source for ROS generation (Qiu et al., 2016; Santos et al., 2016). Zn^{2+} induces NOX-dependent ROS production has been demonstrated in microglial cells (Wu et al., 2012). NOX1, NOX2 and NOX4 are widely expressed in the CNS, including microglial cells.

Similarly to H_2O_2 , Zn^{2+} stimulates PARP-1 activation (Kauppinen et al., 2008; Suh et al., 2007) but it remains elusive how this occurs. An early study suggests that the mitogen-activated protein kinase (MAPK) signalling pathway is important in mediating oxidative stress-induced cell death (Lander, 1997). There is evidence from a recent study to suggest that ROS can activate PARP-1 via extracellular signal-regulated kinase (ERK) (Domercq et al., 2013). In oligodendrocyte and differentiated PC12 neuronal cells, an elevation in the $[Zn^{2+}]_i$ stimulates ERK phosphorylation and activation (Seo et al., 2001; Y.M. Zhang et al., 2006) and, depending on the severity of stimulation and cell types, ERK activation promotes cell death or survival (Seo et al., 2001; Domercq et al., 2011; Domercq et al., 2013). The MEK, phosphorylates and thereby activates the ERK. In addition, it has been shown that the protein tyrosine kinase PYK2 can trigger the MEK/ERK signalling pathway (Yao et al., 2009). PYK2 is highly expressed in the CNS, including in microglial cells (Rolon-Reyes et al., 2015) and sensitive to activation by Ca^{2+} . Furthermore, TRPM2-mediated Ca^{2+} influx or increase in the $[Ca^{2+}]_i$ activates the PYK2/MEK/ERK signalling pathway in monocytes (Yamamoto et al., 2008). The experiments presented in this chapter aim to investigate the signalling mechanisms by which H_2O_2 and Zn^{2+} activates the TRPM2 channel leading to microglial cell death.

4.2 RESULTS

4.2.1 TRPM2 channel in H_2O_2 -induced Ca^{2+} influx in microglial cells

As shown in chapter 3 (section 3.2.1), genetic knockout of the TRPM2 channel expression prevented H_2O_2 -induced increase in the $[Ca^{2+}]_i$ in microglial cells. In this chapter, I further examined the role of TRPM2 channel in mediating H_2O_2 -induced Ca^{2+} signalling in microglial cells by using single cell calcium imaging to measure H_2O_2 -induced increase in the $[Ca^{2+}]_i$ in extracellular Ca^{2+} -containing and Ca^{2+} -free solutions. In contrast with the robust calcium responses in Ca^{2+} -containing solution, H_2O_2 evoked negligible increase in the $[Ca^{2+}]_i$ in Ca^{2+} -free solution (Fig. 4.1a), indicating predominant origin from extracellular Ca^{2+} influx. The increase in the $[Ca^{2+}]_i$ in microglial cells induced by 300 μM H_2O_2 was significantly attenuated in cells pre-loaded with BAPTA-AM, a Ca^{2+} chelator (Fig. 4.1b). Taken together, these findings suggest that TRPM2 channel plays a role in H_2O_2 -induced Ca^{2+} signalling via mediating Ca^{2+} influx.

4.2.2 Effects of TRPM2 channel inhibitors on H_2O_2 -induced microglial cell death

H_2O_2 -induced microglial cell death was prevented in TRPM2-KO microglial cells (section 3.2.2). Here, I investigated the role of TRPM2 channel-mediated Ca^{2+} signalling in mediating H_2O_2 -induced microglial cell death. H_2O_2 -induced microglial cell death was attenuated by pretreatment with BAPTA-AM at 1 μM , but not at lower concentrations (10-100 nM) (Fig. 4.2a). Moreover, H_2O_2 -induced microglial cell death was strongly inhibited by 100 μM 2-APB, a TRPM2 channel inhibitor (Fig. 4.2b). Therefore, the results from genetic knockout of the TRPM2 channel expression (section 3.2.1-3.2.2) and pharmacological inhibition of the TRPM2 channel function have provided consistent evidence to support a role for the TRPM2 channel, particularly TRPM2 channel-mediated Ca^{2+} influx, contributes in mediating H_2O_2 -induced microglial cell death.

4.2.3 PARP-1 in H_2O_2 -induced microglial cell death

An increase in the PARP activity represents a major mechanism by which oxidative stress induces ADPR generation and subsequent TRPM2 channel activation

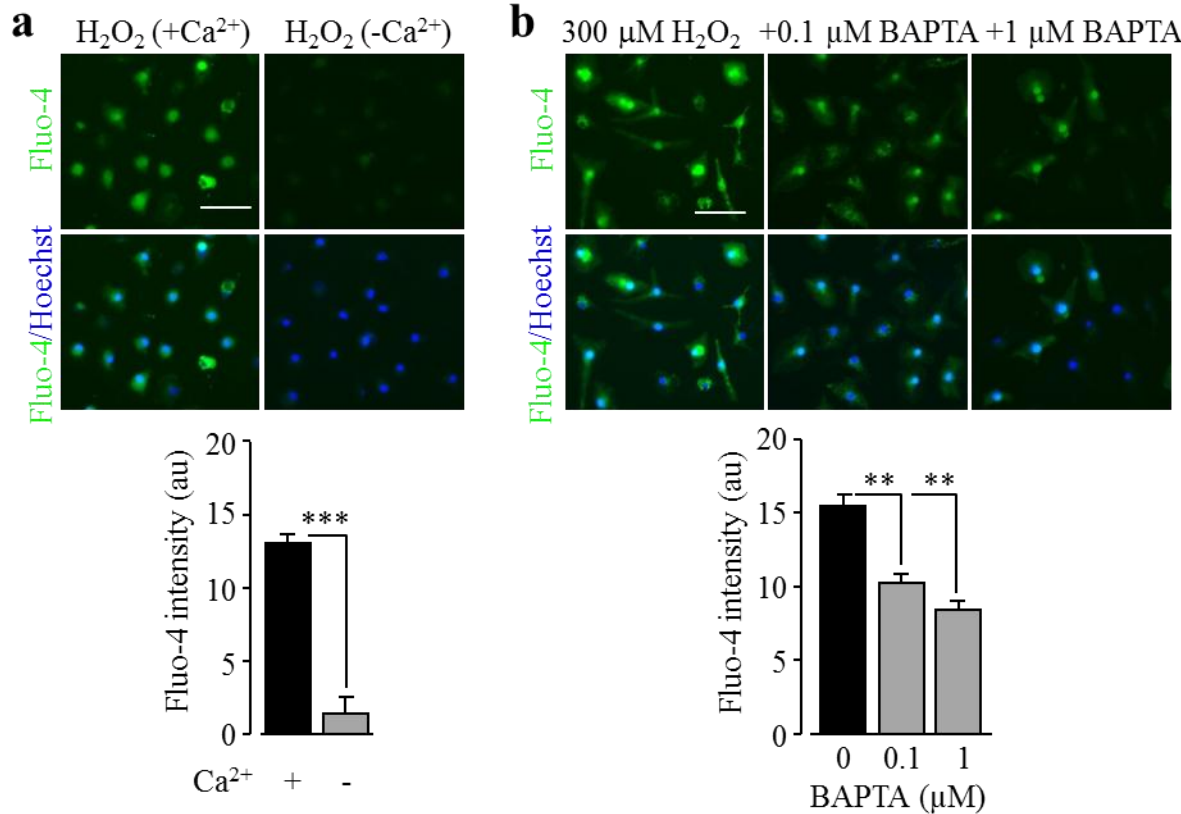


Fig. 4.1 TRPM2 channel is required for H_2O_2 -induced Ca^{2+} signalling in microglial cells.

(a, b) Top, representative single cell images showing Ca^{2+} responses in microglial cells (top row: Fluo-4 fluorescence; bottom row: counter staining with Hoechst). Bottom, summary of the mean H_2O_2 -induced Ca^{2+} responses under indicated conditions for 2 hr from 4 independent experiments, using 3 wells of cells for each condition in each experiment. The conditions are as follows: cells treated with 300 μM H_2O_2 in the presence and absence of Ca^{2+} in extracellular solutions (a) and 300 μM H_2O_2 with treatment of 0.1 and 1 μM BAPTA-AM (b). Cells were treated with BAPTA-AM for 30 min prior to and during exposure to H_2O_2 . Scale bar, 40 μm . **, $p < 0.01$; ***, $p < 0.005$ compared to indicated control group.

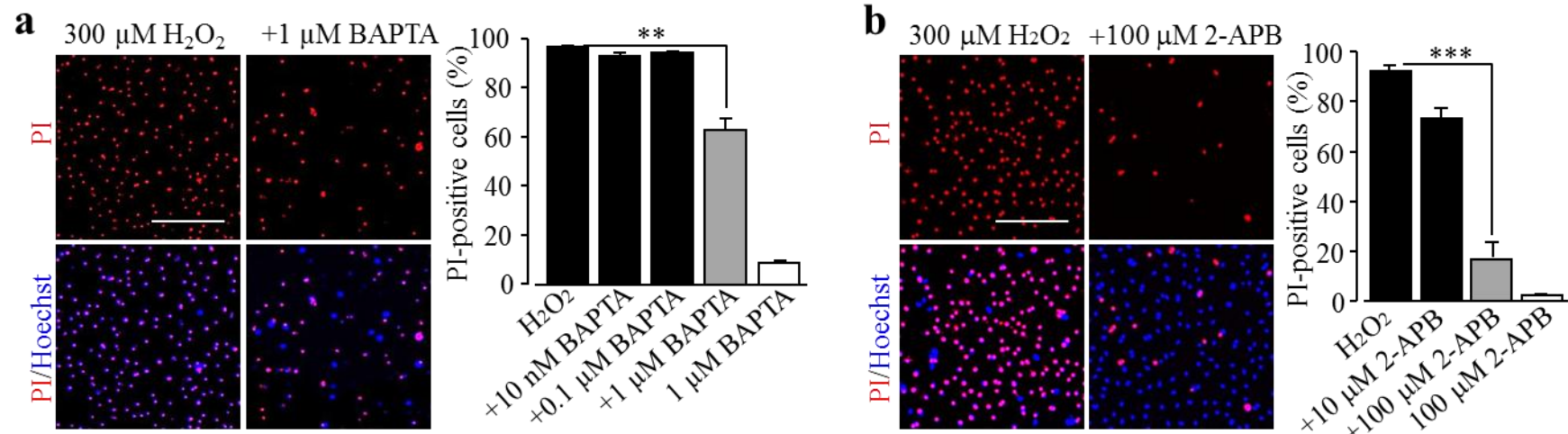


Fig. 4.2 TRPM2 channel-mediated calcium signalling in H_2O_2 -induced microglial cell death.

(a-b) Left, representative images showing microglial cell death (top row: PI-stained dead cells; bottom row: all cells stained with Hoechst). Right, mean H_2O_2 -induced cell death under following conditions: cells were exposed for 24 hr to 300 $\mu\text{M H}_2\text{O}_2$ without or with treatment with 0.01-1 μM BAPTA-AM (a) or 10-100 μM 2-APB (b). Cells were treated with BAPTA-AM or 2-APB for 30 min prior to and during exposure to H_2O_2 . Cells were also treated with each inhibitor at the higher concentration used alone without exposure to H_2O_2 . (a-b) The mean data were from 4 independent experiments, using 3 wells of cells for each condition in each experiment. Scale bar, 20 μm . **, $p < 0.01$; ***, $p < 0.005$ compared to control.

(Jiang et al., 2010). Therefore, I moved on to firstly examine the effect of PARP inhibitors on H₂O₂-induced microglial cell death, using PI staining. H₂O₂-induced cell death was considerably suppressed by PJ34 (Fig. 4.3a) or DPQ (Fig. 4.3b), two structurally different PARP inhibitors, supporting a critical role of PARP in TRPM2 channel-mediated H₂O₂-induced microglial cell death.

To provide direct evidence to show H₂O₂ induces PARP activation, I performed immunofluorescence staining using an antibody that recognizes PAR, the product of PARP activity. Exposure to H₂O₂ for 2 hr stimulated substantial PAR production in microglial cells (Fig. 4.3c). Furthermore, the PAR staining was highly concentrated in the nucleus, as evidenced by the co-localization with DAPI nuclear staining, highly consistent with activation of PARP-1, the major PARP isoform in the nucleus (Kauppinen and Swanson, 2005). H₂O₂-induced PAR production, as anticipated, was almost completely inhibited by PJ34 (Fig. 4.3d). These results collectively provide strong evidence to support that exposure to H₂O₂ stimulates the PARP-1 activity which is important in TRPM2 channel activation in microglial cells.

4.2.4 Effects of PKC/NOX inhibitors on H₂O₂-induced cell death

Next, I performed experiments to investigate the upstream signalling mechanisms, particularly those generating ROS, which stimulates PARP-1. Previous studies showed that PKC and NOX are crucial in the production of ROS (Noh and Koh, 2000; Koh, 2001). It is therefore possible that PKC and NOX play a role in facilitating H₂O₂-induced TRPM2-mediated microglial cell death. The effects of PKC and NOX inhibitors on H₂O₂-induced PARP-1 activity and cell death in microglial cells were investigated by PAR immunofluorescence and PI staining, respectively. H₂O₂-induced PAR production and microglial cell death were completely insensitive to chelerythrine chloride (CTC), a potent PKC inhibitor (Fig. 4.4a-d) and DPI, a generic NOX inhibitor (Fig. 4.4e and g) and GKT137831, a NOX1/4 selective inhibitor (Fig. 4.4f and h). These results indicate that H₂O₂ induced microglial cell death via stimulating the PARP-1 activity and subsequently TRPM2 channel activation, independent of the PKC/NOX signalling pathway.

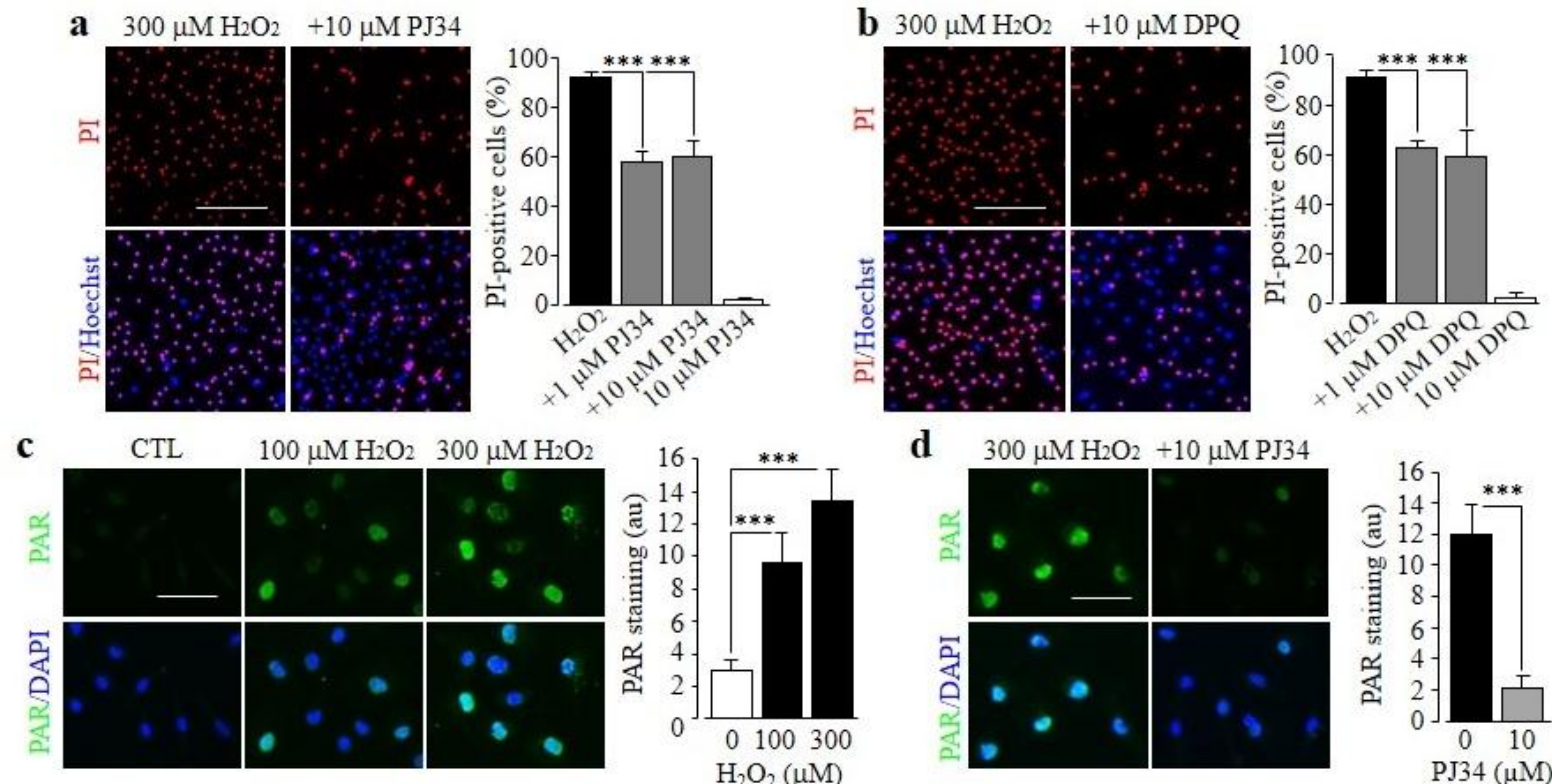


Fig. 4.3 PARP-1 activation is critical in H_2O_2 -induced microglial cell death.

(a-b) Left, representative images showing cell death (top row: PI-stained dead cells; bottom row: all cells stained with Hoechst). Right, mean H_2O_2 -induced cell death under following conditions: cells were exposed for 24 hr to 300 μM H_2O_2 without or with prior treatment with 1-10 μM PJ34 (a) or 1-10 μM DPQ 30 min prior to and during exposure to H_2O_2 (b). Cells were also treated with each inhibitor at higher concentration alone without exposure to H_2O_2 . (c-d) Left, representative images showing PAR staining (top row) and merged images (bottom row) of cells without (CTL) or with exposure for 2 hr to 100 and 300 μM H_2O_2 (c) and, 300 μM H_2O_2 alone or together treatment with 10 μM PJ34 for 30 min prior to and during exposure to H_2O_2 (d). Right, summary of the mean PAR fluorescence intensity in microglial cells. (a-d) The mean data were from four independent experiments, using three wells of cells for each condition in each experiment. Scale bar, 20 μm (a-b) and 40 μm (c-d). ***, p < 0.005 compared to control.

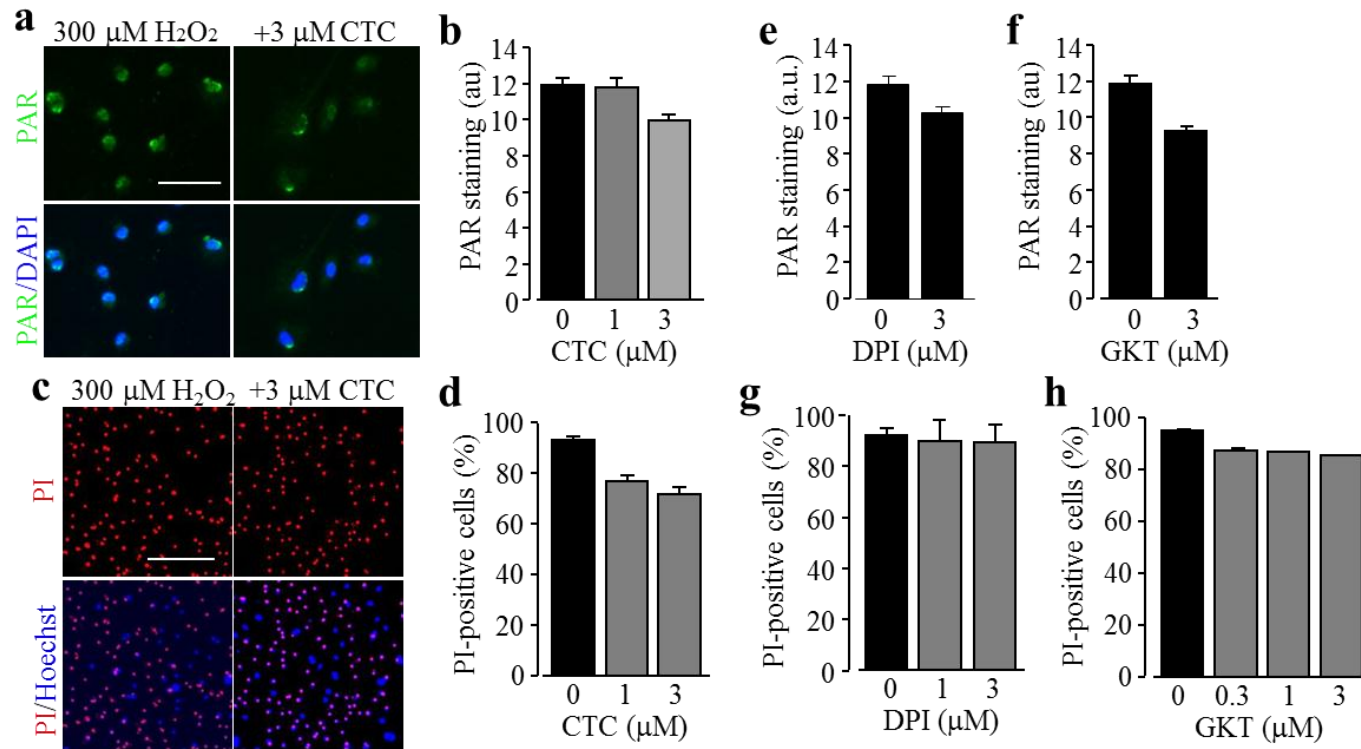


Fig. 4.4 PKC and NOX are not involved in H_2O_2 -induced PARP-1 activation and microglial cell death.

(a) Representative images showing PAR staining (top row) and counter staining with DAPI (bottom row) of microglial cells exposed for 2 hr to 300 μM H_2O_2 alone or together with 3 μM chelerythrine chloride (CTC). (b, e, f) Mean PAR fluorescence intensity in microglial cells exposed for 2 hr to 300 μM H_2O_2 alone or together with CTC (b), diphenyleneiodonium (DPI) (e) and GKT431397 (GKT) (f) from 3 independent experiments, using 3 wells of cells for each condition in each experiment. (c) Representative images showing microglial cell death (top row: PI-stained dead cells; bottom row: all cells stained with Hoechst) after cells were exposed for 24 hr to 300 μM H_2O_2 alone or together with 3 μM CTC. (d, g, h) Mean percentage of cell death in microglial cells exposed for 24 hr to 300 μM H_2O_2 alone or together with CTC (d), DPI (g) and GKT (h) from 3 independent experiments, using 3 wells of cells for each condition in each experiment. Cells were treated with CTC, DPI and GKT for 30 min prior to and during exposure to H_2O_2 . Scale bar, 40 μm (a) and 20 μm (c).

4.2.5 Effects of PYK2 and MEK/ERK inhibitors on H₂O₂-induced cell death

As introduced above, there is evidence to suggest a role of the MEK/ERK signalling in ROS-induced stimulation of PARP-1 activity (Domercq et al., 2013). It is also known that the Ca²⁺-sensitive PYK2 can trigger activation of the MEK/ERK signalling pathway (Lev et al., 1995; Yao et al., 2009). These findings lead to the hypothesis that the initial increase in the [Ca²⁺]_i, resulting from H₂O₂-induced TRPM2 activation, subsequently activates the PYK2/MEK/ERK signalling pathway and further stimulates the PARP-1 activity. Therefore, to test this hypothesis, I examined the effects of PYK2 and MEK/ERK inhibitors on H₂O₂-induced stimulation of PARP-1 activity and cell death in microglial cells. Treatments with PF431396, a potent PYK2 inhibitor (Fig. 4.5a-b), and U0126, an inhibitor of MEK/ERK (Fig. 4.5c-d), resulted in no significant inhibition of H₂O₂-induced stimulation of PARP-1 and cell death in microglial cells. These findings suggest that the PYK2/MEK/ERK signalling pathway is not involved in H₂O₂-induced microglial cell death.

4.2.6 TRPM2 channel in Zn²⁺-induced Ca²⁺ influx in microglial cells

As described in chapter 3 (section 3.2.4), Zn²⁺-induced increase in the [Ca²⁺]_i was prevented by genetic knockout of the TRPM2 channel expression in microglial cells. Here, I performed single cell calcium imaging using extracellular Ca²⁺-containing and Ca²⁺-free solutions to determine the origin of Ca²⁺ resulting in Zn²⁺-induced increase in the [Ca²⁺]_i in microglial cells. Zn²⁺ failed to induce any increase in the [Ca²⁺]_i in extracellular Ca²⁺-free solutions, in stark contrast with the strong Ca²⁺ response in Ca²⁺-containing solution (Fig. 4.6a). These results suggest that extracellular Ca²⁺ influx is responsible for Zn²⁺-induced increase in the [Ca²⁺]_i. In addition, Zn²⁺-induced increase in the [Ca²⁺]_i was strongly suppressed by pretreatment with BAPTA-AM (Fig. 4.6b). Taken together, these data suggest that Zn²⁺-induced Ca²⁺ signalling is dependent of TRPM2 channel-mediated Ca²⁺ influx.

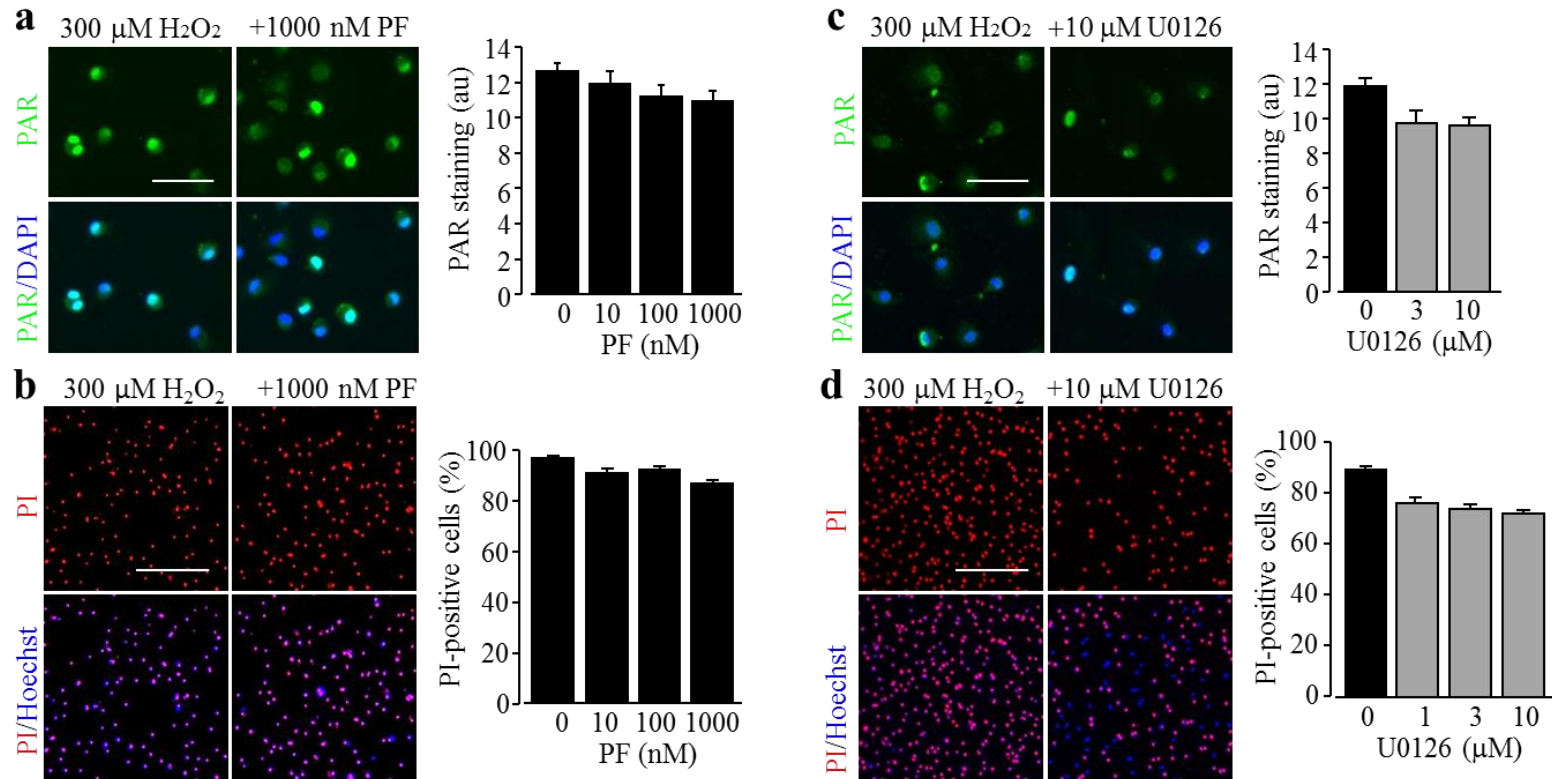


Fig. 4.5 PYK2/MEK signalling is not involved in H_2O_2 -induced PARP-1 activation and microglial cell death.

(a, c) Left, representative images showing PAR (top row) and counter staining with DAPI staining (bottom row) of cells exposed for 2 hr to 300 μM H_2O_2 alone or together with 1000 nM PF431396 (PF) (a) or 10 μM U0126 (c). Right, mean PAR fluorescence intensity in cells under indicated conditions, from 3 independent experiments, using 3 wells of cells for each condition in each experiment. (b, d) Left, representative images showing microglial cell death (top row: PI-stained dead cells; bottom row: counter staining with Hoechst) after cells were exposed for 24 hr to 300 μM H_2O_2 alone or together with 1000 nM PF (b) or 10 μM U0126 (d). Right, mean percentage of cell death under indicated conditions from 3 independent experiments, using 3 wells of cells for each condition in each experiment. Cells were treated with PF or U0126 for 30 min prior to and during exposure to H_2O_2 . Scale bar, 40 μm (a, c) and 20 μm (b, d).

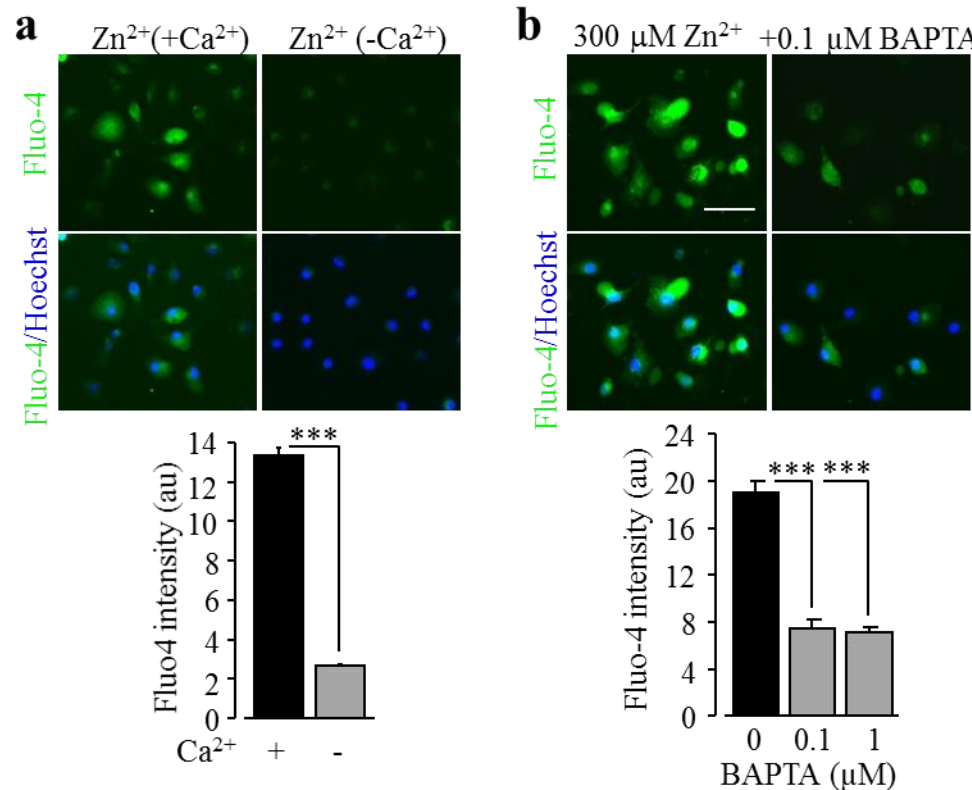


Fig. 4.6 Zn²⁺ induces extracellular Ca²⁺ influx in microglial cells.

(a-b) Top, representative single cell images showing Ca²⁺ responses in microglial cells (top row: Fluo-4 fluorescence; bottom row: counter staining with Hoechst). Bottom, mean Zn²⁺-induced Ca²⁺ responses under indicated conditions for 2 hr from 3 independent experiments, using 3 wells of cells for each condition in each experiment. The conditions are as follows: cells treated with 300 μM Zn²⁺ in the presence and absence of Ca²⁺ in extracellular solutions (a) and 300 μM Zn²⁺ without or with treatment of 0.1 and 1 μM BAPTA-AM (b). Cells were treated with BAPTA-AM for 30 min prior to and during exposure to Zn²⁺. Scale bar, 40 μm. ***, p < 0.005 compared to control.

4.2.7 Effects of TRPM2 channel inhibitors on Zn²⁺-induced microglial cell death

As described in previous chapter (section 3.2.5), studies using a genetic knockout approach have revealed a critical role of the TRPM2 channel in mediating Zn²⁺-induced microglial cell death. Here, I further examined the role of TRPM2 channel-dependent Ca²⁺ influx in Zn²⁺-induced microglial cell death. Zn²⁺-induced cell death was strongly inhibited by pretreatment with BAPTA-AM, at the concentrations as low as 0.01 μM (Fig. 4.7a). These results suggest that TRPM2 channel-mediated Ca²⁺ influx is critical in Zn²⁺-induced microglial cell death. Consistently, inhibition of the TRPM2 channel function with 2-APB significantly attenuated Zn²⁺-induced microglial cell death (Fig. 4.7b). These pharmacological results further confirm a critical role of the TRPM2 channel in mediating Zn²⁺-induced microglial cell death.

4.2.8 PARP-1 in Zn²⁺-induced TRPM2 channel activation and microglial cell death

To investigate whether PARP, particularly PARP-1, is critical in activating TRPM2 channel and subsequently cell death in microglial cells in response to the exposure of Zn²⁺, I examined the effects of PAPR inhibitors on Zn²⁺-induced microglial cell death. Zn²⁺-induced cell death was significantly reduced by PJ34 (Fig 4.8a) or DPQ (Fig. 4.8b). PAR immunofluorescence showed that exposure to 100-300 μM Zn²⁺ for 2 hr potently promoted PAR generation in the nucleus (Fig. 4.8c), which was strongly suppressed by PJ34 (Fig. 4.8d). These results provide strong evidence to suggest that Zn²⁺ induces TRPM2 channel activation in microglial cells by stimulation of PARP-1 activity.

4.2.9 Effects of PKC and NOX inhibitors in Zn²⁺-induced ROS production, PARP-1 activity, TRPM2 channel activation and cell death in microglial cells

Previous studies showed that PKC and NOX are crucial in Zn²⁺-induced ROS generation (Noh and Koh, 2000; Koh, 2001). Therefore, I performed single cell imaging to determine whether exposure to Zn²⁺ promoted ROS production in microglial cells, using DCF, a fluorescent indicator for ROS generation as described in the Materials and Method chapter (section 2.2.6). Exposure to Zn²⁺ resulted in a massive increase in the

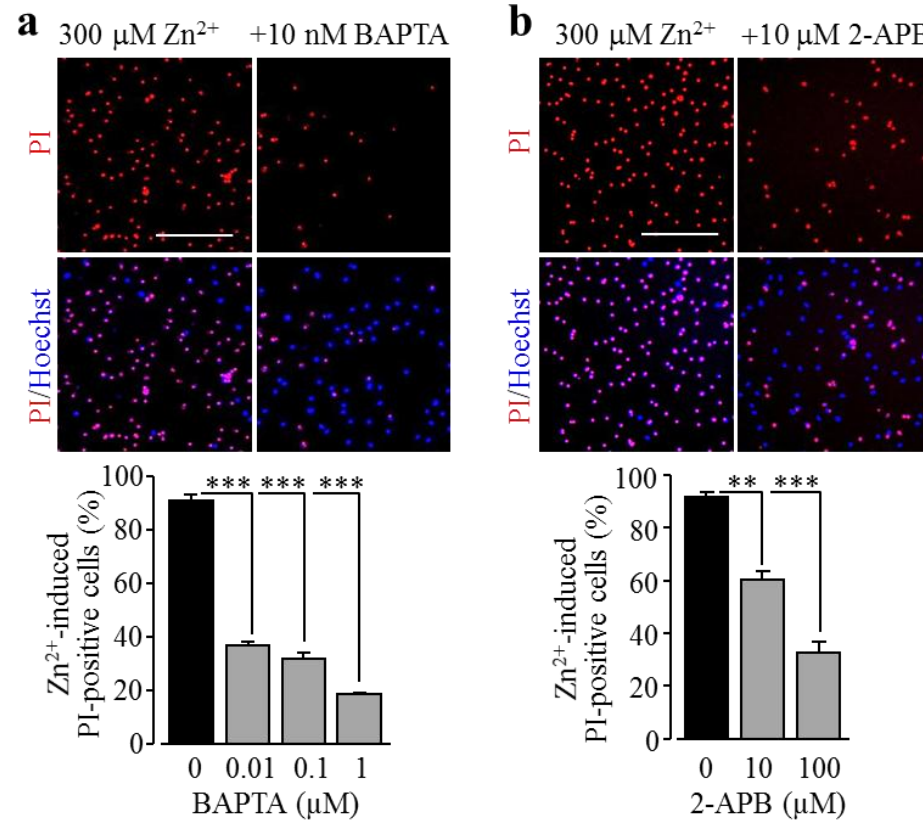


Fig. 4.7 A role of TRPM2 channel in Zn²⁺-induced microglial cell death.

(a-b) Top, representative images showing microglial cell death (top row: PI-stained dead cells; bottom row: all cells stained with Hoechst). Bottom, mean Zn²⁺-induced cell death under the following conditions: cells were exposed for 24 hr to 300 μM Zn²⁺ without or with treatment with 0.01-1 μM BAPTA-AM (a) or 10-100 μM 2-APB (b). Cells were treated with BAPTA-AM or 2-APB for 30 min prior to and during exposure to Zn²⁺. The mean data were from 4 independent experiments, using 3 wells of cells for each condition in each experiment. Scale bar, 20 μm . **, p < 0.01; ***, p < 0.005 compared to control.

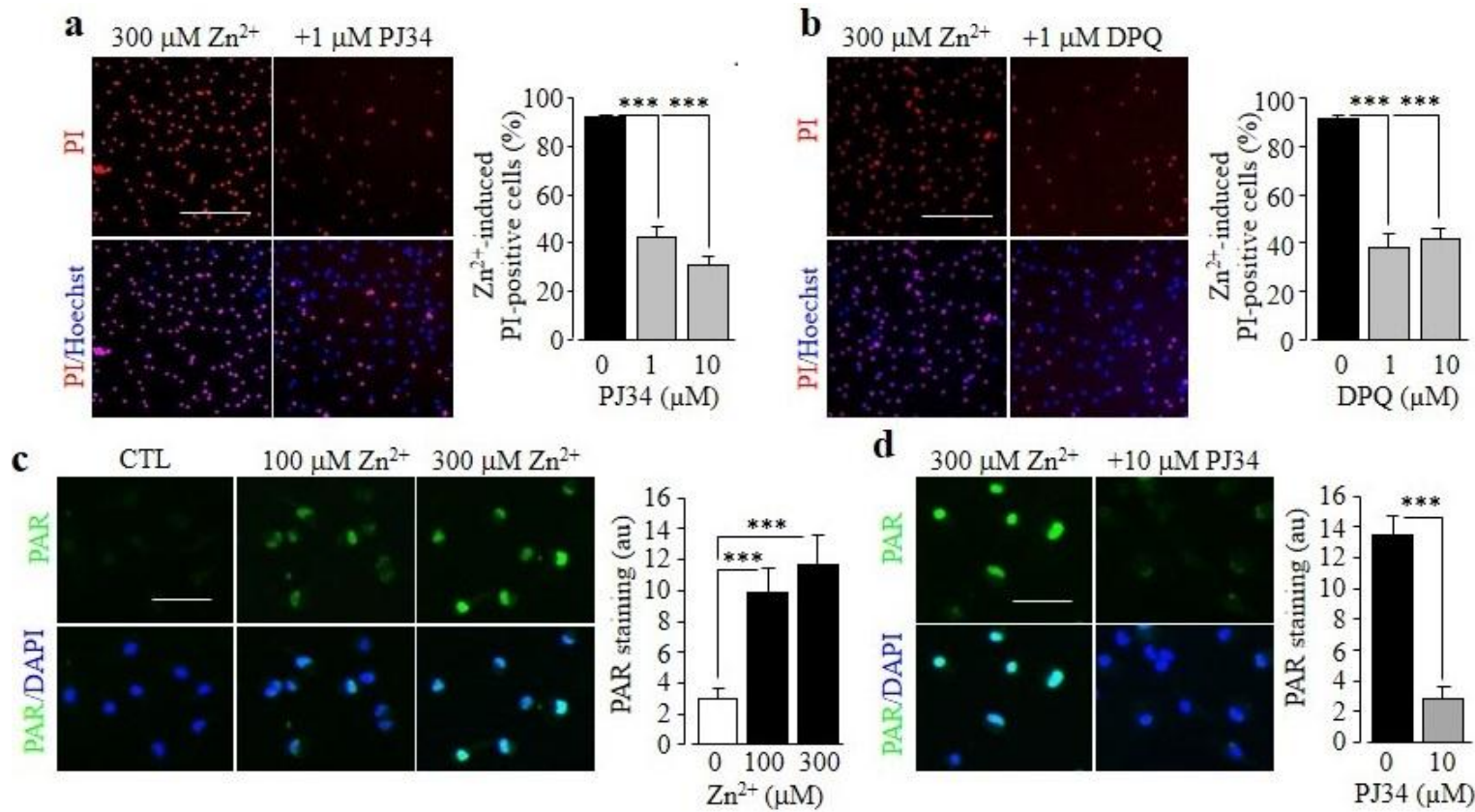


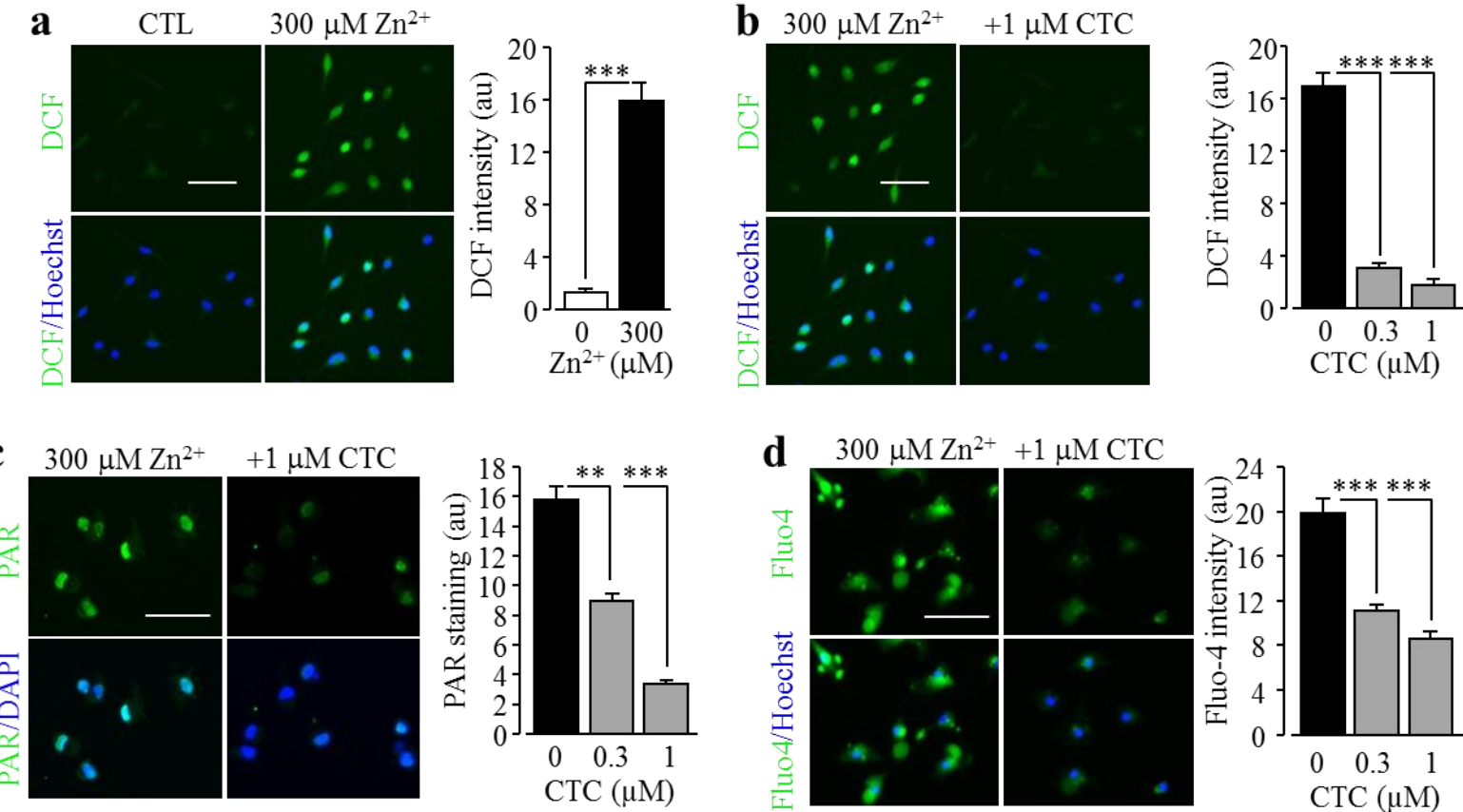
Fig. 4.8 Zn²⁺-induced PARP-1 activation in microglial cells.

(a-b) Left, representative images showing cell death (top row: PI-stained dead cells; bottom row: all cells stained with Hoechst). Right, mean Zn²⁺-induced cell death under the following conditions: cells were exposed for 24 hr to 300 μM Zn²⁺ without or with treatment with 1-10 μM PJ34 (a) or 1-10 μM DPQ (b) 30 min prior to and during exposure to Zn²⁺. (c-d) Left, representative images showing PAR staining (top row) and merged images (bottom row) of cells without (CTL) or with exposure for 2 hrs to 100 μM and 300 μM Zn²⁺ (a), and with 300 μM Zn²⁺ alone or together with 10 μM PJ34 (b). Right, summary of the mean PAR fluorescence intensity in microglial cells. Cells were treated with PJ34 for 30 min prior to and during exposure to Zn²⁺. (a-d) The mean data were from 4 independent experiments, using 3 wells of cells for each condition in each experiment. Scale bar, 20 μm (a-b) and 40 μm (c-d). ***, p < 0.005 compared to control.

cytosolic ROS level (Fig. 4.9a), which was strongly inhibited by CTC (Fig. 4.9b). Treatment with CTC strongly and concentration-dependently inhibited Zn²⁺-induced PAR generation in the nucleus (Fig. 4.9c) and, furthermore, Zn²⁺-induced increase in the [Ca²⁺]_i (Fig. 4.9d) and cell death (Fig. 4.9e) in microglial cells. Similarly, Zn²⁺-induced ROS production, PARP-1 activation, increase in the [Ca²⁺]_i and cell death in microglial cells was strongly and concentration-dependently inhibited by treatment with DPI (Fig. 4.10a-d), GKT137831 (Fig. 4.10e-h) and , albeit to less extent, Phox-I2, a NOX2 selective inhibitor (Fig. 4.10i-l). Taken together, these results provide clear evidence to show a significant role for PKC and NOX, particularly NOX1/4, in Zn²⁺-induced ROS production and PARP-1 activation, leading to TRPM2 channel activation and cell death in microglial cells.

4.2.10 Effects of PYK2 and MEK/ERK inhibitors on PARP-1 activity, TRPM2 channel activation and cell death in microglial cells

As shown and discussed in chapter 3 (section 3.2.5), Zn²⁺-induced microglial cell death occurred only after exposure to Zn²⁺ for 24 hr, which is significantly later than Zn²⁺-induced ROS production, stimulation of PARP-1 and increase in the [Ca²⁺]_i in microglial cell, which were observed after exposure to Zn²⁺ for 2 hr. These findings suggest that additional signalling pathways may be involved as positive feedback mechanisms. As mentioned above (section 4.2.5), the PYK2/MEK/ERK can act as a signalling mechanism downstream of the TRPM2 channel activation. In order to determine whether this is true or not, I performed experiments to examine the effects of PF431396 and U0126 on Zn²⁺-induced stimulation of PARP-1, increase in the [Ca²⁺]_i and cell death in microglial cells. Treatment with PF431396 concentration-dependently inhibited but did not completely prevent Zn²⁺-induced stimulation of PARP-1 (Fig. 4.11a), increase in the [Ca²⁺]_i (Fig. 4.11b) and cell death (Fig. 4.11c). Similarly, treatment with U0126 caused strong but incomplete inhibition of Zn²⁺-induced stimulation of PARP-1 (Fig. 4.11d), increase in the [Ca²⁺]_i (Fig. 4.11e) and cell death (Fig. 4.11f). These results are consistent with the concept that the PYK2/MEK/ERK signalling mechanism plays an important part in Zn²⁺-induced activation of PARP-1 and TRPM2 channel, and cell death in microglial cells.



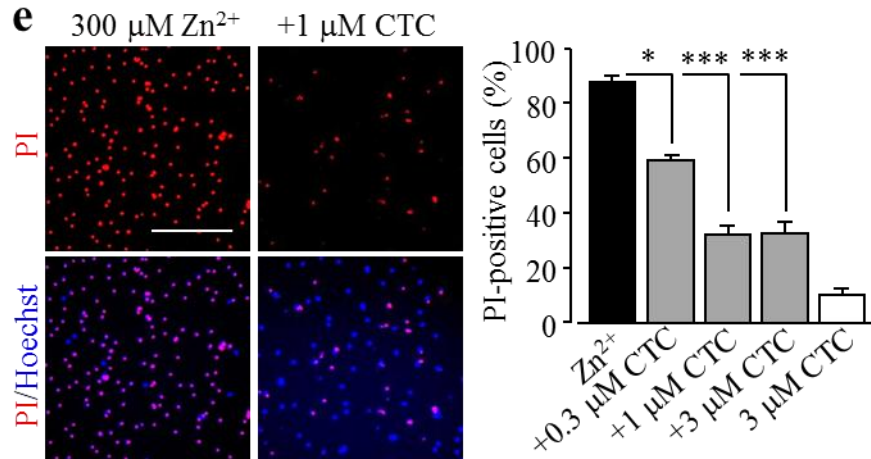
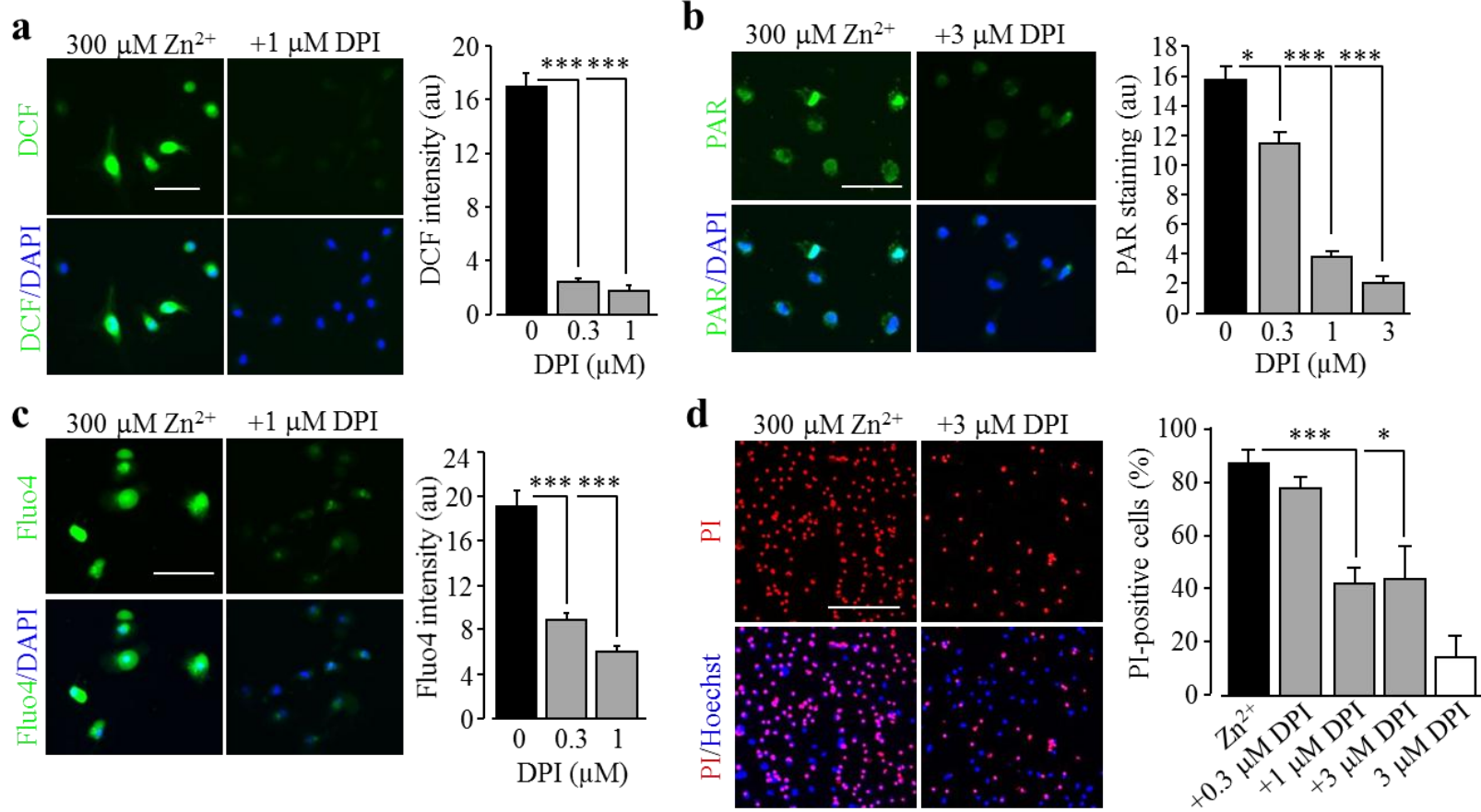


Fig. 4.9 PKC in Zn^{2+} -induced ROS generation, PARP-1 activation increase in the $[\text{Ca}^{2+}]_i$ and cell death in microglial cells.

(a-b) *Left*, representative images showing ROS level (top row: DCF fluorescence; bottom row: counter staining with Hoechst) in microglial cells treated for 2 hr without (CTL) and with exposure to $300 \mu\text{M} \text{Zn}^{2+}$ (a) and with $300 \mu\text{M} \text{Zn}^{2+}$ alone or together with $1 \mu\text{M} \text{CTC}$ (b). *Right*, mean ROS production in microglial cells under indicated conditions from 3 independent experiments, using 3 wells of cells for each condition in each experiment. (c) *Left*, representative images showing PAR staining (top row) and counter staining with DAPI (bottom row) of cells exposed for 2 hr to $300 \mu\text{M} \text{Zn}^{2+}$ alone or together with $1 \mu\text{M} \text{CTC}$. *Right*, mean PAR fluorescence intensity in cells under indicated concentrations from 3 independent experiments, using 3 wells of cells for each condition in each experiment. (d) *Left*, representative single cell images showing Ca^{2+} responses in microglial cells (top row: Fluo-4 fluorescence; bottom row: counterstaining with Hoechst). *Right*, mean Zn^{2+} -induced Ca^{2+} responses in microglial cells under indicated conditions from 3 independent experiments, using 3 wells of cells for each condition in each experiment. (e) *Left*, representative images showing cell death (top row: PI-stained dead cells; bottom row: all cells stained with Hoechst) in microglial cells treated with $300 \mu\text{M} \text{Zn}^{2+}$ alone or together with $1 \mu\text{M} \text{CTC}$ for 24 hr. *Right*, mean percentage of cell death from 3 independent experiments, using 3 wells of cells for each condition in each experiment. In each experiment, cells were treated with CTC for 30 min prior to and during exposure to Zn^{2+} . Scale bar, $40 \mu\text{m}$ (a, b, c, d) and $20 \mu\text{m}$ (e). *, $p < 0.05$; **, $p < 0.01$; ***, $p < 0.005$ compared to group exposed to Zn^{2+} alone. Treatment with the highest concentration of CTC (e) alone resulted in no significant cell death.



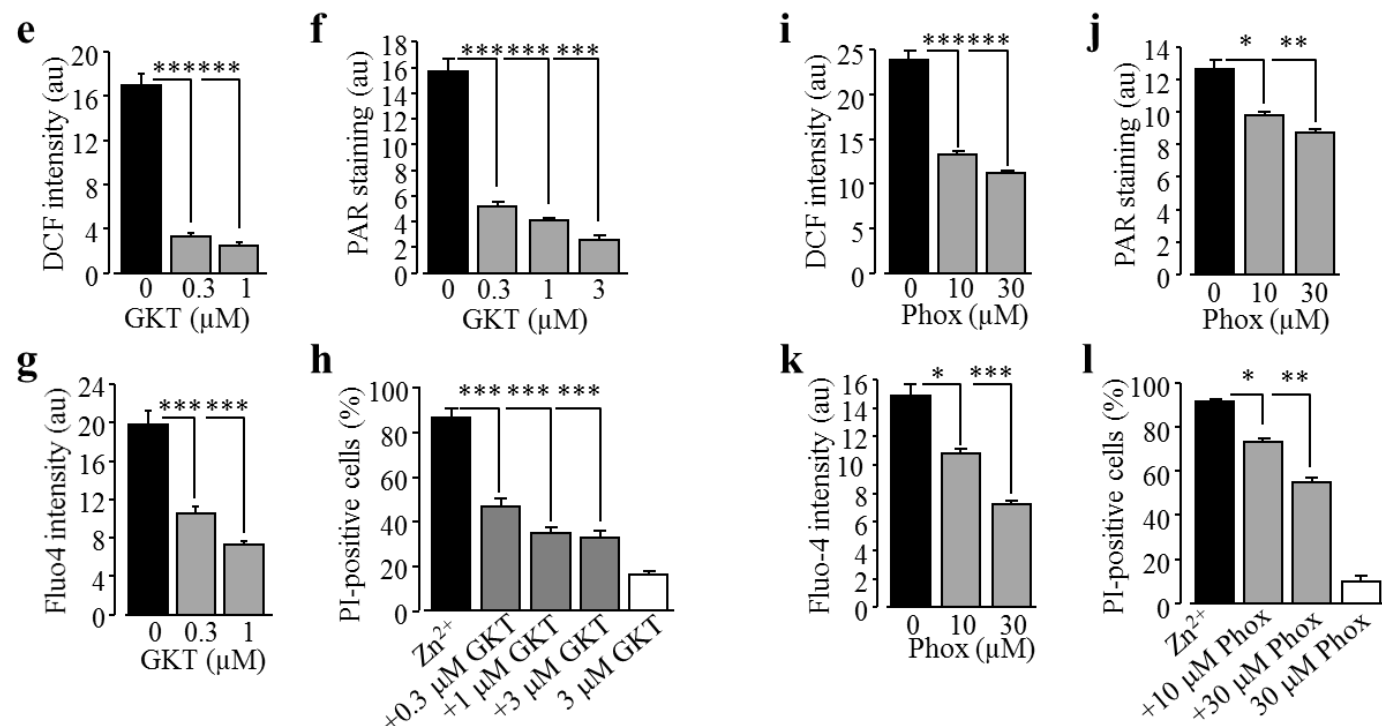
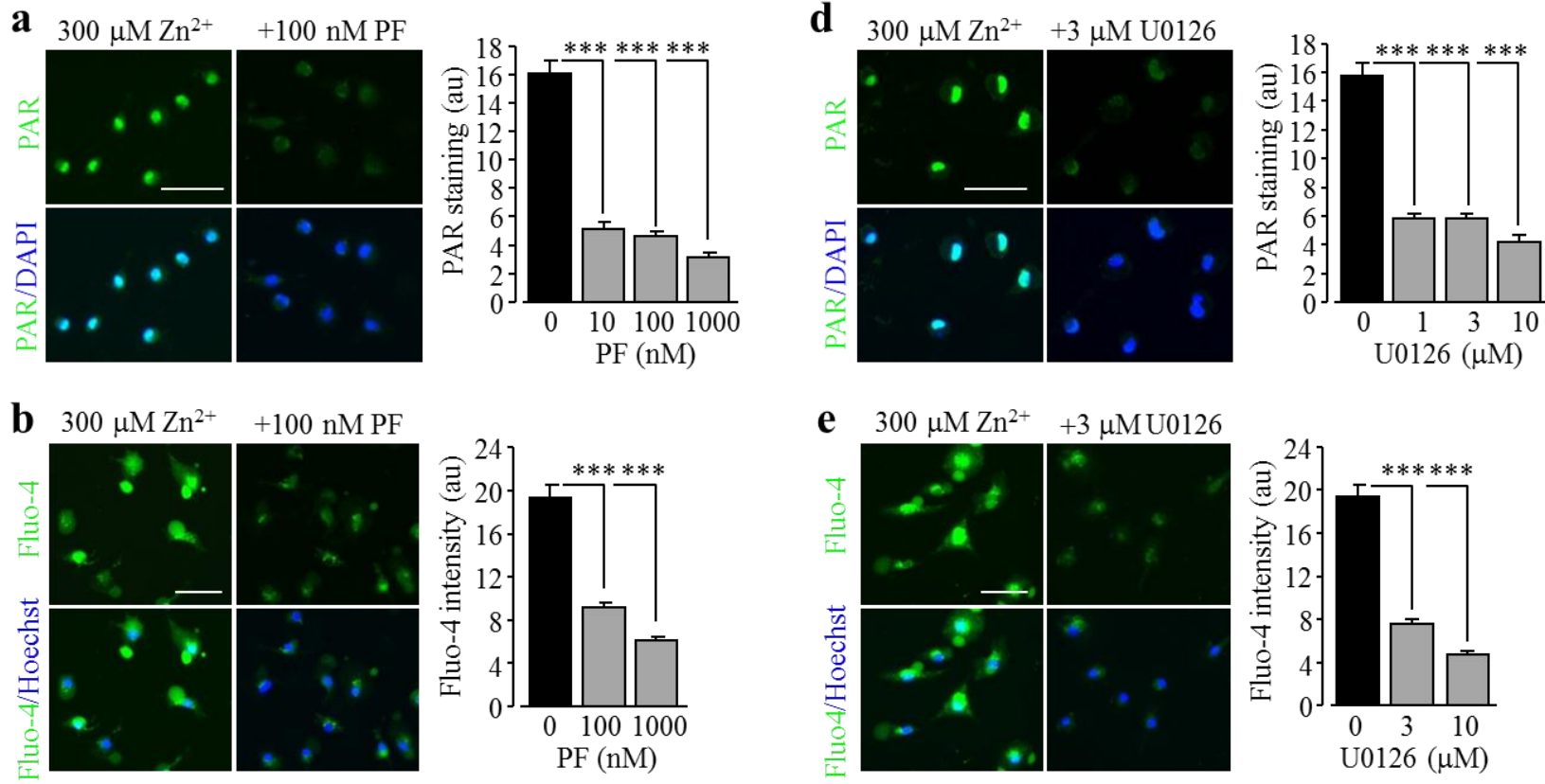


Fig. 4.10 NOX in Zn²⁺-induced ROS generation, PARP-1 activation increase in the [Ca²⁺]_i and cell death in microglial cells.

(a, b, c, d) *Left*, representative images showing DCF fluorescence (top row) and counter staining with Hoechst (bottom row) (a), PAR staining (top row) and counter staining with DAPI (bottom row) (b), Ca²⁺ responses (top row: Fluo-4 fluorescence; bottom row: counterstaining with Hoechst) (c) and cell death (top row: PI-stained dead cells; bottom row: all cells stained with Hoechst) (d) in cells exposed to 300 μM Zn²⁺ alone or together with DPI at indicated concentration. *Right*, mean data from 3 independent experiments, using 3 wells of cells for each condition in each experiment. (e, f, g, h) Mean DCF fluorescence (e), PAR staining (f), Fluo-4 fluorescence (g) and PI staining (h) in microglial cells exposed to 300 μM Zn²⁺ alone or together with GKT at indicated concentrations. (i, j, k, l) Mean DCF fluorescence (i), PAR staining (j), Fluo-4 fluorescence (k) and PI staining (l) in cells exposed to 300 μM Zn²⁺ alone or together with Phox-I2 (Phox) at indicated concentrations. Scale bar, 40 μm (a, b, c) and 20 μm (d). *, p < 0.05; **, p < 0.01; ***, p < 0.005 compared to group exposed to Zn²⁺ alone. Treatment with the highest concentration of DPI (d) or GKT (h) or Phox (l) alone resulted in no significant cell death.



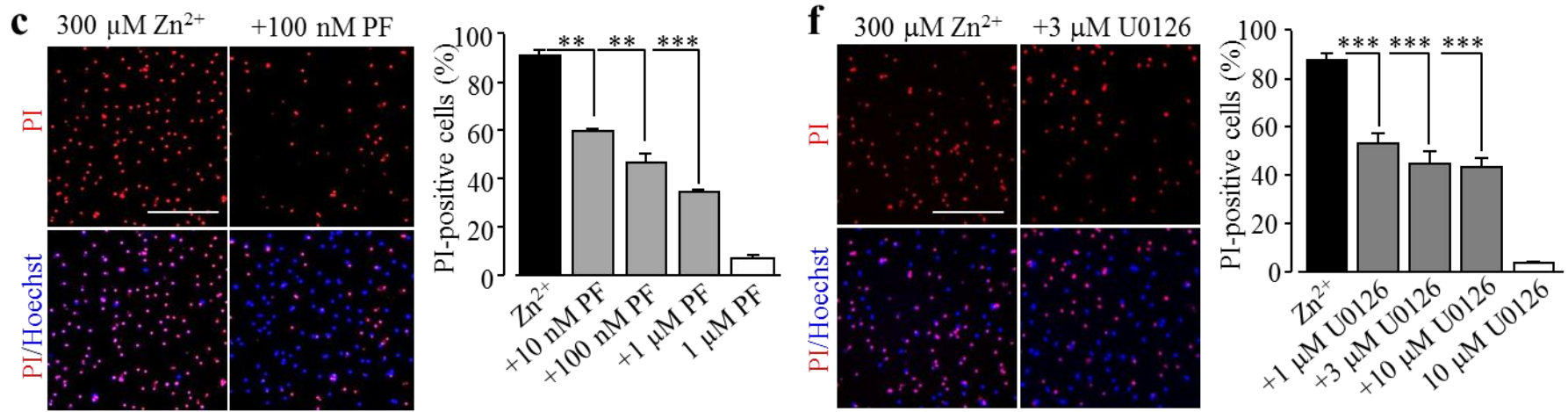
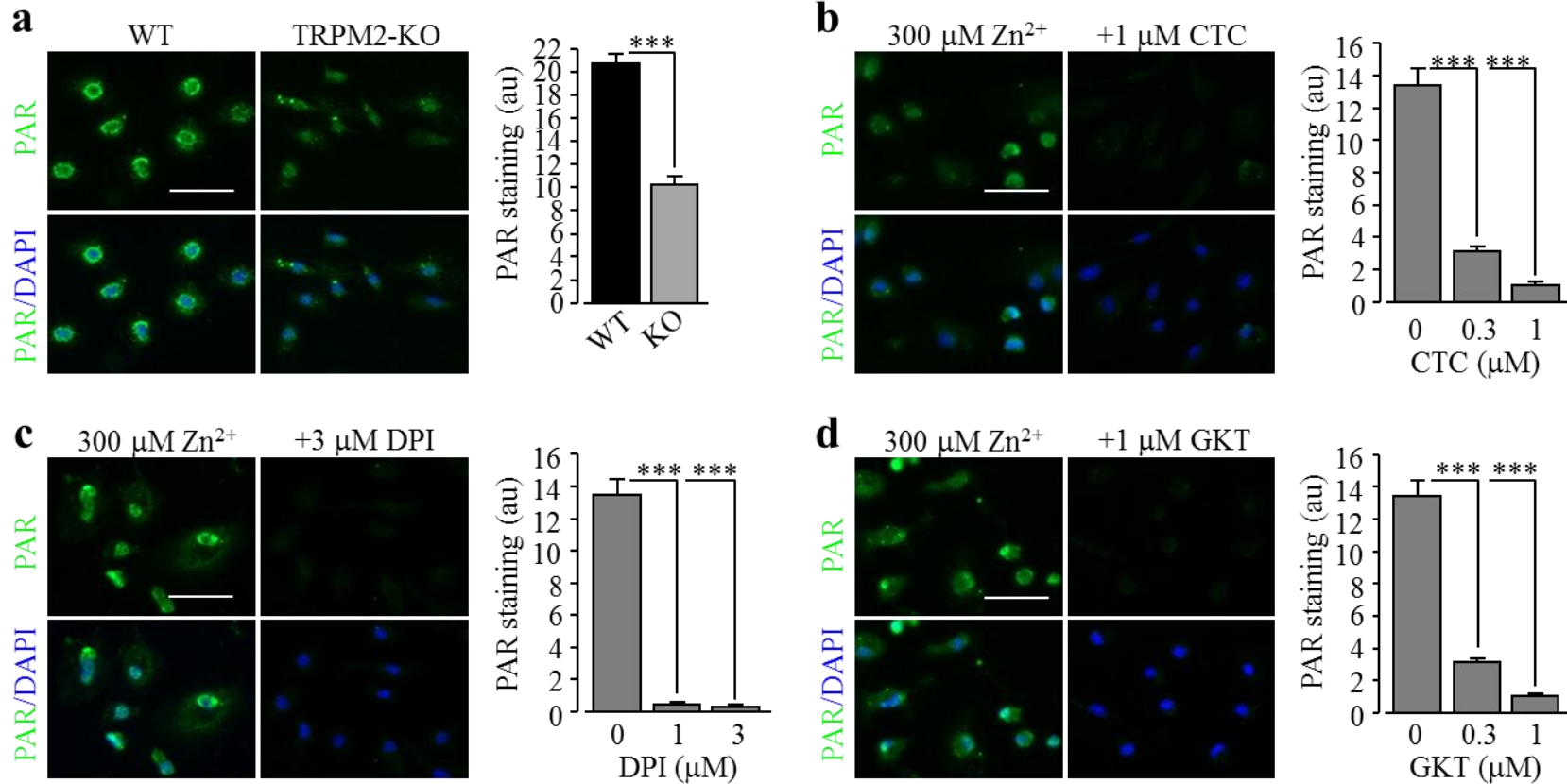


Fig. 4.11 PYK2/MEK/ERK in Zn^{2+} -induced PARP-1 activation, increase in the $[\text{Ca}^{2+}]_i$ and microglial cell death.

(a, d) *Left*, representative images showing the PAR level (top row: PAR fluorescence; bottom row: counterstaining with DAPI) in microglia cells exposed for 2 hr to 300 μM Zn^{2+} alone or together with 100 nM PF 431396 (PF) (a) or 3 μM U0126 (d). *Right*, mean PAR fluorescence intensity in cells under indicated conditions from three independent experiments, using three wells of cells for each condition in each experiment. (b, e) *Left*, representative single cell images showing Ca^{2+} responses (top row: Fluo-4 fluorescence; bottom row: counterstaining with Hoechst) in microglial cells exposed for 2 hr to 300 μM Zn^{2+} alone or together with 100 nM PF (b) or 3 μM U0126 (e). *Right*, mean Zn^{2+} -induced Ca^{2+} responses in microglial cells under indicated conditions from three independent experiments, using three wells of cells for each condition in each experiment. (c, f) *Left*, representative images showing cell death (top row: PI-stained dead cells; bottom row: all cells stained with Hoechst) in cells exposed for 24 hr to 300 μM Zn^{2+} alone or together with 100 nM PF (c) or 3 μM U0126 (f). *Right*, mean percentage of cell death from 3 independent experiments, using 3 wells of cells for each condition in each experiment. Cells were treated with PF or U0126 for 30 min prior to and during exposure to Zn^{2+} . Scale bar, 40 μm (a, b, d and e) and 20 μm (c and f). *, p < 0.05; ***, p < 0.005 compared to the indicated group exposed to with Zn^{2+} alone. Treatment with the highest concentration of PF (c) or U0126 (f) alone resulted in no significant cell death.

To seek further evidence to support the hypothesis that the PKC/NOX-mediated ROS-generating signalling pathway acts as the trigger for the TRPM2 channel activation whereas the PYK2/MEK/ERK signalling pathway serves as a mechanism downstream of the TRPM2 channel activation that promote further TRPM2 channel activation, I performed further experiments. I firstly examined the effects of inhibiting the PKC/NOX signalling pathway with CTC, DPI and GKT137831, and the PYK2/MEK signalling pathway with PF431396 and U0126 on PAR production in TRPM2-KO microglial cells. Zn^{2+} also induced considerable PAR production in TRPM2-KO microglial cells, which was however significantly lower than that in WT microglial cells (Fig. 4.12a), suggesting that the PARP-1 activation plays a role as the signalling mechanism downstream of the TRPM2 channel activation. Furthermore, treatments with CTC (Fig. 4.12b), DPI (Fig. 4.12c) or GKT137831 (Fig. 4.12d) almost completely abolished Zn^{2+} -induced PAR production. In striking contrast, treatment with PF431396 (Fig. 4.12e) or U0126 (Fig. 4.12f) resulted in no significant inhibition. I also investigated whether Zn^{2+} induced any significant increase in the $[Ca^{2+}]_i$ in WT microglial cells pre-treated with PF431396 (Fig. 4.13a) or U0126 (Fig. 4.13b) to inhibit the PYK2/MEK signalling pathway. As anticipated, in microglial cells with the PYK2/MEK signalling pathway being inhibited, Zn^{2+} was still able to induce considerable increase in the $[Ca^{2+}]_i$ and such Zn^{2+} -induced increase in the $[Ca^{2+}]_i$ was completely abolished by treatment with CTC, DPI or GKT137831 (Fig. 4.13a-b). Taken together, these results provide evidence to support the notion that the PKC/NOX signalling pathway is required for Zn^{2+} -induced PARP-1 activation and thereby TRPM2 channel activation, and the PYK2/MEK/ERK signalling pathway is activated downstream of the TRPM2 channel activation (Fig. 4.14).



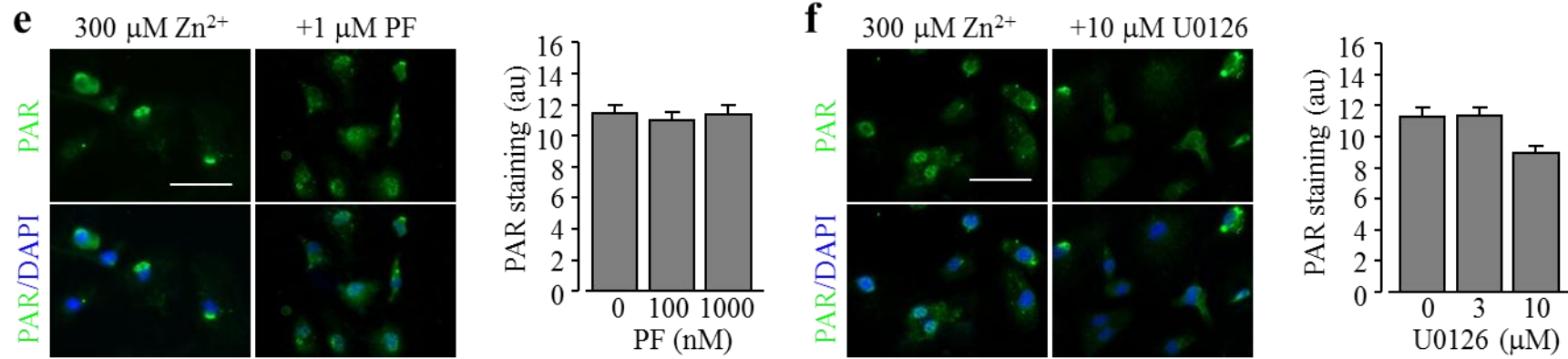


Fig. 4.12 PKC/NOX is required for, and the PYK2/MEK signalling pathway depends on, Zn^{2+} -induced PARP-1 activation.

(a) *Left*, representative images showing the PAR level (top row: PAR fluorescence; bottom row: counterstaining with DAPI) in the WT and TRPM2-KO microglia cells exposed for 2 hr to 300 μ M Zn^{2+} . *Right*, mean Zn^{2+} -induced PAR fluorescence intensity in the WT and TRPM2-KO cells from 3 independent experiments, using 3 wells of cells for each condition in each experiment. (b-f) *Left*, representative images showing the PAR level (top row: PAR fluorescence; bottom row: counter staining with DAPI) in the TRPM2-KO microglia cells exposed for 2 hr to 300 μ M Zn^{2+} alone or together with CTC (b), DPI (c), GKT (d), PF 431396 (PF) (e) or U0126 (f). *Right*, mean PAR fluorescence intensity in microglial cells under indicated conditions from 3 independent experiments, using 3 wells of cells for each condition in each experiment. Scale bar, 40 μ m. ***, p < 0.005 compared to WT cells (a) or cells exposed to Zn^{2+} alone (b-f). Zn^{2+} -induced residual PAR generation in TRPM2-KO microglial cells was strongly inhibited or abolished by treatment with CTC (b), DPI (c) or GKT (d), but not with PF (e) or U0126 (f). Scale bar, 40 μ m. ***, p < 0.005 compared to indicated group exposed to with Zn^{2+} alone.

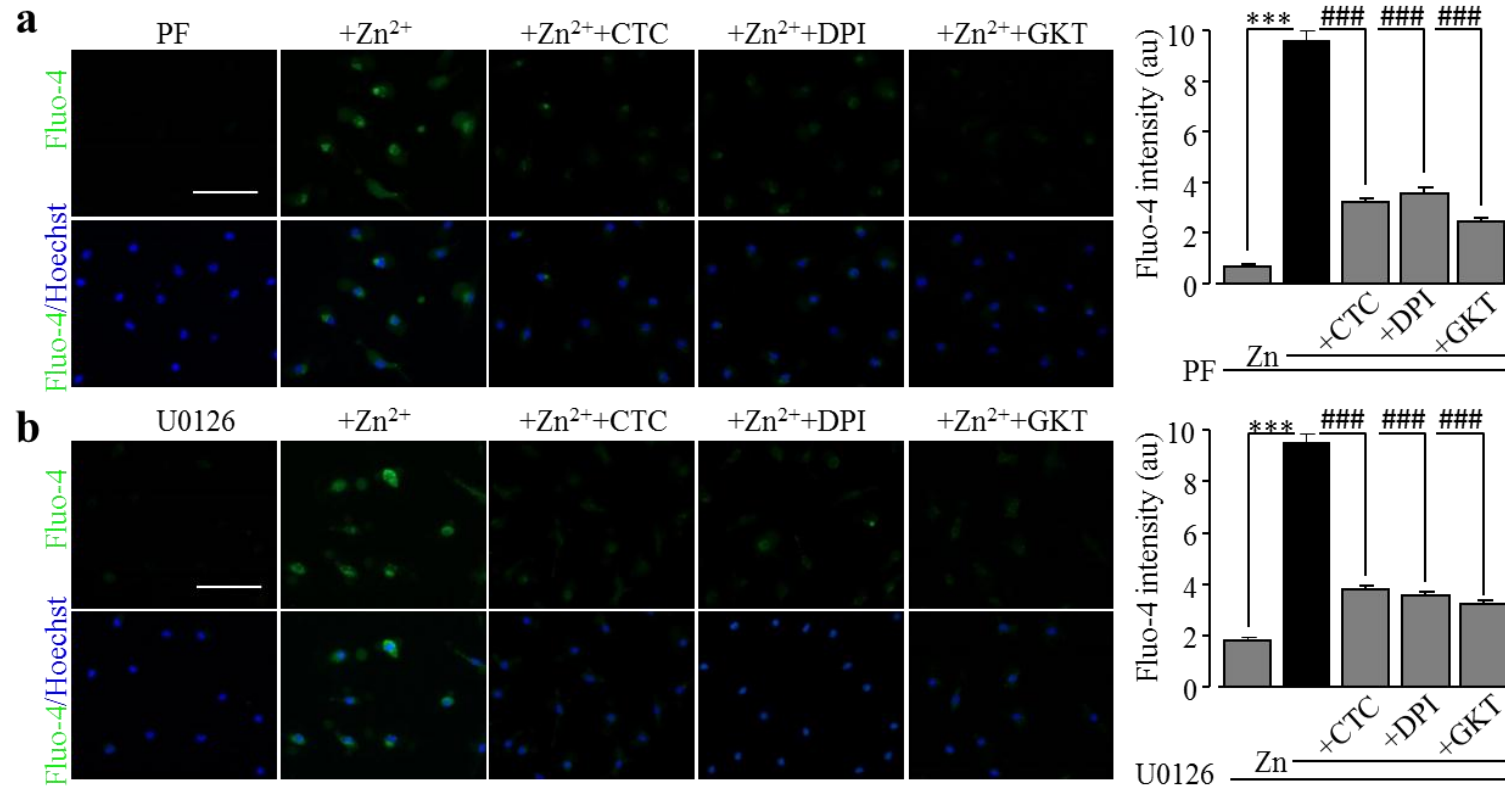


Fig. 4.13 PKC/NOX is required for, and the PYK2/MEK signalling pathway depends on, Zn²⁺-induced TRPM2 channel activation.

(a-b) *Left*, representative images showing the Ca²⁺ responses (top row: Fluo-4 fluorescence; bottom row: counterstaining with Hoechst) in WT microglia cells, treated with 1 μ M PF 431396 (PF) (a) or 3 μ M U0126 (b) alone or together with 1 μ M CTC, 3 μ M DPI, or 1 μ M GKT137831 (GKT) 30 min prior and during 2 hr exposure to 300 μ M Zn²⁺. *Right*, mean Ca²⁺ responses in cells under indicated conditions from at least 3 independent experiments, using 3 wells of cells for each condition in each experiment. In the presence of PF to inhibit PYK2 (a) or U0126 to inhibit MER/ERK (b), Zn²⁺ induced significant increase in the [Ca²⁺]_c in WT microglial cells, which was strongly inhibited by treatment with CTC, DPI or GKT. Scale bar, 40 μ m. ***, p < 0.005 compared to control group treated with PF or U0126 alone, and **#, p < 0.005 compared to cells exposed to Zn²⁺ and treated with PF or U0126.

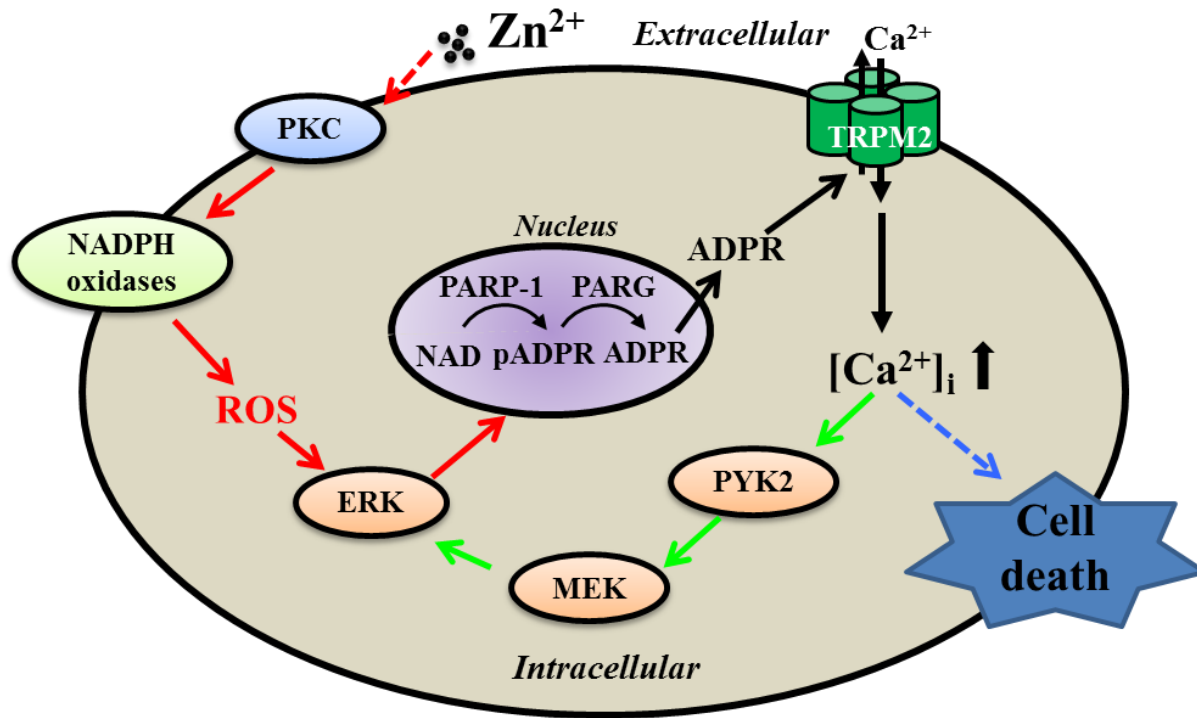


Fig. 4.14 Summary of the signalling mechanisms mediating Zn^{2+} -induced TRPM2 channel activation and cell death in microglial cells.

Zn^{2+} activates cell surface TRPM2 channel involving multiple-step signalling pathways. Zn^{2+} stimulates PKC and NADPH oxidases to generate ROS. ROS activates PARP-1 and PARG in the nucleus leading to ADPR production and subsequent activation of TRPM2-dependent Ca^{2+} influx to increase the intracellular Ca^{2+} concentrations ($[Ca^{2+}]_i$). Elevated $[Ca^{2+}]_i$ in turn results in activation of the PYK2/MEK/ERK signalling pathway as a positive feedback mechanism that amplifies activation of PARP-1, leading to TRPM2-mediated Ca^{2+} overloading and cell death. Abbreviations: PRC, protein kinase C; NADPH oxidase, nicotinamide adenine dinucleotide phosphate-dependent oxidase; ROS, reactive oxygen species; ERK, extracellular signal-regulated kinase; NAD, nicotinamide adenine dinucleotide; pADPR, poly(ADP-ribose) moiety; ADPR, ADP-ribose; PARP-1, poly(ADP-ribose) polymerase 1; PARG, poly(ADP-ribose) glycohydrolase; MEK, mitogen-activated kinase; PYK2, protein tyrosine kinase 2.

4.3 DISCUSSION

In the present study, I used pharmacological approaches to examine the signalling mechanisms underlying TRPM2 channel-mediated microglial cell death induced by H₂O₂ and Zn²⁺. H₂O₂-induced stimulation of PARP-1 activity mediates TRPM2 channel activation and cell death in microglial cells. Such microglial cell death however is independent of the PKC/NOX and PYK2/MEK/ERK signalling pathways. Zn²⁺-induced TRPM2 channel activation and cell death are dependent of PKC/NOX-mediated ROS production and PARP-1 activation. Furthermore, the PYK2/MEK/ERK signalling pathway acts downstream of the TRPM2 channel activation as a positive feedback mechanism that drives Ca²⁺ overloading and cell death in response to Zn²⁺, as illustrated in Fig. 4.14.

In the previous chapter (section 3.2.1), I have shown the importance of the TRPM2 channel in mediating H₂O₂-induced increase in the [Ca²⁺]_i in microglial cells. In this chapter I further performed experiments to examine TRPM2 channel-mediated Ca²⁺ signalling in microglial cells and its role in microglial cell death induced by H₂O₂. H₂O₂-induced increase in the [Ca²⁺]_i in microglial cells was largely abolished in the absence of extracellular Ca²⁺ (Fig. 4.1a) or attenuated by BAPTA-AM (Fig. 4.1b). These results provide consistent evidence to indicate that TRPM2 channel plays a role in H₂O₂-induced Ca²⁺ signalling via mediating extracellular Ca²⁺ influx, consistent with the finding from a previous study examining macrophages (Zou et al., 2013). H₂O₂-induced microglial cell death was attenuated by pretreatment with BAPTA-AM (Fig. 4.2a) and 2-APB (Fig. 4.2b). These results provide further evidence to indicate a crucial role of the TRPM2 channel activation, particularly TRPM2 channel-mediated Ca²⁺ signalling, is critical in mediating H₂O₂-induced microglial cell death.

As mentioned in the Introduction chapter, oxidative stress-induced PARP activation is one of the major signalling mechanisms contributes to the production of ADPR leading to the TRPM2 channel activation (Jiang et al., 2010). Consistently, H₂O₂-induced microglial cell death was remarkably inhibited by PJ34 and DPQ (Fig. 4.3a-b). In addition, immunofluorescence staining examining PAR formation indicates that H₂O₂ stimulated the PARP-1 activity in the nucleus in microglial cells (Fig. 4.3c), which was also prevented by PJ34 (Fig. 4.3d). Taken together, these results suggest that PARP-1 activity is critical in H₂O₂-induced TRPM2 channel activation in microglial cells.

I also attempted to investigate the signalling mechanisms by which H₂O₂ stimulates the PARP-1 activity, TRPM2 channel activation and subsequent cell death in microglial cells. PKC and NOX signalling pathway is widely known to act upstream of ROS generation. However, H₂O₂-induced PARP-1 activation and microglial cell death were completely insensitive to inhibitors of PKC and NOX (Figs. 4.4a-h). Similarly, inhibition of the PYK2 and MEK/ERK failed to inhibit H₂O₂-induced PARP-1 activation and cell death in microglial cells (Fig. 4.5a-d). These results indicate that H₂O₂ induced microglial cell death via stimulating the PARP-1 activity and subsequently TRPM2 channel activation but is independent of the PKC/NOX signalling pathway and the PYK2/MEK/ERK signalling pathway.

My studies presented in the previous chapter reveal an important role of the TRPM2 channel in Zn²⁺-evoked Ca²⁺ response and cell death in microglial cells (sections 3.2.4 and 3.2.5). In this chapter, I further showed that Zn²⁺-induced increase in the [Ca²⁺]_i in microglial cells was prevented in the absence of extracellular Ca²⁺ (Fig. 4.6a) and inhibited by BAPTA-AM (Fig. 4.6b). Taken together, these results suggest that Zn²⁺-induced Ca²⁺ signalling results from extracellular Ca²⁺ influx. Zn²⁺-induced microglial cell death were strongly suppressed by BAPTA-AM, even at 10-100 nM (Fig. 4.7a). In addition, Zn²⁺-induced microglial cell death was prevented by 2-APB (Fig. 4.7b). These results support a critical role for not only the TRPM2 channel but TRPM2-mediated Ca²⁺ signalling in mediating Zn²⁺ toxicity to microglial cells.

Zn²⁺-induced PARP-1 activation has been reported in microglial cells (Kauppinen et al., 2008) and I have confirmed this finding by demonstrating that Zn²⁺ stimulates PAR formation in the nucleus (Fig. 4.8c-d). Furthermore, Zn²⁺-induced cell death was strongly attenuated by PJ34 and DPQ (Fig. 4.8a-b). These results suggest that PARP-1 activation in Zn²⁺-induced TRPM2-mediated microglial cell death. It is known that Zn²⁺ induces NOX-dependent ROS production (Wu et al., 2012) and PKC stimulates NOX (Min et al., 2004). Consistently, here I showed that Zn²⁺-induced ROS generation were strongly reduced by inhibiting PKC (Fig. 4.9a) and NOX, including NOX1/4 (Fig. 4.10a and e) and NOX2 (Fig. 4.10i). In addition, Zn²⁺-induced stimulation of PARP-1, the increase in the [Ca²⁺]_i and cell death in microglial cells were prevented by PKC (Fig. 4.9c-d) and NOX inhibitors (4.10f-h and 4.10j-l). These results provide strong evidence to show that PKC/NOX-mediated ROS generation is critical in Zn²⁺-induced stimulation of PARP-1 activity, TRPM2 channel activation and cell death in microglial cells.

In monocytes, TRPM2 channel-mediated Ca^{2+} influx activates the PYK2/MEK/ERK signalling pathway, which is important in chemokine generation in response to ROS *in vitro* or *in vivo* (Yamamoto et al., 2008). Here, I showed that Zn^{2+} -induced stimulation of PARP-1 activity, increase in the $[\text{Ca}^{2+}]_i$ and cell death was strongly suppressed by inhibiting the PYK2/MEK/ERK signalling pathway (Fig. 4.11a-f). I have provided further evidence to show that the PYK2/MEK/ERK signalling pathway constitutes a positive feedback mechanism that amplifies Zn^{2+} -induced stimulation of PARP-1 and TRPM2 channel activation that ultimately drive microglial cell death (Figs. 4.12 and 4.13).

In conclusion, the studies presented in this chapter provide evidence to show TRPM2 channel activation, particularly TRPM2 channel-mediated Ca^{2+} influx, as a critical mechanism mediating H_2O_2 - and Zn^{2+} -induced cell death in microglial cells. H_2O_2 -induced microglial cell death is strongly dependent of PARP-1 but not PKC/NOX or PYK2/MEK/ERK signalling pathways. Stimulation of PARP-1 is also critical for Zn^{2+} -induced TRPM2 channel activation and cell death in microglial cells. Furthermore, activation of the PKC/NOX signalling pathway is an important mechanism in Zn^{2+} -induced stimulation of PARP-1 and TRPM2 channel activation. Additionally, activation of the PYK2/MEK/ERK signalling pathway acts as a positive feedback signalling mechanism that further amplifies Zn^{2+} -induced stimulation of PARP-1 and TRPM2 channel activation. Activation of these signalling mechanisms, in response to prolonged exposure to excessive Zn^{2+} , ultimately drives Ca^{2+} overloading and cell death in microglial cells (Fig. 4.14).

CHAPTER 5

SIGNALLING MECHANISMS FOR A β ₄₂-INDUCED TRPM2-MEDIATED MICROGLIAL ACTIVATION AND TNF- α GENERATION

5.1 INTRODUCTION

Chronic or dysregulated microglial cell activation and excessive generation of neurotoxic mediators including pro-inflammatory cytokines, such as TNF- α , IL-1 β and ROS, can give rise to neuroinflammation (Liu and Hong, 2003; Block et al., 2007; Colonna and Butovsky, 2017; Regen et al., 2017; Wolf et al., 2017). Accruing evidence from preclinical and clinical studies support the notion that an imbalance between generation and removal of A β is an early and initiating factor in AD (Mucke and Selkoe, 2012; Hong et al., 2016; Selkoe and Hardy, 2016).

Studies over the years have widely demonstrated that A β induces activation of microglial cells and production of inflammatory mediators, particularly TNF- α (Jekabsone et al., 2006; Wyss-Coray and Rogers, 2012; Shi et al., 2015). A β -induced activation of microglial cells as well as TNF- α production have been shown to be significantly suppressed by curcumin (Shi et al., 2015), which has recently reported as a TRPM2 channel blocker (Kheradpezhoh et al., 2016). A recent study has shown that genetic ablation of the TRPM2 channel expression strongly suppressed microglial activation in the APP/PS1 AD mouse brain (Ostapchenko et al., 2015), indicating a critical role for the TRPM2 channel in A β -induced microglial activation and neuroinflammation. Consistently, the study presented in chapter 3 shows that A β_{42} induces microglial cell activation. However, the mechanisms by which A β_{42} activates the TRPM2 channel and its relationship to neuroinflammation, including production of TNF- α , were not defined. As introduced in the Introduction chapter, NOX in microglial cells have a significant role in ROS production in AD (Block et al., 2007; Cheret et al., 2008; Harrigan et al., 2008). Studies have also proposed that NOX-dependent ROS production is important in A β -induced microglial cell activation (Jekabsone et al., 2006; Brown and Neher, 2010). In addition, PKC and NOX have been reported for ganglioside-induced microglial activation (Min et al., 2004). Furthermore, it has been shown that genetic ablation of PARP-1 suppresses A β -induced microglial activation (Kauppinen et al., 2011), indicating PARP-1 activation as part of the signalling pathway microglial activation. There is evidence that the activation of ERK is induced in microglial cells following exposure to A β_{42} (Sondag et al., 2009; Liu and Bian, 2010).

In this chapter, I will describe the experiments aimed to investigate the signalling mechanisms by which A β_{42} induces TRPM2 channel activation, and the role for the TRPM2 channel in mediating A β_{42} -induced microglial activation and TNF- α generation.

5.2 RESULTS

5.2.1 TRPM2 channel role in A β ₄₂-induced Ca²⁺ influx

TRPM2 channel activation mediates extracellular Ca²⁺ influx leading to an increase in the [Ca²⁺]_i in microglial cells, as shown in chapter 4 as well as previous studies (Kraft et al., 2004; Miyake et al., 2014; Jeong et al., 2017). I examined whether A β ₄₂ also induced TRPM2-dependent Ca²⁺ influx. A β ₄₂-induced increase in the [Ca²⁺]_i was observed in extracellular Ca²⁺-containing solution, but not in Ca²⁺-free solution (Fig. 5.1a-b), Furthermore, A β ₄₂-induced increase in the [Ca²⁺]_i in WT microglial cells were abolished by treatment with 2-APB (Fig. 5.1c-d). These results, together with the loss of A β ₄₂-induced increase in the [Ca²⁺]_i in TRPM2-KO microglial cells (section 3.2.4), strongly support A β ₄₂-induced TRPM2 channel activation leading to Ca²⁺ influx and increase in the [Ca²⁺]_i.

5.2.2 Effects of TRPM2 channel inhibitor on A β ₄₂-induced microglial cell activation

A β ₄₂-induced microglial cell activation was prevented in TRPM2-KO microglial cells (section 3.2.6). I further examined the effect of 2-APB on A β ₄₂-induced microglial cell activation. A β ₄₂-induced change in the morphology of WT microglial cells was prevented with treatment, prior to and during exposure to A β ₄₂, with 2-APB (Fig 5.2a-c). The results from genetic and pharmacological interventions provide consistent evidence to show a critical role for the TRPM2 channel in determining A β ₄₂-induced microglial activation.

5.2.3 A β ₄₂-induced TNF- α production is TRPM2-dependent

As already introduced above, TNF- α represents the major pro-inflammatory cytokine generated by microglial cells, and A β -induced TNF- α production plays an important role in AD-related neuroinflammation. I performed immunocytochemistry to examine the TNF- α expression in microglial cells after 48 hr exposure to A β ₄₂ and, furthermore, ELISA assay to determine TNF- α released into the culture medium after 72 hr exposure to A β ₄₂. Exposure to 10-300 nM A β ₄₂ induced a concentration-dependent

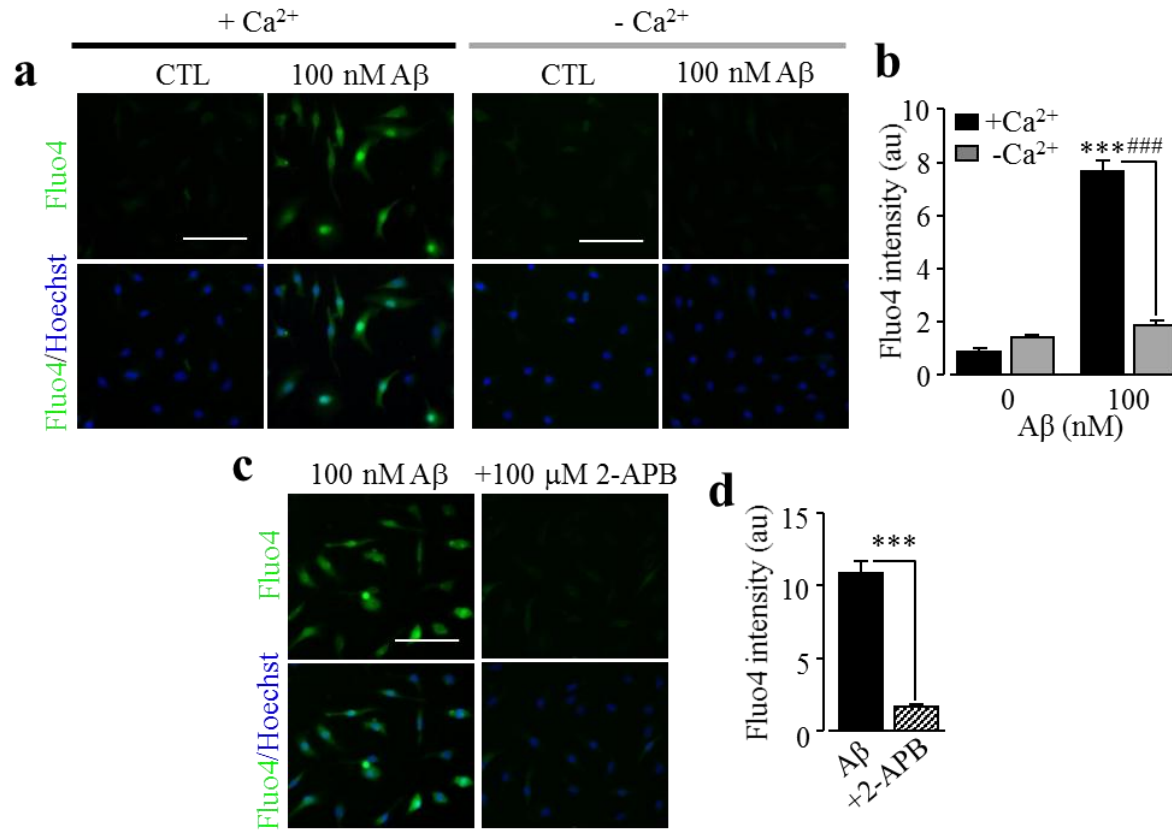


Fig. 5.1 Aβ₄₂ induces Ca²⁺ influx through the TRPM2 channel in microglial cells.

(a, c) Representative single cell images showing intracellular Ca²⁺ levels in microglial cells (top row: Fluo4 fluorescence; bottom row: counter staining with Hoechst) after exposed to 100 nM Aβ₄₂ for 8 hr in extracellular Ca²⁺-containing (+Ca²⁺) or Ca²⁺-free (-Ca²⁺) solutions (a) and, 100 nM Aβ₄₂ for 8 hr alone or treatment with 100 μM 2-APB (c), 30 min prior to and during exposure to Aβ₄₂. (b, d) Mean Aβ₄₂-induced Fluo4 fluorescence intensity, indicative of the intracellular Ca²⁺ levels in cells under indicated conditions from 3 independent experiments, using 3 wells of cells for each condition in each experiment. Scale bar, 40 μm. ***, p < 0.005 compared to control. ##, p < 0.005 compared between cells exposed to Aβ₄₂ in the presence and absence of extracellular Ca²⁺.

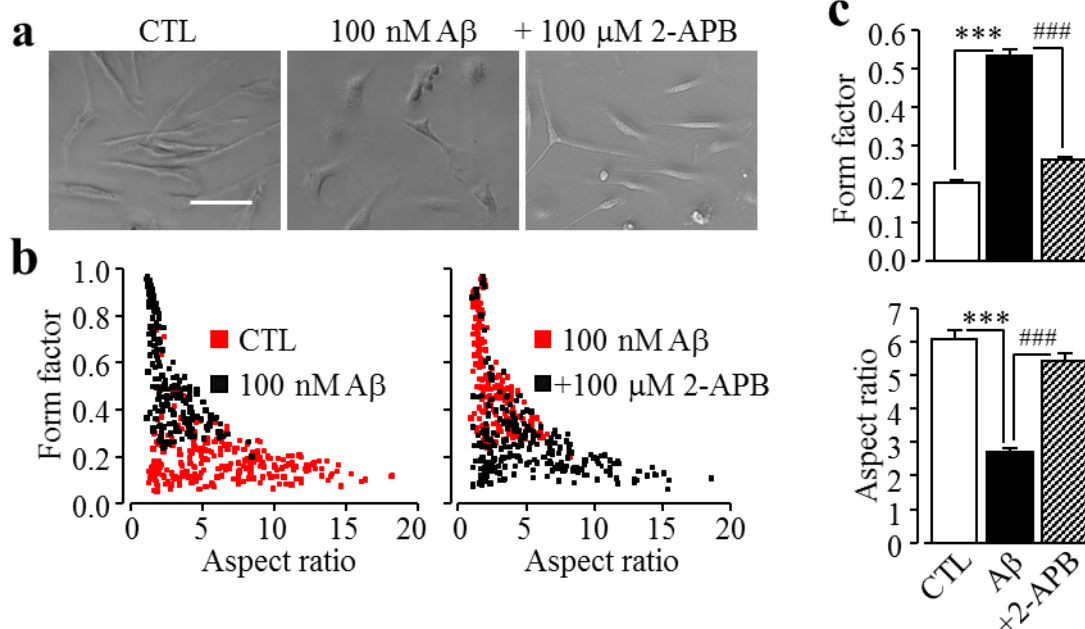


Fig. 5.2 A role of TRPM2 channel in A β ₄₂-induced microglial cell activation.

(a) Representative phase-contrast images showing cell morphology of microglial cells after exposure to 100 nM A β ₄₂ for 24 hr alone or treatment with 100 μ M 2-APB, 30 min prior to and during exposure to A β ₄₂, captured using an EVOS microscope with a 40x object lens. (b) Scatter plot showing distribution of form factor and aspect ratio of individual WT microglial cells after exposure to 100 nM A β ₄₂ for 24 hr alone or treatment with 100 μ M 2-APB, 30 min prior and duration exposure to A β ₄₂. (c) Mean values of form factor (top) and aspect ratio (bottom) of microglial cells under indicated conditions from at least 3 independent experiments, using 3 wells of cells for each condition in each experiment. Scale bar, 50 μ m. ***, p < 0.005 compared to control. **, p < 0.005 compared to cells exposed to A β ₄₂ alone.

increase in both TNF- α expression (Fig. 5.3a-b) and TNF- α release (Fig. 5.3c) by WT microglial cells.

In contrast with WT microglial cells, treatment with 30-300 nM A β ₄₂ induced no TNF- α expression in TRPM2-KO microglial cells (Fig. 5.4a-b). Consistently, there was no TNF- α release from TRPM2-KO microglial cells after treatment with A β ₄₂ (Fig. 5.4c). A β ₄₂-induced TNF- α release from WT microglial cells was also strongly suppressed by treatment with 2-APB (Fig. 5.4d). These results provide compelling evidence to indicate a critical role for the TRPM2 channel in A β ₄₂-induced TNF- α generation.

5.2.4 PARP-1 in A β ₄₂-induced TRPM2 channel activation, cell activation and TNF- α production in microglial cells

Previous studies provide evidence to support that PARP-1 activation is critical for A β - or traumatic brain injury-induced microglial cell activation (Kauppinen et al., 2011; Stoica et al., 2014). In order to further test the hypothesis that A β ₄₂ induced PARP activation results in TRPM2 channel activation, I examined the effect of PARP inhibitor on the increase in [Ca²⁺]_i in microglial cells. Treatment of WT microglial cells with PJ34 prevented A β ₄₂-induced increase in the [Ca²⁺]_i (Fig. 5.5a-b), and strongly inhibited A β ₄₂-induced change in the cell morphology (Fig. 5.5c-f). Furthermore, treatment with PJ34 and DPQ significantly inhibited A β ₄₂-induced TNF- α production (Fig. 5.5g). These results suggest that PARP has a critical role in TRPM2-mediated A β ₄₂-induced microglial cell activation and TNF- α production.

In order to investigate whether A β ₄₂ stimulated PARP-1 in microglial cells, I performed immunofluorescence staining using an anti-PAR antibody. Exposure to A β ₄₂ resulted in massive PAR production in microglial cells and that such PAR production was predominantly concentrated in the nucleus, as illustrated by the co-localization of PAR immunoreactivity with DAPI counterstaining (Fig. 5.6a-b), indicating PARP-1 activation. A β ₄₂ also induced considerable PAR production in TRPM2-KO microglial cells, which was however significantly lower than that in WT microglial cells (Fig. 5.6c-d). As anticipated, A β ₄₂-induced PAR production in both WT and TRPM2-KO cells was completely prevented by treatment with PJ34 (Fig. 5.6c-d). Taken together, these results support that A β ₄₂ activates the TRPM2 channel via stimulating the PARP-1 activity.

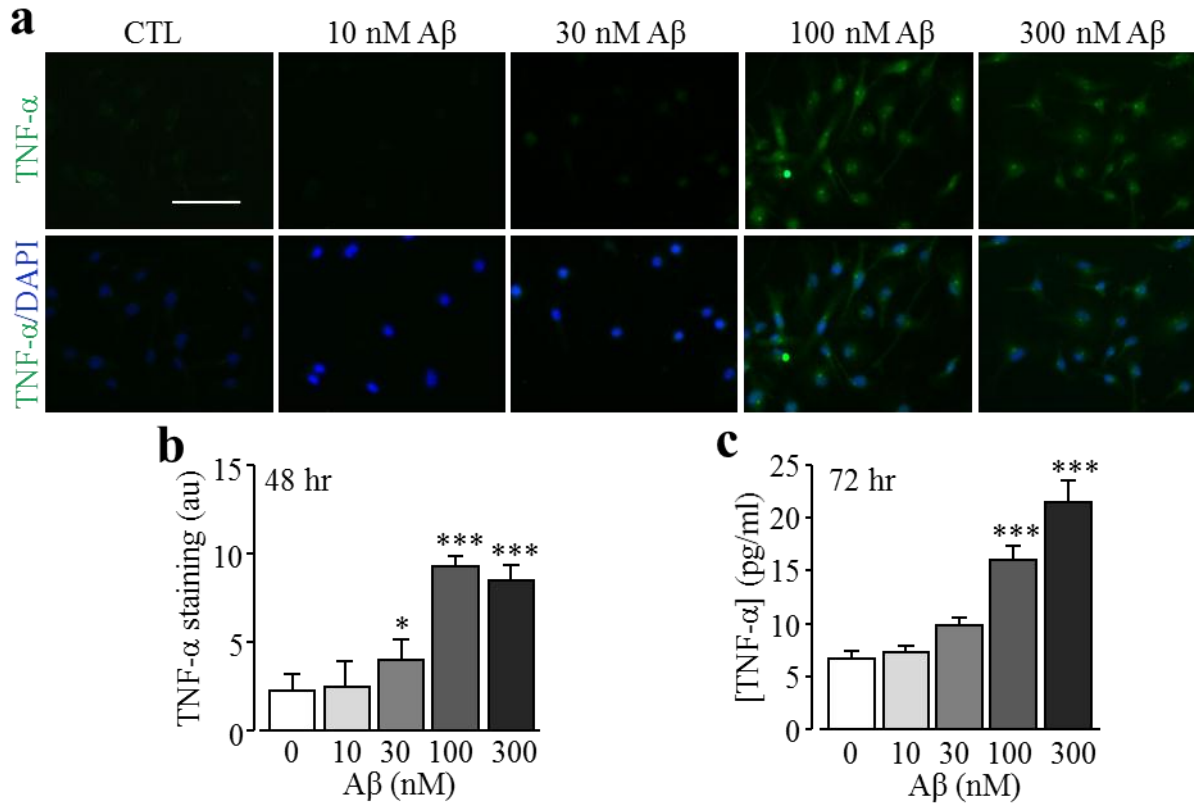


Fig. 5.3 A β_{42} induces TNF- α production in microglial cells.

(a) Representative fluorescent images showing TNF- α immunoreactivity in cells without (CTL) and with exposure to A β_{42} at indicated concentrations for 48 hr. Cells were counterstained with DAPI. (b) Summary of mean TNF- α expression in cells under indicated conditions from 3 independent experiments, using 3 wells of cells for each condition in each experiment. (c) Summary of ELISA assay of TNF- α release by cells after exposed to A β_{42} at indicated concentrations for 72 hr from 3 independent experiments, using 3 wells of cells for each condition in each experiment. Scale bar, 40 μ m. *, p < 0.05; ***, p < 0.005 compared to control.

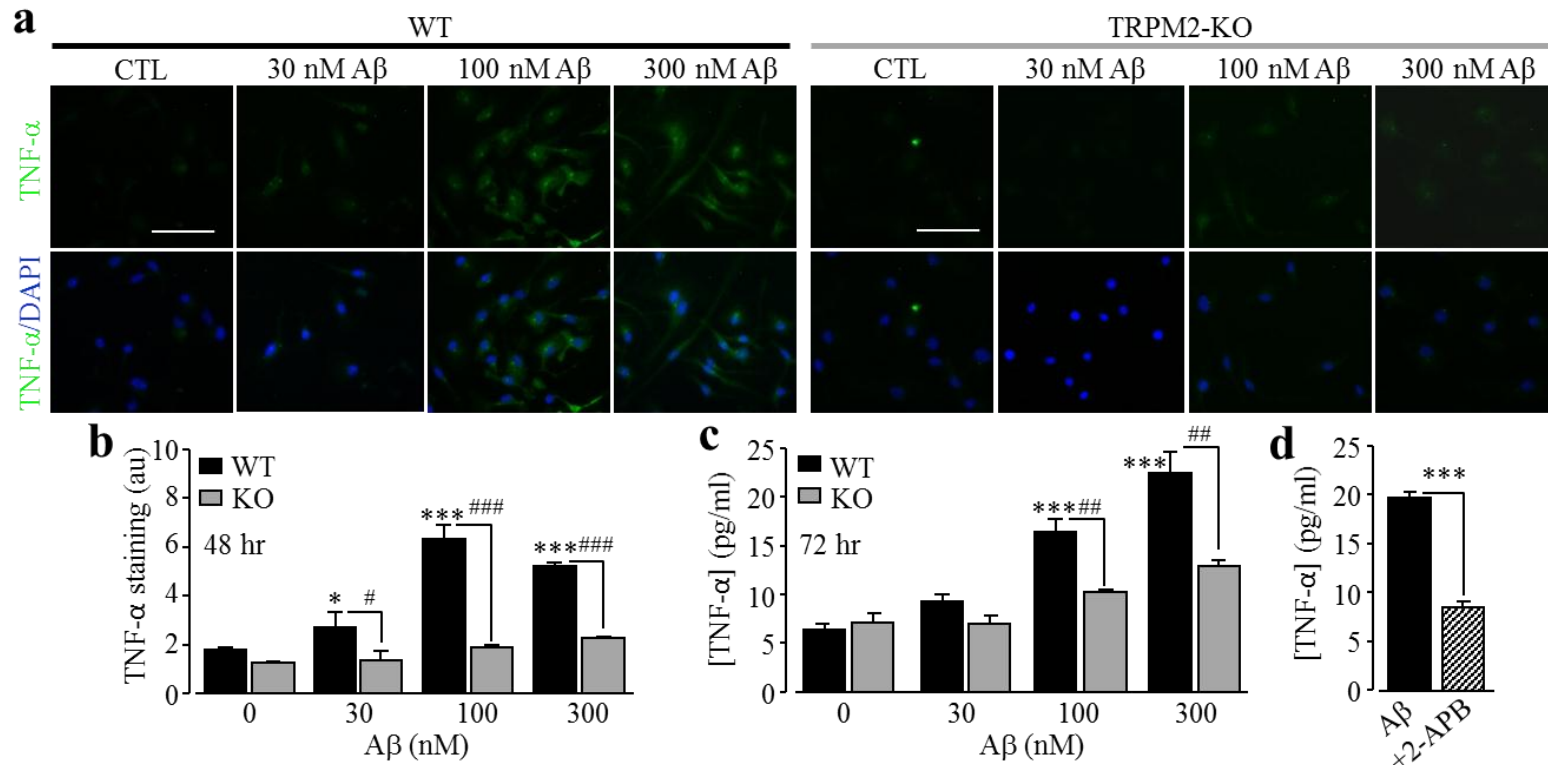
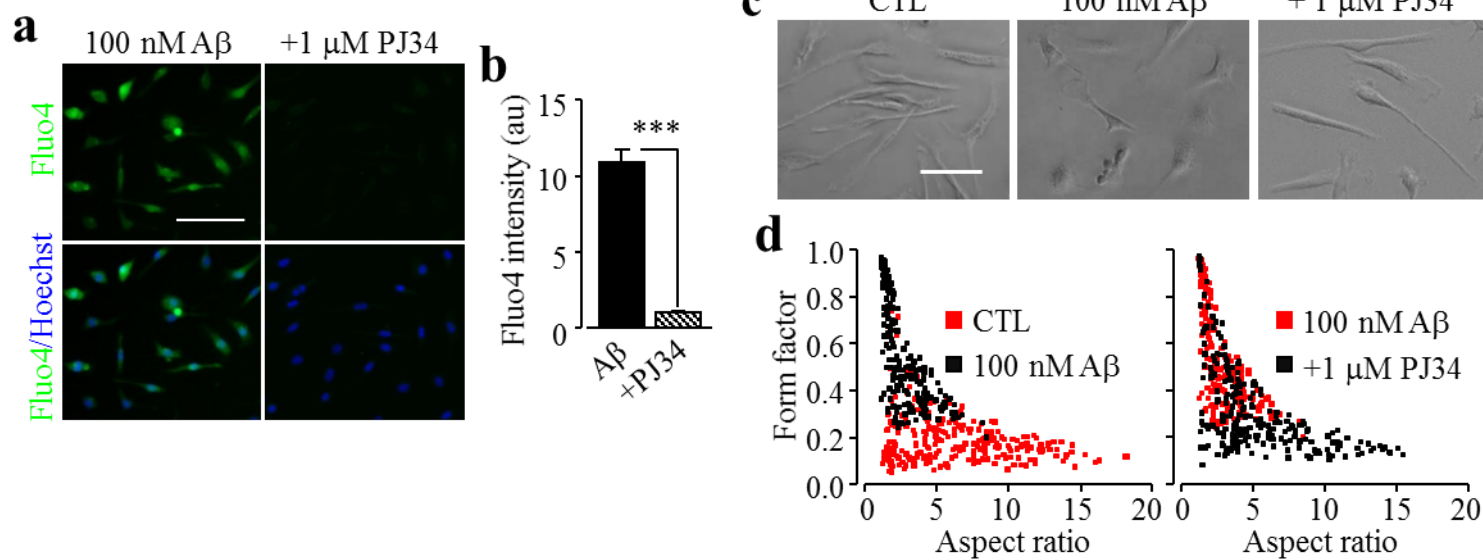


Fig. 5.4 TRPM2 is required for A β_{42} -induced TNF- α production by microglial cells.

(a) Representative fluorescent images showing TNF- α immunoreactivity in cells from WT and TRPM2-KO mice without (CTL) and with exposure to A β_{42} at indicated concentrations for 48 hr. Cells were counterstained with DAPI. (b) Mean TNF- α expression under indicated conditions from 3 independent experiments, using 3 wells of cells for each condition in each experiment. (c) Summary of ELISA assay of TNF- α release by WT and TRPM2-KO cells after exposure to A β_{42} at indicated concentrations for 72 hr from 3 independent experiments, using 3 wells of cells for each condition in each experiment. (d) Summary of ELISA assay of TNF- α release after exposure to 100 nM A β_2 for 72 hr alone or treatment with 100 μ M 2-APB, 30 min prior to during exposure to A β_{42} from 3 independent experiments, using 3 wells of cells for each condition in each experiment. Scale bar, 40 μ m. *, p < 0.05; **, p < 0.01; ***, p < 0.005 compared to control. #, p < 0.05; ##, p < 0.01; ###, p < 0.005 compared between WT and TRPM2-KO cells under the same treatment.



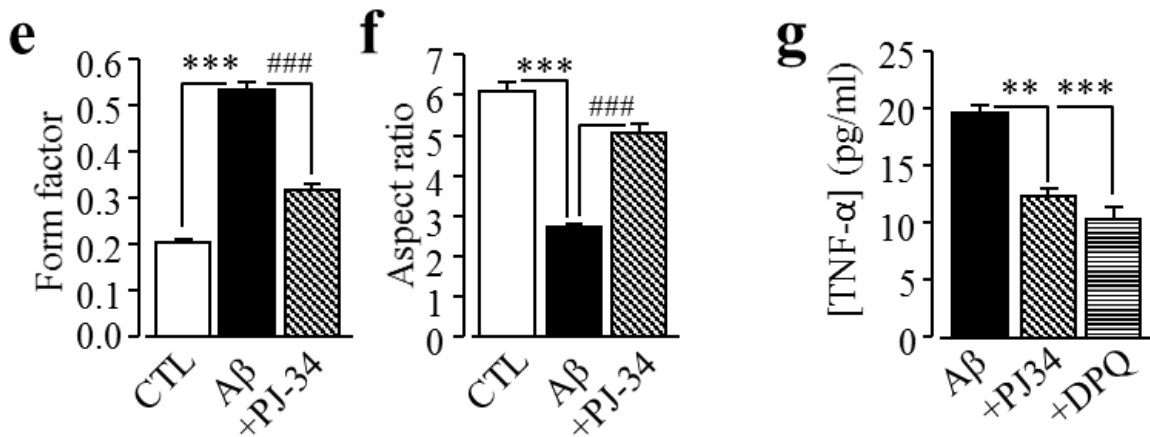


Fig. 5.5 A role of PARP in A β ₄₂-induced cell activation and TNF- α production in microglial cells.

(a) Representative single cell images showing intracellular Ca²⁺ levels in microglial cells (top row: Fluo4 fluorescence; bottom row: counter staining with Hoechst) after exposed to 100 nM A β ₄₂ for 8 hr alone or treatment with 1 μ M PJ34, 30 min prior to and during exposure to A β ₄₂. (b) Mean A β ₄₂-induced Fluo4 fluorescence intensity, indicative of the intracellular Ca²⁺ levels in cells under indicated conditions from 3 independent experiments, using 3 wells of cells for each condition in each experiment. (c) Representative phase-contrast images showing cell morphology of microglial cells after exposure to A β ₄₂ for 24 hr alone or treatment with 1 μ M PJ34, 30 min prior to and during exposure to A β ₄₂, captured using an EVOS microscope with a 40x object lens. (d) Scatter plot showing distribution of form factor and aspect ratio of individual WT microglial cells after exposure to 100 nM A β ₄₂ for 24 hr alone or treatment with 1 μ M PJ34, 30 min prior and duration exposure to A β ₄₂. (e-f) Mean values of form factor (e) and aspect ratio (f) of microglial cells under indicated conditions from at least 3 independent experiments, using 3 wells of cells for each condition in each experiment. (g) Summary of ELISA assay of TNF- α release after exposure to 100 nM A β ₄₂ for 72 hr alone or treatment with 1 μ M PJ34 or 10 μ M DPQ, 30 min prior to during exposure to A β ₄₂ from 3 independent experiments, using 3 wells of cells for each condition in each experiment. Scale bar, 40 μ m (a) and 50 μ m (c). **, p < 0.01; ***, p < 0.005 compared to control. ###, p < 0.005 compared to cells exposed to A β ₄₂ alone.

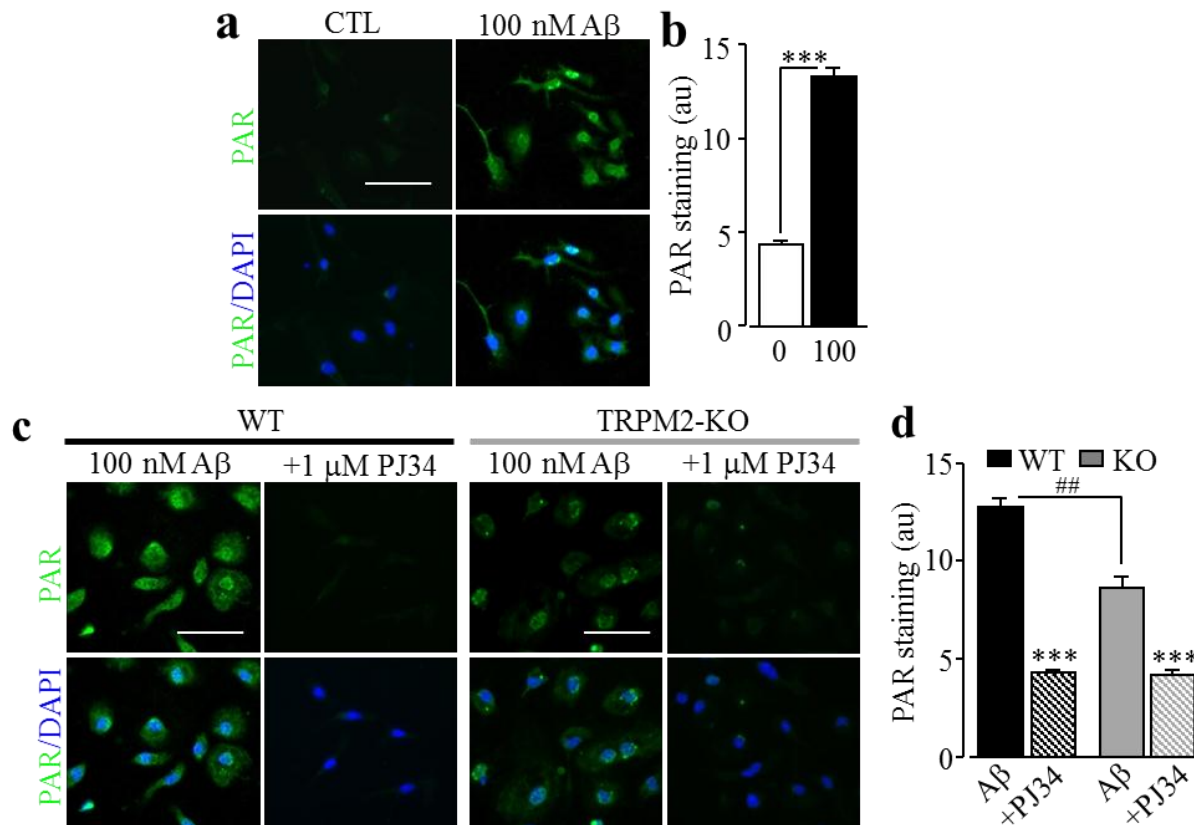


Fig. 5.6 A β ₄₂ induces PARP-1 activation in microglial cells.

(a, c) Representative fluorescent images showing PAR staining (top row) and counterstaining with DAPI (bottom row) in cells without (CTL) and with exposure to 100 nM A β ₄₂ for 8 hr in WT cells (a), or after exposure to with 100 nM A β ₄₂ for 8 hr alone or treatment with 1 μ M PJ34, 30 min prior to and during exposure to A β ₄₂, in WT and KO-TRPM2 cells (c). (b, d) Mean PAR fluorescence intensity in cells under indicated conditions from 3 independent experiments, using 3 wells of cells for each condition in each experiment. Scale bar, 40 μ m. ***, p < 0.005 compared to control and, ##, p < 0.01 compared between WT and TRPM2-KO cells under the same treatment.

5.2.5 PKC and NOX in A β ₄₂-induced ROS production, activation of PARP-1 and TRPM2 and TNF- α production in microglial cells

PKC and NOX are crucial in the production of ROS in microglial cells in response to Zn²⁺ shown in chapter 4 (see section 4.2.9) or in response to ganglioside shown in a previous study (Min et al., 2004). NOX-dependent ROS production is important in A β -induced microglial cell activation and plays a critical role in AD pathogenesis (Jakebson et al., 2006; Brown & Neher 2010). Hence, I examined ROS production after exposure to different concentrations of A β ₄₂ (30-300 nM) for 8 hr, using DCF. Exposure to A β ₄₂ led to a salient and concentration-dependent increase in DCF fluorescence intensity (Fig. 5.7a), indicating A β ₄₂-induced ROS production. In addition, treatment with CTC (Fig. 5.7b) and, DPI, GKT or Phox (Fig. 5.7c) strongly inhibited or completely prevented A β ₄₂-induced ROS production. These findings suggest that PKC and NOX are involved in A β ₄₂-induced ROS production in microglial cells.

Next, I examined whether PKC/NOX-mediated ROS production is important in A β ₄₂-induced stimulation of PARP-1, TRPM2 channel activation, cell activation and TNF- α production in microglial cells. Treatment with CTC and, DPI, GKT or Phox strongly suppressed or completely abolished A β ₄₂-induced PAR formation (Fig. 5.8a and c) and increases in the [Ca²⁺]_i (Fig. 5.8b and d). These pharmacological treatments also blocked A β ₄₂-induced change in the morphology of microglial cells (Fig. 5.9a-e) and, furthermore, strongly suppressed A β ₄₂-induced TNF- α production (Fig. 5.9f). These results therefore suggest a critical role for PKC/NOX mediated ROS generation in A β ₄₂-induced PARP-1 and TRPM2 channel activation, microglial cell activation and TNF- α production.

5.2.6 PYK2 and MEK/ERK in A β ₄₂-induced activation of PARP-1 and TRPM2-activation and TNF- α production in microglial cells

As shown in studies presented in chapter 4, the PYK2-MEK-ERK signalling pathway acts as a positive feedback mechanism, downstream of TRPM2 channel activation, to stimulate PARP-1 activation in microglial cells following exposure to Zn²⁺ (section 4.2.10). Therefore, I investigated whether such a signalling pathway also participated in A β ₄₂-induced stimulation of PARP-1 and TRPM2 channel activation.

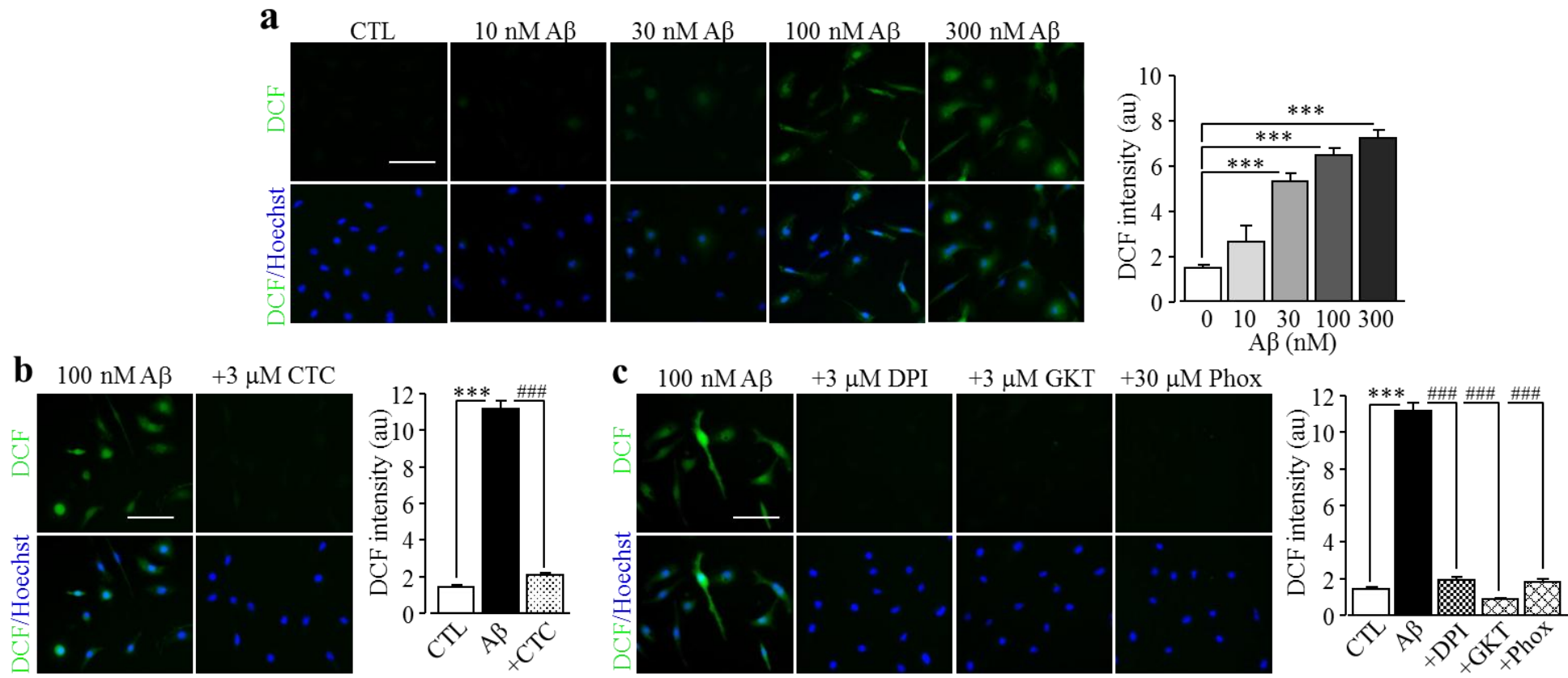


Fig. 5.7 A role for PKC and NOX in A β ₄₂-induced ROS production in microglial cells.

(a-c) *Left*, representative images showing cellular ROS levels (top row: DCF fluorescence; bottom row: counter staining with Hoechst) in cells without (CTL) and with exposure to A β ₄₂ at indicated concentrations for 8 hr (a) and, in cells after exposure for 8 hr to 100 nM A β ₄₂ alone or treatment with 3 μ M CTC (b), 3 μ M DPI, 3 μ M GKT or 30 μ M Phox (c). *Right*, mean A β ₄₂-induced ROS production in microglial cells under indicated conditions, from 3 independent experiments, using three wells of cells for each condition in each experiment. Scale bar, 40 μ m. ***, p < 0.005 compared to control. ##, p < 0.005 compared to the group exposed to A β ₄₂ alone.

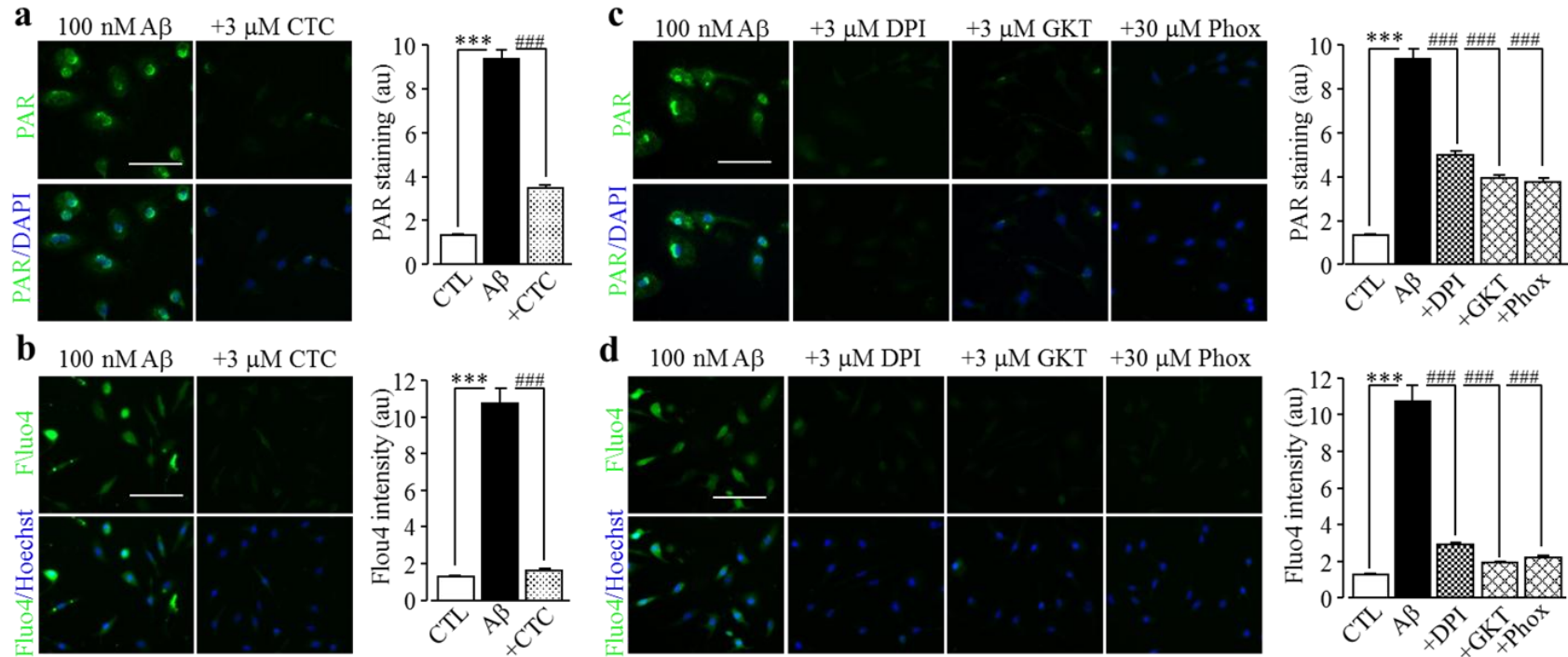
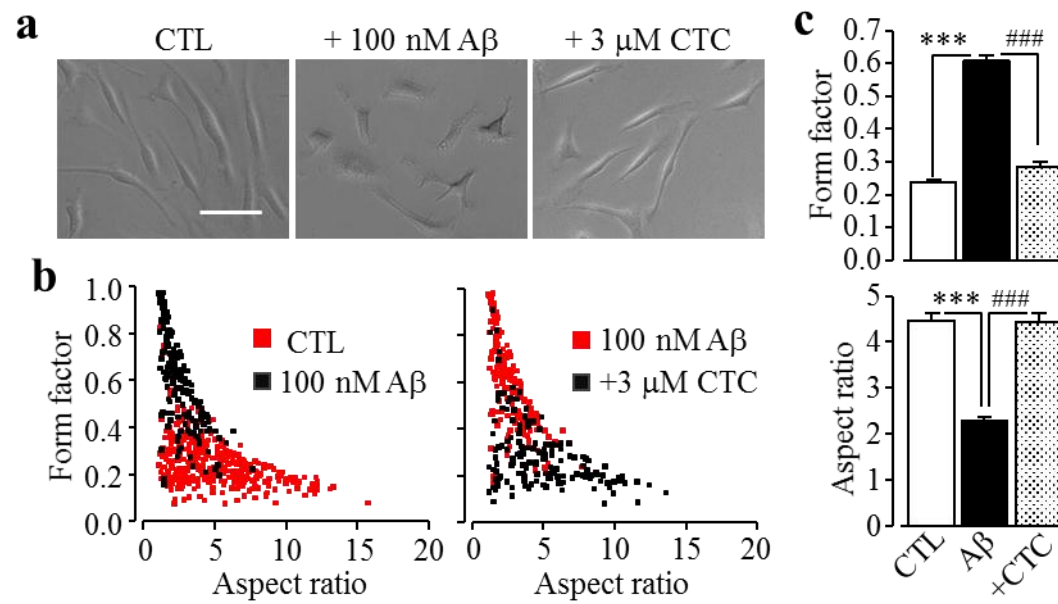


Fig. 5.8 PKC and NOX in A β ₄₂-induced PARP-1 activation and TRPM2 channel activation in microglial cells.

(a, c) Left, representative images showing PAR staining (top row) and counter staining with DAPI (bottom row) of microglial cells after exposure for 8 hr to 100 nM A β ₄₂ alone or treatment with CTC (b), DPI, GKT or Phox (e). Right, mean A β ₄₂-induced PAR staining in microglial cells under indicated conditions from 3 independent experiments, using three wells of cells for each condition in each experiment. (b, d) Left, representative single cell images showing Ca²⁺ responses in microglial cells (top row: Fluo-4 fluorescence; bottom row: counter staining with Hoechst). Right, mean A β ₄₂-induced Ca²⁺ responses in microglial cells under indicated conditions from 3 independent experiments, using 3 wells of cells for each condition in each experiment. Cells were treated with CTC, DPI, GKT or Phox for 30 min prior to and during exposure to A β ₄₂. Scale bar, 40 μ m. ***, p < 0.005 compared between cells without (CTL) and with exposure to 100 nM A β ₄₂. ###, p < 0.005 compared to the group exposed to A β ₄₂ alone.



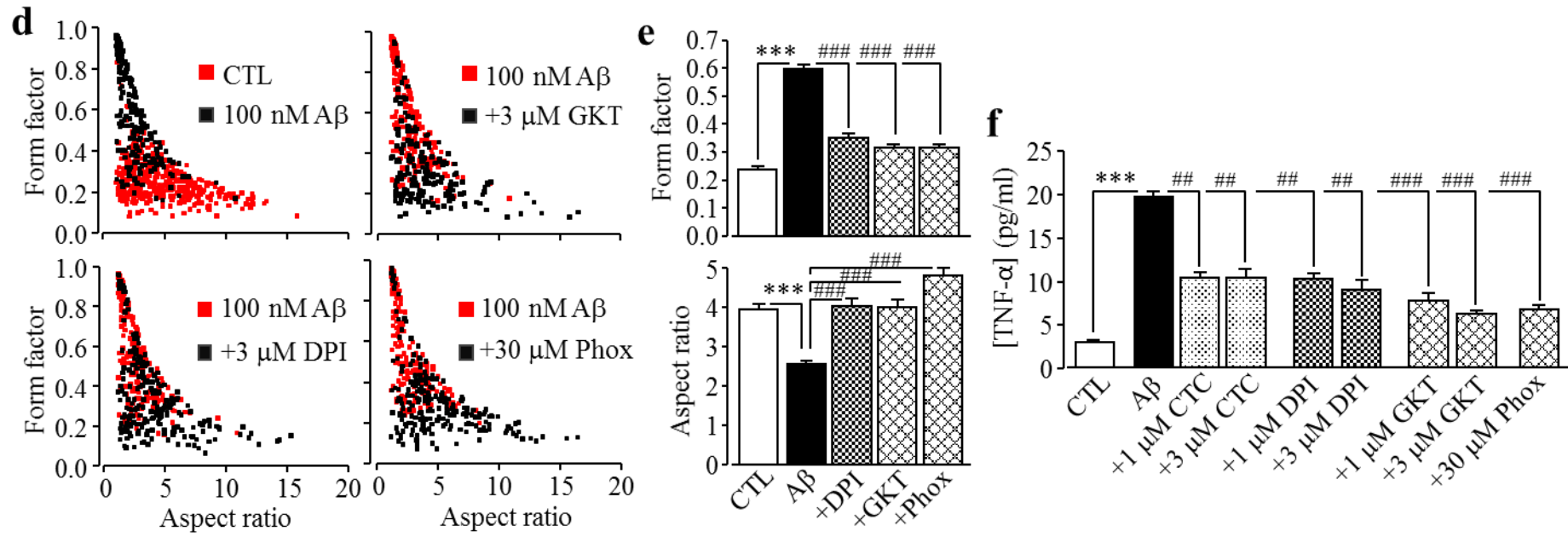


Fig. 5.9 PKC and NOX in A β ₄₂-induced microglial activation and TNF- α production.

(a) Representative phase-contrast images showing cell morphology of microglial cells after exposure to A β ₄₂ for 24 hr alone or treatment with 3 μ M CTC, 30 min prior to and during exposure to A β ₄₂. (b, d) Scatter plot showing distribution of form factor and aspect ratio values for individual cells after exposure for 24 hr to 100 nM A β ₄₂ alone or treatment with 3 μ M CTC (b), 3 μ M DPI, 3 μ M GKT or 30 μ M Phox (d), 30 min prior to and during exposure to A β ₄₂. (c, e) Mean values of form factor (top) and aspect ratio (bottom) in cells under indicated conditions from 3 independent experiments, using 3 wells of cells for each condition in each experiment. (f) Summary of ELISA assay of TNF- α release from cells without (CTL) and with exposure to 100 nM A β ₄₂ alone or treatment with CTC, DPI, GKT or Phox at indicated concentrations from 3 independent experiments, using 3 wells of cells for each condition in each experiment. Cells were treated with CTC, DPI, GKT or Phox for 30 min prior to and during exposure to A β ₄₂. ***, p < 0.005 compared between cells without and with exposure to 100 nM A β ₄₂. ##, p < 0.01; ###, p < 0.005 compared to group exposed to A β ₄₂ alone.

Treatment with PF431296 or U0126 strongly inhibited A β ₄₂-induced PAR production (Fig. 5.10a-b) and increases in the [Ca²⁺]_i (Fig. 5.10c-d). These results support a role for the PYK2-MEK-ERK signalling pathway in A β ₄₂-induced activation of PARP-1 and TRPM2 channel. I also examined the effects of PYK2 and MEK/ERK inhibitors on A β ₄₂-induced microglial activation and TNF- α production. Treatment with PF431396 or U0126 largely prevented A β ₄₂-induced microglial activation (Fig. 5.11a-b), and TNF- α production (Fig. 5.11c). These results further suggest a critical role of the PYK2-MEK-ERK signalling pathway in A β ₄₂-induced microglial cell activation and TNF- α production.

If PKC-dependent NOX activation and the PYK2-MEK-ERK signalling pathways act respectively upstream or downstream of the TRPM2 channel activation in A β ₄₂-induced PARP-1 activation, one expects that the residual A β ₄₂-induced PARP-1 activity in TRPM2-KO microglial cells is exclusively sensitive to the PKC and NOX inhibitors, but not to the PYK2 and MEK/ERK inhibitors. Indeed, A β ₄₂-induced PAR production in TRPM2-KO microglial cells was completely blunted by treatment with CTC and, DPI, GKT or Phox (Fig. 5.12a-d), but totally unaffected by treatment with PF or U0126 (Fig. 5.12e-f). These contrasting results are consistent with notion that the PYK2-MEK-ERK signalling pathway acts downstream of TRPM2 channel activation as a positive feedback mechanism to stimulate PARP-1 and TRPM2 channel activation.

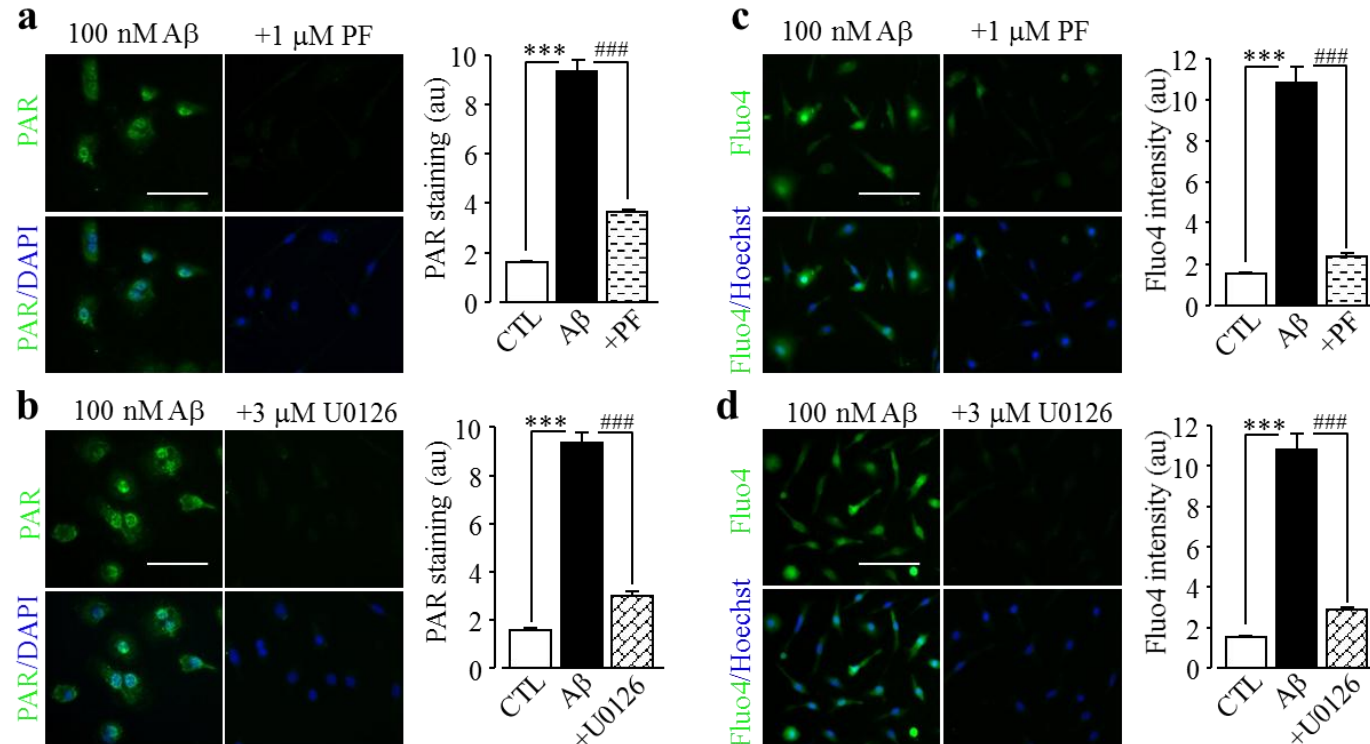


Fig. 5.10 PYK2/MEK/ERK in A β ₄₂-induced PARP-1 activation and TRPM2 channel activation in microglial cells.

(a, b) *Left*, representative images showing PAR level (top row: PAR fluorescence; bottom row: counter staining with DAPI) in cells exposed for 8 hr to 100 nM A β ₄₂ alone or together with 1 μ M PF 431396 (PF) (a) or 3 μ M U0126 (b). *Right*, mean PAR fluorescence intensity in cells without (CTL) and with exposure to 100 nM A β ₄₂ alone or together with 1 μ M PF (a) or 3 μ M U0126 (b) from 3 independent experiments, using 3 wells of cells for each condition in each experiment. (c, d) *Left*, representative single cell images showing Ca²⁺ responses (top row: Fluo-4 fluorescence; bottom row: counterstaining with Hoechst) in cells exposed to 100 nM A β ₄₂ without and with treatment with 1 μ M PF (c) or 3 μ M U0126 (d). *Right*, mean A β ₄₂-induced Ca²⁺ responses in cells under indicated conditions from 3 independent experiments, using 3 wells of cells for each condition in each experiment. ***, p < 0.005 compared between cells without (CTL) and with exposure to 100 nM A β ₄₂ alone and, ###, p < 0.005 compared to group exposed to A β ₄₂ alone.

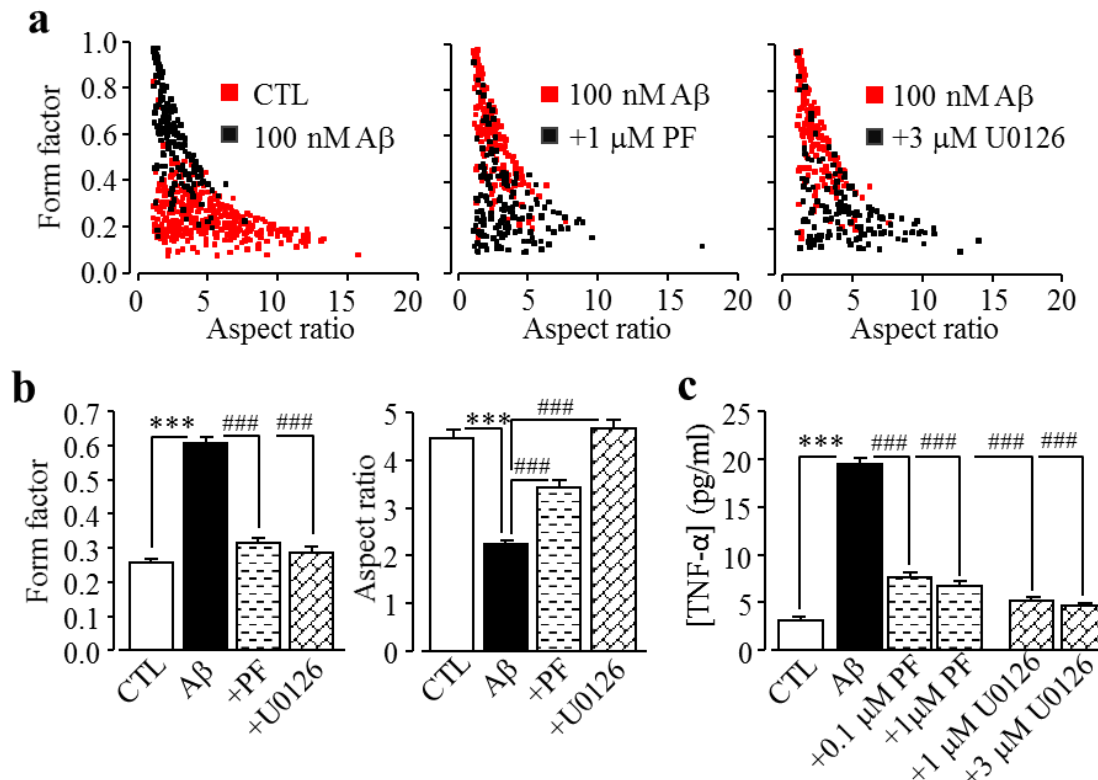
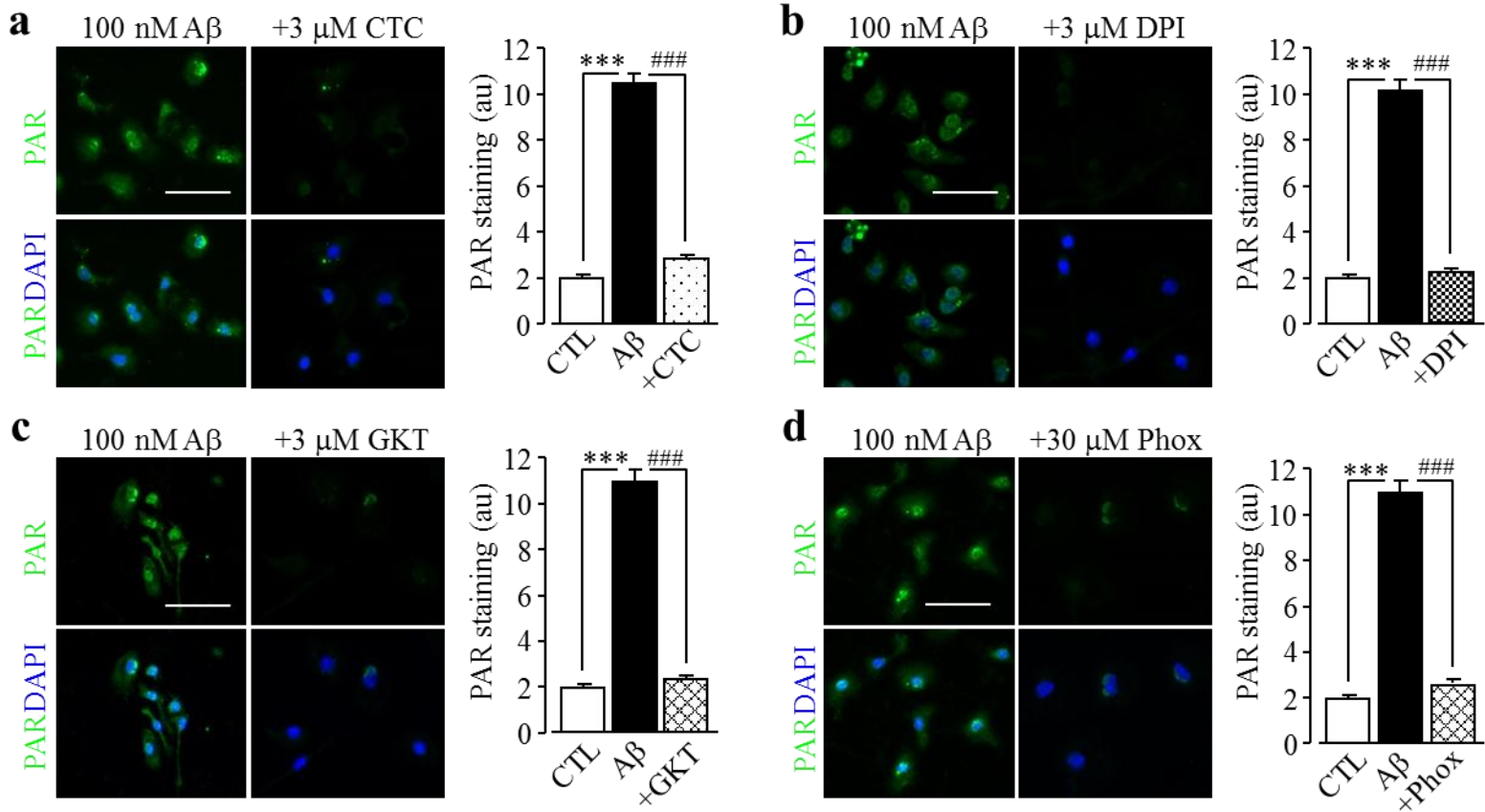


Fig. 5.11 PYK2/MEK/ERK in A β ₄₂-induced microglial cell activation and TNF- α production.

(a) Scatter plot showing distribution of form factor and aspect ratio values of individual cells without (CTL) and with exposure for 24 hr to 100 nM A β ₄₂ alone or treatment with 1 μ M PF or 3 μ M U0126. (b) Mean values of form factor (left) and aspect ratio (right) in cells under indicated conditions from 3 independent experiments, using 3 wells of cells for each condition in each experiment. (c) Summary of ELISA assay of TNF- α release by cells without (CTL) and with exposure for 72 hr to 100 nM A β ₄₂ alone or treatment with PF or U0126 at indicated concentrations from 3 independent experiments, using 3 wells of cells for each condition in each experiment. Cells were treated with PF and U0126 for 30 min prior to and during exposure to 100 nM A β ₄₂. ***, p < 0.005 compared between cells without (CTL) and with exposure to A β ₄₂. **#, p < 0.005 compared to group exposed to A β ₄₂ alone.



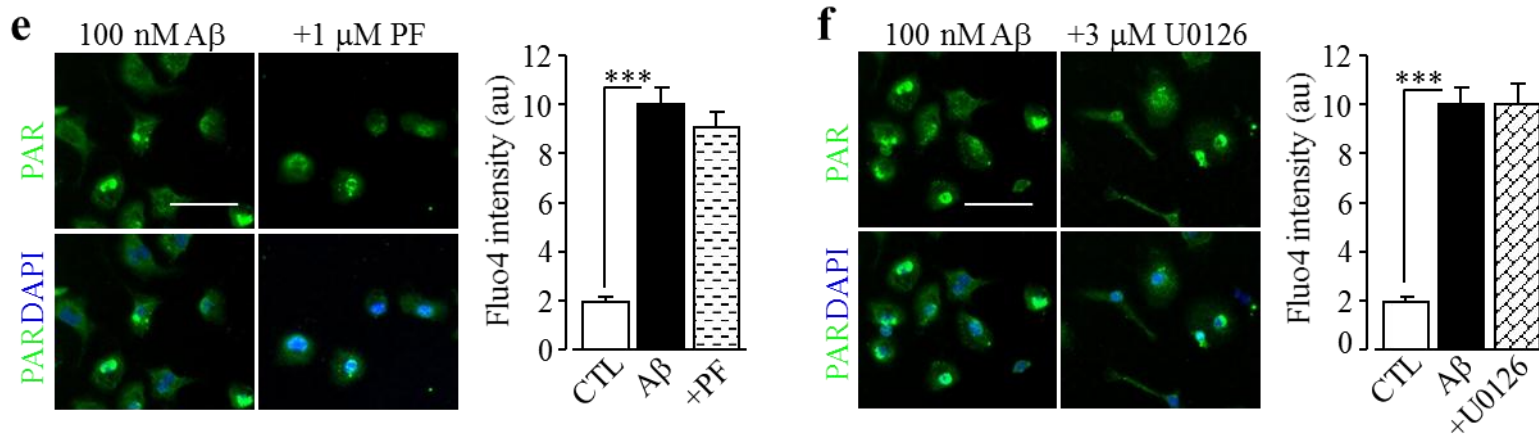


Fig. 5.12 PKC/NOX activation is required for, and PYK2/MEK activation depends on, A β ₄₂-induced TRPM2 channel activation.

(a-f) *Left*, representative images showing PAR level (top row: PAR fluorescence; bottom row: counterstaining with DAPI) in TRPM2-KO microglia cells exposed for 8 hr to 100 nM A β ₄₂ alone or together with 3 μ M CTC (a), 3 μ M DPI (b), 3 μ M GKT (c), 30 μ M Phox (d), 1 μ M PF (e) or 3 μ M U0126 (f), 30 min prior to and during exposure to A β ₄₂. *Right*, mean PAR fluorescence intensity in microglial cells under indicated conditions from 3 independent cell preparations, using 3 wells of cells for each condition in each experiment. Scale bar, 40 μ m. ***, p < 0.005 compared between cells without (CTL) and with exposure to A β ₄₂ alone and, **, p < 0.005 compared to group exposed to A β ₄₂ alone.

5.3 DISCUSSION

Studies presented in this chapter provide evidence to show that PKC/NOX-mediated ROS production and PARP-1 activation are required for A β ₄₂-induced TRPM2 channel activation. Furthermore, the PYK2-MEK-ERK signalling pathway, as a positive feedback mechanism downstream of the TRPM2 channel activation, facilitates activation of PARP-1 and TRPM2 channel. These molecular and signalling mechanisms are important in A β ₄₂-induced microglial cell activation and TNF- α production (Fig. 5.13).

As shown in chapter 3 (section 3.2.4), the TRPM2 channel plays a crucial role in mediating A β ₄₂-induced increase in the [Ca²⁺]_i in microglial cells. Here, I further showed that removal of extracellular Ca²⁺ (Fig. 5.1a-b) or treatment with the TRPM2 channel inhibitor 2-APB (Fig. 5.1c-d) prevented A β ₄₂-induced increase in the [Ca²⁺]_i in microglial cells indicating that TRPM2 channel-mediated Ca²⁺ influx leads to A β ₄₂-induced increase in the [Ca²⁺]_i. Consistently with that A β ₄₂-induced change in the morphology of microglial cells was inhibited by TRPM2-KO (section 3.2.6), treatment with 2-APB significantly inhibited A β ₄₂-induced change in the cell morphology (Fig. 5.2a-c), supporting a critical role for the TRPM2 channel in A β ₄₂-induced microglial activation.

TRPM2-dependent microglial activation is strongly implicated in A β -induced neuroinflammation (Ostapchenko et al., 2015), but evidence supporting the role for the TRPM2 channel in A β -induced neuroinflammation is still lacking. As introduced above, it has been well recognized that TNF- α , a major pro-inflammatory cytokine produced by activated microglial cells, is potent in inducing neurotoxicity and A β -induced TNF- α generation significantly contributes to neuroinflammation in AD pathogenesis (Block et al., 2007; Heppner et al., 2015; Alam et al., 2016; Krabbe et al., 2017). In this chapter, I showed that exposure to A β ₄₂ induced TNF- α generation by microglial cells (Fig. 5.3a-c). Interestingly, A β ₄₂-induced TNF- α generation was deficient in TRPM2-KO microglial cells (Fig. 5.4a-c), and strongly attenuated by the TRPM2 channel inhibitor 2-APB (Fig. 5.4d). It has been shown that ROS-induced TRPM2 channel activation caused microglial cell death (section 3.2.2). However, exposure to A β ₄₂ up to 300 nM for 72 hr, a condition used for TNF- α release assay, induced no significant necrotic microglial cell death (section 3.2.5), largely ruling out the possibility that A β ₄₂-induced TNF- α release results from microglial cell death. These results provide compelling evidence for the first time to show a critical role of the TRPM2 channel in A β -induced

TNF- α generation, therefore offering novel insights into A β -induced inflammation. Furthermore, considering the well-known neurotoxicity of TNF- α , these findings suggest a significant role of A β -induced neuroinflammation in AD pathogenesis.

The results described in this chapter also have provided insights into the signalling mechanisms by which A β_{42} induces TRPM2 channel activation in microglial cells. As introduced above, A β -induced PARP-1 activation in microglial cells was shown in a previous study (Kauppinen et al., 2011). Consistently, exposure to A β_{42} strongly increased PAR formation, which was highly concentrated in the nucleus (Fig. 5.6a-b), suggesting A β_{42} -induced PARP-1 activation. In addition A β_{42} -induced PAR formation was prevented by treatment with PJ34 (Fig. 5.6c-d). Furthermore, A β_{42} -induced increase in the $[Ca^{2+}]_i$ (Fig. 5.5a-b), change in the cell morphology (Fig. 5.5c-f) and TNF- α production (Fig. 5.5g) in microglial cells were prevented by treatment with PJ34. These results are consistent with PARP-1 being a critical factor in A β -induced microglial cell activation (Kauppinen et al., 2011).

In this chapter, I also showed that the sequential activation of PKC and NOX, including NOX1/4 and NOX2, NOX-mediated ROS production, and PARP-1 activation are important in A β_{42} -induced TRPM2 channel-mediated microglial cell activation and TNF- α production (Figs. 5.7, 5.8 and 5.9).

In the previous chapter (section 4.2.10), TRPM2 channel activation, possibly TRPM2 channel-mediated Ca^{2+} influx, triggers the PYK2-MEK-ERK signalling pathway as a positive feedback mechanism that enhances PARP-1 activation and subsequent TRPM2 channel activation in microglial cell in response to prolonged exposure to Zn $^{2+}$. Here, I showed that inhibition of this signalling pathway prevented A β_{42} -induced PARP-1 activation (Fig. 5.10a-b) and increase in the $[Ca^{2+}]_i$ in WT microglial cells (Fig. 5.10c-d). Genetic deletion of the TRPM2 channel expression significantly attenuated, but did not completely prevent, A β_{42} -induced PARP-1 activation (Fig. 5.6c-d), supporting critical involvement of TRPM2 channel in A β_{42} -induced stimulation of PARP-1. Furthermore, the remaining A β_{42} -induced PARP-1 activation in TRPM2-KO microglial cells was totally abolished by inhibiting PKC and NOX (Fig. 5.12a-d), but was not altered by inhibiting PYK2 and MEK/ERK (Fig. 5.12e-f). These differentiating results support the notion that A β_{42} -induced PKC/NOX-mediated ROS production and PARP-1 activation initiates the TRPM2 channel activation, which leads to, possibly via TRPM2-mediated Ca^{2+} influx, activation of the PYK2-MEK-ERK signalling pathway to further facilitate activation of PARP-1 and

TRPM2 channel. Interestingly, A β ₄₂-induced microglial activation and TNF- α production were prevented by inhibition of these signalling mechanisms (Fig. 5.11a-c).

In conclusion, the studies presented in this chapter provide evidence to show that PKC-dependent NOX-mediated ROS production and PARP-1 activation are required for A β ₄₂-induced TRPM2 channel activation and the PYK2-MEK-ERK signalling pathway as a positive feedback mechanism further stimulates activation of PARP-1 and TRPM2 channel (Fig. 5.13). These novel findings afford mechanistic insights into A β -induced neuroinflammation in AD pathogenesis.

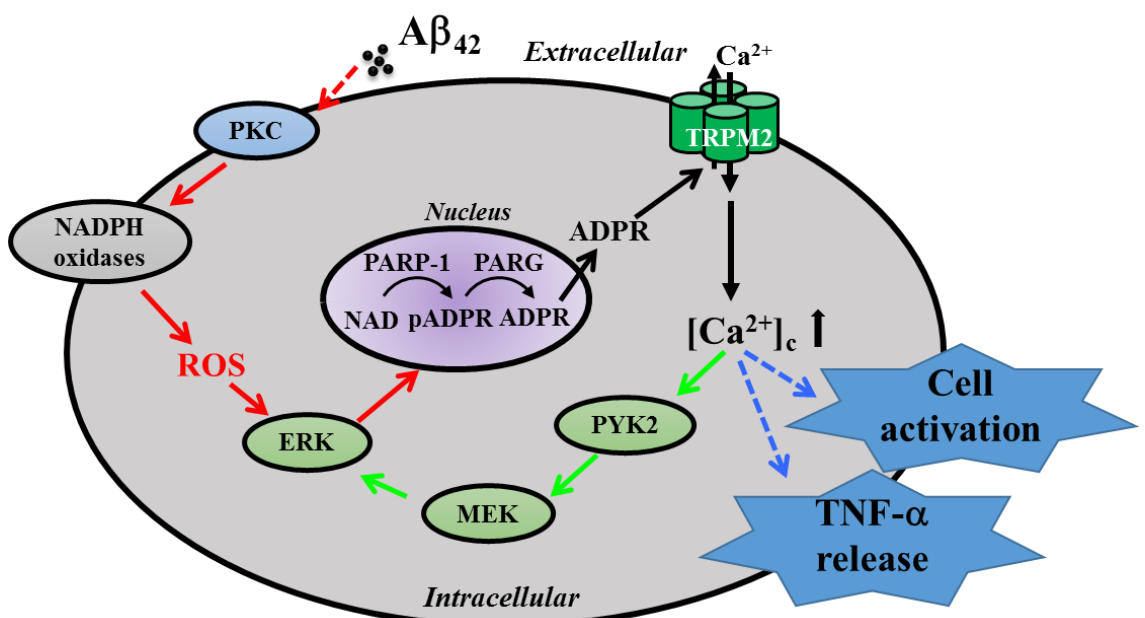


Fig. 5.13 Schematic summary of the signalling mechanisms mediating A β ₄₂-induced TRPM2 channel and microglial activation as well as TNF- α generation.

A β ₄₂ activates the TRPM2 channel involving multiple-step intracellular signalling pathways in microglial cell activation and TNF- α generation. A β ₄₂ stimulates PKC and NOX. ROS activates PARP-1 and PARG in the nucleus leading to ADPR production and subsequent activation of TRPM2-dependent Ca²⁺ influx to increase the cytoplasmic Ca²⁺ concentrations ([Ca²⁺]_c). Elevated [Ca²⁺]_c in turn activate the PYK2/MEK/ERK signalling pathway as a positive feedback mechanism that amplifies activation of PARP-1, leading to TRPM2-mediated Ca²⁺ overloading, microglial cell activation and TNF- α generation.

CHAPTER 6

TNF- α AUTOCRINE/PARACRINE SIGNALLING MECHANISMS VIA TRPM2 CHANNEL IN MICROGLIAL CELLS

6.1 INTRODUCTION

It has been long known that TNF- α is involved in initiating and propagating the inflammatory responses and in the pathogenesis of multiple neurodegenerative diseases, including AD, rheumatoid arthritis (RA) and Crohn's disease (Van Deventer, 1997; Feldmann, 2002; Paouri et al., 2017). Studies have shown promising application of anti-TNF- α drugs in reducing cognitive impairments associated with AD (Shi et al., 2011). Application of TNF- α inhibitor or deletion of the TNF- α receptors in mouse AD models results in a significant reduction in A β accumulation (Gabbita et al., 2015).

Microglial cells represents the major source of TNF- α generation in the CNS (Krabbe et al., 2017; Paouri et al., 2017). TNF- α , on one hand, is generated by activated microglial cells in response to DAMP molecules, such as A β ₄₂ shown in the previous study, and on the other, acts as a DAMP to stimulate the microglial cell activation (Meda et al., 1995). Therefore, TNF- α serves as an autocrine or paracrine signalling molecule. A previous study provides evidence to show that TNF- α stimulates a positive autocrine loop as a result from the prolonged activation of microglial cells by LPS (Kuno et al., 2005). It is also suggested that TNF- α , when applied exogenously, can induce activation of microglial cells (Kauppinen and Swanson, 2005).

There is evidence to show the activation of TRPM2 channel by TNF- α (Roberge et al., 2014). In addition, studies presented in the previous chapter (chapter 3) showed a critical role of the TRPM2 channel for TNF- α -induced microglial cell activation. However, the signalling mechanisms involved in TNF- α -induced TRPM2 channel activation and subsequently microglial cell activation, particularly production of TNF- α itself still remain unclear. Genetic deletion of the NOX expression in endothelial cells strongly inhibited TNF- α -induced ROS production (Frey et al., 2002), indicating a critical role for NOX in TNF- α -induced ROS production. In addition, NOX-dependent ROS production is required for TNF- α -induced microglial cell activation (Jekabsone et al., 2006). ROS in turn can up-regulate TNF- α expression via activation of MAPK signalling pathway (Nakao et al., 2008).

In this chapter, I investigated the role of the TRPM2 channel in microglial cell activation and TNF- α production in response to TNF- α and the signalling mechanisms involved in TNF- α -induced TRPM2 channel activation, microglial cell activation and TNF- α generation.

6.2 RESULTS

6.2.1 TRPM2 channel in TNF- α -induced Ca^{2+} influx and microglial cell activation

The results presented in chapter 3 show that the TRPM2 channel is critical in mediating TNF- α -induced increase in the $[\text{Ca}^{2+}]_i$ (section 3.2.4). To better understand the role of the TRPM2 channel in TNF- α -induced Ca^{2+} signalling, I examined TNF- α -induced increase in the $[\text{Ca}^{2+}]_i$ in microglial cells in extracellular Ca^{2+} -containing and Ca^{2+} -free solutions. TNF- α -induced increase in the $[\text{Ca}^{2+}]_i$ was observed in Ca^{2+} -containing solution, but not in Ca^{2+} -free solution (Fig. 6.1a), indicating TNF- α -induced TRPM2 channel-mediated Ca^{2+} signalling via Ca^{2+} influx. In addition, treatment of the TRPM2 channel inhibitor 2-APB attenuated TNF- α -induced increase in the $[\text{Ca}^{2+}]_i$ (Fig. 6.1b). These findings consistently support TNF- α -induced TRPM2 channel activation, leading to extracellular Ca^{2+} influx and increase in the $[\text{Ca}^{2+}]_i$.

As shown in previous chapter (section 3.2.6), studies using a genetic knockout approach have revealed a role of the TRPM2 channel in mediating TNF- α -induced microglial cell activation. To further confirm this finding, I examined the effects of the TRPM2 channel inhibitor 2-APB on TNF- α -induced microglial cell activation. TNF- α -induced change in the morphology of microglial cells was prevented by 2-APB (Fig 6.2a-c). These pharmacological results further support a critical role of the TRPM2 channel for TNF- α -induced microglial cell activation.

6.2.2 TRPM2 channel in TNF- α induced TNF- α production in microglial cells

As introduced above, TNF- α is the major pro-inflammatory cytokine generated by microglial cells following exposure to various DAMP molecules. Consistently, studies presented in the previous chapter show $\text{A}\beta_{42}$ induces TNF- α production in microglial cells (section 5.2.3). TNF- α can acts as an autocrine/paracrine signalling molecule and mediates microglial cell activation, as shown in chapter 3 (section 3.2.6) as well as in previous studies (Kuno et al., 2005). Therefore, it is interesting to investigate whether TNF- α -induced microglial cell activation promotes TNF- α production. I examined the TNF- α expression in microglial cells after 48 hr exposure to TNF- α and, TNF- α released

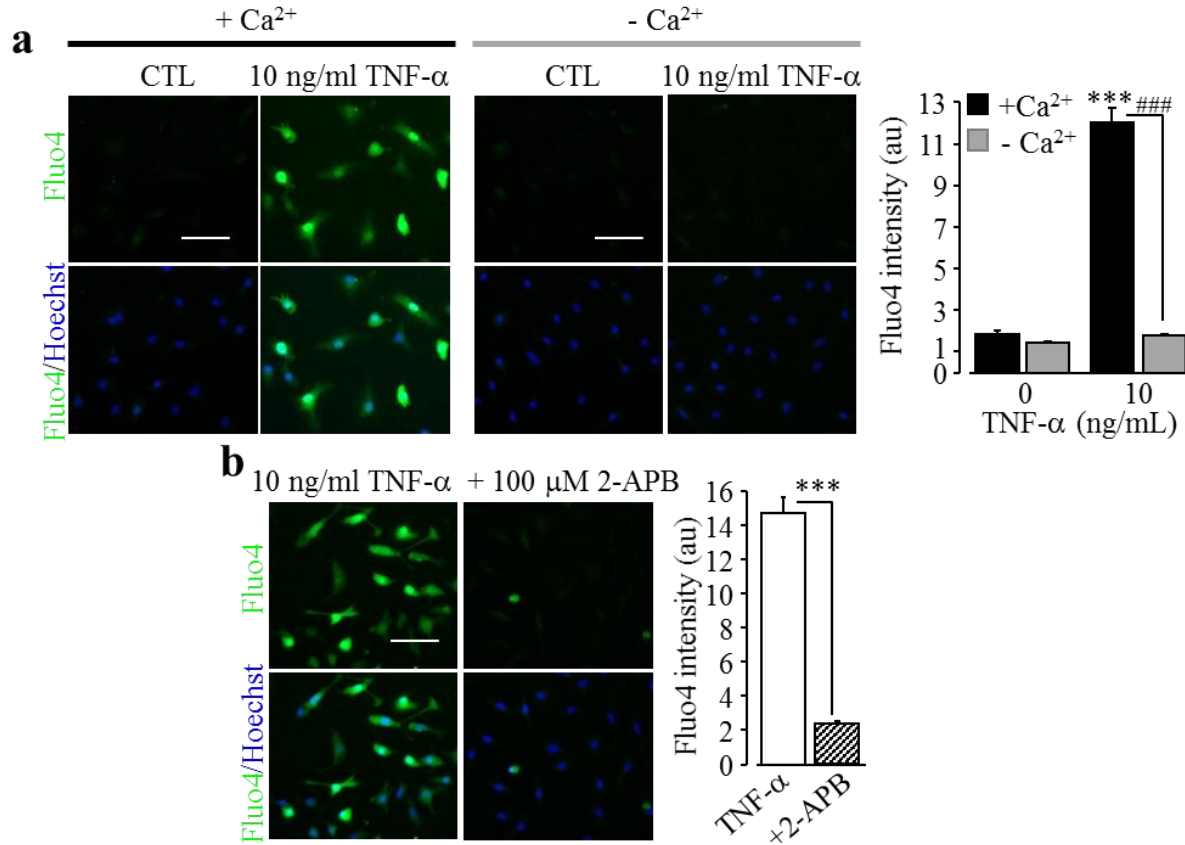


Fig. 6.1 TNF-α induces Ca²⁺ influx through the TRPM2 channel in microglial cells.

(a, b) Left, representative single cell images showing intracellular Ca²⁺ levels in cells (top row: Fluo4 fluorescence; bottom row: counter staining with Hoechst) after exposed to 10 ng/ml TNF-α for 8 hr in Ca²⁺-containing (+Ca²⁺) or Ca²⁺-free (-Ca²⁺) solutions (a) and, 10 ng/ml TNF-α for 8 hr alone or treatment with 100 μM 2-APB (b), 30 min prior to and during exposure to TNF-α. Right, mean TNF-α-induced Fluo4 fluorescence intensity, indicative of intracellular Ca²⁺ levels, in cells under indicated conditions from 3 independent experiments, using 3 wells of cells for each condition in each experiment. Scale bar, 40 μm. *, p < 0.05; ***, p < 0.005 compared to control. ###, p < 0.005 ###, between cells exposed to TNF-α in the presence and absence of extracellular Ca²⁺.

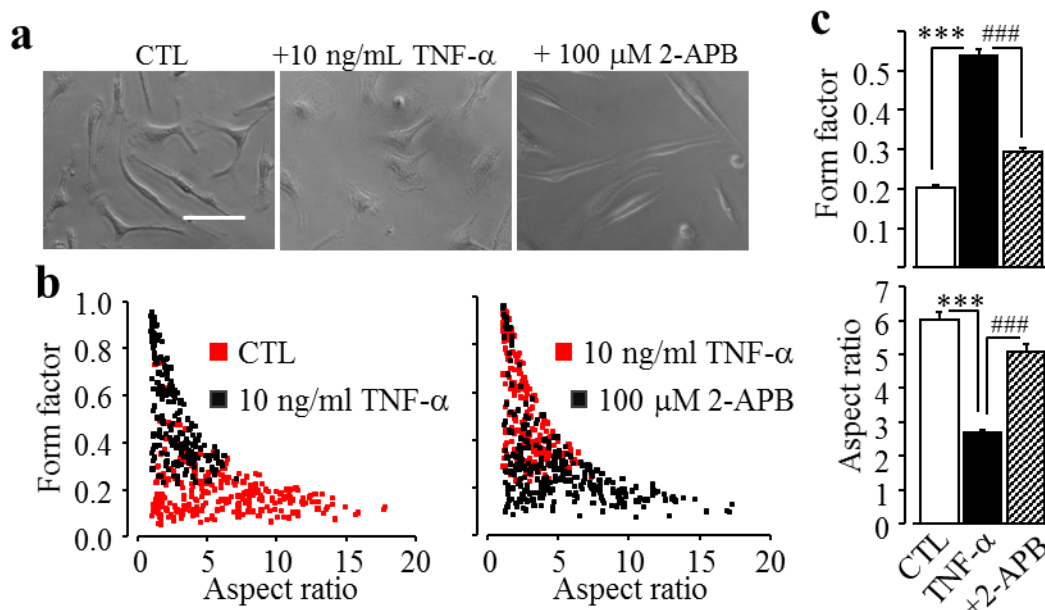


Fig. 6.2 Activation of TRPM2 channel is required for TNF- α -induced microglial cell activation.

(a) Representative phase-contrast images showing cell morphology of microglial cells after exposure to 10 ng/ml TNF- α for 24 hr alone or treatment with 100 μ M 2-APB, 30 min prior to and during exposure to TNF- α , captured using an EVOS microscope with a 40x object lens. (b) Scatter plot showing distribution of form factor and aspect ratio of individual WT microglial cells after exposure to 10 ng/ml TNF- α for 24 hr alone or treatment with 100 μ M 2-APB, 30 min prior and duration exposure to TNF- α . (c) Mean values of form factor (top) and aspect ratio (bottom) of microglial cells under indicated conditions from at least 3 independent experiments, using 3 wells of cells for each condition in each experiment. Scale bar, 50 μ m. ***, p < 0.005 compared to control. ****, p < 0.005 compared to cells exposed to TNF- α alone.

into the culture medium after 72 hr exposure to TNF- α . Exposure to TNF- α at 10-100 ng/ml for 48 hr induced significant and concentration-dependent increase in the TNF- α expression in microglial cells (Fig. 6.3a-b). Consistently, there was a concentration-dependent increase in TNF- α release (Fig. 6.3c). These results strongly suggest that TNF- α serves as an autocrine/paracrine signalling molecule.

Next I examined whether the TRPM2 channel is involved in such a positive feedback loop signalling mechanism by using genetic and pharmacological approaches. In contrast with strong increase in the TNF- α generation seen in WT microglial cells, no or very modest TNF- α expression was observed in TRPM2-KO microglial cells (Fig. 6.4a-b). Consistently, there was no TNF- α release by TRPM2-KO microglial cells following exposure to TNF- α (Fig. 6.4c). Furthermore, treatment with 2-APB strongly attenuated TNF- α generation in WT microglial cells in response to exposure to TNF- α (Fig. 6.4d). These results provide compelling evidence to indicate a critical role for the TRPM2 channel in TNF- α -induced microglial cell activation and TNF- α generation.

6.2.3 PARP-1 is required in TNF- α -induced TRPM2 channel activation and TNF- α generation in microglial cells

Studies presented in the previous chapter have demonstrated a critical role for PARP-1 activation in TRPM2 channel-mediated A β ₄₂-induced microglial cell activation (section 5.2.4). So, I further tested the hypothesis that PARP-1 is involved in TNF- α -induced TRPM2 channel activation and subsequently microglial cell activation by examining the effects of PARP inhibitors on TNF- α -induced increase in the [Ca²⁺]_i, microglial cell activation and TNF- α production. TNF- α -induced increase in the [Ca²⁺]_i (Fig. 6.5a-b) and microglial cell activation (Fig. 6.5c-f) were strongly inhibited by treatment with PJ34. Furthermore, TNF- α generation in microglial cell induced by TNF- α was significantly inhibited by PJ34 and DPQ (Fig. 6.5g). PAR immunofluorescence staining showed that exposure to TNF- α resulted in massive PAR production in microglial cells and that PAR was co-localized with DAPI staining (Fig. 6.6a-b). TNF- α -induced PAR production was detected in the TRPM2-KO microglial cells but lesser than that in WT microglial cells (Fig. 6.6c-d). As expected, treatment with PJ34 strongly inhibited TNF- α -induced PAR production in both WT and TRPM2-KO cells (Fig. 6.6c-d). Taken together, these results support that PARP-1 plays a crucial role in mediating

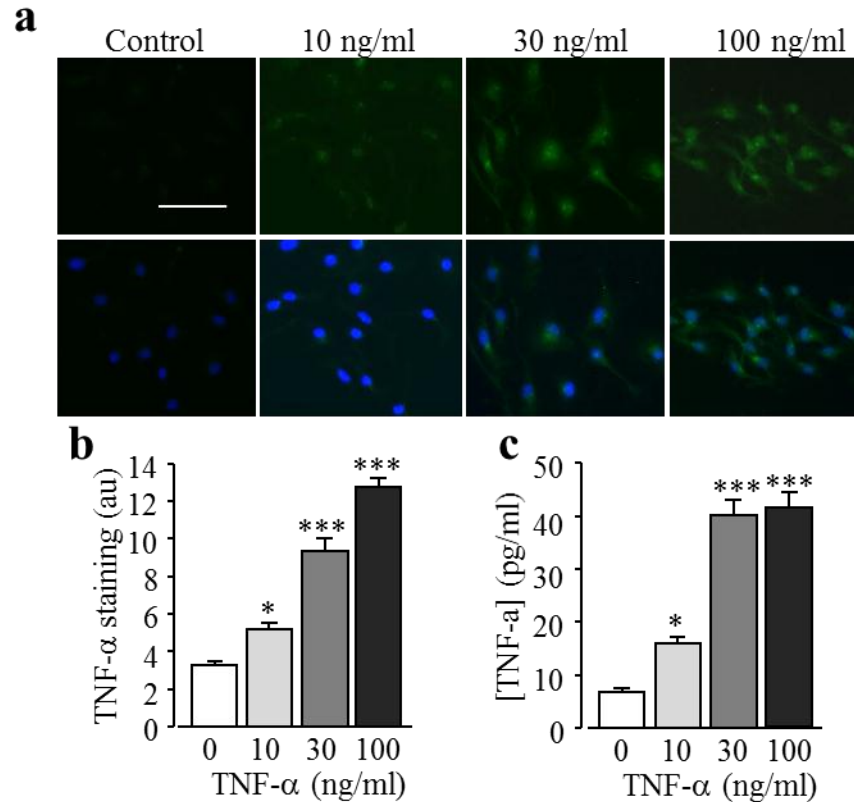


Fig. 6.3 TNF- α induces autocrine/paracrine action by producing TNF- α in microglial cells.

(a) Representative fluorescent images showing TNF- α immunoreactivity labelled with an anti-TNF- α antibody in microglial cells without (CTL) and with exposure to TNF- α at indicated concentrations for 48 hr. Cells were counterstained with DAPI. (b) Summary of mean TNF- α expression in microglial cells under indicated conditions from 3 independent experiments, using 3 wells of cells for each condition in each experiment. (c) Summary of ELISA assay of TNF- α release by microglial cells after exposed to TNF- α at indicated concentrations for 72 hr from 3 independent experiments, using 3 wells of cells for each condition in each experiment. Scale bar, 40 μ m. *, p < 0.05; ***, p < 0.005 compared to indicated control group.

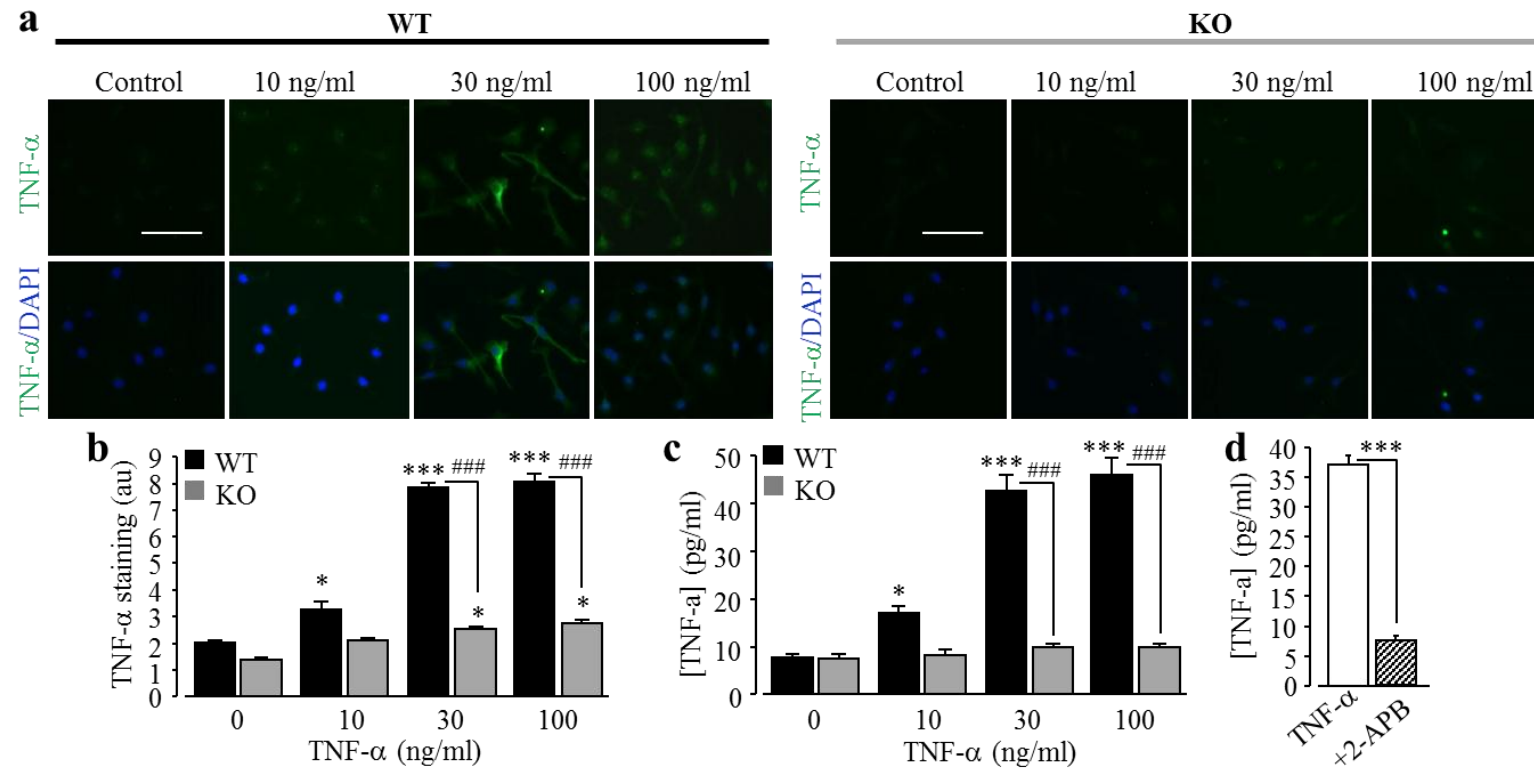
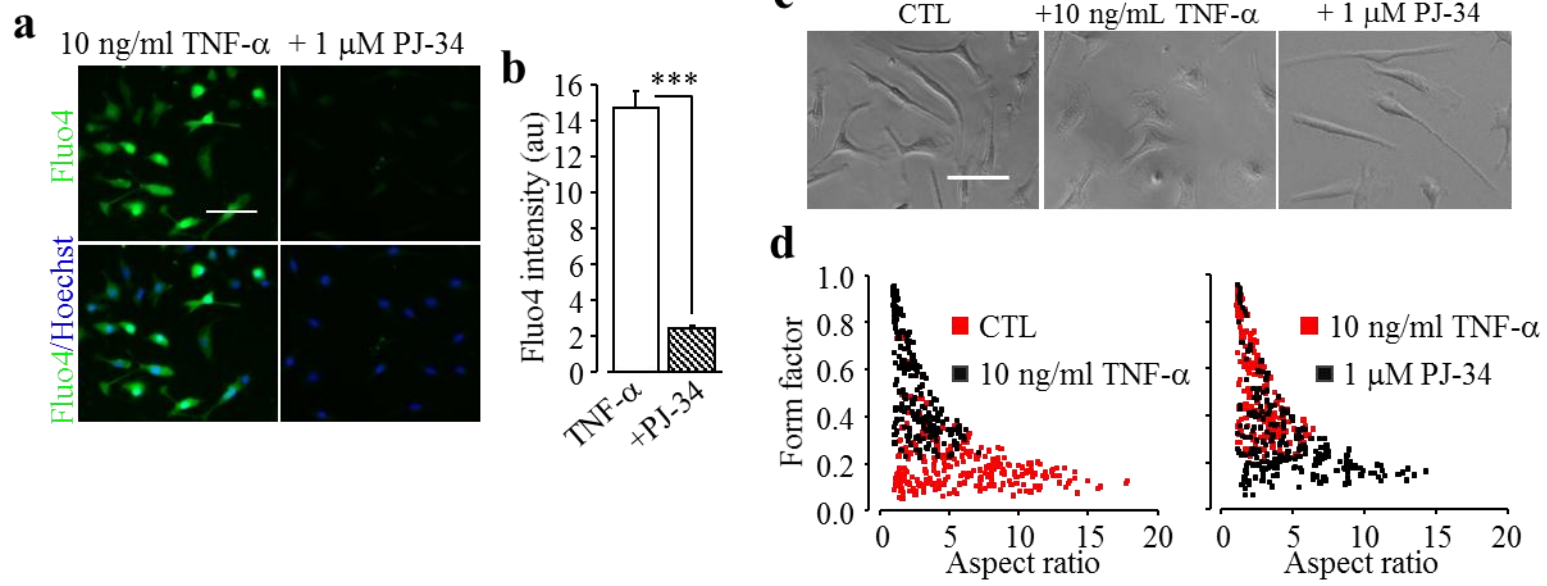


Fig. 6.4 TRPM2 channel is required for TNF- α -induced TNF- α production by microglial cells.

(a) Representative fluorescent images showing TNF- α immunoreactivity in microglial WT and TRPM2-KO cells without (CTL) and with exposure to TNF- α at indicated concentrations for 48 hr. Cells were counterstained with DAPI. (b) Summary of mean TNF- α expression under indicated conditions from 3 independent experiments, using 3 wells of cells for each condition in each experiment. (c) Summary of ELISA assay of TNF- α release by WT and TRPM2-KO cells after exposure to TNF- α at indicated concentrations for 72 hr from 3 independent experiments, using 3 wells of cells for each condition in each experiment. (d) Summary of ELISA assay of TNF- α release after exposure to 30 ng/ml TNF- α for 72 hr alone or treatment with 100 μ M 2-APB, 30 min prior to during exposure to TNF- α from 3 independent experiments, using 3 wells of cells for each condition in each experiment. Scale bar, 40 μ m. *, p < 0.05; ***, p < 0.005 compared to control. #, p < 0.05; ###, p < 0.005 compared between WT and TRPM2-KO cells under the same treatment.



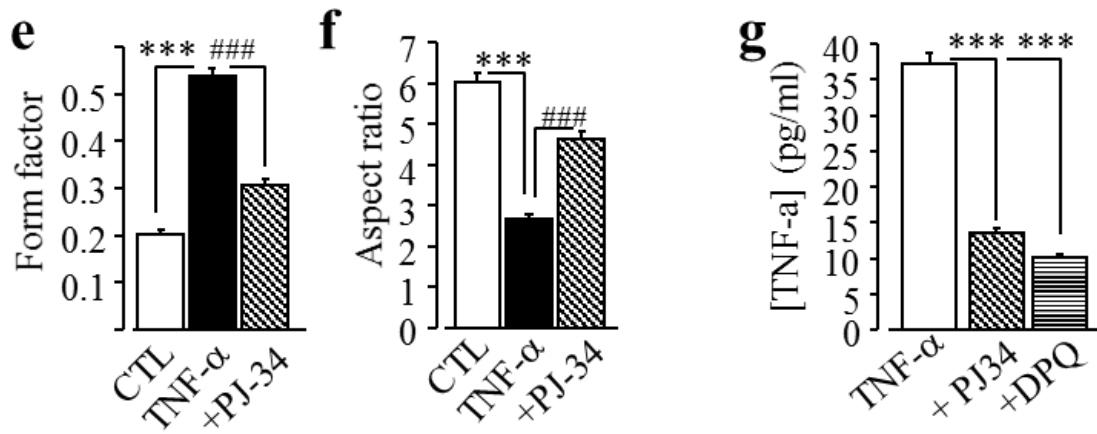


Fig. 6.5 Activation of PARP is required for TNF- α -induced microglial cell activation.

(a) Representative single cell images showing intracellular Ca^{2+} levels in microglial cells (top row: Fluo4 fluorescence; bottom row: counter staining with Hoechst) after exposed to 10 ng/ml TNF- α for 8 hr alone or treatment with 1 μM PJ34, 30 min prior to and during exposure to TNF- α . (b) Mean TNF- α -induced Fluo4 fluorescence intensity, indicative of the intracellular Ca^{2+} levels in cells under indicated conditions from 3 independent experiments, using 3 wells of cells for each condition in each experiment. (c) Representative phase-contrast images showing cell morphology of microglial cells after exposure to 10 ng/ml TNF- α for 24 hr alone or treatment with 1 μM PJ34, 30 min prior to and during exposure to TNF- α , captured using an EVOS microscope with a 40x object lens. (d) Scatter plot showing distribution of form factor and aspect ratio of individual WT microglial cells after exposure to 10 ng/ml TNF- α for 24 hr alone or treatment with 1 μM PJ34, 30 min prior and duration exposure to TNF- α . (e-f) Mean values of form factor (e) and aspect ratio (f) of microglial cells under indicated conditions from at least 3 independent experiments, using 3 wells of cells for each condition in each experiment. (g) Summary of ELISA assay of TNF- α release after exposure to 30 ng/ml TNF- α for 72 hr alone or treatment with 1 μM PJ34 or 10 μM DPQ, 30 min prior to during exposure to TNF- α from 3 independent experiments, using 3 wells of cells for each condition in each experiment. Scale bar, 40 μm (a) and 50 μm (c). **, p < 0.01; ***, p < 0.005 compared to control. ###, p < 0.005 compared to cells exposed to TNF- α alone.

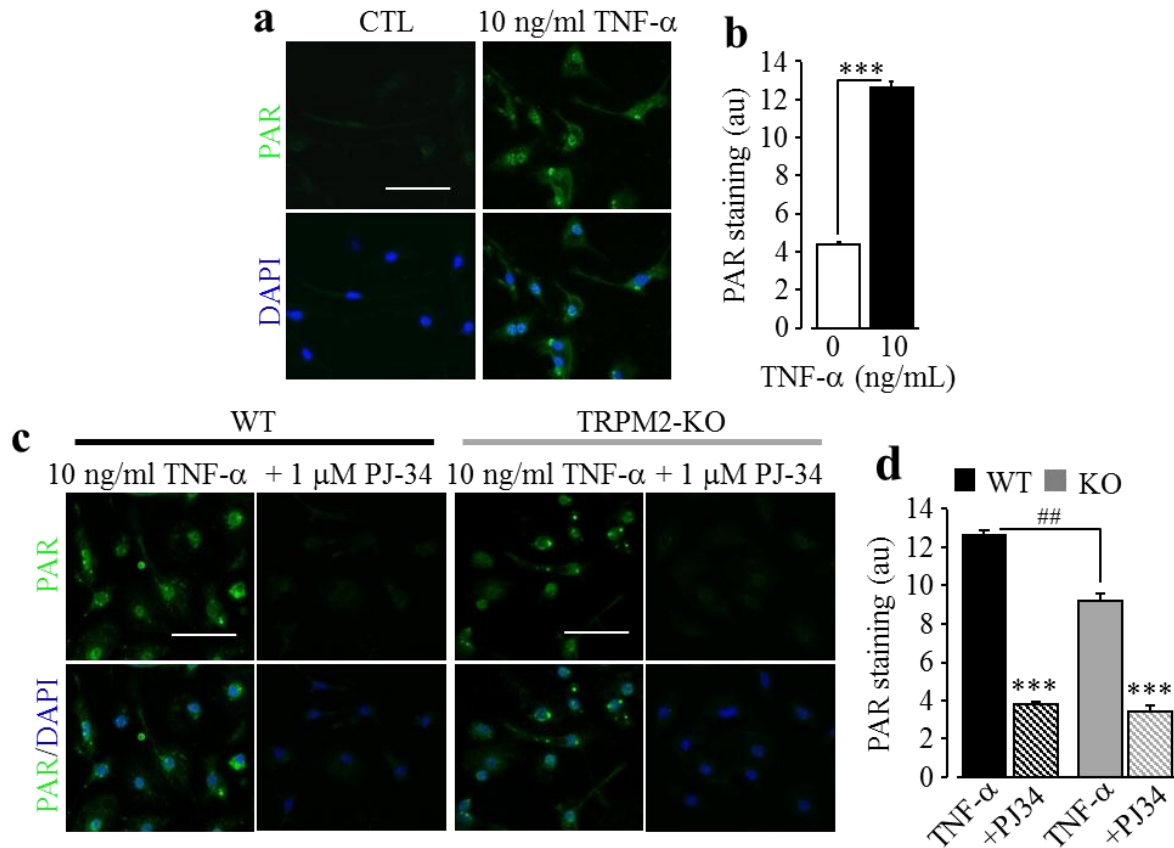


Fig. 6.6 TNF- α induces PARP-1 activation in microglial cells.

(a, c) Representative fluorescent images showing PAR staining (top row) and counter staining with DAPI (bottom row) without (CTL) and with exposure to 10 ng/ml TNF- α for 8 hr (a), or after exposure to 10 ng/ml TNF- α for 8 hr alone or treatment with 1 μ M PJ34 in WT and TRPM2-KO cells 30 min prior to and during exposure to TNF- α (c). (b, d) Summary of mean PAR fluorescence intensity under indicated conditions from 3 independent experiments, using 3 wells of cells for each condition in each experiment. Scale bar, 40 μ m. ***, p < 0.005 compared to control. **, p < 0.01 compared between WT and TRPM2-KO cells under the same treatment.

TNF- α -induced TRPM2 channel activation, microglial cell activation and TNF- α generation in microglial cells.

6.2.4 PKC and NOX in TNF- α -induced ROS production, activation of PARP-1 and TRPM2 channel, and TNF- α generation in microglial cells

Exposure to 10-100 ng/ml TNF- α resulted in a concentration-dependent increase in the ROS level in microglial cells (Fig. 6.7a). As discussed above in the introduction, it has been reported that NOX is the main source of ROS production responsible for TNF- α -induced microglial cell activation (Jekabsone et al., 2006) and PKC can induce NOX action (section 4.2.9 and section 5.2.5). I conducted experiments to examine the effects of PKC and NOX inhibitors on TNF- α -induced ROS production. TNF- α -induced increase in the ROS production in microglial cells was almost completely inhibited by CTC (Fig. 6.7b), or DPI, GKT and Phox (Fig. 6.7c), supporting a critical role for PKC and NOX in ROS generation.

Next, I examined whether PKC/NOX-mediated ROS generation is important in TNF- α -induced stimulation of PARP-1 activity, TRPM2 channel activation, microglial cell activation and TNF- α production in microglial cells. Treatment with CTC, DPI, GKT or Phox remarkably inhibited A β ₄₂-induced PARP-1 activity (Fig. 6.8a and c), increases in the [Ca²⁺]_i (Fig. 6.8b and d), change in the cell morphology (Fig. 6.9a-e) and TNF- α generation (Fig. 6.9a-e). Taken together, these results suggest that PKC/NOX-dependent ROS generation has a critical role in mediating TNF- α -induced activation of PARP-1 and TRPM2 channel, microglial cell activation and TNF- α generation in microglial cells.

6.2.5 PYK2-MEK/ERK signalling as a positive feedback in TNF- α -induced microglial cell activation and TNF- α generation

The PYK2-MEK-ERK signalling pathway serves as a positive feedback mechanism in facilitating TRPM2 channel that is important in A β ₄₂-induced microglial cell activation and TNF- α generation (section 5.2.6). I therefore examined whether such a signalling pathway also participates in TNF- α -induced microglial activation and TNF- α generation. TNF- α -induced microglial cell activation (Fig. 6.10a-b) and TNF- α generation (Fig. 6.10c) were strongly inhibited by treatment with PF431396 or U0126.

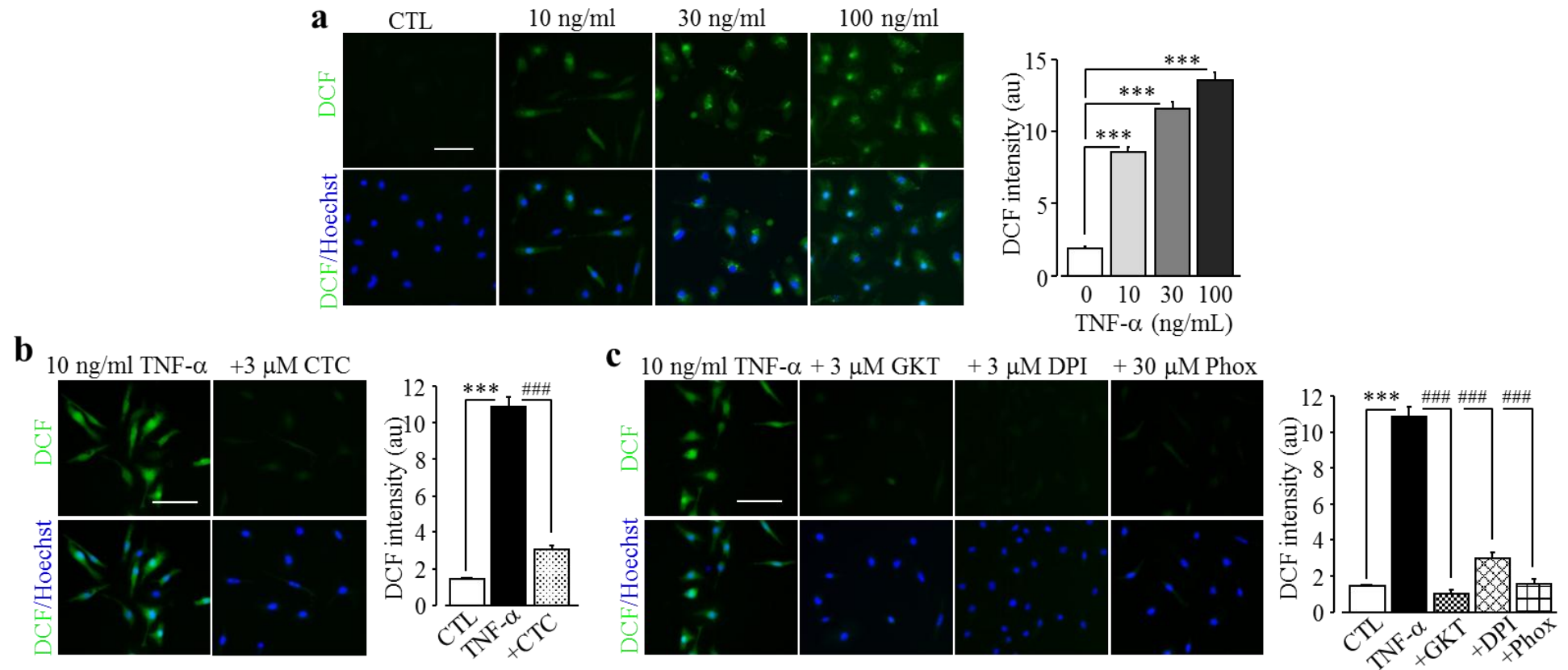


Fig. 6.7 A role of PKC and NOX in TNF- α -induced ROS production in microglial cells.

(a-c) *Left*, representative images showing cellular ROS levels (top row: DCF fluorescence; bottom row: counter staining with Hoechst) in cells without (CTL) and with exposure to TNF- α at indicated concentrations for 8 hr (a) and, in cells after exposure for 8 hr to 10 ng/ml TNF- α alone or treatment with 3 μ M CTC (c), 3 μ M DPI, 3 μ M GKT or 30 μ M Phox (d). *Right*, mean TNF- α -induced ROS production in microglial cells under indicated conditions, from 3 independent experiments, using three wells of cells for each condition in each experiment. Scale bar, 40 μ m. ***, p < 0.005 compared between cells without (CTL) and with exposure to 10 ng/ml TNF- α . ###, p < 0.005 compared to the group exposed to TNF- α alone.

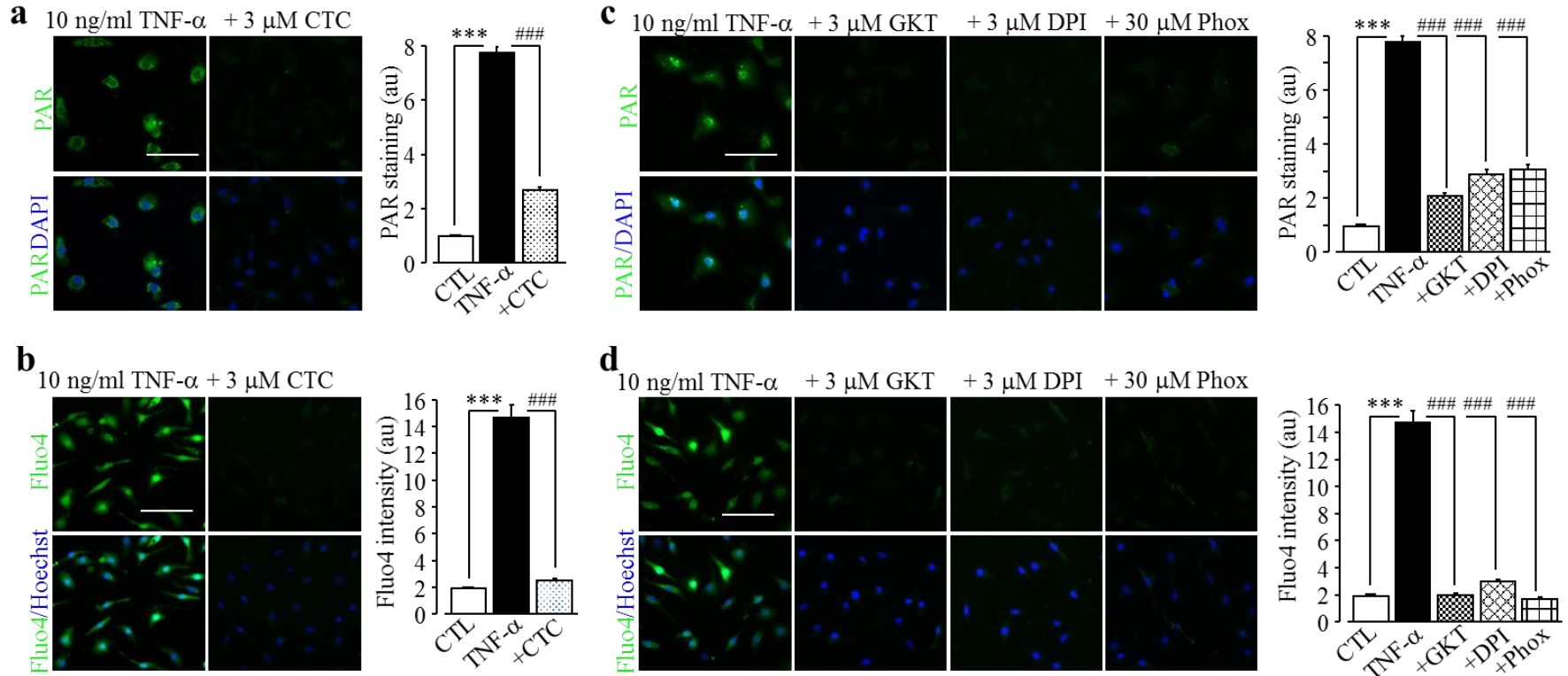
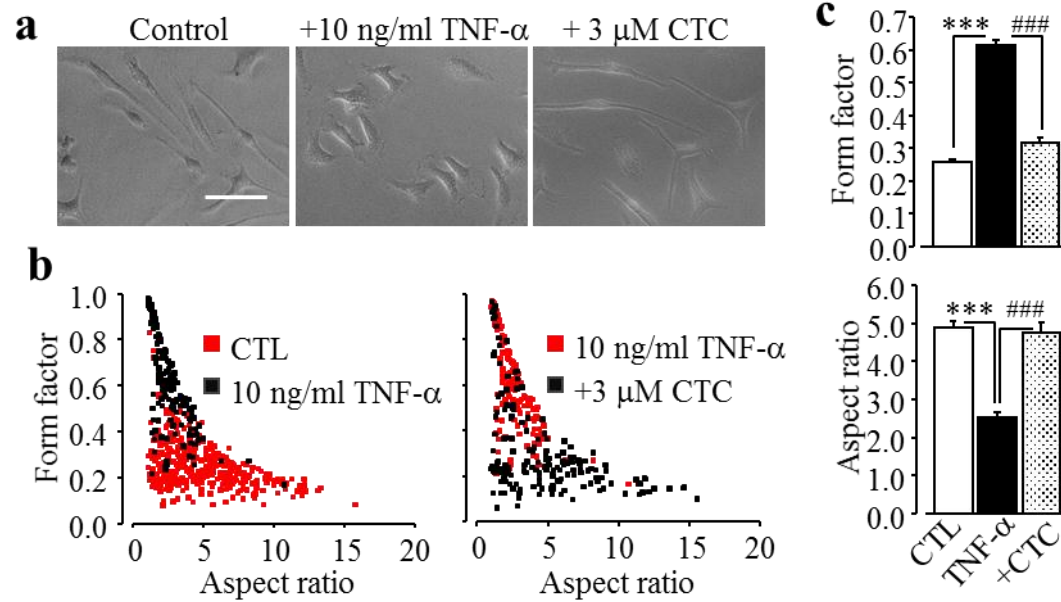


Fig. 6.8 PKC and NOX in TNF- α -induced PARP-1 activation and TRPM2 channel activation in microglial cells.

(a, c) Left, representative images showing PAR staining (top row) and counter staining with DAPI (bottom row) of microglial cells after exposure for 8 hr to 10 ng/ml TNF- α alone or treatment with CTC (b), DPI, GKT or Phox (e). Right, mean TNF- α -induced PAR staining in microglial cells under indicated conditions from 3 independent experiments, using three wells of cells for each condition in each experiment. (b, d) Left, representative single cell images showing Ca^{2+} responses in microglial cells (top row: Fluo-4 fluorescence; bottom row: counter staining with Hoechst). Right, mean TNF- α -induced Ca^{2+} responses in microglial cells under indicated conditions from 3 independent experiments, using 3 wells of cells for each condition in each experiment. Cells were treated with CTC, DPI, GKT or Phox for 30 min prior to and during exposure to TNF- α . Scale bar, 40 μ m. ***, p < 0.005 compared between cells without (CTL) and with exposure to 10 ng/ml TNF- α . ###, p < 0.005 compared to the group exposed to TNF- α alone.



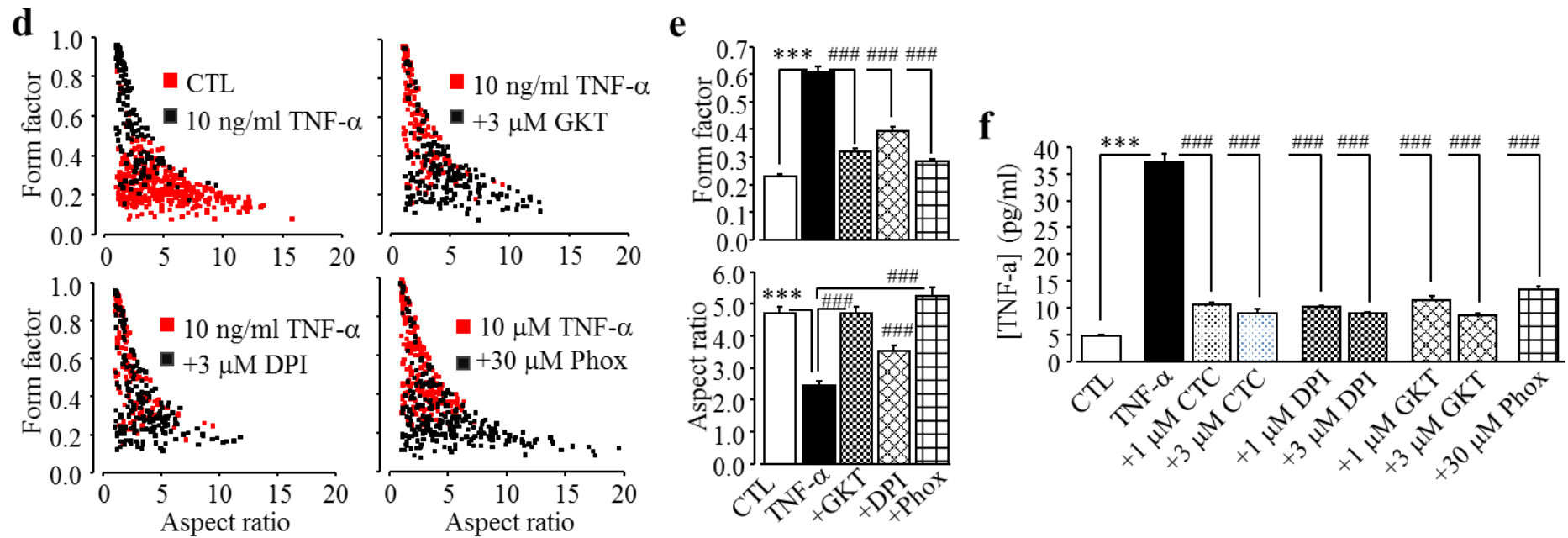


Fig. 6.9 PKC/NOX is critical in TNF- α -induced microglial activation and TNF- α production.

(a) Representative phase-contrast images showing cell morphology of microglial cells after exposure to 10 ng/ml TNF- α for 24 hr alone or treatment with 3 μ M CTC, 30 min prior to and during exposure to TNF- α , captured using an EVOS microscope with a 40x object lens. (b, d) Scatter plot showing distribution of form factor and aspect ratio values for individual cells after exposure for 24 hr to 10 ng/ml TNF- α alone or treatment with 3 μ M CTC (b), 3 μ M DPI, 3 μ M GKT or 30 μ M Phox (d), 30 min prior to and during exposure to TNF- α . (c, e) Mean values of form factor (top) and aspect ratio (bottom) in cells under indicated conditions from 3 independent experiments, using 3 wells of cells for each condition in each experiment. (f) Summary of ELISA assay of TNF- α release from cells without (CTL) and with exposure to 30 ng/ml TNF- α alone or treatment with CTC, DPI, GKT or Phox at indicated concentrations from 3 independent experiments, using 3 wells of cells for each condition in each experiment. Cells were treated with CTC, DPI, GKT or Phox for 30 min prior to and during exposure to TNF- α . ***, p < 0.005 compared between cells without (CTL) and with exposure to TNF- α (f). ##, p < 0.01; ###, p < 0.005 compared to group exposed to TNF- α alone.

These results suggest that the PYK2-MEK-ERK signalling pathway is important in microglial cell activation and TNF- α production. Furthermore, such treatments strongly inhibited TNF- α -induced PARP-1 (Fig. 6.11a-b) and increases in the $[Ca^{2+}]_i$ (Fig. 6.11c-d). These results strongly support involvement of the PYK2-MEK-ERK signalling pathway in TNF- α -induced activation of PARP-1 and TRPM2 channel.

To further seek the roles of PKC-dependent NOX activation and the PYK2-MEK-ERK signalling pathway, I examined the PARP-1 activity in TRPM2-KO microglial cells by immunofluorescence staining. As shown in Figure 6.12a-d, TNF- α -induced PAR production in TRPM2-KO microglial cells was completely suppressed by inhibiting PKC and NOX with CTC, DPI, GKT or Phox. In contrast, no inhibition was observed in TRPM2-KO microglial cells after treatment with PF431396 or U0126 (Fig. 6.12e-f). Taken together, these results indicate that PKC-dependent NOX activation occurs upstream of PARP-1 activation leading to TRPM2 channel activation. The results also suggest that the PYK2-MEK-ERK signalling pathway acts downstream of the TRPM2 channel activation as a positive feedback mechanism to stimulate PARP-1 and thereby TRPM2 channel activation.

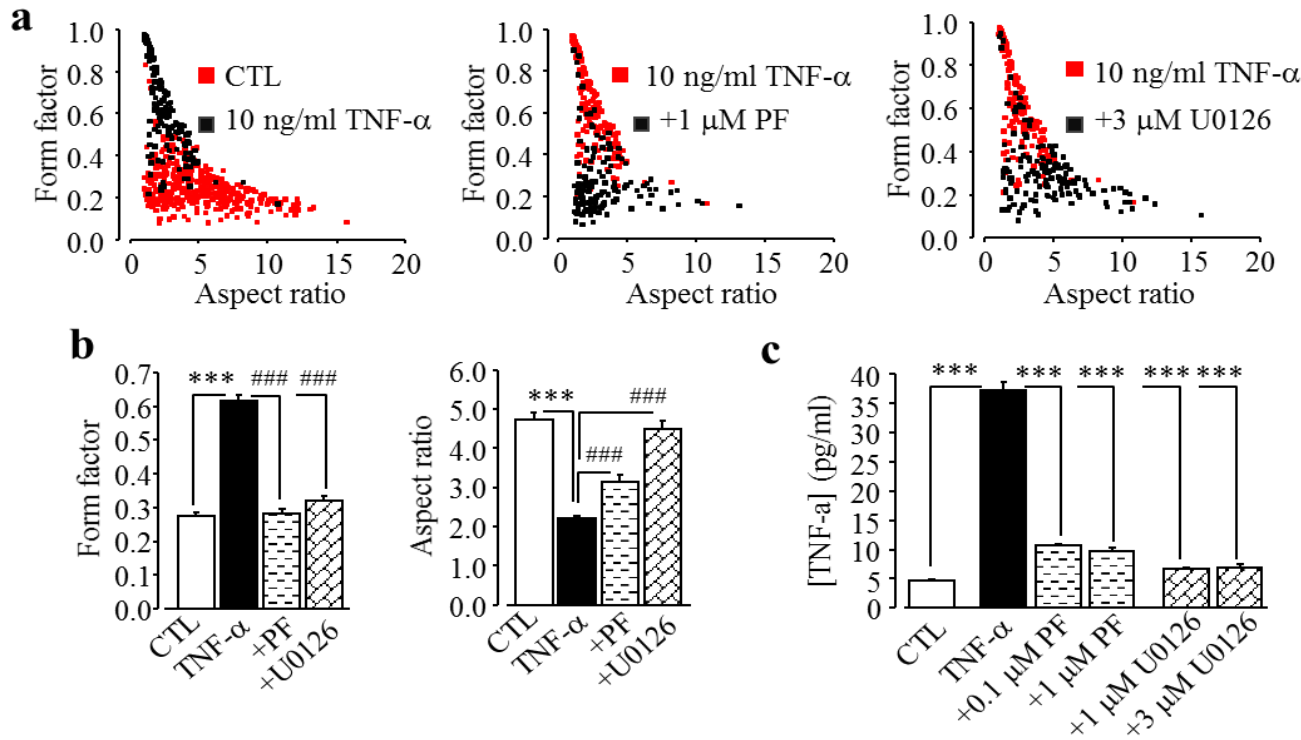


Fig. 6.10 PYK2/MEK/ERK is involved in TNF- α -induced microglial cell activation and TNF- α production.

(a) Scatter plot showing distribution of form factor and aspect ratio values of individual cells without (CTL) and with exposure for 24 hr to 10 ng/ml TNF- α alone or treatment with 1 μ M PF or 3 μ M U0126, 30 min prior to and during exposure to TNF- α . (b) Mean values of form factor (left) and aspect ratio (right) in microglial cells under conditions indicated in (a) from 3 independent experiments, using 3 wells of cells for each condition in each experiment. (c) Summary of ELISA assay of TNF- α release by microglial cells without (CTL) and with exposure for 72 hr to 30 ng/ml TNF- α alone or treatment with PF or U0126 at indicated concentrations from 3 independent experiments, using 3 wells of cells for each condition in each experiment. Cells were treated with PF and U0126 for 30 min prior to and during exposure to 30 ng/ml TNF- α . ***, p < 0.005 compared between cells without (CTL) and with exposure to TNF- α . ###, p < 0.005 compared to group exposed to TNF- α alone.

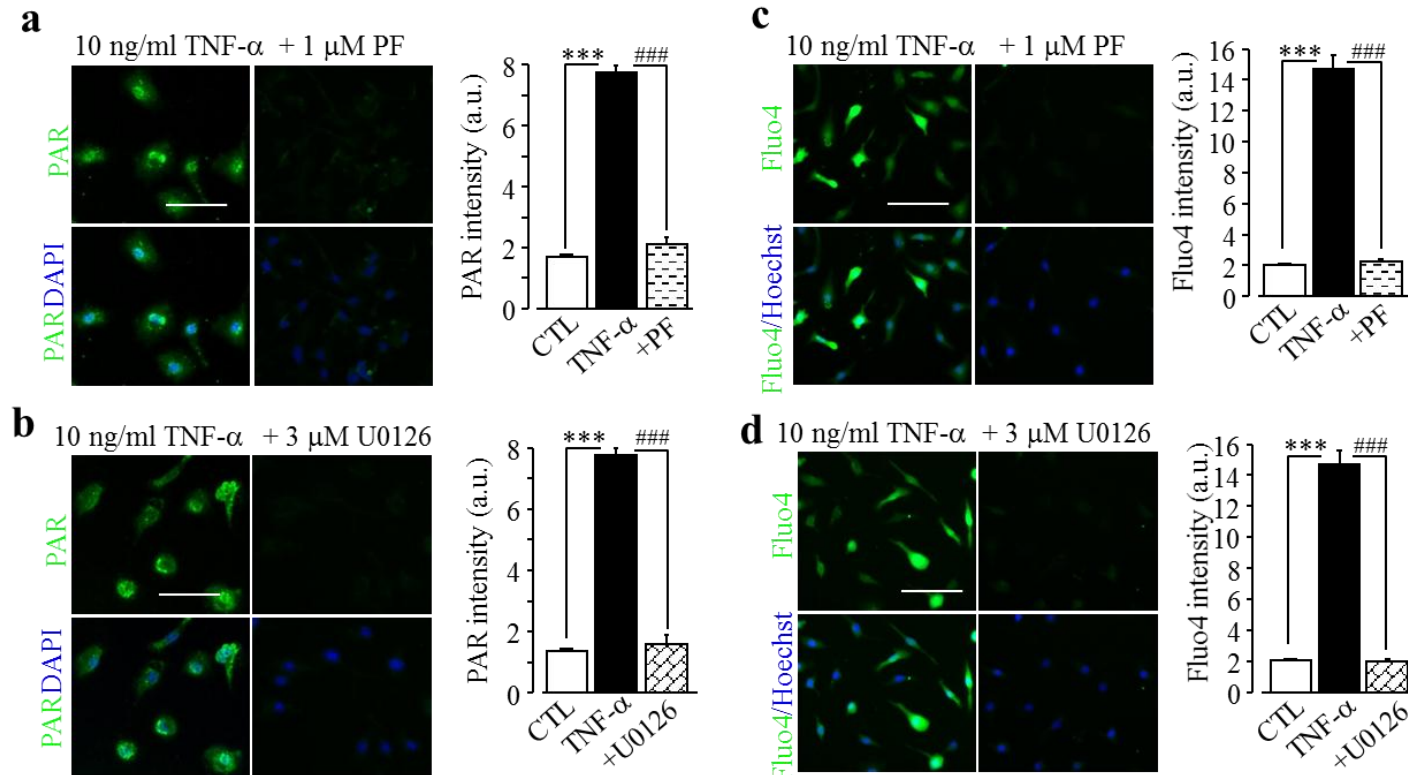
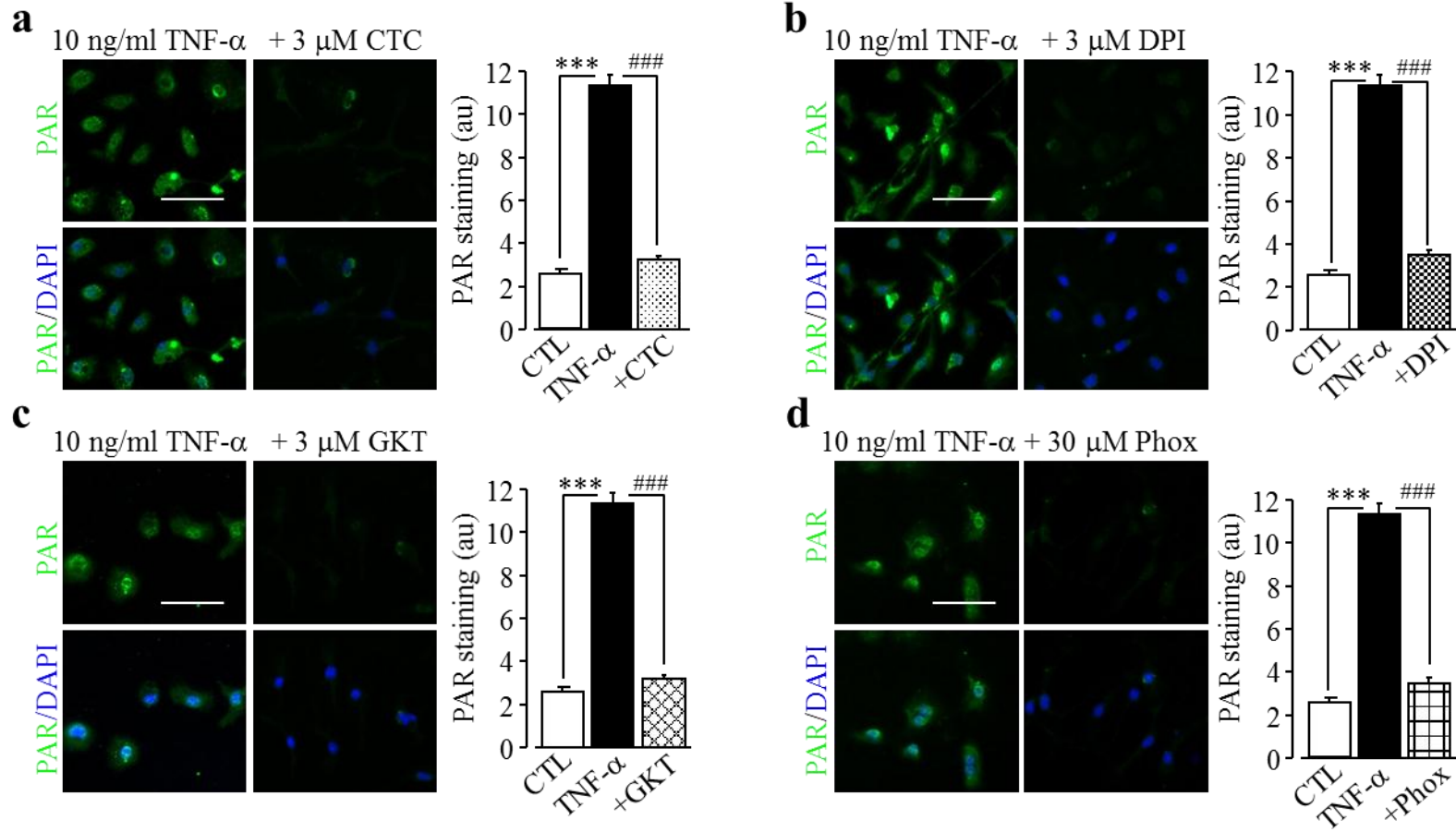


Fig. 6.11 PYK2/MEK/ERK is involved in TNF- α -induced PARP-1 activation and TRPM2 channel activation in microglial cells.

(a-b) Left, representative images showing PAR level (top row: PAR fluorescence; bottom row: counter staining with DAPI) in cells exposed for 8 hr to 10 ng/ml TNF- α alone or together with 1 μ M PF (a) or 3 μ M U0126 (b), 30 min prior to and during exposure to TNF- α . Right, summary of PAR fluorescence intensity under conditions indicated in (a and b), from 3 independent experiments, using 3 wells of cells for each condition in each experiment. (c-d) Left, representative single cell images showing Ca^{2+} responses (top row: Fluo-4 fluorescence; bottom row: counter staining with Hoechst) in cells exposed to 10 ng/ml TNF- α without and with treatment with 1 μ M PF (c) or 3 μ M U0126 (d). Right, mean Ca^{2+} responses in cells under indicated conditions from 3 independent experiments, using 3 wells of cells for each condition in each experiment. ***, p < 0.005 compared between cells without (CTL) and with exposure to TNF- α . ###, p < 0.005 compared to group exposed to TNF- α alone.



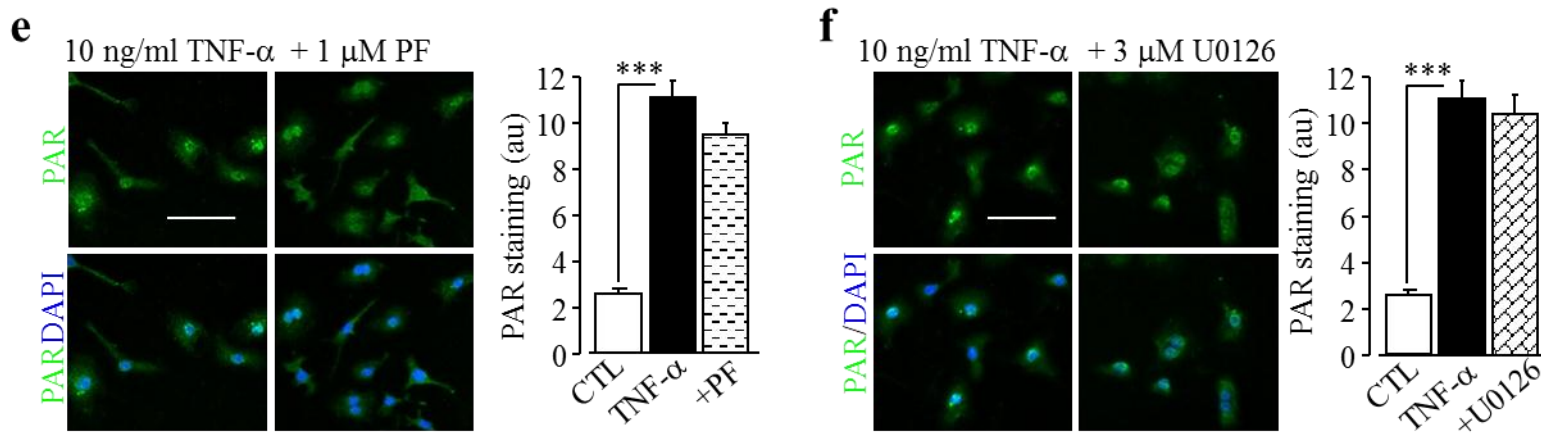


Fig. 6.12 PKC/NOX activation is required for, and PYK2/MEK activation depends on, TNF- α -induced TRPM2 channel activation.

(a-f) *Left*, representative images showing PAR level (top row: PAR fluorescence; bottom row: counter staining with DAPI) in TRPM2-KO cells exposed for 8 hr to 10 ng/ml TNF- α alone or together with 3 μ M CTC (a), 3 μ M DPI (b), 3 μ M GKT (c), 30 μ M Phox (d), 1 μ M PF (e) or 3 μ M U0126 (f), 30 min prior to and during exposure to 10 ng/ml TNF- α . *Right*, mean PAR fluorescence intensity in cells under indicated conditions, from 3 independent cell preparations, using three wells of cells for each condition in each experiment. Scale bar, 40 μ m. ***, p < 0.005 compared between cells without (CTL) and with exposure to TNF- α alone and, ###, p < 0.005 compared to group exposed to TNF- α alone.

6.3 DISCUSSION

The studies presented in this chapter show that the TRPM2 channel plays a crucial role in TNF- α autocrine/paracrine signalling mechanism in microglial cells, in which TNF- α induces microglial cell activation and TNF- α production. In addition, PKC/NOX-mediated ROS production and subsequent PARP-1 activation are required for TNF- α -induced TRPM2 channel activation. Furthermore, the PYK2-MEK-ERK signalling pathway acts a positive feedback mechanism downstream of the TRPM2 channel activation to further enhance activation of PARP-1 and TRPM2 channel (Fig. 6.13).

The findings described in the previous chapter show that genetic deletion of the TRPM2 channel expression resulted in loss of TNF- α -induced increase in the $[Ca^{2+}]_i$ in microglial cells (section 3.2.3), suggesting a crucial role of TRPM2 channel in TNF- α -induced Ca^{2+} signalling. In the present chapter, I further showed that TNF- α induced increase in the $[Ca^{2+}]_i$ in WT microglial cells was largely absent upon removal of extracellular Ca^{2+} (Fig. 6.1a). In addition, TNF- α -induced increase in the $[Ca^{2+}]_i$ was almost completely abolished by inhibition of the TRPM2 channel using 2-APB (Fig. 6.1b). These findings strengthen the notion that suggest the TRPM2 channel-mediated extracellular Ca^{2+} influx mediates TNF- α -induced Ca^{2+} signalling in microglial cells. Microglial cell activation induced by TNF- α was significantly inhibited in TRPM2-KO cells, as shown in the previous chapter (section 3.2.6). Treatment with 2-APB significantly inhibited TNF- α -induced microglial cell activation (Fig. 6.2a-c), confirming a critical role for the TRPM2 channel in TNF- α -induced microglial activation.

TNF- α is a major inflammatory mediator generated by microglial cells upon activation by various DAMP molecules such as $A\beta_{42}$ as shown in chapter 5, and strongly implicated in multiple neurodegenerative diseases (Paouri et al., 2017; Feldmaan, et al., 2002). It is also known that TNF- α itself can induce microglial cell activation via TNF- α receptor (Kuno et al., 2005). Studies presented in the previous chapter show a critical role for the TRPM2 channel in mediating $A\beta_{42}$ -induced microglial cell activation and TNF- α generation (see section 5.2.3). However, it was unclear whether the TRPM2 channel is critically involved in TNF- α induced microglial cell activation and generation of itself. In the present study, treatment of WT microglial cells with TNF- α increased the TNF- α expression (Fig. 6.3a-b) and release (Fig 6.3c). Such responses were remarkably inhibited in TRPM2-KO microglial cells (Fig. 6.4a-c),

and abolished upon inhibition of the TRPM2 channel using 2-APB (Fig 6.4d). PI staining assay showed no necrotic cell death after treatment with TNF- α (section 3.2.5), strongly suggesting that release of TNF- α is not due to microglial cell death. Collectively, the results presented in this chapter provide strong evidence to show an important role of the TRPM2 channel in mediating TNF- α -induced microglial activation and TNF- α generation.

So far, studies using genetic and pharmacological approaches have provided compelling evidence to show an important role of the TRPM2 channel in TNF- α induced cell activation and TNF- α production in microglial cells. However, the underlying signalling mechanisms were not clearly defined. Studies presented in chapter 5 suggest that stimulation of PARP-1 is crucial in A β ₄₂-induced TRPM2 channel activation and microglial cell activation (section 5.2.4). Consistently, a significant increase in the PAR generation, which was concentrated in the nucleus, was observed in microglial cells following exposure to TNF- α (Fig. 6.6a-b). Such an increase in the PAR generation was abolished by treatment with PJ34 (Fig. 6.6c-d). These results suggest TNF- α stimulated the PAPR-1 activity. In addition, TNF- α -induced increase in the [Ca²⁺]_i (Fig. 6.5a-b), change in the cell morphology (Fig. 6.5c-f) and TNF- α generation (Fig. 6.5g) in microglial cells were prevented by treatment with PJ34, further suggesting that PARP-1 activation is involved in TNF- α -induced TRPM2-mediated microglial cell activation and TNF- α generation.

TNF- α -induced NOX activation has been shown in various cell types to results in accumulation of intracellular ROS (Morgan and Liu, 2011; Moe et al., 2006). In addition, a previous study suggested a crucial role of PKC in the ROS generation via NOX activation following exposure to TNF- α (Frey et al., 2002). As found for A β ₄₂-induced microglial cell activation (section 5.2.5), TNF- α -induced ROS production in microglial cells (Fig 6.7a) was prevented by inhibiting PKC and NOX (Fig. 6.7b-c), suggesting a role of PKC and NOX is also involved in TNF- α -induced ROS production. Studies presented in this chapter also showed that PKC/NOX-mediated ROS production is important in TNF- α -induced activation of PARP-1 (Fig. 6.8a and c) and TRPM2 channel (Fig. 6.8b and d). Activation of these mechanisms is critical in TNF- α -induced microglial cells activation (Fig 6.9a-e) and TNF- α generation (Fig. 6.9f). Collectively, these results provide compelling evidence to show that PKC/NOX-mediated ROS production is critical in TNF- α -induced activation of PARP-1 and TRPM2 channel that leads to microglial cell activation and TNF- α generation.

A previous study showed involvement of PYK2 in TNF- α -induced ROS generation (Zhao and Bokoch, 2005). Furthermore, as shown in the previous chapter, the PYK2-MEK-ERK signalling pathway acts as a positive feedback mechanism, downstream of the TRPM2 channel activation, to enhance activation of PARP-1 and TRPM2 channel in A β ₄₂-induced microglial cell activation and TNF- α production (section 5.2.10). Here, I showed a similar role of such mechanisms in TNF- α -induced activation of PARP-1 (Fig. 6.11a and b) and TRPM2 channel (Fig. 6.11c and d), microglial cell activation (Fig. 6.10a and b) and TNF- α production (Fig. 6.10c). As shown A β ₄₂-induced microglial cell activation in previous chapters, the signalling mechanisms engaging TNF- α -induced microglial cell activation and TNF- α production involve sequential activation of PKC/NOX-mediated ROS production and PARP-1 activation, which acts upstream of the TRPM2 channel activation, and the PYK2-MEK-ERK that positively feeds back into activation of PARP-1 (Fig. 6.12).

Overall, studies described in this chapter have demonstrated an important role of the TRPM2 channel in mediating TNF- α -induced autocrine/paracrine signalling in microglial cells. PKC-dependent NOX-mediated ROS production and PARP-1 activation are required for TNF- α -induced TRPM2 channel activation and the PYK2-MEK-ERK signalling pathway as a positive feedback mechanism further stimulates activation of PARP-1 and TRPM2 channel (Fig. 6.13). These novel findings suggest a positive autocrine/paracrine loop in the activation of microglial cells via TNF- α and therefore, offer new insights into the role of TNF- α as one of the major factors in multiple CNS pathologies.

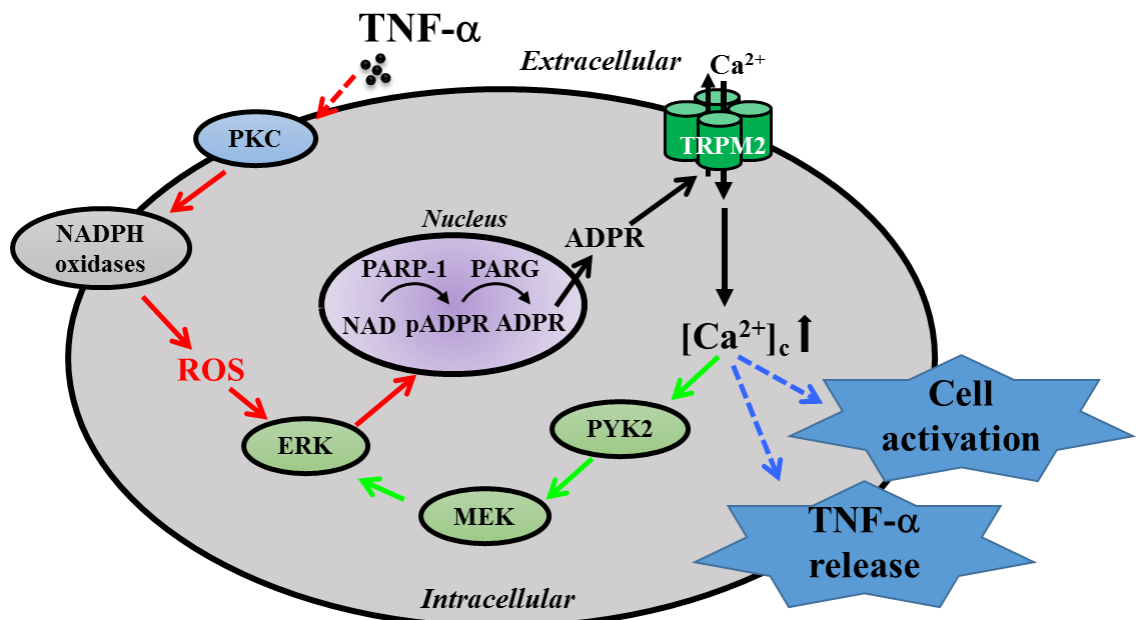


Fig. 6.13 Schematic summary of the TNF- α -induced autocrine/paracrine signalling mechanisms via TRPM2 channel in microglial cells.

TNF- α activates the TRPM2 channel involving multiple-step intracellular signalling pathways in microglial cell activation and TNF- α generation. TNF- α stimulates PKC and NOX. ROS activates PARP-1 and PARG in the nucleus leading to ADPR production and subsequent activation of TRPM2-dependent Ca^{2+} influx to increase the cytosolic Ca^{2+} concentrations ($[\text{Ca}^{2+}]_c$). Elevated $[\text{Ca}^{2+}]_c$ in turn activate the PYK2/MEK/ERK signalling pathway as a positive feedback mechanism that amplifies activation of PARP-1, leading to TRPM2-mediated Ca^{2+} overloading, microglial cell activation and TNF- α generation.

CHAPTER 7

GENERAL DISCUSSION AND CONCLUSIONS

7.1 GENERAL DISCUSSION AND CONCLUSIONS

The studies presented in this thesis have provided valuable insights into the critical role of TRPM2 channel in microglial cell functions, including cell death, cell activation and pro-inflammatory cytokine TNF- α release, in response to DAMPs such as Zn²⁺, A β ₄₂ and TNF- α as well as H₂O₂ (Fig. 7.1). In addition, the studies have revealed novel signalling mechanisms by which these stimuli activates the TRPM2 channel (Fig. 7.1). This chapter will summarise the key findings and discuss the future direction.

Studies over the past several years suggest that the Ca²⁺-permeable TRPM2 channel on the cell surface acts as a major molecular mechanism for ROS-induced Ca²⁺ signalling in immune cells (Mortadza et al., 2015). Previous studies provide evidence to show an increase in the [Ca²⁺]_i in response to H₂O₂, A β and TNF- α in different cell types (Kraft et al., 2004; Fonfria et al., 2005; Zhang et al., 2006). The studies presented in this thesis confirmed that the increase in the [Ca²⁺]_i was induced by H₂O₂, Zn²⁺, A β ₄₂ and TNF- α in microglial cells (chapter 3), and further showed that such Ca²⁺ signalling was lost in TRPM2-KO microglial cells or largely abolished in the absence of extracellular Ca²⁺. These results provide compelling evidence to indicate that the TRPM2 channel plays a major role in H₂O₂- or DAMP-induced Ca²⁺ signalling via mediating Ca²⁺ influx.

The experiments conducted in this thesis further showed that exposure to H₂O₂ or Zn²⁺ evoked substantial cell death in WT microglial cells, which was abolished in TRPM2-KO microglial cells (chapter 3) and, in addition, attenuated by 2-APB (chapter 4). These results indicate a crucial role for the TRPM2 channel in mediating H₂O₂- or Zn²⁺-induced microglial cell death. The signalling mechanisms by which exposure to H₂O₂ and Zn²⁺ induces the TRPM2 channel activation were further investigated in WT microglial cells (chapter 4). Similarly to H₂O₂, Zn²⁺ stimulated PARP-1 dependent PAR generation in the nucleus. Further studies demonstrated that H₂O₂- and Zn²⁺-induced microglial cell death was antagonised by PJ-34 and DPQ. Such results suggest that PARP-1 is responsible for the TRPM2 channel activation following the exposure to H₂O₂ or Zn²⁺, resulting in microglial cell death. As discussed in section 1.8, microglial and macrophage cells share several functions. Study by single cell Ca²⁺ imaging showed that the TRPM2 channel in macrophage cells functions as a Ca²⁺-permeable channel that mediates Ca²⁺ influx upon exposure to H₂O₂ (Zou et al., 2013). Such a Ca²⁺ signalling mechanism is responsible for the H₂O₂-induced macrophage cell death.

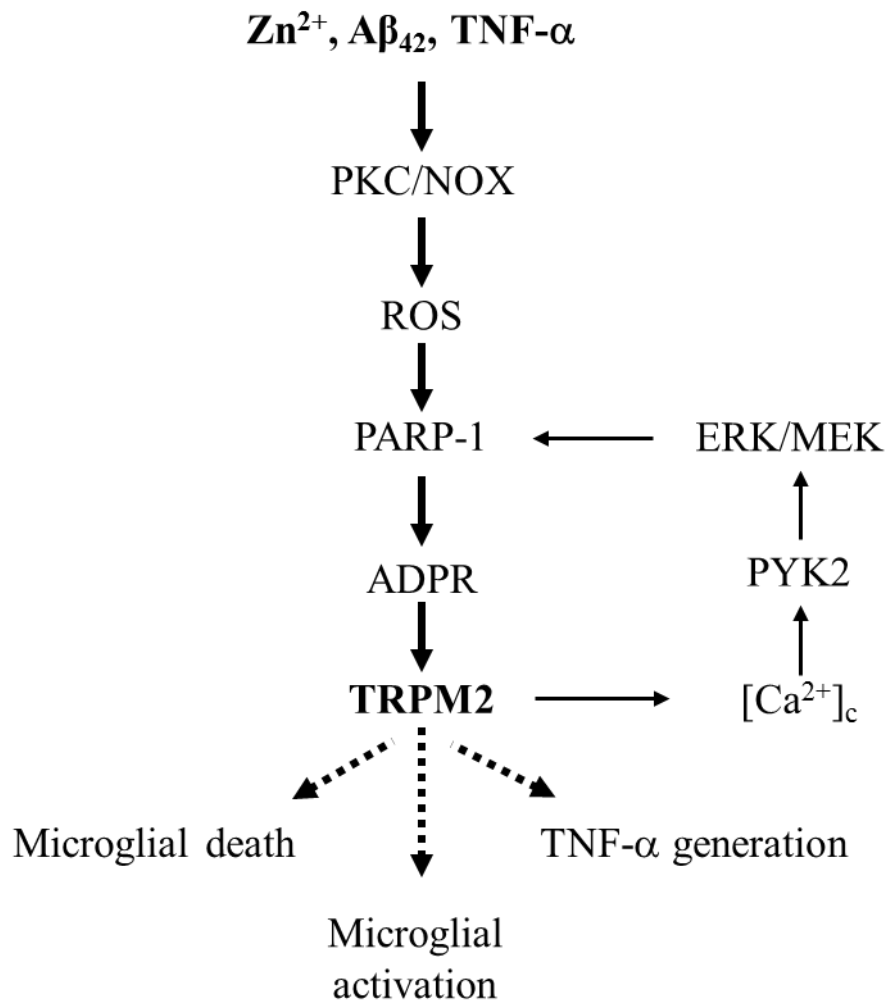


Fig. 7.1 Schematic summary of the signalling mechanisms mediating Zn^{2+} , $\text{A}\beta_{42}$ - and $\text{TNF-}\alpha$ -induced TRPM2 channel activation, microglial activation and $\text{TNF-}\alpha$ generation.

Exposure to Zn^{2+} , $\text{A}\beta_{42}$ - and $\text{TNF-}\alpha$ induces activation of protein kinase C (PKC) and NADPH oxidases (NOX), including NOX1/4 and NOX2, leading to generation of ROS. ROS stimulate activation of poly(ADP-ribose) polymerase-1 (PARP-1) in the nucleus to generate ADP-ribose (ADPR). ADPR binds to activates the TRPM2 channel, resulting extracellular Ca^{2+} influx to increase the cytosolic Ca^{2+} concentrations ($[\text{Ca}^{2+}]_c$). Intracellular Ca^{2+} stimulates the PYK2/MEK/ERK signalling pathway to further enhance activation of PARP-1 and TRPM2 channel. TRPM2 channel activation is required for Zn^{2+} -induced microglial cell death as well as $\text{A}\beta_{42}$ - and $\text{TNF-}\alpha$ -induced microglial activation and generation of $\text{TNF-}\alpha$, a key proinflammatory cytokine implicated in neuroinflammation.

Furthermore, H₂O₂-induced macrophage cell death was significantly reduced by PJ-34 and TRPM2 channel deficiency. The results from both previous (Zou et al., 2013) and present studies provide consistent evidence to suggest that the TRPM2 channels in macrophage and microglial cells functions as a cell surface Ca²⁺-permeable channel and TRPM2-mediated extracellular Ca²⁺ influx constitutes the principal mechanism resulting in H₂O₂-induced macrophage/microglial cell death.

NOX represents an important source for ROS generation in the brain and PKC stimulates NOX. Zn²⁺-induced ROS production, PARP-1 activity, increase in the [Ca²⁺]_i and cell death were strongly reduced by inhibiting PKC and NOX, including NOX1/4 and NOX2. These results provide strong evidence to show that PKC/NOX-mediated ROS generation is critical in Zn²⁺-induced stimulation of PARP-1 activity, TRPM2-mediated increase in the [Ca²⁺]_i and cell death in microglial cells. Previous studies suggest that ROS can stimulate PARP-1 via the MEK/ERK signalling. In monocytes, TRPM2 channel-mediated Ca²⁺ influx activates the PYK2/MEK/ERK signalling pathway in response to H₂O₂ *in vitro* or oxidative stress *in vivo*, which is important in chemokine generation (Yamamoto et al., 2008). Here, I showed that the PYK2/MEK/ERK signalling pathway is important in Zn²⁺-induced stimulation of PARP-1, TRPM2-mediated increase in the [Ca²⁺]_i and cell death.

It is worth mentioning many of the inhibitors used in the study are limited in their specificity. Nonetheless, the results obtained using pharmacological inhibitors are consistent with the hypothesis that the PYK2/MEK/ERK signalling pathway constitutes a positive feedback mechanism that amplifies Zn²⁺-induced stimulation of PARP-1, TRPM2 channel activation, and increase in the [Ca²⁺]_i that ultimately drives cell death. Activation of such signalling mechanisms offers a feasible explanation for the significant delay in Zn²⁺-induced cell death as compared to Zn²⁺-induced increase in the [Ca²⁺]_i.

In striking contrast with Zn²⁺, H₂O₂-induced effects were completely insensitive to inhibitors of the PKC/NOX and PYK2/MEK/ERK signalling mechanisms. Such differentiating results could be due to much lower concentrations of ROS produced in microglial cells in response to Zn²⁺ than the concentration of exogenous H₂O₂. It is also worth mentioning that when heterologously expressed in HEK293 cells, the TRPM2 channel in the open state but not in the closed state becomes inactivated upon exposure to extracellular Zn²⁺ at concentrations used in this study (Yang et al., 2011). The exact reason for the discrepancy in terms of Zn²⁺ inhibition of the endogenous and

heterologously overexpressed TRPM2 channels is currently unclear, and may arise from the different TRPM2 expression level. Alternatively or additionally, Zn²⁺ has been rapidly transported by yet defined Zn²⁺-transporting mechanisms into the cytosol in order to induce PKC activation and as a result, extracellular Zn²⁺ concentrations insufficiently inhibit the TRPM2 channel. The findings reported in chapter 4, despite their relevance to Zn²⁺-related brain damage *in vivo* remaining to be further explored, should help to evolve a better and mechanistic insight into Zn²⁺-induced cytotoxicity. This part of the work has been recently published in Scientific Reports (Mortadza et al., 2017).

A β , a major DAMP inducing neuroinflammation via microglial activation and excessive generation of pro-inflammatory mediators, contributes in AD pathogenesis. Microglial cell activation and TNF- α production in response to A β_{42} have been of particular interest. Emerging evidence supports a role for the TRPM2 channel in A β -induced neuroinflammation. I have examined the role of the TRPM2 channel in mediating A β_{42} -induced microglial activation and TNF- α generation (chapter 5). A β_{42} -induced microglial activation and TNF- α generation were observed in WT microglial cells but were ablated by genetic or pharmacological inhibition of the TRPM2 channel. Exposure to A β_{42} raised the [Ca²⁺]_i via promoting Ca²⁺ influx, which was prevented by TRPM2-KO. A β_{42} induced ROS production and PARP-1 activation. A β_{42} -induced ROS production and PARP-1 activation as well as an increase in the [Ca²⁺]_i, microglial activation and TNF- α production, were suppressed by inhibiting PKC and NOX. Furthermore, A β_{42} -induced PARP-1 activation, increase in the [Ca²⁺]_i, microglial activation and TNF- α production were attenuated by inhibiting the Ca²⁺-sensitive PYK2 and downstream MEK/ERK kinases. These results provide compelling evidence to support a critical role for the TRPM2 channel in A β_{42} -induced microglial activation and TNF- α production. The results also suggest that A β_{42} activates the TRPM2 channel via PKC/NOX-mediated ROS production and PARP-1 activation, which is further enhanced by the PYK2/MEK/ERK signalling pathway as a positive feedback mechanism. These findings provide novel insights into the mechanisms underlying A β -induced neuroinflammation.

The studies presented in this thesis also showed TNF- α as an autocrine/paracrine mediator in microglial cells (chapter 6). TNF- α induced microglial cell activation and TNF- α production confirming the finding from a previous study that stimulation of microglial cells with TNF- α significantly increases TNF- α production (Kuno et al.,

2005). The studies presented in this thesis further showed a critical role of the TRPM2 channel in such TNF- α -induced autocrine or paracrine signalling. TNF- α induced TRPM2 channel activation involves ROS production and PARP-1 activation. Additionally, the PYK2/MEK/ERK signalling pathway acts as a positive feedback signalling mechanism that further amplifies TNF- α -induced activation of PARP-1 and TRPM2 channel, and subsequently drives microglia cell activation and TNF- α production. TNF- α -induced autocrine/paracrine activation in microglial cells may explain the prolonged activation of microglial cells that occurs in the chronic stages of inflammatory and neurodegenerative diseases. A limitation of this study is that the data of the TNF- α release from microglial cells was analysed based on the total amount of TNF- α presents in the culture media without excluding the possible contamination of residual exogenous TNF- α . In fact, the amount of TNF- α release by microglial cells was much less than the amount of exogenous TNF- α applied. The reason for such discrepancy is presently unclear. As such, further investigation is required, to exclude the possible contribution of exogenous TNF- α . The findings from such investigations would provide clearer evidence to conclude the role of the TRPM2 channel in mediating production of TNF- α by TNF- α -stimulated microglial cells.

In conclusion, the studies presented in this thesis demonstrate that the microglia TRPM2 channel is an exciting avenue to enable a better understanding of CNS pathologies and selective TRPM2 inhibitors may provide a plausible therapeutic treatment for multiple neurodegenerative diseases.

List of References

- Aarts, M., Iihara, K., Wei, W.L., Xiong, Z.G., Arundine, M., Cerwinski, W., MacDonald, J.F. and Tymianski, M. 2003. A key role for TRPM7 channels in anoxic neuronal death. *Cell.* **115**(7),pp.863–877.
- Abid, M.R., Kachra, Z., Spokes, K.C. and Aird, W.C. 2000. NADPH oxidase activity is required for endothelial cell proliferation and migration. *FEBS letters.* **486**(3),pp.252–256.
- Abramov, A.Y., Jacobson, J., Wientjes, F., Hothersall, J., Canevari, L. and Duchen, M.R. 2005. Expression and modulation of an NADPH oxidase in mammalian astrocytes. *The Journal of Neuroscience: The Official Journal of the Society for Neuroscience.* **25**(40),pp.9176–9184.
- Ago, T., Takeya, R., Hiroaki, H., Kurabayashi, F., Ito, T., Kohda, D. and Sumimoto, H. 2001. The PX domain as a novel phosphoinositide- binding module. *Biochemical and Biophysical Research Communications.* **287**(3),pp.733–738.
- Aguiari, G., Banzi, M., Gessi, S., Cai, Y.Q., Zeggio, E., Manzati, E., Piva, R., Lambertini, E., Ferrari, L., Peters, D.J., Lanza, F., Harris, P.C., Borea, P.A., Somlo, S. and del Senno, L. 2004. Deficiency of polycystin-2 reduces Ca²⁺ channel activity and cell proliferation in ADPKD lymphoblastoid cells. *Faseb Journal.* **18**(3),p.884–.
- Ahern, G.P. 2003. Activation of TRPV1 by the satiety factor oleoylethanolamide. *J Biol Chem.* **278**(33),pp.30429–34.
- Ahluwalia, J., Rang, H. and Nagy, I. 2002. The putative role of vanilloid receptor-like protein-1 in mediating high threshold noxious heat-sensitivity in rat cultured primary sensory neurons. *Eur J Neurosci.* **16**(8),pp.1483–9.
- Ahmad, M., Kelly, M.R., Zhao, X., Kandhi, S. and Wolin, M.S. 2010. Roles for Nox4 in the contractile response of bovine pulmonary arteries to hypoxia. *Am J Physiol Heart Circ Physiol.* **298**(6),pp.H1879-88.
- Ahmmmed, G.U. and Malik, A.B. 2005. Functional role of TRPC channels in the regulation of endothelial permeability. *Pflugers Archiv: European Journal of Physiology.* **451**(1),pp.131–142.
- Ahmmmed, G.U., Mehta, D., Vogel, S., Holinstat, M., Paria, B.C., Tiruppathi, C. and Malik, A.B. 2004. Protein kinase Calpha phosphorylates the TRPC1 channel and regulates store-operated Ca²⁺ entry in endothelial cells. *J Biol Chem.* **279**(20),pp.20941–9.
- Alam, Q., Alam, M.Z., Mushtaq, G., Damanhouri, G.A., Rasool, M., Kamal, M.A. and Haque, A. 2016. Inflammatory Process in Alzheimer's and Parkinson's Diseases: Central Role of Cytokines. *Curr Pharm Des.* **22**(5),pp.541–8.
- Alessandri-Haber, N., Yeh, J.J., Boyd, A.E., Parada, C.A., Chen, X., Reichling, D.B. and Levine, J.D. 2003. Hypotonicity induces TRPV4-mediated nociception in rat. *Neuron.* **39**(3),pp.497–511.

- Alim, I., Teves, L., Li, R.W., Mori, Y. and Tymianski, M. 2013. Modulation of NMDAR Subunit Expression by TRPM2 Channels Regulates Neuronal Vulnerability to Ischemic Cell Death. *Journal of Neuroscience*. **33**(44),pp.17264–17277.
- Allen, R.G. and Tresini, M. 2000. Oxidative stress and gene regulation. *Free Radical Biology and Medicine*. **28**(3),pp.463–499.
- Amaral, M.D. and Pozzo-Miller, L. 2007. TRPC3 channels are necessary for brain-derived neurotrophic factor to activate a nonselective cationic current and to induce dendritic spine formation. *The Journal of Neuroscience: The Official Journal of the Society for Neuroscience*. **27**(19),pp.5179–5189.
- Ambasta, R.K., Kumar, P., Griendling, K.K., Schmidt, H.H.H.W., Busse, R. and Brandes, R.P. 2004. Direct interaction of the novel Nox proteins with p22phox is required for the formation of a functionally active NADPH oxidase. *The Journal of Biological Chemistry*. **279**(44),pp.45935–45941.
- Andrade, Y.N., Fernandes, J., Vazquez, E., Fernandez-Fernandez, J.M., Arniges, M., Sanchez, T.M., Villalon, M. and Valverde, M.A. 2005. TRPV4 channel is involved in the coupling of fluid viscosity changes to epithelial ciliary activity. *J Cell Biol*. **168**(6),pp.869–74.
- Angelov, D.N., Arnhold, S., Andressen, C., Grabsch, H., Puschmann, M., Hescheler, J. and Addicks, K. 1998. Temporospatial relationships between macroglia and microglia during in vitro differentiation of murine stem cells. *Developmental Neuroscience*. **20**(1),pp.42–51.
- Angus, D.C. and van der Poll, T. 2013. Severe sepsis and septic shock. *The New England Journal of Medicine*. **369**(9),pp.840–851.
- Aoyagi, K., Ohara-Imaizumi, M., Nishiwaki, C., Nakamichi, Y. and Nagamatsu, S. 2010. Insulin/phosphoinositide 3-kinase pathway accelerates the glucose-induced first-phase insulin secretion through TrpV2 recruitment in pancreatic beta-cells. *Biochem J*. **432**(2),pp.375–86.
- Assaf, S.Y. and Chung, S.H. 1984. Release of endogenous Zn²⁺ from brain tissue during activity. *Nature*. **308**(5961),pp.734–736.
- Babior, B.M. 2000. Phagocytes and oxidative stress. *The American Journal of Medicine*. **109**(1),pp.33–44.
- Babior, B.M., Kipnes, R.S. and Curnutte, J.T. 1973. Biological defense mechanisms. The production by leukocytes of superoxide, a potential bactericidal agent. *J Clin Invest*. **52**(3),pp.741–4.
- Bach, G. 2001. Mucolipidosis type IV. *Molecular Genetics and Metabolism*. **73**(3),pp.197–203.
- Bach, G. 2005. Mucolipin 1: endocytosis and cation channel--a review. *Pflugers Arch*. **451**(1),pp.313–7.

- Bai, C.-X., Giamarchi, A., Rodat-Despoix, L., Padilla, F., Downs, T., Tsikas, L. and Delmas, P. 2008. Formation of a new receptor-operated channel by heteromeric assembly of TRPP2 and TRPC1 subunits. *EMBO reports*. **9**(5),pp.472–479.
- Bai, J.Z. and Lipski, J. 2010. Differential expression of TRPM2 and TRPV4 channels and their potential role in oxidative stress-induced cell death in organotypic hippocampal culture. *Neurotoxicology*. **31**(2),pp.204–14.
- Bandell, M., Story, G.M., Hwang, S.W., Viswanath, V., Eid, S.R., Petrus, M.J., Earley, T.J. and Patapoutian, A. 2004. Noxious cold ion channel TRPA1 is activated by pungent compounds and bradykinin. *Neuron*. **41**(6),pp.849–857.
- Banfi, B., Clark, R.A., Steger, K. and Krause, K.H. 2003. Two novel proteins activate superoxide generation by the NADPH oxidase NOX1. *J Biol Chem*. **278**(6),pp.3510–3.
- Banfi, B., Molnar, G., Maturana, A., Steger, K., Hegedus, B., Demaurex, N. and Krause, K.H. 2001. A Ca(2+)-activated NADPH oxidase in testis, spleen, and lymph nodes. *J Biol Chem*. **276**(40),pp.37594–601.
- Banfi, B., Tirone, F., Durussel, I., Knisz, J., Moskwa, P., Molnar, G.Z., Krause, K.H. and Cox, J.A. 2004. Mechanism of Ca²⁺ activation of the NADPH oxidase 5 (NOX5). *J Biol Chem*. **279**(18),pp.18583–91.
- Barbet, G., Demion, M., Moura, I.C., Serafini, N., Léger, T., Vrtovsnik, F., Monteiro, R.C., Guinamard, R., Kinet, J.-P. and Launay, P. 2008. The calcium-activated nonselective cation channel TRPM4 is essential for the migration but not the maturation of dendritic cells. *Nature Immunology*. **9**(10),pp.1148–1156.
- Barcia, C., Sanchez Bahillo, A., Fernandez-Villalba, E., Bautista, V., Poza, Y.P.M., Fernandez-Barreiro, A., Hirsch, E.C. and Herrero, M.T. 2004. Evidence of active microglia in substantia nigra pars compacta of parkinsonian monkeys 1 year after MPTP exposure. *Glia*. **46**(4),pp.402–9.
- Bari, M.R., Akbar, S., Eweida, M., Kühn, F.J.P., Gustafsson, A.J., Lückhoff, A. and Islam, M.S. 2009. H₂O₂-induced Ca²⁺ influx and its inhibition by N-(p-amylocinnamoyl) anthranilic acid in the beta-cells: involvement of TRPM2 channels. *Journal of Cellular and Molecular Medicine*. **13**(9B),pp.3260–3267.
- Bauer, C., Duewell, P., Mayer, C., Lehr, H.A., Fitzgerald, K.A., Dauer, M., Tschopp, J., Endres, S., Latz, E. and Schnurr, M. 2010. Colitis induced in mice with dextran sulfate sodium (DSS) is mediated by the NLRP3 inflammasome. *Gut*. **59**(9),pp.1192–1199.
- Bautista, D.M., Jordt, S.-E., Nikai, T., Tsuruda, P.R., Read, A.J., Poblete, J., Yamoah, E.N., Basbaum, A.I. and Julius, D. 2006. TRPA1 mediates the inflammatory actions of environmental irritants and proalgesic agents. *Cell*. **124**(6),pp.1269–1282.
- Beaulieu, C., Dyck, R. and Cynader, M. 1992. ENRICHMENT OF GLUTAMATE IN ZINC-CONTAINING TERMINALS OF THE CAT VISUAL-CORTEX. *Neuroreport*. **3**(10),pp.861–864.

- Beck, A., Kolisek, M., Bagley, L.A., Fleig, A. and Penner, R. 2006. Nicotinic acid adenine dinucleotide phosphate and cyclic ADP-ribose regulate TRPM2 channels in T lymphocytes. *Faseb Journal*. **20**(7),pp.962–+.
- Bedard, K. and Krause, K.H. 2007. The NOX family of ROS-generating NADPH oxidases: Physiology and pathophysiology. *Physiol Rev*. **87**(1),pp.245–313.
- Beech, D.J., Muraki, K. and Flemming, R. 2004. Non-selective cationic channels of smooth muscle and the mammalian homologues of *Drosophila* TRP. *Journal of Physiology-London*. **559**(3),pp.685–706.
- Behl, C., Davis, J.B., Lesley, R. and Schubert, D. 1994. HYDROGEN-PEROXIDE MEDIATES AMYLOID-BETA PROTEIN TOXICITY. *Cell*. **77**(6),pp.817–827.
- Behrendt, H.-J., Germann, T., Gillen, C., Hatt, H. and Jostock, R. 2004. Characterization of the mouse cold-menthol receptor TRPM8 and vanilloid receptor type-1 VR1 using a fluorometric imaging plate reader (FLIPR) assay. *British Journal of Pharmacology*. **141**(4),pp.737–745.
- Ben-Mabrouk, F. and Tryba, A.K. 2010. Substance P modulation of TRPC3/7 channels improves respiratory rhythm regularity and ICAN-dependent pacemaker activity. *European Journal of Neuroscience*. **31**(7),pp.1219–1232.
- Benna, J.E., Dang, P.M.-C., Gaudry, M., Fay, M. le, More, F., Hakim, J. and Gougerot-Pocidalo, M.-A. 1997. Phosphorylation of the Respiratory Burst Oxidase Subunit p67phox during Human Neutrophil Activation. *THE JOURNAL OF BIOLOGICAL CHEMISTRY*.
- van den Berge, S.A., van Strien, M.E., Korecka, J.A., Dijkstra, A.A., Sluijs, J.A., Kooijman, L., Eggers, R., De Filippis, L., Vescovi, A.L., Verhaagen, J., van de Berg, W.D. and Hol, E.M. 2011. The proliferative capacity of the subventricular zone is maintained in the parkinsonian brain. *Brain*. **134**(Pt 11),pp.3249–63.
- von Bernhardi, R., Tichauer, J.E. and Eugenin, J. 2010. Aging-dependent changes of microglial cells and their relevance for neurodegenerative disorders. *J Neurochem*. **112**(5),pp.1099–114.
- Berry, E.V. and Toms, N.J. 2006. Pyruvate and oxaloacetate limit zinc-induced oxidative HT-22 neuronal cell injury. *Neurotoxicology*. **27**(6),pp.1043–1051.
- Bezprozvanny, I. and Mattson, M.P. 2008. Neuronal calcium mishandling and the pathogenesis of Alzheimer's disease. *Trends Neurosci*. **31**(9),pp.454–63.
- Bezzerides, V.J., Ramsey, I.S., Kotecha, S., Greka, A. and Clapham, D.E. 2004. Rapid vesicular translocation and insertion of TRP channels. *Nat Cell Biol*. **6**(8),pp.709–20.
- Bleier, L. and Dröse, S. 2013. Superoxide generation by complex III: from mechanistic rationales to functional consequences. *Biochimica Et Biophysica Acta*. **1827**(11–12),pp.1320–1331.
- Blesa, J. and Przedborski, S. 2014. Parkinson's disease: animal models and dopaminergic cell vulnerability. *Front Neuroanat*. **8**,p.155.

- Block, M.L., Zecca, L. and Hong, J.-S. 2007. Microglia-mediated neurotoxicity: uncovering the molecular mechanisms. *Nature Reviews. Neuroscience*. **8**(1),pp.57–69.
- Bödding, M. 2007. TRP proteins and cancer. *Cellular Signalling*. **19**(3),pp.617–624.
- Bödding, M., Wissenbach, U. and Flockerzi, V. 2002. The recombinant human TRPV6 channel functions as Ca²⁺ sensor in human embryonic kidney and rat basophilic leukemia cells. *The Journal of Biological Chemistry*. **277**(39),pp.36656–36664.
- Boll, M.C., Alcaraz-Zubeldia, M. and Rios, C. 2011. Medical management of Parkinson's disease: focus on neuroprotection. *Curr Neuropharmacol*. **9**(2),pp.350–9.
- Bollimuntha, S., Selvaraj, S. and Singh, B.B. 2011. Emerging roles of canonical TRP channels in neuronal function. *Adv Exp Med Biol*. **704**,pp.573–93.
- Bosco, E.E., Kumar, S., Marchionni, F., Biesiada, J., Kordos, M., Szczur, K., Meller, J., Seibel, W., Mizrahi, A., Pick, E., Filippi, M.D. and Zheng, Y. 2012. Rational design of small molecule inhibitors targeting the Rac GTPase-p67(phox) signaling axis in inflammation. *Chem Biol*. **19**(2),pp.228–42.
- Boueiz, A. and Hassoun, P.M. 2009. Regulation of endothelial barrier function by reactive oxygen and nitrogen species. *Microvasc Res*. **77**(1),pp.26–34.
- Boveris, A., Cadena, E. and Stoppani, A.O. 1976. Role of ubiquinone in the mitochondrial generation of hydrogen peroxide. *Biochem J*. **156**(2),pp.435–44.
- Boveris, A. and Chance, B. 1973. The mitochondrial generation of hydrogen peroxide. General properties and effect of hyperbaric oxygen. *Biochem J*. **134**(3),pp.707–16.
- Brauchi, S., Krapivinsky, G., Krapivinsky, L. and Clapham, D.E. 2008. TRPM7 facilitates cholinergic vesicle fusion with the plasma membrane. *Proceedings of the National Academy of Sciences of the United States of America*. **105**(24),pp.8304–8308.
- Brixel, L.R., Monteilh-Zoller, M.K., Ingenbrandt, C.S., Fleig, A., Penner, R., Enklaar, T., Zabel, B.U. and Prawitt, D. 2010. TRPM5 regulates glucose-stimulated insulin secretion. *Pflugers Arch*. **460**(1),pp.69–76.
- Brodacki, B., Staszewski, J., Toczyłowska, B., Kozłowska, E., Drela, N., Chalimoniuk, M. and Stepien, A. 2008. Serum interleukin (IL-2, IL-10, IL-6, IL-4), TNFalpha, and INFgamma concentrations are elevated in patients with atypical and idiopathic parkinsonism. *Neurosci Lett*. **441**(2),pp.158–62.
- Brown, G.C. and Neher, J.J. 2010. Inflammatory neurodegeneration and mechanisms of microglial killing of neurons. *Molecular Neurobiology*. **41**(2–3),pp.242–247.
- Buelow, B., Song, Y. and Scharenberg, A.M. 2008. The Poly(ADP-ribose) polymerase PARP-1 is required for oxidative stress-induced TRPM2 activation in lymphocytes. *J Biol Chem*. **283**(36),pp.24571–83.

- Caiafa, P., Guastafierro, T. and Zampieri, M. 2009. Epigenetics: poly(ADP-ribosyl)ation of PARP-1 regulates genomic methylation patterns. *FASEB journal: official publication of the Federation of American Societies for Experimental Biology*. **23**(3),pp.672–678.
- Cape, J.L., Bowman, M.K. and Kramer, D.M. 2007. A semiquinone intermediate generated at the Qo site of the cytochrome bc1 complex: importance for the Q-cycle and superoxide production. *Proceedings of the National Academy of Sciences of the United States of America*. **104**(19),pp.7887–7892.
- Carter, R.N., Tolhurst, G., Walmsley, G., Vizuete-Forster, M., Miller, N. and Mahaut-Smith, M.P. 2006. Molecular and electrophysiological characterization of transient receptor potential ion channels in the primary murine megakaryocyte. *The Journal of Physiology*. **576**(Pt 1),pp.151–162.
- Cassel, S.L., Eisenbarth, S.C., Iyer, S.S., Sadler, J.J., Colegio, O.R., Tephly, L.A., Carter, A.B., Rothman, P.B., Flavell, R.A. and Sutterwala, F.S. 2008. The Nalp3 inflammasome is essential for the development of silicosis. *Proceedings of the National Academy of Sciences of the United States of America*. **105**(26),pp.9035–9040.
- Castor, L.R., Locatelli, K.A. and Ximenes, V.F. 2010. Pro-oxidant activity of apocynin radical. *Free Radic Biol Med*. **48**(12),pp.1636–43.
- Caterina, M.J., Leffler, A., Malmberg, A.B., Martin, W.J., Trafton, J., Petersen-Zeitz, K.R., Koltzenburg, M., Basbaum, A.I. and Julius, D. 2000. Impaired nociception and pain sensation in mice lacking the capsaicin receptor. *Science (New York, N.Y.)*. **288**(5464),pp.306–313.
- Chang, Q., Gyftogianni, E., van de Graaf, S.F., Hoefs, S., Weidema, F.A., Bindels, R.J. and Hoenderop, J.G. 2004. Molecular determinants in TRPV5 channel assembly. *J Biol Chem*. **279**(52),pp.54304–11.
- Chen, G.-L., Zeng, B., Eastmond, S., Elsenussi, S.E., Boa, A.N. and Xu, S.-Z. 2012. Pharmacological comparison of novel synthetic fenamate analogues with econazole and 2-APB on the inhibition of TRPM2 channels. *British Journal of Pharmacology*. **167**(6),pp.1232–1243.
- Chen, Q., Vazquez, E.J., Moghaddas, S., Hoppel, C.L. and Lesnefsky, E.J. 2003. Production of reactive oxygen species by mitochondria: central role of complex III. *J Biol Chem*. **278**(38),pp.36027–31.
- Chen, X.Z., Vassilev, P.M., Basora, N., Peng, J.B., Nomura, H., Segal, Y., Brown, E.M., Reeders, S.T., Hediger, M.A. and Zhou, J. 1999. Polycystin-L is a calcium-regulated cation channel permeable to calcium ions. *Nature*. **401**(6751),pp.383–6.
- Chen, Y., Zhang, Z., Lv, X.Y., Wang, Y.D., Hu, Z.G., Sun, H., Tan, R.Z., Liu, Y.H., Bian, G.H., Xiao, Y., Li, Q.W., Yang, Q.T., Ai, J.Z., Feng, L., Yang, Y., Wei, Y.Q. and Zhou, Q. 2008. Expression of Pkd2l2 in testis is implicated in spermatogenesis. *Biological & Pharmaceutical Bulletin*. **31**(8),pp.1496–1500.

- Cheng, G., Cao, Z., Xu, X., van Meir, E.G. and Lambeth, J.D. 2001. Homologs of gp91phox: cloning and tissue expression of Nox3, Nox4, and Nox5. *Gene*. **269**(1–2),pp.131–40.
- Cheret, C., Gervais, A., Lelli, A., Colin, C., Amar, L., Ravassard, P., Mallet, J., Cumano, A., Krause, K.H. and Mallat, M. 2008. Neurotoxic Activation of Microglia Is Promoted by a Nox1-Dependent NADPH Oxidase. *Journal of Neuroscience*. **28**(46),pp.12039–12051.
- Chinta, S.J., Rane, A., Yadava, N., Andersen, J.K., Nicholls, D.G. and Polster, B.M. 2009. Reactive oxygen species regulation by AIF- and complex I-depleted brain mitochondria. *Free Radic Biol Med*. **46**(7),pp.939–47.
- Chouchani, E.T., Pell, V.R., James, A.M., Work, L.M., Saeb-Parsy, K., Frezza, C., Krieg, T. and Murphy, M.P. 2016. A Unifying Mechanism for Mitochondrial Superoxide Production during Ischemia-Reperfusion Injury. *Cell Metab*. **23**(2),pp.254–63.
- Chung, K.K., Freestone, P.S. and Lipski, J. 2011. Expression and functional properties of TRPM2 channels in dopaminergic neurons of the substantia nigra of the rat. *J Neurophysiol*. **106**(6),pp.2865–75.
- Chung, M.K., Guler, A.D. and Caterina, M.J. 2005. Biphasic currents evoked by chemical or thermal activation of the heat-gated ion channel, TRPV3. *Journal of Biological Chemistry*. **280**(16),pp.15928–15941.
- Chung, M.K., Lee, H., Mizuno, A., Suzuki, M. and Caterina, M.J. 2004. 2-aminoethoxydiphenyl borate activates and sensitizes the heat-gated ion channel TRPV3. *J Neurosci*. **24**(22),pp.5177–82.
- Citron, M., Diehl, T.S., Capell, A., Haass, C., Teplow, D.B. and Selkoe, D.J. 1996. Inhibition of amyloid beta-protein production in neural cells by the serine protease inhibitor AEBSF. *Neuron*. **17**(1),pp.171–9.
- Clapham, D.E. 2003. TRP channels as cellular sensors. *Nature*. **426**(6966),pp.517–524.
- Clark, K., Langeslag, M., van Leeuwen, B., Ran, L., Ryazanov, A.G., Figidor, C.G., Moolenaar, W.H., Jalink, K. and van Leeuwen, F.N. 2006. TRPM7, a novel regulator of actomyosin contractility and cell adhesion. *The EMBO journal*. **25**(2),pp.290–301.
- Clausen, B.H., Lambertsen, K.L., Babcock, A.A., Holm, T.H., Dagnaes-Hansen, F. and Finsen, B. 2008. Interleukin-1beta and tumor necrosis factor-alpha are expressed by different subsets of microglia and macrophages after ischemic stroke in mice. *Journal of Neuroinflammation*. **5**,p.46.
- Colonna, M. and Butovsky, O. 2017. Microglia Function in the Central Nervous System During Health and Neurodegeneration. *Annual Review of Immunology*. **35**,pp.441–468.
- Colonna, M. and Wang, Y. 2016. TREM2 variants: new keys to decipher Alzheimer disease pathogenesis. *Nature Reviews Neuroscience*. **17**(4),pp.201–207.

- Coombes, E., Jiang, J., Chu, X.P., Inoue, K., Seeds, J., Branigan, D., Simon, R.P. and Xiong, Z.G. 2011. Pathophysiologically relevant levels of hydrogen peroxide induce glutamate-independent neurodegeneration that involves activation of transient receptor potential melastatin 7 channels. *Antioxid Redox Signal.* **14**(10),pp.1815–27.
- Corey, D.P., Garcia-Anoveros, J., Holt, J.R., Kwan, K.Y., Lin, S.Y., Vollrath, M.A., Amalfitano, A., Cheung, E.L.M., Derfler, B.H., Duggan, A., Geleoc, G.S.G., Gray, P.A., Hoffman, M.P., Rehm, H.L., Tamasauskas, D. and Zhang, D.S. 2004. TRPA1 is a candidate for the mechanosensitive transduction channel of vertebrate hair cells. *Nature.* **432**(7018),pp.723–730.
- Cosens, D.J. and Manning, A. 1969. ABNORMAL ELECTRORETINOGRAM FROM A DROSOPHILA MUTANT. *Nature.* **224**(5216),pp.285–287.
- Cover, C., Liu, J., Farhood, A., Malle, E., Waalkes, M.P., Bajt, M.L. and Jaeschke, H. 2006. Pathophysiological role of the acute inflammatory response during acetaminophen hepatotoxicity. *Toxicol Appl Pharmacol.* **216**(1),pp.98–107.
- Cover, C., Mansouri, A., Knight, T.R., Bajt, M.L., Lemasters, J.J., Pessayre, D. and Jaeschke, H. 2005. Peroxynitrite-induced mitochondrial and endonuclease-mediated nuclear DNA damage in acetaminophen hepatotoxicity. *J Pharmacol Exp Ther.* **315**(2),pp.879–87.
- Cramer, W.A., Hasan, S.S. and Yamashita, E. 2011. The Q cycle of cytochrome bc complexes: a structure perspective. *Biochimica Et Biophysica Acta.* **1807**(7),pp.788–802.
- Crofts, A.R., Barquera, B., Gennis, R.B., Kuras, R., Guergova-Kuras, M. and Berry, E.A. 1999. Mechanism of ubiquinol oxidation by the bc(1) complex: different domains of the quinol binding pocket and their role in the mechanism and binding of inhibitors. *Biochemistry.* **38**(48),pp.15807–26.
- Cross, A.R. and Segal, A.W. 2004. The NADPH oxidase of professional phagocytes--prototype of the NOX electron transport chain systems. *Biochim Biophys Acta.* **1657**(1),pp.1–22.
- Cruz, C.M., Rinna, A., Forman, H.J., Ventura, A.L.M., Persechini, P.M. and Ojcius, D.M. 2007. ATP Activates a Reactive Oxygen Species-dependent Oxidative Stress Response and Secretion of Proinflammatory Cytokines in Macrophages. *Journal of Biological Chemistry.* **282**(5),pp.2871–2879.
- Cunningham, C., Wilcockson, D.C., Campion, S., Lunnon, K. and Perry, V.H. 2005. Central and systemic endotoxin challenges exacerbate the local inflammatory response and increase neuronal death during chronic neurodegeneration. *The Journal of Neuroscience: The Official Journal of the Society for Neuroscience.* **25**(40),pp.9275–9284.
- Czlonkowska, A., Kohutnicka, M., Kurkowska-Jastrzebska, I. and Czlonkowski, A. 1996. Microglial reaction in MPTP (1-methyl-4-phenyl-1,2,3,6-tetrahydropyridine) induced Parkinson's disease mice model. *Neurodegeneration.* **5**(2),pp.137–43.

- Dalrymple, A., Slater, D.M., Poston, L. and Tribe, R.M. 2004. Physiological induction of transient receptor potential canonical proteins, calcium entry channels, in human myometrium: Influence of pregnancy, labor, and interleukin-1 beta. *Journal of Clinical Endocrinology & Metabolism*. **89**(3),pp.1291–1300.
- Davidson, D.G. and Eastham, W.N. 1966. ACUTE LIVER NECROSIS FOLLOWING OVERDOSE OF PARACETAMOL. *British Medical Journal*. **2**(5512),p.497-.
- De Deken, X., Wang, D., Dumont, J.E. and Miot, F. 2002. Characterization of ThOX proteins as components of the thyroid H(2)O(2)-generating system. *Exp Cell Res.* **273**(2),pp.187–96.
- DeCaen, P.G., Delling, M., Vien, T.N. and Clapham, D.E. 2013. Direct recording and molecular identification of the calcium channel of primary cilia. *Nature*. **504**(7479),pp.315–8.
- Del Rio-Hortega P. (1932) Microglia. In: Cytology and Cellular Pathology of the Nervous System, edited by Penfield W. New York: Hoeber, 1932, p. **482**–1924–534.
- Delany, N.S., Hurle, M., Facer, P., Alnadaf, T., Plumpton, C., Kinghorn, I., See, C.G., Costigan, M., Anand, P., Woolf, C.J., Crowther, D., Sanseau, P. and Tate, S.N. 2001. Identification and characterization of a novel human vanilloid receptor-like protein, VRL-2. *Physiol Genomics*. **4**(3),pp.165–74.
- DeLeo, F.R., Nauseef, W.M., Jesaitis, A.J., Burritt, J.B., Clark, R.A. and Quinn, M.T. 1995. A domain of p47phox that interacts with human neutrophil flavocytochrome b558. *J Biol Chem*. **270**(44),pp.26246–51.
- Delling, M., DeCaen, P.G., Doerner, J.F., Febvay, S. and Clapham, D.E. 2013. Primary cilia are specialized calcium signalling organelles. *Nature*. **504**(7479),pp.311–4.
- Delmas, P. 2004. Polycystins: from mechanosensation to gene regulation. *Cell*. **118**(2),pp.145–8.
- Delmas, P. 2005. Polycystins: polymodal receptor/ion-channel cellular sensors. *Pflugers Archiv-European Journal of Physiology*. **451**(1),pp.264–276.
- Dewas, C., Fay, M., Gougerot-Pocidalo, M.A. and El-Benna, J. 2000. The mitogen-activated protein kinase extracellular signal-regulated kinase 1/2 pathway is involved in formyl-methionyl-leucyl-phenylalanine-induced p47phox phosphorylation in human neutrophils. *J Immunol*. **165**(9),pp.5238–44.
- Di Palma, F., Belyantseva, I.A., Kim, H.J., Vogt, T.F., Kachar, B. and Noben-Trauth, K. 2002. Mutations in Mcoln3 associated with deafness and pigmentation defects in varitint-waddler (Va) mice. *Proc Natl Acad Sci U S A*. **99**(23),pp.14994–14999.
- Diatchuk, V., Lotan, O., Koshkin, V., Wikstroem, P. and Pick, E. 1997. Inhibition of NADPH oxidase activation by 4-(2-aminoethyl)-benzenesulfonyl fluoride and related compounds. *J Biol Chem*. **272**(20),pp.13292–301.

Diebold, B.A. and Bokoch, G.M. 2001. Molecular basis for Rac2 regulation of phagocyte NADPH oxidase. *Nat Immunol.* **2**(3),pp.211–5.

Diestel, A., Aktas, O., Hackel, D., Hake, I., Meier, S., Raine, C.S., Nitsch, R., Zipp, F. and Uhrich, O. 2003. Activation of microglial poly(ADP-ribose)-polymerase-1 by cholesterol breakdown products during neuroinflammation: a link between demyelination and neuronal damage. *Journal of Experimental Medicine.* **198**(11),pp.1729–1740.

Djenoune, L., Khabou, H., Joubert, F., Quan, F.B., Figueiredo, S.N., Bodineau, L., Del Bene, F., Burckle, C., Tostivint, H. and Wyart, C. 2014. Investigation of spinal cerebrospinal fluid-contacting neurons expressing PKD2L1 evidence for a conserved system from fish to primates. *Frontiers in Neuroanatomy*. [Online]. **8**. Available from: ://WOS:000335371600001.

Doerner, J.F., Gisselmann, G., Hatt, H. and Wetzel, C.H. 2007. Transient receptor potential channel A1 is directly gated by calcium ions. *J Biol Chem.* **282**(18),pp.13180–9.

Domercq, M., Alberdi, E., Sanchez-Gomez, M.V., Ariz, U., Perez-Samartin, A. and Matute, C. 2011. Dual-specific Phosphatase-6 (Dusp6) and ERK Mediate AMPA Receptor-induced Oligodendrocyte Death. *Journal of Biological Chemistry.* **286**(13),pp.11825–11836.

Domercq, M., Mato, S., Soria, F.N., Sanchez-Gomez, M.V., Alberdi, E. and Matute, C. 2013. Zn²⁺-induced ERK activation mediates PARP-1-dependent ischemic-reoxygenation damage to oligodendrocytes. *Glia.* **61**(3),pp.383–393.

Dong, X.P., Cheng, X.P., Mills, E., Delling, M., Wang, F.D., Kurz, T. and Xu, H.X. 2008. The type IV mucolipidosis-associated protein TRPML1 is an endolysosomal iron release channel. *Nature.* **455**(7215),pp.992-U78.

Dong, X.P., Wang, X. and Xu, H. 2010. TRP channels of intracellular membranes. *J Neurochem.* **113**(2),pp.313–28.

Dostert, C., Pétrilli, V., Van Bruggen, R., Steele, C., Mossman, B.T. and Tschoopp, J. 2008. Innate immune activation through Nalp3 inflammasome sensing of asbestos and silica. *Science (New York, N.Y.).* **320**(5876),pp.674–677.

Du, J.Y., Xie, J. and Yue, L.X. 2009. Intracellular calcium activates TRPM2 and its alternative spliced isoforms. *Proceedings of the National Academy of Sciences of the United States of America.* **106**(17),pp.7239–7244.

Duncan, L.M., Deeds, J., Hunter, J., Shao, J., Holmgren, L.M., Woolf, E.A., Tepper, R.I. and Shyjan, A.W. 1998. Down-regulation of the novel gene melastatin correlates with potential for melanoma metastasis. *Cancer Research.* **58**(7),pp.1515–1520.

Dupuy, C., Ohayon, R., Valent, A., Noel-Hudson, M.S., Deme, D. and Virion, A. 1999. Purification of a novel flavoprotein involved in the thyroid NADPH oxidase. Cloning of the porcine and human cdnas. *J Biol Chem.* **274**(52),pp.37265–9.

Eisfeld, J. and Luckhoff, A. 2007. Trpm2. *Handb Exp Pharmacol.* (179),pp.237–52.

- El Benna, J., Faust, R.P., Johnson, J.L. and Babior, B.M. 1996. Phosphorylation of the respiratory burst oxidase subunit p47phox as determined by two-dimensional phosphopeptide mapping. Phosphorylation by protein kinase C, protein kinase A, and a mitogen-activated protein kinase. *J Biol Chem.* **271**(11),pp.6374–8.
- El Benna, J., Han, J., Park, J.W., Schmid, E., Ulevitch, R.J. and Babior, B.M. 1996. Activation of p38 in stimulated human neutrophils: phosphorylation of the oxidase component p47phox by p38 and ERK but not by JNK. *Arch Biochem Biophys.* **334**(2),pp.395–400.
- El-Benna, J., Dang, P.M.-C., Gougerot-Pocidalo, M.-A. and Elbim, C. 2005. Phagocyte NADPH oxidase: a multicomponent enzyme essential for host defenses. *Archivum Immunologiae Et Therapiae Experimentalis.* **53**(3),pp.199–206.
- El-Benna, J., Dang, P.M.-C., Gougerot-Pocidalo, M.-A., Marie, J.-C. and Braut-Boucher, F. 2009. p47phox, the phagocyte NADPH oxidase/NOX2 organizer: structure, phosphorylation and implication in diseases. *Experimental and Molecular Medicine.* **41**(4),p.217.
- Ellmark, S.H., Dusting, G.J., Fui, M.N., Guzzo-Pernell, N. and Drummond, G.R. 2005. The contribution of Nox4 to NADPH oxidase activity in mouse vascular smooth muscle. *Cardiovasc Res.* **65**(2),pp.495–504.
- Erler, I., Al-Ansary, D.M., Wissenbach, U., Wagner, T.F., Flockerzi, V. and Niemeyer, B.A. 2006. Trafficking and assembly of the cold-sensitive TRPM8 channel. *J Biol Chem.* **281**(50),pp.38396–404.
- Esatbeyoglu, T., Huebbe, P., Ernst, I.M.A., Chin, D., Wagner, A.E. and Rimbach, G. 2012. Curcumin--from molecule to biological function. *Angewandte Chemie (International Ed. in English).* **51**(22),pp.5308–5332.
- Fauzee, N.J.S., Pan, J. and Wang, Y. 2010. PARP and PARG inhibitors--new therapeutic targets in cancer treatment. *Pathology oncology research: POR.* **16**(4),pp.469–478.
- Feldmann, M. 2002. Development of anti-TNF therapy for rheumatoid arthritis. *Nat Rev Immunol.* **2**(5),pp.364–71.
- Fernandes, J., Lorenzo, I.M., Andrade, Y.N., Garcia-Elias, A., Serra, S.A., Fernández-Fernández, J.M. and Valverde, M.A. 2008. IP₃ sensitizes TRPV4 channel to the mechano- and osmotransducing messenger 5'-6'-epoxyeicosatrienoic acid. *The Journal of Cell Biology.* **181**(1),pp.143–155.
- Fleig, A. and Penner, R. 2004a. Emerging roles of TRPM channels. *Novartis Found Symp.* **258**,pp.248-58; discussion 258-66.
- Fleig, A. and Penner, R. 2004b. The TRPM ion channel subfamily: molecular, biophysical and functional features. *Trends Pharmacol Sci.* **25**(12),pp.633–9.
- Flemming, R., Xu, S.Z. and Beech, D.J. 2003. Pharmacological profile of store-operated channels in cerebral arteriolar smooth muscle cells. *Br J Pharmacol.* **139**(5),pp.955–65.

- Fonfria, E., Marshall, I.C.B., Benham, C.D., Boyfield, I., Brown, J.D., Hill, K., Hughes, J.P., Skaper, S.D. and McNulty, S. 2004. TRPM2 channel opening in response to oxidative stress is dependent on activation of poly(ADP-ribose) polymerase. *British Journal of Pharmacology*. **143**(1),pp.186–192.
- Fonfria, E., Marshall, I.C.B., Boyfield, I., Skaper, S.D., Hughes, J.P., Owen, D.E., Zhang, W., Miller, B.A., Benham, C.D. and McNulty, S. 2005. Amyloid beta-peptide(1-42) and hydrogen peroxide-induced toxicity are mediated by TRPM2 in rat primary striatal cultures. *Journal of Neurochemistry*. **95**(3),pp.715–723.
- Fonfria, E., Mattei, C., Hill, K., Brown, J.T., Randall, A., Benham, C.D., Skaper, S.D., Campbell, C.A., Crook, B., Murdock, P.R., Wilson, J.M., Maurio, F.P., Owen, D.E., Tilling, P.L. and McNulty, S. 2006. TRPM2 is elevated in the tMCAO stroke model, transcriptionally regulated, and functionally expressed in C13 microglia. *Journal of Receptors and Signal Transduction*. **26**(3),pp.179–198.
- Forman, H.J. and Kennedy, J.A. 1974. Role of superoxide radical in mitochondrial dehydrogenase reactions. *Biochem Biophys Res Commun*. **60**(3),pp.1044–50.
- Frangogiannis, N.G. 2014. The inflammatory response in myocardial injury, repair, and remodelling. *Nature Reviews Cardiology*. **11**(5),pp.255–265.
- Frautschy, S.A., Yang, F., Irrizarry, M., Hyman, B., Saido, T.C., Hsiao, K. and Cole, G.M. 1998. Microglial response to amyloid plaques in APPsw transgenic mice. *Am J Pathol*. **152**(1),pp.307–17.
- Frederickson, C.J., Cuajungco, M.P. and Frederickson, C.J. 2005. Is zinc the link between compromises of brain perfusion (excitotoxicity) and Alzheimer's disease? *Journal of Alzheimers Disease*. **8**(2),pp.155–160.
- Freichel, M., Suh, S.H., Pfeifer, A., Schweig, U., Trost, C., Weissgerber, P., Biel, M., Philipp, S., Freise, D., Droogmans, G., Hofmann, F., Flockerzi, V. and Nilius, B. 2001. Lack of an endothelial store-operated Ca²⁺ current impairs agonist-dependent vasorelaxation in TRP4^{-/-} mice. *Nat Cell Biol*. **3**(2),pp.121–7.
- Frey, R.S., Rahman, A., Kefer, J.C., Minshall, R.D. and Malik, A.B. 2002. PKC ζ regulates TNF-alpha-induced activation of NADPH oxidase in endothelial cells. *Circ Res*. **90**(9),pp.1012–9.
- Gabbita, S.P., Johnson, M.F., Kobritz, N., Eslami, P., Poteshkina, A., Varadarajan, S., Turman, J., Zemlan, F. and Harris-White, M.E. 2015. Oral TNF α Modulation Alters Neutrophil Infiltration, Improves Cognition and Diminishes Tau and Amyloid Pathology in the 3xTgAD Mouse Model. *Plos One*. **10**(10),p.e0137305.
- Gao, X., Kim, H.K., Chung, J.M. and Chung, K. 2007. Reactive oxygen species (ROS) are involved in enhancement of NMDA-receptor phosphorylation in animal models of pain. *Pain*. **131**(3),pp.262–71.
- Gao, Y.J. and Ji, R.R. 2010. Chemokines, neuronal-glial interactions, and central processing of neuropathic pain. *Pharmacol Ther*. **126**(1),pp.56–68.
- Geiszt, M. and Leto, T.L. 2004. The Nox family of NAD(P)H oxidases: host defense and beyond. *The Journal of Biological Chemistry*. **279**(50),pp.51715–51718.

- Gelderblom, M., Melzer, N., Schattling, B., Gob, E., Hicking, G., Arunachalam, P., Bittner, S., Ufer, F., Herrmann, A.M., Bernreuther, C., Glatzel, M., Gerloff, C., Kleinschmitz, C., Meuth, S.G., Friese, M.A. and Magnus, T. 2014. Transient Receptor Potential Melastatin Subfamily Member 2 Cation Channel Regulates Detrimental Immune Cell Invasion in Ischemic Stroke. *Stroke*. **45**(11),pp.3395–3402.
- Genova, T., Grolez, G.P., Camillo, C., Bernardini, M., Bokhobza, A., Richard, E., Scianna, M., Lemonnier, L., Valdembri, D., Munaron, L., Philips, M.R., Mattot, V., Serini, G., Prevarskaya, N., Gkika, D. and Pla, A.F. 2017. TRPM8 inhibits endothelial cell migration via a non-channel function by trapping the small GTPase Rap1. *Journal of Cell Biology*. **216**(7),pp.2107–2130.
- George, J.L., Mok, S., Moses, D., Wilkins, S., Bush, A.I., Cherny, R.A. and Finkelstein, D.I. 2009. Targeting the progression of Parkinson's disease. *Curr Neuropharmacol*. **7**(1),pp.9–36.
- Gerhard, A., Pavese, N., Hotton, G., Turkheimer, F., Es, M., Hammers, A., Eggert, K., Oertel, W., Banati, R.B. and Brooks, D.J. 2006. In vivo imaging of microglial activation with [11C](R)-PK11195 PET in idiopathic Parkinson's disease. *Neurobiol Dis*. **21**(2),pp.404–12.
- Gianni, D., Taulet, N., Zhang, H., DerMardirossian, C., Kister, J., Martinez, L., Roush, W.R., Brown, S.J., Bokoch, G.M. and Rosen, H. 2010. A Novel and Specific NADPH Oxidase-1 (Nox1) Small-Molecule Inhibitor Blocks the Formation of Functional Invadopodia in Human Colon Cancer Cells. *Acs Chemical Biology*. **5**(10),pp.981–993.
- Gloire, G., Legrand-Poels, S. and Piette, J. 2006. NF-kappaB activation by reactive oxygen species: fifteen years later. *Biochemical Pharmacology*. **72**(11),pp.1493–1505.
- van de Graaf, S.F.J., Hoenderop, J.G.J., van der Kemp, A.W.C.M., Gisler, S.M. and Bindels, R.J.M. 2006. Interaction of the epithelial Ca²⁺ channels TRPV5 and TRPV6 with the intestine- and kidney-enriched PDZ protein NHERF4. *Pflugers Archiv: European Journal of Physiology*. **452**(4),pp.407–417.
- Gray, S.P., Di Marco, E., Okabe, J., Szyndralewiez, C., Heitz, F., Montezano, A.C., de Haan, J.B., Koulis, C., El-Osta, A., Andrews, K.L., Chin-Dusting, J.P., Touyz, R.M., Wingler, K., Cooper, M.E., Schmidt, H.H. and Jandeleit-Dahm, K.A. 2013. NADPH oxidase 1 plays a key role in diabetes mellitus-accelerated atherosclerosis. *Circulation*. **127**(18),pp.1888–902.
- Greka, A., Navarro, B., Oancea, E., Duggan, A. and Clapham, D.E. 2003. TRPC5 is a regulator of hippocampal neurite length and growth cone morphology. *Nature Neuroscience*. **6**(8),pp.837–845.
- Grigolava, I.V., Ksenzenko, Mi., Konstantinob, A.A., Tikhonov, A.N. and Kerimov, T.M. 1980. [Tiron as a spin-trap for superoxide radicals produced by the respiratory chain of submitochondrial particles]. *Biokhimiia*. **45**(1),pp.75–82.
- Grimm, C., Kraft, R., Sauerbruch, S., Schultz, G. and Harteneck, C. 2003. Molecular and functional characterization of the melastatin-related cation channel TRPM3. *Journal of Biological Chemistry*. **278**(24),pp.21493–21501.

- Grimm, C., Kraft, R., Schultz, G. and Harteneck, C. 2005. Activation of the melastatin-related cation channel TRMP3 by D-erythro-sphingosine. *Molecular Pharmacology*. **67**(3),pp.798–805.
- de Groot, T., Bindels, R.J.M. and Hoenderop, J.G.J. 2008. TRPV5: an ingeniously controlled calcium channel. *Kidney International*. **74**(10),pp.1241–1246.
- Grubisha, O., Rafty, L.A., Takanishi, C.L., Xu, X., Tong, L., Perraud, A.L., Scharenberg, A.M. and Denu, J.M. 2006. Metabolite of SIR2 reaction modulates TRPM2 ion channel. *J Biol Chem*. **281**(20),pp.14057–65.
- Guinamard, R., Simard, C. and Del Negro, C. 2013. Flufenamic acid as an ion channel modulator. *Pharmacology & Therapeutics*. **138**(2),pp.272–284.
- Guler, A.D., Lee, H., Iida, T., Shimizu, I., Tominaga, M. and Caterina, M. 2002. Heat-evoked activation of the ion channel, TRPV4. *J Neurosci*. **22**(15),pp.6408–14.
- Gunthorpe, M.J., Benham, C.D., Randall, A. and Davis, J.B. 2002. The diversity in the vanilloid (TRPV) receptor family of ion channels. *Trends in Pharmacological Sciences*. **23**(4),pp.183–191.
- Guo, L., Schreiber, T.H., Weremowicz, S., Morton, C.C., Lee, C. and Zhou, J. 2000. Identification and characterization of a novel polycystin family member, polycystin-L2, in mouse and human: Sequence, expression, alternative splicing, and chromosomal localization. *Genomics*. **64**(3),pp.241–251.
- Ha, J.S., Lee, J.E., Lee, J.R., Lee, C.S., Maeng, J.S., Bae, Y.S., Kwon, K.S. and Park, S.S. 2010. Nox4-dependent H₂O₂ production contributes to chronic glutamate toxicity in primary cortical neurons. *Exp Cell Res*. **316**(10),pp.1651–61.
- Hagenston, A.M., Rudnick, N.D., Boone, C.E. and Yeckel, M.F. 2009. 2-Aminoethoxydiphenyl-borate (2-APB) increases excitability in pyramidal neurons. *Cell Calcium*. **45**(3),pp.310–7.
- Ham, H.-Y., Hong, C.-W., Lee, S.-N., Kwon, M.-S., Kim, Y.-J. and Song, D.-K. 2012. Sulfur mustard primes human neutrophils for increased degranulation and stimulates cytokine release via TRPM2/p38 MAPK signaling. *Toxicology and Applied Pharmacology*. **258**(1),pp.82–88.
- Hanaoka, K., Qian, F., Boletta, A., Bhunia, A.K., Piontek, K., Tsikas, L., Sukhatme, V.P., Guggino, W.B. and Germino, G.G. 2000. Co-assembly of polycystin-1 and -2 produces unique cation-permeable currents. *Nature*. **408**(6815),pp.990–4.
- Hanisch, U.K. 2002. Microglia as a source and target of cytokines. *Glia*. **40**(2),pp.140–55.
- Hara, H., Taniguchi, M., Kobayashi, M., Kamiya, T. and Adachi, T. 2015. Plasma-activated medium-induced intracellular zinc liberation causes death of SH-SY5Y cells. *Archives of Biochemistry and Biophysics*. **584**,pp.51–60.
- Hara, Y., Wakamori, M., Ishii, M., Maeno, E., Nishida, M., Yoshida, T., Yamada, H., Shimizu, S., Mori, E., Kudoh, J., Shimizu, N., Kurose, H., Okada, Y., Imoto, K. and Mori, Y. 2002. LTRPC2 Ca²⁺-permeable channel activated by changes in

- redox status confers susceptibility to cell death. *Molecular Cell.* **9**(1),pp.163–173.
- Haraguchi, K., Kawamoto, A., Isami, K., Maeda, S., Kusano, A., Asakura, K., Shirakawa, H., Mori, Y., Nakagawa, T. and Kaneko, S. 2012. TRPM2 Contributes to Inflammatory and Neuropathic Pain through the Aggravation of Pronociceptive Inflammatory Responses in Mice. *Journal of Neuroscience.* **32**(11),pp.3931–3941.
- Hardie, R.C. and Minke, B. 1992. THE TRP GENE IS ESSENTIAL FOR A LIGHT-ACTIVATED CA₂₊ CHANNEL IN DROSOPHILA PHOTORECEPTORS. *Neuron.* **8**(4),pp.643–651.
- Hardy, J. 2006. A hundred years of Alzheimer's disease research. *Neuron.* **52**(1),pp.3–13.
- Hardy, J. and Selkoe, D.J. 2002. The amyloid hypothesis of Alzheimer's disease: progress and problems on the road to therapeutics. *Science.* **297**(5580),pp.353–6.
- Harrigan, T.J., Abdullaev, I.F., Jourd'heuil, D. and Mongin, A.A. 2008. Activation of microglia with zymosan promotes excitatory amino acid release via volume-regulated anion channels: the role of NADPH oxidases. *Journal of Neurochemistry.* **106**(6),pp.2449–2462.
- Harteneck, C., Frenzel, H. and Kraft, R. 2007. N-(p-Amylcinnamoyl)anthranilic Acid (ACA): A Phospholipase A2 Inhibitor and TRP Channel Blocker: ACA AND TRP CHANNELS. *Cardiovascular Drug Reviews.* **25**(1),pp.61–75.
- Hartmann, J., Dragicevic, E., Adelsberger, H., Henning, H.A., Sumser, M., Abramowitz, J., Blum, R., Dietrich, A., Freichel, M., Flockerzi, V., Birnbaumer, L. and Konnerth, A. 2008. TRPC3 channels are required for synaptic transmission and motor coordination. *Neuron.* **59**(3),pp.392–398.
- Hasegawa, T., Kikuyama, M., Sakurai, K., Kambayashi, Y., Adachi, M., Saniabadi, A.R., Kuwano, H. and Nakano, M. 2002. Mechanism of superoxide anion production by hepatic sinusoidal endothelial cells and Kupffer cells during short-term ethanol perfusion in the rat. *Liver.* **22**(4),pp.321–329.
- Hassock, S.R., Zhu, M.X., Trost, C., Flockerzi, V. and Authi, K.S. 2002. Expression and role of TRPC proteins in human platelets: evidence that TRPC6 forms the store-independent calcium entry channel. *Blood.* **100**(8),pp.2801–11.
- Hazan, A., Kumar, R., Matzner, H. and Priel, A. 2015. The pain receptor TRPV1 displays agonist-dependent activation stoichiometry. *Sci Rep.* **5**,p.12278.
- Hecquet, C.M., Ahmmmed, G.U., Vogel, S.M. and Malik, A.B. 2008. Role of TRPM2 channel in mediating H₂O₂-induced Ca₂₊ entry and endothelial hyperpermeability. *Circulation Research.* **102**(3),pp.347–355.
- Hecquet, C.M. and Malik, A.B. 2009. Role of H₂O₂-activated TRPM2 calcium channel in oxidant-induced endothelial injury. *Thrombosis and Haemostasis.* **101**(4),pp.619–625.

- Heiner, I., Eisfeld, J., Halaszovich, C.R., Wehage, E., Jungling, E., Zitt, C. and Luckhoff, A. 2003. Expression profile of the transient receptor potential (TRP) family in neutrophil granulocytes: evidence for currents through long TRP channel 2 induced by ADP-ribose and NAD. *Biochemical Journal*. **371**, pp.1045–1053.
- Heiner, I., Eisfeld, J., Warnstedt, M., Radukina, N., Jüngling, E. and Lückhoff, A. 2006. Endogenous ADP-ribose enables calcium-regulated cation currents through TRPM2 channels in neutrophil granulocytes. *Biochemical Journal*. **398**(2), pp.225–232.
- Heinloth, A., Heermeier, K., Raff, U., Wanner, C. and Galle, J. 2000. Stimulation of NADPH oxidase by oxidized low-density lipoprotein induces proliferation of human vascular endothelial cells. *Journal of the American Society of Nephrology: JASN*. **11**(10), pp.1819–1825.
- Hellwig, N., Albrecht, N., Harteneck, C., Schultz, G. and Schaefer, M. 2005. Homo- and heteromeric assembly of TRPV channel subunits. *Journal of Cell Science*. **118**(5), pp.917–928.
- Heneka, M.T., Golenbock, D.T. and Latz, E. 2015. Innate immunity in Alzheimer's disease. *Nat Immunol*. **16**(3), pp.229–36.
- Heneka, M.T., Kummer, M.P., Stutz, A., Delekate, A., Schwartz, S., Vieira-Saecker, A., Griep, A., Axt, D., Remus, A., Tzeng, T.C., Gelpi, E., Halle, A., Korte, M., Latz, E. and Golenbock, D.T. 2013. NLRP3 is activated in Alzheimer's disease and contributes to pathology in APP/PS1 mice. *Nature*. **493**(7434), pp.674–8.
- Heppner, F.L., Ransohoff, R.M. and Becher, B. 2015. Immune attack: the role of inflammation in Alzheimer disease. *Nat Rev Neurosci*. **16**(6), pp.358–72.
- Hermosura, M.C., Monteilh-Zoller, M.K., Scharenberg, A.M., Penner, R. and Fleig, A. 2002. Dissociation of the store-operated calcium current/(CRAC) and the Mg-nucleotide-regulated metal ion current MagNuM. *Journal of Physiology-London*. **539**(2), pp.445–458.
- Herson, P.S. and Ashford, M.L. 1999. Reduced glutathione inhibits beta-NAD+-activated non-selective cation currents in the CRI-G1 rat insulin-secreting cell line. *J Physiol*. **514** (Pt 1), pp.47–57.
- Herson, P.S., Dulock, K.A. and Ashford, M.L. 1997. Characterization of a nicotinamide-adenine dinucleotide-dependent cation channel in the CRI-G1 rat insulinoma cell line. *J Physiol*. **505** (Pt 1), pp.65–76.
- Hilenski, L.L., Clempus, R.E., Quinn, M.T., Lambeth, J.D. and Griendling, K.K. 2004. Distinct subcellular localizations of Nox1 and Nox4 in vascular smooth muscle cells. *Arterioscler Thromb Vasc Biol*. **24**(4), pp.677–83.
- Hill, K., Benham, C.D., McNulty, S. and Randall, A.D. 2004. Flufenamic acid is a pH-dependent antagonist of TRPM2 channels. *Neuropharmacology*. **47**(3), pp.450–460.

- Hill, K., McNulty, S. and Randall, A.D. 2004. Inhibition of TRPM2 channels by the antifungal agents clotrimazole and econazole. *Naunyn Schmiedebergs Arch Pharmacol.* **370**(4),pp.227–37.
- Hines, D.J., Choi, H.B., Hines, R.M., Phillips, A.G. and MacVicar, B.A. 2013. Prevention of LPS-induced microglia activation, cytokine production and sickness behavior with TLR4 receptor interfering peptides. *PloS One.* **8**(3),p.e60388.
- Hinwood, M., Morandini, J., Day, T.A. and Walker, F.R. 2012. Evidence that microglia mediate the neurobiological effects of chronic psychological stress on the medial prefrontal cortex. *Cereb Cortex.* **22**(6),pp.1442–54.
- Hirano, T., Yamaguchi, R., Asami, S., Iwamoto, N. and Kasai, H. 1996. 8-Hydroxyguanine levels in nuclear DNA and its repair activity in rat organs associated with age. *Journals of Gerontology Series a-Biological Sciences and Medical Sciences.* **51**(5),pp.B303–B307.
- Hiroi, T., Wajima, T., Negoro, T., Ishii, M., Nakano, Y., Kiuchi, Y., Mori, Y. and Shimizu, S. 2013. Neutrophil TRPM2 channels are implicated in the exacerbation of myocardial ischaemia/reperfusion injury. *Cardiovascular Research.* **97**(2),pp.271–281.
- Hirota, K., Sonoda, E., Kawamoto, T., Motegi, A., Masutani, C., Hanaoka, F., Szuts, D., Iwai, S., Sale, J.E., Lehmann, A. and Takeda, S. 2010. Simultaneous Disruption of Two DNA Polymerases, Pol eta and Pol zeta, in Avian DT40 Cells Unmasks the Role of Pol eta in Cellular Response to Various DNA Lesions. *Plos Genetics.* [Online]. **6**(10). Available from: ://WOS:000283647800035.
- Hirst, J., Carroll, J., Fearnley, I.M., Shannon, R.J. and Walker, J.E. 2003. The nuclear encoded subunits of complex I from bovine heart mitochondria. *Biochimica Et Biophysica Acta.* **1604**(3),pp.135–150.
- Hoffman, N.E., Miller, B.A., Wang, J.F., Elrod, J.W., Rajan, S., Gao, E., Song, J.L., Zhang, X.Q., Hirschler-Laszkiewicz, I., Shanmughapriya, S., Koch, W.J., Feldman, A.M., Madesh, M. and Cheung, J.Y. 2015. Ca²⁺ entry via Trpm2 is essential for cardiac myocyte bioenergetics maintenance. *American Journal of Physiology-Heart and Circulatory Physiology.* **308**(6),pp.H637–H650.
- Hoffmann, A., Kann, O., Ohlemeyer, C., Hanisch, U.-K. and Kettenmann, H. 2003. Elevation of basal intracellular calcium as a central element in the activation of brain macrophages (microglia): suppression of receptor-evoked calcium signaling and control of release function. *The Journal of Neuroscience: The Official Journal of the Society for Neuroscience.* **23**(11),pp.4410–4419.
- Hofmann, T., Chubanov, V., Gudermann, T. and Montell, C. 2003. TRPM5 is a voltage-modulated and Ca²⁺-activated monovalent selective cation channel. *Current Biology.* **13**(13),pp.1153–1158.
- Hofmann, T., Obukhov, A.G., Schaefer, M., Harteneck, C., Gudermann, T. and Schultz, G. 1999. Direct activation of human TRPC6 and TRPC3 channels by diacylglycerol. *Nature.* **397**(6716),pp.259–263.

- Holzmann, C., Kappel, S., Kilch, T., Jochum, M.M., Urban, S.K., Jung, V., Stöckle, M., Rother, K., Greiner, M. and Peinelt, C. 2015. Transient receptor potential melastatin 4 channel contributes to migration of androgen-insensitive prostate cancer cells. *Oncotarget*. **6**(39),pp.41783–41793.
- Hong, S., Beja-Glasser, V.F., Nfonoyim, B.M., Frouin, A., Li, S., Ramakrishnan, S., Merry, K.M., Shi, Q., Rosenthal, A., Barres, B.A., Lemere, C.A., Selkoe, D.J. and Stevens, B. 2016. Complement and microglia mediate early synapse loss in Alzheimer mouse models. *Science*. **352**(6286),pp.712–716.
- Howell, G.A., Welch, M.G. and Frederickson, C.J. 1984. Stimulation-induced uptake and release of zinc in hippocampal slices. *Nature*. **308**(5961),pp.736–738.
- Hoyal, C.R., Gutierrez, A., Young, B.M., Catz, S.D., Lin, J.H., Tsichlis, P.N. and Babior, B.M. 2003. Modulation of p47PHOX activity by site-specific phosphorylation: Akt-dependent activation of the NADPH oxidase. *Proc Natl Acad Sci U S A*. **100**(9),pp.5130–5.
- Hu, H.Z., Gu, Q., Wang, C., Colton, C.K., Tang, J., Kinoshita-Kawada, M., Lee, L.Y., Wood, J.D. and Zhu, M.X. 2004. 2-aminoethoxydiphenyl borate is a common activator of TRPV1, TRPV2, and TRPV3. *J Biol Chem*. **279**(34),pp.35741–8.
- Huang, A.L., Chen, X.K., Hoon, M.A., Chandrashekhar, J., Guo, W., Trankner, D., Ryba, N.J.P. and Zuker, C.S. 2006. The cells and logic for mammalian sour taste detection. *Nature*. **442**(7105),pp.934–938.
- Hughes, J., Ward, C.J., Peral, B., Aspinwall, R., Clark, K., San Millán, J.L., Gamble, V. and Harris, P.C. 1995. The polycystic kidney disease 1 (PKD1) gene encodes a novel protein with multiple cell recognition domains. *Nature Genetics*. **10**(2),pp.151–160.
- Hurley, S.D., O'Banion, M.K., Song, D.D., Arana, F.S., Olschowka, J.A. and Haber, S.N. 2003. Microglial response is poorly correlated with neurodegeneration following chronic, low-dose MPTP administration in monkeys. *Exp Neurol*. **184**(2),pp.659–68.
- Huynh, K.W., Cohen, M.R., Jiang, J.S., Samanta, A., Lodowski, D.T., Zhou, Z.H. and Moiseenkova-Bell, V.Y. 2016. Structure of the full-length TRPV2 channel by cryo-EM. *Nature Communications*. [Online]. **7**. Available from: ://WOS:000373120200001.
- Hyslop, P.A., Zhang, Z., Pearson, D.V. and Phebus, L.A. 1995. Measurement of striatal H₂O₂ by microdialysis following global forebrain ischemia and reperfusion in the rat: correlation with the cytotoxic potential of H₂O₂ in vitro. *Brain Res*. **671**(2),pp.181–6.
- Iadecola, C., Zhang, F.Y., Niwa, K., Eckman, C., Turner, S.K., Fischer, E., Younkin, S., Borchelt, D.R., Hsiao, K.K. and Carlson, G.A. 1999. SOD1 rescues cerebral endothelial dysfunction in mice overexpressing amyloid precursor protein. *Nature Neuroscience*. **2**(2),pp.157–161.
- Inamura, K., Sano, Y., Mochizuki, S., Yokoi, H., Miyake, A., Nozawa, K., Kitada, C., Matsushime, H. and Furuichi, K. 2003. Response to ADP-ribose by activation of

- TRPM2 in the CRI-G1 insulinoma cell line. *Journal of Membrane Biology.* **191**(3),pp.201–207.
- Infanger, D.W., Sharma, R.V. and Davisson, R.L. 2006. NADPH oxidases of the brain: distribution, regulation, and function. *Antioxidants & Redox Signaling.* **8**(9–10),pp.1583–1596.
- Inoue, R., Jensen, L.J., Shi, J., Morita, H., Nishida, M., Honda, A. and Ito, Y. 2006. Transient receptor potential channels in cardiovascular function and disease. *Circulation Research.* **99**(2),pp.119–131.
- Inoue, R., Okada, T., Onoue, H., Hara, Y., Shimizu, S., Naitoh, S., Ito, Y. and Mori, Y. 2001. The transient receptor potential protein homologue TRP6 is the essential component of vascular alpha(1)-adrenoceptor-activated Ca(2+)-permeable cation channel. *Circ Res.* **88**(3),pp.325–32.
- Iordanov, I., Mihalyi, C., Toth, B. and Csanady, L. 2016. The proposed channel-enzyme transient receptor potential melastatin 2 does not possess ADP ribose hydrolase activity. *Elife.* [Online]. **5**. Available from: ://WOS:000380856900001.
- Irizarry, M.C., McNamara, M., Fedorchak, K., Hsiao, K. and Hyman, B.T. 1997. APPSw transgenic mice develop age-related A beta deposits and neuropil abnormalities, but no neuronal loss in CA1. *J Neuropathol Exp Neurol.* **56**(9),pp.965–73.
- Ishii, M., Shimizu, S., Hagiwara, T., Wajima, T., Miyazaki, A., Mori, Y. and Kiuchi, Y. 2006. Extracellular-added ADP-ribose increases intracellular free Ca²⁺ concentration through Ca²⁺ release from stores, but not through TRPM2-mediated Ca²⁺ entry, in rat beta-cell line RIN-5F. *J Pharmacol Sci.* **101**(2),pp.174–8.
- Ishii, M., Shimizu, S., Hara, Y., Hagiwara, T., Miyazaki, A., Mori, Y. and Kiuchi, Y. 2006. Intracellular-produced hydroxyl radical mediates H₂O₂-induced Ca²⁺ influx and cell death in rat beta-cell line RIN-5F. *Cell Calcium.* **39**(6),pp.487–94.
- Ishimaru, Y., Inada, H., Kubota, M., Zhuang, H., Tominaga, M. and Matsunami, H. 2006. Transient receptor potential family members PKD1L3 and PKD2L1 form a candidate sour taste receptor. *Proc Natl Acad Sci U S A.* **103**(33),pp.12569–12574.
- Isogai, A., Lee, K., Mitsui, R. and Hashitani, H. 2016. Functional coupling of TRPV4 channels and BK channels in regulating spontaneous contractions of the guinea pig urinary bladder. *Pflugers Arch.* **468**(9),pp.1573–85.
- Iwata, Y., Katanosaka, Y., Arai, Y., Komamura, K., Miyatake, K. and Shigekawa, M. 2003. A novel mechanism of myocyte degeneration involving the Ca²⁺-permeable growth factor-regulated channel. *Journal of Cell Biology.* **161**(5),pp.957–967.
- Iyer, G.Y., Islam, M.F. and Quastel, J.H. 1961. BIOCHEMICAL ASPECTS OF PHAGOCYTOSIS. *Nature.* **192**(480),p.535-.

- Jankowsky, J.L., Xu, G., Fromholt, D., Gonzales, V. and Borchelt, D.R. 2003. Environmental enrichment exacerbates amyloid plaque formation in a transgenic mouse model of Alzheimer disease. *J Neuropathol Exp Neurol.* **62**(12),pp.1220–7.
- Jay, D.B., Papaharalambus, C.A., Seidel-Rogol, B., Dikalova, A.E., Lassegue, B. and Griendling, K.K. 2008. Nox5 mediates PDGF-induced proliferation in human aortic smooth muscle cells. *Free Radic Biol Med.* **45**(3),pp.329–35.
- Jekabsone, A., Mander, P.K., Tickler, A., Sharpe, M. and Brown, G.C. 2006. Fibrillar beta-amyloid peptide Abeta1-40 activates microglial proliferation via stimulating TNF-alpha release and H₂O₂ derived from NADPH oxidase: a cell culture study. *Journal of Neuroinflammation.* **3**,p.24.
- Jeong, H.-K., Jou, I. and Joe, E. 2010. Systemic LPS administration induces brain inflammation but not dopaminergic neuronal death in the substantia nigra. *Experimental & Molecular Medicine.* **42**(12),pp.823–832.
- Jiang, L.H., Yang, W., Zou, J. and Beech, D.J. 2010. TRPM2 channel properties, functions and therapeutic potentials. *Expert Opinion on Therapeutic Targets.* **14**(9),pp.973–988.
- Jung, S., Strotmann, R., Schultz, G. and Plant, T.D. 2002. TRPC6 is a candidate channel involved in receptor-stimulated cation currents in A7r5 smooth muscle cells. *Am J Physiol Cell Physiol.* **282**(2),pp.C347-59.
- Jungnickel, M.K., Marrero, H., Birnbaumer, L., Lemos, J.R. and Florman, H.M. 2001. Trp2 regulates entry of Ca²⁺ into mouse sperm triggered by egg ZP3. *Nat Cell Biol.* **3**(5),pp.499–502.
- Kalogeris, T., Bao, Y. and Korthuis, R.J. 2014. Mitochondrial reactive oxygen species: a double edged sword in ischemia/reperfusion vs preconditioning. *Redox Biol.* **2**,pp.702–14.
- Kamata, H. and Hirata, H. 1999. Redox regulation of cellular signalling. *Cellular Signalling.* **11**(1),pp.1–14.
- Kamizato, M., Nishida, K., Masuda, K., Takeo, K., Yamamoto, Y., Kawai, T., Teshima-Kondo, S., Tanahashi, T. and Rokutan, K. 2009. Interleukin 10 inhibits interferon gamma- and tumor necrosis factor alpha-stimulated activation of NADPH oxidase 1 in human colonic epithelial cells and the mouse colon. *J Gastroenterol.* **44**(12),pp.1172–84.
- Kaneko, S., Kawakami, S., Hara, Y., Wakamori, M., Itoh, E., Minami, T., Takada, Y., Kume, T., Katsuki, H., Mori, Y. and Akaike, A. 2006. A critical role of TRPM2 in neuronal cell death by hydrogen peroxide. *J Pharmacol Sci.* **101**(1),pp.66–76.
- Kanzaki, M. 1999. Molecular identification of a eukaryotic, stretch-activated nonselective cation channel (vol 285, pg 882, 1999). *Science.* **285**(5433),pp.1493–1493.
- Kanzaki, M., Zhang, Y.Q., Mashima, H., Li, L., Shibata, H. and Kojima, I. 1999. Translocation of a calcium-permeable cation channel induced by insulin-like growth factor-I. *Nature Cell Biology.* **1**(3),pp.165–170.

- Karacsonyi, C., Miguel, A.S. and Puertollano, R. 2007. Mucolipin-2 localizes to the Arf6-associated pathway and regulates recycling of GPI-APs. *Traffic*. **8**(10),pp.1404–14.
- Karathanassis, D., Stahelin, R.V., Bravo, J., Perisic, O., Pacold, C.M., Cho, W. and Williams, R.L. 2002. Binding of the PX domain of p47(phox) to phosphatidylinositol 3,4-bisphosphate and phosphatidic acid is masked by an intramolecular interaction. *EMBO J.* **21**(19),pp.5057–68.
- Kashiba, H., Uchida, Y., Takeda, D., Nishigori, A., Ueda, Y., Kuribayashi, K. and Ohshima, M. 2004. TRPV2-immunoreactive intrinsic neurons in the rat intestine. *Neuroscience Letters*. **366**(2),pp.193–196.
- Kashio, M., Sokabe, T., Shintaku, K., Uematsu, T., Fukuta, N., Kobayashi, N., Mori, Y. and Tominaga, M. 2012. Redox signal-mediated sensitization of transient receptor potential melastatin 2 (TRPM2) to temperature affects macrophage functions. *Proceedings of the National Academy of Sciences of the United States of America*. **109**(17),pp.6745–6750.
- Kashio, M. and Tominaga, M. 2015. Redox Signal-mediated Enhancement of the Temperature Sensitivity of Transient Receptor Potential Melastatin 2 (TRPM2) Elevates Glucose-induced Insulin Secretion from Pancreatic Islets. *Journal of Biological Chemistry*. **290**(19),pp.12435–12442.
- Katanosaka, Y., Iwasaki, K., Ujihara, Y., Takatsu, S., Nishitsuji, K., Kanagawa, M., Sudo, A., Toda, T., Katanosaka, K., Mohri, S. and Naruse, K. 2014. TRPV2 is critical for the maintenance of cardiac structure and function in mice. *Nature Communications*. [Online]. **5**. Available from: ://WOS:000337505100004.
- Katsuyama, M. 2010. NOX/NADPH oxidase, the superoxide-generating enzyme: its transcriptional regulation and physiological roles. *Journal of Pharmacological Sciences*. **114**(2),pp.134–146.
- Kauppinen, T.M., Higashi, Y., Suh, S.W., Escartin, C., Nagasawa, K. and Swanson, R.A. 2008. Zinc triggers microglial activation. *Journal of Neuroscience*. **28**(22),pp.5827–5835.
- Kauppinen, T.M., Suh, S.W., Higashi, Y., Berman, A.E., Escartin, C., Won, S.J., Wang, C., Cho, S.-H., Gan, L. and Swanson, R.A. 2011. Poly(ADP-ribose)polymerase-1 modulates microglial responses to amyloid beta. *Journal of Neuroinflammation*. [Online]. **8**. Available from: ://WOS:000298946200001.
- Kauppinen, T.M. and Swanson, R.A. 2005. Poly(ADP-ribose) polymerase-1 promotes microglial activation, proliferation, and matrix metalloproteinase-9-mediated neuron death. *Journal of Immunology*. **174**(4),pp.2288–2296.
- Keeney, P.M., Xie, J., Capaldi, R.A. and Bennett, J.P., Jr. 2006. Parkinson's disease brain mitochondrial complex I has oxidatively damaged subunits and is functionally impaired and misassembled. *J Neurosci*. **26**(19),pp.5256–64.
- Keller, S.A., Jones, J.M., Boyle, A., Barrow, L.L., Killen, P.D., Green, D.G., Kapousta, N.V., Hitchcock, P.F., Swank, R.T. and Meisler, M.H. 1994. Kidney and retinal defects (Krd), a transgene-induced mutation with a deletion of mouse chromosome 19 that includes the Pax2 locus. *Genomics*. **23**(2),pp.309–320.

- Kheradpezhouh, E., Barritt, G.J. and Rychkov, G.Y. 2016. Curcumin inhibits activation of TRPM2 channels in rat hepatocytes. *Redox Biol.* **7**, pp.1–7.
- Kheradpezhouh, E., Ma, L.L., Morphett, A., Barritt, G.J. and Rychkov, G.Y. 2014. TRPM2 channels mediate acetaminophen-induced liver damage. *Proc Natl Acad Sci U S A.* **111**(8), pp.3176–3181.
- Kikuchi, H., Hikage, M., Miyashita, H. and Fukumoto, M. 2000. NADPH oxidase subunit, gp91(phox) homologue, preferentially expressed in human colon epithelial cells. *Gene.* **254**(1–2), pp.237–43.
- Kim, H.J., Li, Q., Tjon-Kon-Sang, S., So, I., Kiselyov, K. and Muallem, S. 2007. Gain-of-function mutation in TRPML3 causes the mouse Varitint-Waddler phenotype. *J Biol Chem.* **282**(50), pp.36138–42.
- Kim, H.J., Li, Q., Tjon-Kon-Sang, S., So, I., Kiselyov, K., Soyombo, A.A. and Muallem, S. 2008. A novel mode of TRPML3 regulation by extracytosolic pH absent in the varitint-waddler phenotype. *EMBO J.* **27**(8), pp.1197–205.
- Kim, H.J., Soyombo, A.A., Tjon-Kon-Sang, S., So, I. and Muallem, S. 2009. The Ca(2+) channel TRPML3 regulates membrane trafficking and autophagy. *Traffic.* **10**(8), pp.1157–67.
- Kim, H.K., Park, S.K., Zhou, J.L., Taglialatela, G., Chung, K., Coggeshall, R.E. and Chung, J.M. 2004. Reactive oxygen species (ROS) play an important role in a rat model of neuropathic pain. *Pain.* **111**(1–2), pp.116–24.
- Kim, S.J., Kim, Y.S., Yuan, J.P., Petralia, R.S., Worley, P.F. and Linden, D.J. 2003. Activation of the TRPC1 cation channel by metabotropic glutamate receptor mGluR1. *Nature.* **426**(6964), pp.285–91.
- Kim, Y.H. and Koh, J.Y. 2002. The role of NADPH oxidase and neuronal nitric oxide synthase in zinc-induced poly(ADP-ribose) polymerase activation and cell death in cortical culture. *Experimental Neurology.* **177**(2), pp.407–418.
- Klose, C., Straub, I., Riehle, M., Ranta, F., Krautwurst, D., Ullrich, S., Meyerhof, W. and Harteneck, C. 2011. Fenamates as TRP channel blockers: mefenamic acid selectively blocks TRPM3. *British Journal of Pharmacology.* **162**(8), pp.1757–1769.
- Knaus, U.G., Morris, S., Dong, H.J., Chernoff, J. and Bokoch, G.M. 1995. Regulation of human leukocyte p21-activated kinases through G protein--coupled receptors. *Science (New York, N.Y.).* **269**(5221), pp.221–223.
- Knowles, H., Heizer, J.W., Li, Y., Chapman, K., Ogden, C.A., Andreasen, K., Shapland, E., Kucera, G., Mogan, J., Humann, J., Lenz, L.L., Morrison, A.D. and Perraud, A.L. 2011. Transient Receptor Potential Melastatin 2 (TRPM2) ion channel is required for innate immunity against *Listeria monocytogenes*. *Proceedings of the National Academy of Sciences of the United States of America.* **108**(28), pp.11578–11583.
- Koga, H., Terasawa, H., Nunoi, H., Takeshige, K., Inagaki, F. and Sumimoto, H. 1999. Tetratricopeptide repeat (TPR) motifs of p67(phox) participate in interaction

- with the small GTPase Rac and activation of the phagocyte NADPH oxidase. *J Biol Chem.* **274**(35),pp.25051–60.
- Koh, J.-Y. 2005. Endogenous Zinc in Neurological Diseases. *Journal of Clinical Neurology.* **1**(2),p.121.
- Koh, J.Y. 2001. Zinc and disease of the brain. *Molecular Neurobiology.* **24**(1–3),pp.99–106.
- Koh, J.Y., Suh, S.W., Gwag, B.J., He, Y.Y., Hsu, C.Y. and Choi, D.W. 1996. The role of zinc in selective neuronal death after transient global cerebral ischemia. *Science.* **272**(5264),pp.1013–1016.
- Koike, C., Obara, T., Uriu, Y., Numata, T., Sanuki, R., Miyata, K., Koyasu, T., Ueno, S., Funabiki, K., Tani, A., Ueda, H., Kondo, M., Mori, Y., Tachibana, M. and Furukawa, T. 2010. TRPM1 is a component of the retinal ON bipolar cell transduction channel in the mGluR6 cascade. *Proc Natl Acad Sci U S A.* **107**(1),pp.332–337.
- Kolisek, M., Beck, A., Fleig, A. and Penner, R. 2005. Cyclic ADP-ribose and hydrogen peroxide synergize with ADP-ribose in the activation of TRPM2 channels. *Mol Cell.* **18**(1),pp.61–9.
- Konrad, R.J., Jolly, Y.C., Major, C. and Wolf, B.A. 1992. Inhibition of phospholipase A2 and insulin secretion in pancreatic islets. *Biochimica Et Biophysica Acta.* **1135**(2),pp.215–220.
- Konstantinov, A.A., Peskin, A.V., Popova, E., Khomutov, G.B. and Ruuge, E.K. 1987. Superoxide generation by the respiratory chain of tumor mitochondria. *Biochim Biophys Acta.* **894**(1),pp.1–10.
- Korshunov, S.S., Skulachev, V.P. and Starkov, A.A. 1997. High protonic potential actuates a mechanism of production of reactive oxygen species in mitochondria. *FEBS Lett.* **416**(1),pp.15–8.
- Kottgen, M. 2007. TRPP2 and autosomal dominant polycystic kidney disease. *Biochim Biophys Acta.* **1772**(8),pp.836–50.
- Kottgen, M., Hofherr, A., Li, W., Chu, K., Cook, S., Montell, C. and Watnick, T. 2011. Drosophila sperm swim backwards in the female reproductive tract and are activated via TRPP2 ion channels. *Plos One.* **6**(5),p.e20031.
- Koulen, P., Cai, Y., Geng, L., Maeda, Y., Nishimura, S., Witzgall, R., Ehrlich, B.E. and Somlo, S. 2002. Polycystin-2 is an intracellular calcium release channel. *Nat Cell Biol.* **4**(3),pp.191–7.
- Krabbe, G., Minami, S.S., Etchegaray, J.I., Taneja, P., Djukic, B., Davalos, D., Le, D., Lo, I., Zhan, L., Reichert, M.C., Sayed, F., Merlini, M., Ward, M.E., Perry, D.C., Lee, S.E., Sias, A., Parkhurst, C.N., Gan, W., Akassoglou, K., Miller, B.L., Farese, R.V. and Gan, L. 2017. Microglial NF κ B-TNF α hyperactivation induces obsessive-compulsive behavior in mouse models of progranulin-deficient frontotemporal dementia. *Proceedings of the National Academy of Sciences.* **114**(19),pp.5029–5034.

- Kraft, R., Grimm, C., Frenzel, H. and Harteneck, C. 2006. Inhibition of TRPM2 cation channels by N-(p-amylcinnamoyl)anthranilic acid. *Br J Pharmacol.* **148**(3),pp.264–73.
- Kraft, R., Grimm, C., Grosse, K., Hoffmann, A., Sauerbruch, S., Kettenmann, H., Schultz, G. and Harteneck, C. 2004. Hydrogen peroxide and ADP-ribose induce TRPM2-mediated calcium influx and cation currents in microglia. *American Journal of Physiology-Cell Physiology.* **286**(1),pp.C129–C137.
- Kudin, A.P., Bimpang-Buta, N.Y., Vielhaber, S., Elger, C.E. and Kunz, W.S. 2004. Characterization of superoxide-producing sites in isolated brain mitochondria. *J Biol Chem.* **279**(6),pp.4127–35.
- Kuhn, F.J., Knop, G. and Luckhoff, A. 2007. The transmembrane segment S6 determines cation versus anion selectivity of TRPM2 and TRPM8. *J Biol Chem.* **282**(38),pp.27598–609.
- Kuhn, F.J., Kuhn, C., Naziroglu, M. and Luckhoff, A. 2009. Role of an N-terminal splice segment in the activation of the cation channel TRPM2 by ADP-ribose and hydrogen peroxide. *Neurochem Res.* **34**(2),pp.227–33.
- Kuhn, F.J. and Luckhoff, A. 2004. Sites of the NUDT9-H domain critical for ADP-ribose activation of the cation channel TRPM2. *J Biol Chem.* **279**(45),pp.46431–7.
- Kuhn, F.J.P., Kuhn, C. and Luckhoff, A. 2015. Functional Characterisation of a TRPM2 orthologue from the sea anemone *Nematostella vectensis* in human cells. *Scientific Reports.* [Online]. **5**. Available from: ://WOS:000348291800019.
- Kumar, A., Majhi, R.K., Swain, N., Giri, S.C., Kar, S., Samanta, L. and Goswami, C. 2016. TRPV4 is endogenously expressed in vertebrate spermatozoa and regulates intracellular calcium in human sperm. *Biochem Biophys Res Commun.* **473**(4),pp.781–788.
- Kumar, M.J., Nicholls, D.G. and Andersen, J.K. 2003. Oxidative alpha-ketoglutarate dehydrogenase inhibition via subtle elevations in monoamine oxidase B levels results in loss of spare respiratory capacity: implications for Parkinson's disease. *J Biol Chem.* **278**(47),pp.46432–9.
- Kuno, R., Wang, J., Kawanokuchi, J., Takeuchi, H., Mizuno, T. and Suzumura, A. 2005. Autocrine activation of microglia by tumor necrosis factor-alpha. *J Neuroimmunol.* **162**(1–2),pp.89–96.
- Kurashina, T., Dezaki, K., Yoshida, M., Sukma Rita, R., Ito, K., Taguchi, M., Miura, R., Tominaga, M., Ishibashi, S., Kakei, M. and Yada, T. 2015. The β-cell GHSR and downstream cAMP/TRPM2 signaling account for insulinostatic and glycemic effects of ghrelin. *Scientific Reports.* [Online]. **5**(1). [Accessed 1 September 2017]. Available from: <http://www.nature.com/articles/srep14041>.
- Kurkowska-Jastrzebska, I., Wronska, A., Kohutnicka, M., Czlonkowski, A. and Czlonkowska, A. 1999. The inflammatory reaction following 1-methyl-4-phenyl-1,2,3, 6-tetrahydropyridine intoxication in mouse. *Exp Neurol.* **156**(1),pp.50–61.

- Kushnareva, Y., Murphy, A.N. and Andreyev, A. 2002. Complex I-mediated reactive oxygen species generation: modulation by cytochrome c and NAD(P)+ oxidation-reduction state. *The Biochemical Journal*. **368**(Pt 2),pp.545–553.
- Kussmaul, L. and Hirst, J. 2006. The mechanism of superoxide production by NADH:ubiquinone oxidoreductase (complex I) from bovine heart mitochondria. *Proceedings of the National Academy of Sciences of the United States of America*. **103**(20),pp.7607–7612.
- Kwan, H.Y., Huang, Y. and Yao, X. 2007. TRP channels in endothelial function and dysfunction. *Biochim Biophys Acta*. **1772**(8),pp.907–14.
- Lambertsen, K.L., Biber, K. and Finsen, B. 2012. Inflammatory Cytokines in Experimental and Human Stroke. *Journal of Cerebral Blood Flow & Metabolism*. **32**(9),pp.1677–1698.
- Lander, H.M. 1997. An essential role for free radicals and derived species in signal transduction. *Faseb Journal*. **11**(2),pp.118–124.
- Lange, I., Penner, R., Fleig, A. and Beck, A. 2008. Synergistic regulation of endogenous TRPM2 channels by adenine dinucleotides in primary human neutrophils. *Cell Calcium*. **44**(6),pp.604–615.
- Lange, I., Yamamoto, S., Partida-Sanchez, S., Mori, Y., Fleig, A. and Penner, R. 2009. TRPM2 Functions as a Lysosomal Ca²⁺-Release Channel in beta Cells. *Science Signaling*. [Online]. **2**(71). Available from: ://WOS:000275474700004.
- Lapouge, K., Smith, S.J., Walker, P.A., Gamblin, S.J., Smerdon, S.J. and Rittinger, K. 2000. Structure of the TPR domain of p67phox in complex with Rac.GTP. *Mol Cell*. **6**(4),pp.899–907.
- Larson, A.M., Polson, J., Fontana, R.J., Davern, T.J., Lalani, E., Hynan, L.S., Reisch, J.S., Schiodt, F.V., Ostapowicz, G., Shakil, A.O., Lee, W.M. and Acute Liver Failure Study, G. 2005. Acetaminophen-induced acute liver failure: results of a United States multicenter, prospective study. *Hepatology*. **42**(6),pp.1364–72.
- Launay, P., Fleig, A., Perraud, A.L., Scharenberg, A.M., Penner, R. and Kinet, J.P. 2002. TRPM4 is a Ca²⁺-activated nonselective cation channel mediating cell membrane depolarization. *Cell*. **109**(3),pp.397–407.
- Lee, C.R., Machold, R.P., Witkovsky, P. and Rice, M.E. 2013. TRPM2 channels are required for NMDA-induced burst firing and contribute to H₂O₂-dependent modulation in substantia nigra pars reticulata GABAergic neurons. *J Neurosci*. **33**(3),pp.1157–68.
- Lee, J., Cha, S.-K., Sun, T.-J. and Huang, C.-L. 2005. PIP2 activates TRPV5 and releases its inhibition by intracellular Mg²⁺. *The Journal of General Physiology*. **126**(5),pp.439–451.
- Lee, J.K., Tran, T. and Tansey, M.G. 2009. Neuroinflammation in Parkinson's disease. *J Neuroimmune Pharmacol*. **4**(4),pp.419–29.

- Lee, M., Cho, T., Jantaratnotai, N., Wang, Y.T., McGeer, E. and McGeer, P.L. 2010. Depletion of GSH in glial cells induces neurotoxicity: relevance to aging and degenerative neurological diseases. *Faseb Journal*. **24**(7),pp.2533–2545.
- Leech, C.A., Dzhura, I., Chepurny, O.G., Schwede, F., Genieser, H.-G. and Holz, G.G. 2010. Facilitation of β -cell K(ATP) channel sulfonylurea sensitivity by a cAMP analog selective for the cAMP-regulated guanine nucleotide exchange factor Epac. *Islets*. **2**(2),pp.72–81.
- Lepage, P.K., Lussier, M.P., Barajas-Martinez, H., Bousquet, S.M., Blanchard, A.P., Francoeur, N., Dumaine, R. and Boulay, G. 2006. Identification of two domains involved in the assembly of transient receptor potential canonical channels. *J Biol Chem*. **281**(41),pp.30356–64.
- Leto, T.L., Adams, A.G. and de Mendez, I. 1994. Assembly of the phagocyte NADPH oxidase: binding of Src homology 3 domains to proline-rich targets. *Proc Natl Acad Sci U S A*. **91**(22),pp.10650–4.
- Lev, S., Moreno, H., Martinez, R., Canoll, P., Peles, E., Musacchio, J.M., Plowman, G.D., Rudy, B. and Schlessinger, J. 1995. PROTEIN-TYROSINE KINASE PYK2 INVOLVED IN CA₂₊-INDUCED REGULATION OF ION-CHANNEL AND MAP KINASE FUNCTIONS. *Nature*. **376**(6543),pp.737–745.
- Lewis, E.M., Sergeant, S., Ledford, B., Stull, N., Dinauer, M.C. and McPhail, L.C. 2010. Phosphorylation of p22phox on threonine 147 enhances NADPH oxidase activity by promoting p47phox binding. *The Journal of Biological Chemistry*. **285**(5),pp.2959–2967.
- Li, C.K., Meng, L., Li, X., Li, D.L. and Jiang, L.H. 2015. Non-NMDAR neuronal Ca₂₊-permeable channels in delayed neuronal death and as potential therapeutic targets for ischemic brain damage. *Expert Opinion on Therapeutic Targets*. **19**(7),pp.879–892.
- Li, F., Abuarab, N. and Sivaprasadarao, A. 2016. Reciprocal regulation of actin cytoskeleton remodelling and cell migration by Ca₂₊ and Zn₂₊: role of TRPM2 channels. *J Cell Sci*. **129**(10),pp.2016–29.
- Li, J.M., Fan, L.M., Christie, M.R. and Shah, A.M. 2005. Acute tumor necrosis factor alpha signaling via NADPH oxidase in microvascular endothelial cells: role of p47phox phosphorylation and binding to TRAF4. *Mol Cell Biol*. **25**(6),pp.2320–30.
- Li, M., Jiang, J. and Yue, L. 2006. Functional characterization of homo- and heteromeric channel kinases TRPM6 and TRPM7. *J Gen Physiol*. **127**(5),pp.525–37.
- Li, Q., Liu, Y., Zhao, W. and Chen, X.Z. 2002. The calcium-binding EF-hand in polycystin-L is not a domain for channel activation and ensuing inactivation. *FEBS Lett*. **516**(1–3),pp.270–8.
- Liao, M.F., Cao, E.H., Julius, D. and Cheng, Y.F. 2013. Structure of the TRPV1 ion channel determined by electron cryo-microscopy. *Nature*. **504**(7478),p.107–.

- Liedtke, W., Choe, Y., Marti-Renom, M.A., Bell, A.M., Denis, C.S., Sali, A., Hudspeth, A.J., Friedman, J.M. and Heller, S. 2000. Vanilloid receptor-related osmotically activated channel (VR-OAC), a candidate vertebrate osmoreceptor. *Cell*. **103**(3),pp.525–35.
- Lievremont, J.-P., Bird, G.S. and Putney, J.W. 2005. Mechanism of inhibition of TRPC cation channels by 2-aminoethoxydiphenylborane. *Molecular Pharmacology*. **68**(3),pp.758–762.
- Lièvremont, J.-P., Bird, G.S.J. and Putney, J.W. 2004. Canonical transient receptor potential TRPC7 can function as both a receptor- and store-operated channel in HEK-293 cells. *American Journal of Physiology. Cell Physiology*. **287**(6),pp.C1709-1716.
- Liman, E.R. 2010. A TRP channel contributes to insulin secretion by pancreatic beta-cells. *Islets*. **2**(5),pp.331–333.
- Liman, E.R. 2007. TRPM5 and taste transduction. *Handbook of Experimental Pharmacology*. (179),pp.287–298.
- Liman, E.R., Corey, D.P. and Dulac, C. 1999. TRP2: a candidate transduction channel for mammalian pheromone sensory signaling. *Proceedings of the National Academy of Sciences of the United States of America*. **96**(10),pp.5791–5796.
- Liou, G.Y. and Storz, P. 2010. Reactive oxygen species in cancer. *Free Radic Res.* **44**(5),pp.479–96.
- Lista, S., O'Bryant, S.E., Blennow, K., Dubois, B., Hugon, J., Zetterberg, H. and Hampel, H. 2015. Biomarkers in Sporadic and Familial Alzheimer's Disease. *J Alzheimers Dis*. **47**(2),pp.291–317.
- Liu, B. and Hong, J.S. 2003. Role of microglia in inflammation-mediated neurodegenerative diseases: mechanisms and strategies for therapeutic intervention. *J Pharmacol Exp Ther*. **304**(1),pp.1–7.
- Liu, D. and Liman, E.R. 2003. Intracellular Call and the phospholipid PIP2 regulate the taste transduction ion channel TRPM5. *Proc Natl Acad Sci U S A*. **100**(25),pp.15160–15165.
- Liu, L., Zhu, W., Zhang, Z.-S., Yang, T., Grant, A., Oxford, G. and Simon, S.A. 2004. Nicotine inhibits voltage-dependent sodium channels and sensitizes vanilloid receptors. *Journal of Neurophysiology*. **91**(4),pp.1482–1491.
- Liu, Y.Y. and Bian, J.S. 2010. Hydrogen sulfide protects amyloid-beta induced cell toxicity in microglia. *J Alzheimers Dis*. **22**(4),pp.1189–200.
- Liu, Z., Wu, H., Wei, Z., Wang, X., Shen, P., Wang, S., Wang, A., Chen, W. and Lu, Y. 2016. TRPM8: a potential target for cancer treatment. *J Cancer Res Clin Oncol*. **142**(9),pp.1871–81.
- Lockwich, T., Singh, B.B., Liu, X.B. and Ambudkar, I.S. 2001. Stabilization of cortical actin induces internalization of transient receptor potential 3 (Trp3)-associated caveolar Ca²⁺ signaling complex and loss of Ca²⁺ influx without disruption of

- Trp3-inositol trisphosphate receptor association. *Journal of Biological Chemistry.* **276**(45),pp.42401–42408.
- LopezJimenez, N.D., Cavenagh, M.M., Sainz, E., Cruz-Ithier, M.A., Battey, J.F. and Sullivan, S.L. 2006. Two members of the TRPP family of ion channels, Pkd1l3 and Pkd2l1, are co-expressed in a subset of taste receptor cells. *Journal of Neurochemistry.* **98**(1),pp.68–77.
- Lorenzo, I.M., Liedtke, W., Sanderson, M.J. and Valverde, M.A. 2008. TRPV4 channel participates in receptor-operated calcium entry and ciliary beat frequency regulation in mouse airway epithelial cells. *Proceedings of the National Academy of Sciences of the United States of America.* **105**(34),pp.12611–12616.
- Lores Arnaiz, S., Llesuy, S., Cutrin, J.C. and Boveris, A. 1995. Oxidative stress by acute acetaminophen administration in mouse liver. *Free Radic Biol Med.* **19**(3),pp.303–10.
- Loschen, G., Azzi, A., Richter, C. and Flohe, L. 1974. Superoxide radicals as precursors of mitochondrial hydrogen peroxide. *FEBS Lett.* **42**(1),pp.68–72.
- Lounsbury, K.M., Hu, Q. and Ziegelstein, R.C. 2000. Calcium signaling and oxidant stress in the vasculature. *Free Radic Biol Med.* **28**(9),pp.1362–9.
- Lubisch W., Grandel R., Kock M., Mueller R., Hoeger T., Schult S. New azepinoindole derivatives are PARP inhibitors – useful for the treatment of e.g. stroke, Alzheimer's, Parkinson's or Huntington's disease, epilepsy, kidney damage, acute myocardial infarction, tumors, tumor metastasis, sepsis and ARDS 2001(DE10039610-A1), Patent
- Lucas, P., Ukhanov, K., Leinders-Zufall, T. and Zufall, F. 2003. A diacylglycerol-gated cation channel in vomeronasal neuron dendrites is impaired in TRPC2 mutant mice: mechanism of pheromone transduction. *Neuron.* **40**(3),pp.551–61.
- Lund, F., Solvason, N., Grimaldi, J.C., Parkhouse, R.M. and Howard, M. 1995. Murine CD38: an immunoregulatory ectoenzyme. *Immunology Today.* **16**(10),pp.469–473.
- Lund, F.E. 2006. Signaling properties of CD38 in the mouse immune system: enzyme-dependent and -independent roles in immunity. *Molecular Medicine (Cambridge, Mass.).* **12**(11–12),pp.328–333.
- Ma, H.T., Venkatachalam, K., Parys, J.B. and Gill, D.L. 2002. Modification of store-operated channel coupling and inositol trisphosphate receptor function by 2-aminoethoxydiphenyl borate in DT40 lymphocytes. *J Biol Chem.* **277**(9),pp.6915–22.
- MacEwan, D.J. 2002. TNF receptor subtype signalling: differences and cellular consequences. *Cell Signal.* **14**(6),pp.477–92.
- Macpherson, L.J., Geierstanger, B.H., Viswanath, V., Bandell, M., Eid, S.R., Hwang, S. and Patapoutian, A. 2005. The pungency of garlic: Activation of TRPA1 and TRPV1 in response to allicin. *Current Biology.* **15**(10),pp.929–934.

- Malavasi, F., Deaglio, S., Ferrero, E., Funaro, A., Sancho, J., Ausiello, C.M., Ortolan, E., Vaisitti, T., Zubiaur, M., Fedele, G., Aydin, S., Tibaldi, E.V., Durelli, I., Lusso, R., Cozno, F. and Horenstein, A.L. 2006. CD38 and CD157 as receptors of the immune system: a bridge between innate and adaptive immunity. *Molecular Medicine (Cambridge, Mass.).* **12**(11–12),pp.334–341.
- Mander, P. and Brown, G.C. 2005. Activation of microglial NADPH oxidase is synergistic with glial iNOS expression in inducing neuronal death: a dual-key mechanism of inflammatory neurodegeneration. *Journal of Neuroinflammation.* **2**,p.20.
- Mander, P.K., Jekabsone, A. and Brown, G.C. 2006. Microglia proliferation is regulated by hydrogen peroxide from NADPH oxidase. *Journal of Immunology (Baltimore, Md.: 1950).* **176**(2),pp.1046–1052.
- Marin-Teva, J.L., Dusart, I., Colin, C., Gervais, A., van Rooijen, N. and Mallat, M. 2004. Microglia promote the death of developing Purkinje cells. *Neuron.* **41**(4),pp.535–47.
- Maroto, R., Raso, A., Wood, T.G., Kurosky, A., Martinac, B. and Hamill, O.P. 2005. TRPC1 forms the stretch-activated cation channel in vertebrate cells. *Nature Cell Biology.* **7**(2),pp.179-U99.
- Martinez, M.C. and Andriantsitohaina, R. 2009. Reactive Nitrogen Species: Molecular Mechanisms and Potential Significance in Health and Disease. *Antioxidants & Redox Signaling.* **11**(3),pp.669–702.
- Martins, A.S., Shkryl, V.M., Nowycky, M.C. and Shirokova, N. 2008. Reactive oxygen species contribute to Ca²⁺ signals produced by osmotic stress in mouse skeletal muscle fibres. *The Journal of Physiology.* **586**(1),pp.197–210.
- Matsushita, M., Kozak, J.A., Shimizu, Y., McLachlin, D.T., Yamaguchi, H., Wei, F.Y., Tomizawa, K., Matsui, H., Chait, B.T., Cahalan, M.D. and Nairn, A.C. 2005. Channel function is dissociated from the intrinsic kinase activity and autophosphorylation of TRPM7/ChaK1. *J Biol Chem.* **280**(21),pp.20793–803.
- Maurel, A., Hernandez, C., Kunduzova, O., Bompard, G., Cambon, C., Parini, A. and Frances, B. 2003. Age-dependent increase in hydrogen peroxide production by cardiac monoamine oxidase A in rats. *Am J Physiol Heart Circ Physiol.* **284**(4),pp.H1460-7.
- McCoy, M.K. and Tansey, M.G. 2008. TNF signaling inhibition in the CNS: implications for normal brain function and neurodegenerative disease. *Journal of Neuroinflammation.* **5**(1),p.45.
- McGeer, P.L. and McGeer, E.G. 2008. Glial reactions in Parkinson's disease. *Mov Disord.* **23**(4),pp.474–83.
- McHugh, D., Flemming, R., Xu, S.-Z., Perraud, A.-L. and Beech, D.J. 2003. Critical intracellular Ca²⁺ dependence of transient receptor potential melastatin 2 (TRPM2) cation channel activation. *The Journal of Biological Chemistry.* **278**(13),pp.11002–11006.

- McKemy, D.D. 2005. How cold is it? TRPM8 and TRPA1 in the molecular logic of cold sensation. *Molecular Pain*. [Online]. **1**. Available from: ://WOS:000202941000001.
- McKemy, D.D., Neuhausser, W.M. and Julius, D. 2002. Identification of a cold receptor reveals a general role for TRP channels in thermosensation. *Nature*. **416**(6876),pp.52–8.
- McLennan, H.R. and Degli Esposti, M. 2000. The contribution of mitochondrial respiratory complexes to the production of reactive oxygen species. *J Bioenerg Biomembr*. **32**(2),pp.153–62.
- Meda, L., Cassatella, M.A., Szendrei, G.I., Ottos, L., Baron, P., Villalba, M., Ferrari, D. and Rossi, F. 1995. Activation of microglial cells by beta-amyloid protein and interferon-gamma. *Nature*. **374**(6523),pp.647–650.
- Mederos y Schnitzler, M., Waring, J., Gudermann, T. and Chubanov, V. 2008. Evolutionary determinants of divergent calcium selectivity of TRPM channels. *FASEB J*. **22**(5),pp.1540–51.
- Mei, Z.Z., Mao, H.J. and Jiang, L.H. 2006. Conserved cysteine residues in the pore region are obligatory for human TRPM2 channel function. *American Journal of Physiology-Cell Physiology*. **291**(5),pp.C1022–C1028.
- Meier, B., Radeke, H.H., Selle, S., Younes, M., Sies, H., Resch, K. and Habermehl, G.G. 1989. Human fibroblasts release reactive oxygen species in response to interleukin-1 or tumour necrosis factor-alpha. *The Biochemical Journal*. **263**(2),pp.539–545.
- de Mendez, I., Homayounpour, N. and Leto, T.L. 1997. Specificity of p47phox SH3 domain interactions in NADPH oxidase assembly and activation. *Mol Cell Biol*. **17**(4),pp.2177–85.
- Miller, B.A. 2004. Inhibition of TRPM2 function by PARP inhibitors protects cells from oxidative stress-induced death. *British Journal of Pharmacology*. **143**(5),pp.515–516.
- Miller, B.A., Wang, J., Hirschler-Laszkiewicz, I., Gao, E., Song, J., Zhang, X.-Q., Koch, W.J., Madesh, M., Mallilankaraman, K., Gu, T., Chen, S., Keefer, K., Conrad, K., Feldman, A.M. and Cheung, J.Y. 2013. The second member of transient receptor potential-melastatin channel family protects hearts from ischemia-reperfusion injury. *American Journal of Physiology. Heart and Circulatory Physiology*. **304**(7),pp.H1010-1022.
- Min, K.J., Pyo, H.K., Yang, M.S., Ji, K.A., Jou, I. and Joe, E.H. 2004. Gangliosides activate microglia via protein kinase C and NADPH oxidase. *Glia*. **48**(3),pp.197–206.
- Minke, B., Wu, C. and Pak, W.L. 1975. Induction of photoreceptor voltage noise in the dark in Drosophila mutant. *Nature*. **258**(5530),pp.84–7.
- Mitchell, J.R., Jollow, D.J., Potter, W.Z., Davis, D.C., Gillette, J.R. and Brodie, B.B. 1973. Acetaminophen-induced hepatic necrosis. I. Role of drug metabolism. *J Pharmacol Exp Ther*. **187**(1),pp.185–94.

- Miwa, S., St-Pierre, J., Partridge, L. and Brand, M.D. 2003. Superoxide and hydrogen peroxide production by Drosophila mitochondria. *Free Radical Biology & Medicine*. **35**(8),pp.938–948.
- Miyake, T., Shirakawa, H., Kusano, A., Sakimoto, S., Konno, M., Nakagawa, T., Mori, Y. and Kaneko, S. 2014. TRPM2 contributes to LPS/IFN gamma-induced production of nitric oxide via the p38/JNK pathway in microglia. *Biochem Biophys Res Commun*. **444**(2),pp.212–217.
- Mizuno, Y., Ohta, S., Tanaka, M., Takamiya, S., Suzuki, K., Sato, T., Oya, H., Ozawa, T. and Kagawa, Y. 1989. Deficiencies in complex I subunits of the respiratory chain in Parkinson's disease. *Biochem Biophys Res Commun*. **163**(3),pp.1450–5.
- Mochizuki, T., Wu, G.Q., Hayashi, T., Xenophontos, S.L., Veldhuisen, B., Saris, J.J., Reynolds, D.M., Cai, Y.Q., Gabow, P.A., Pierides, A., Kimberling, W.J., Breuning, M.H., Deltas, C.C., Peters, D.J.M. and Somlo, S. 1996. PKD2, a gene for polycystic kidney disease that encodes an integral membrane protein. *Science*. **272**(5266),pp.1339–1342.
- Moe, K.T., Aulia, S., Jiang, F., Chua, Y.L., Koh, T.H., Wong, M.C. and Dusting, G.J. 2006. Differential upregulation of Nox homologues of NADPH oxidase by tumor necrosis factor-alpha in human aortic smooth muscle and embryonic kidney cells. *Journal of Cellular and Molecular Medicine*. **10**(1),pp.231–239.
- Mogi, M., Harada, M., Riederer, P., Narabayashi, H., Fujita, K. and Nagatsu, T. 1994. Tumor necrosis factor-alpha (TNF-alpha) increases both in the brain and in the cerebrospinal fluid from parkinsonian patients. *Neurosci Lett*. **165**(1–2),pp.208–10.
- Monsonego, A. and Weiner, H.L. 2003. Immunotherapeutic approaches to Alzheimer's disease. *Science (New York, N.Y.)*. **302**(5646),pp.834–838.
- Montell, C. 2005. The TRP superfamily of cation channels. *Sci STKE*. **2005**(272),p.re3.
- Montell, C., Birnbaumer, L., Flockerzi, V., Bindels, R.J., Brudorf, E.A., Caterina, M.J., Clapham, D.E., Harteneck, C., Heller, S., Julius, D., Kojima, I., Mori, Y., Penner, R., Prawitt, D., Scharenberg, A.M., Schultz, G., Shimizu, N. and Zhu, M.X. 2002. A unified nomenclature for the superfamily of TRP cation channels. *Molecular Cell*. **9**(2),pp.229–231.
- Montell, C. and Rubin, G.M. 1989. MOLECULAR CHARACTERIZATION OF THE DROSOPHILA TRP LOCUS - A PUTATIVE INTEGRAL MEMBRANE-PROTEIN REQUIRED FOR PHOTOTRANSDUCTION. *Neuron*. **2**(4),pp.1313–1323.
- Montgomery, S.L., Mastrangelo, M.A., Habib, D., Narrow, W.C., Knowlden, S.A., Wright, T.W. and Bowers, W.J. 2011. Ablation of TNF-RI/RII expression in Alzheimer's disease mice leads to an unexpected enhancement of pathology: implications for chronic pan-TNF- α suppressive therapeutic strategies in the brain. *The American Journal of Pathology*. **179**(4),pp.2053–2070.
- Montgomery, S.L., Narrow, W.C., Mastrangelo, M.A., Olschowka, J.A., O'Banion, M.K. and Bowers, W.J. 2013. Chronic Neuron- and Age-Selective Down-Regulation of TNF Receptor Expression in Triple-Transgenic Alzheimer

- Disease Mice Leads to Significant Modulation of Amyloid- and Tau-Related Pathologies. *The American Journal of Pathology*. **182**(6),pp.2285–2297.
- Moqrich, A., Hwang, S.W., Earley, T.J., Petrus, M.J., Murray, A.N., Spencer, K.S.R., Andahazy, M., Story, G.M. and Patapoutian, A. 2005. Impaired thermosensation in mice lacking TRPV3, a heat and camphor sensor in the skin. *Science*. **307**(5714),pp.1468–1472.
- Morgan, M.J. and Liu, Z.G. 2011. Crosstalk of reactive oxygen species and NF-kappaB signaling. *Cell Res*. **21**(1),pp.103–15.
- Mori, Y., Wakamori, M., Miyakawa, T., Hermosura, M., Hara, Y., Nishida, M., Hirose, K., Mizushima, A., Kurosaki, M., Mori, E., Gotoh, K., Okada, T., Fleig, A., Penner, R., Iino, M. and Kurosaki, T. 2002. Transient receptor potential 1 regulates capacitative Ca²⁺ entry and Ca²⁺ release from endoplasmic reticulum in B lymphocytes. *J Exp Med*. **195**(6),pp.673–81.
- Mortadza, S.A.S., Wang, L., Li, D.L. and Jiang, L.H. 2015. TRPM2 channel-mediated ROS-sensitive Ca²⁺ signaling mechanisms in immune cells. *Frontiers in Immunology*. [Online]. **6**. Available from: ://WOS:000359471400001.
- Mortadza, S.S., Sim, J.A., Stacey, M. and Jiang, L.H. 2017. Signalling mechanisms mediating Zn²⁺-induced TRPM2 channel activation and cell death in microglial cells. *Sci Rep*. **7**,p.45032.
- Motterlini, R. and Foresti, R. 2014. Heme oxygenase-1 as a target for drug discovery. *Antioxidants & Redox Signaling*. **20**(11),pp.1810–1826.
- Mucke, L. and Selkoe, D.J. 2012. Neurotoxicity of amyloid beta-protein: synaptic and network dysfunction. *Cold Spring Harb Perspect Med*. **2**(7),p.a006338.
- Mukerji, G., Yianguo, Y., Corcoran, S.L., Selmer, I.S., Smith, G.D., Benham, C.D., Bountra, C., Agarwal, S.K. and Anand, P. 2006. Cool and menthol receptor TRPM8 in human urinary bladder disorders and clinical correlations. *BMC Urol*. **6**,p.6.
- Munoz, F.M., Gao, R., Tian, Y., Henstenburg, B.A., Barrett, J.E. and Hu, H. 2017. Neuronal P2X7 receptor-induced reactive oxygen species production contributes to nociceptive behavior in mice. *Sci Rep*. **7**(1),p.3539.
- Munsch, T., Freichel, M., Flockerzi, V. and Pape, H.C. 2003. Contribution of transient receptor potential channels to the control of GABA release from dendrites. *Proc Natl Acad Sci U S A*. **100**(26),pp.16065–70.
- Muraki, K., Iwata, Y., Katanosaka, Y., Ito, T., Ohya, S., Shigekawa, M. and Imaizumi, Y. 2003. TRPV2 is a component of osmotically sensitive cation channels in murine aortic myocytes. *Circulation Research*. **93**(9),pp.829–838.
- Murphy, M.P. 2009. How mitochondria produce reactive oxygen species. *The Biochemical Journal*. **417**(1),pp.1–13.
- Murphy, M.P. and LeVine, H., 3rd 2010. Alzheimer's disease and the amyloid-beta peptide. *J Alzheimers Dis*. **19**(1),pp.311–23.

- Nagamine, K., Kudoh, J., Minoshima, S., Kawasaki, K., Asakawa, S., Ito, F. and Shimizu, N. 1998. Molecular cloning of a novel putative Ca²⁺ channel protein (TRPC7) highly expressed in brain. *Genomics*. **54**(1),pp.124–31.
- Nagata, K., Duggan, A., Kumar, G. and Garcia-Anoveros, J. 2005. Nociceptor and hair cell transducer properties of TRPA1, a channel for pain and hearing. *J Neurosci*. **25**(16),pp.4052–61.
- Nagata, K., Zheng, L., Madathany, T., Castiglioni, A.J., Bartles, J.R. and Garcia-Anoveros, J. 2008. The varitint-waddler (Va) deafness mutation in TRPML3 generates constitutive, inward rectifying currents and causes cell degeneration. *Proc Natl Acad Sci U S A*. **105**(1),pp.353–8.
- Nagatsu, T. and Sawada, M. 2007. Biochemistry of postmortem brains in Parkinson's disease: historical overview and future prospects. *J Neural Transm Suppl*. (72),pp.113–20.
- Nakabo, Y. and Pabst, M.J. 1996. Lysis of leukemic cells by human macrophages: inhibition by 4-(2-aminoethyl)-benzenesulfonyl fluoride (AEBSF), a serine protease inhibitor. *J Leukoc Biol*. **60**(3),pp.328–36.
- Nakamura, Y., Si, Q.S. and Kataoka, K. 1999. Lipopolysaccharide-induced microglial activation in culture: temporal profiles of morphological change and release of cytokines and nitric oxide. *Neuroscience Research*. **35**(2),pp.95–100.
- Nakao, N., Kurokawa, T., Nonami, T., Tumurkhuu, G., Koide, N. and Yokochi, T. 2008. Hydrogen peroxide induces the production of tumor necrosis factor-alpha in RAW 264.7 macrophage cells via activation of p38 and stress-activated protein kinase. *Innate Immun*. **14**(3),pp.190–6.
- Nathan, J.D., Patel, A.A., McVey, D.C., Thomas, J.E., Prpic, V., Vigna, S.R. and Liddle, R.A. 2001. Capsaicin vanilloid receptor-1 mediates substance P release in experimental pancreatitis. *Am J Physiol Gastrointest Liver Physiol*. **281**(5),pp.G1322-8.
- Nauli, S.M., Alenghat, F.J., Luo, Y., Williams, E., Vassilev, P., Li, X., Elia, A.E.H., Lu, W., Brown, E.M., Quinn, S.J., Ingber, D.E. and Zhou, J. 2003. Polycystins 1 and 2 mediate mechanosensation in the primary cilium of kidney cells. *Nature Genetics*. **33**(2),pp.129–137.
- Nawashiro, H., Martin, D. and Hallenbeck, J.M. 1997. Neuroprotective effects of TNF binding protein in focal cerebral ischemia. *Brain Res*. **778**(2),pp.265–71.
- Naylor, J., Li, J., Milligan, C.J., Zeng, F., Sukumar, P., Hou, B., Sedo, A., Yuldasheva, N., Majeed, Y., Beri, D., Jiang, S., Seymour, V.A., McKeown, L., Kumar, B., Harteneck, C., O'Regan, D., Wheatcroft, S.B., Kearney, M.T., Jones, C., Porter, K.E. and Beech, D.J. 2010. Pregnenolone sulphate- and cholesterol-regulated TRPM3 channels coupled to vascular smooth muscle secretion and contraction. *Circ Res*. **106**(9),pp.1507–15.
- Naziroğlu, M. and Lückhoff, A. 2008. A calcium influx pathway regulated separately by oxidative stress and ADP-Ribose in TRPM2 channels: single channel events. *Neurochemical Research*. **33**(7),pp.1256–1262.

- Naziroglu, M., Luckhoff, A. and Jungling, E. 2007. Antagonist effect of flufenamic acid on TRPM2 cation channels activated by hydrogen peroxide. *Cell Biochemistry and Function*. **25**(4),pp.383–387.
- Naziroglu, M., Ozgul, C., Celik, O., Cig, B. and Sozbir, E. 2011. Aminoethoxydiphenyl Borate and Flufenamic Acid Inhibit Ca²⁺ Influx Through TRPM2 Channels in Rat Dorsal Root Ganglion Neurons Activated by ADP-Ribose and Rotenone. *Journal of Membrane Biology*. **241**(2),pp.69–75.
- Ni, Z., Hou, S., Barton, C.H. and Vaziri, N.D. 2004. Lead exposure raises superoxide and hydrogen peroxide in human endothelial and vascular smooth muscle cells. *Kidney Int.* **66**(6),pp.2329–36.
- Nicotera, P. and Bano, D. 2003. The enemy at the gates. Ca²⁺ entry through TRPM7 channels and anoxic neuronal death. *Cell*. **115**(7),pp.768–770.
- Niethammer, P., Grabher, C., Look, A.T. and Mitchison, T.J. 2009. A tissue-scale gradient of hydrogen peroxide mediates rapid wound detection in zebrafish. *Nature*. **459**(7249),pp.996–9.
- Nieto, F.R., Clark, A.K., Grist, J., Hathway, G.J., Chapman, V. and Malcangio, M. 2016. Neuron-immune mechanisms contribute to pain in early stages of arthritis. *J Neuroinflammation*. **13**(1),p.96.
- Nijenhuis, T., Hoenderop, J.G.J. and Bindels, R.J.M. 2005. TRPV5 and TRPV6 in Ca(2+) (re)absorption: regulating Ca(2+) entry at the gate. *Pflugers Archiv: European Journal of Physiology*. **451**(1),pp.181–192.
- Nijenhuis, T., Hoenderop, J.G.J., van der Kemp, A.W.C.M. and Bindels, R.J.M. 2003. Localization and regulation of the epithelial Ca²⁺ channel TRPV6 in the kidney. *Journal of the American Society of Nephrology: JASN*. **14**(11),pp.2731–2740.
- Nijenhuis, T., Renkema, K.Y., Hoenderop, J.G.J. and Bindels, R.J.M. 2006. Acid-base status determines the renal expression of Ca²⁺ and Mg²⁺ transport proteins. *Journal of the American Society of Nephrology: JASN*. **17**(3),pp.617–626.
- Nilius, B. 2007. TRP channels in disease. *Biochim Biophys Acta*. **1772**(8),pp.805–12.
- Nilius, B. and Droogmans, G. 2001. Ion channels and their functional role in vascular endothelium. *Physiol Rev*. **81**(4),pp.1415–59.
- Nilius, B., Prenen, J., Droogmans, G., Voets, T., Vennekens, R., Freichel, M., Wissenbach, U. and Flockerzi, V. 2003. Voltage dependence of the Ca²⁺-activated cation channel TRPM4. *Journal of Biological Chemistry*. **278**(33),pp.30813–30820.
- Nilius, B., Voets, T. and Peters, J. 2005. TRP channels in disease. *Sci STKE*. **2005**(295),p.re8.
- Nilius, B., Watanabe, H. and Vriens, J. 2003. The TRPV4 channel: structure-function relationship and promiscuous gating behaviour. *Pflugers Archiv-European Journal of Physiology*. **446**(3),pp.298–303.

- Nimmerjahn, A., Kirchhoff, F. and Helmchen, F. 2005. Resting microglial cells are highly dynamic surveillants of brain parenchyma in vivo. *Science*. **308**(5726),pp.1314–1318.
- Nisimoto, Y., Motalebi, S., Han, C.H. and Lambeth, J.D. 1999. The p67(phox) activation domain regulates electron flow from NADPH to flavin in flavocytochrome b(558). *J Biol Chem*. **274**(33),pp.22999–3005.
- Noh, K.M. and Koh, J.Y. 2000. Induction and activation by zinc of NADPH oxidase in cultured cortical neurons and astrocytes. *Journal of Neuroscience*. **20**(23),p.art. no.-RC111.
- Nomura, H., Turco, A.E., Pei, Y., Kalaydjieva, L., Schiavello, T., Weremowicz, S., Ji, W.Z., Morton, C.C., Meisler, M., Reeders, S.T. and Zhou, J. 1998. Identification of PKDL, a novel polycystic kidney disease 2-like gene whose murine homologue is deleted in mice with kidney and retinal defects. *Journal of Biological Chemistry*. **273**(40),pp.25967–25973.
- Oancea, E., Vriens, J., Brauchi, S., Jun, J., Splawski, I. and Clapham, D.E. 2009. TRPM1 forms ion channels associated with melanin content in melanocytes. *Science Signaling*. **2**(70),p.ra21.
- Oberwinkler, J., Lis, A., Giehl, K.M., Flockerzi, V. and Philipp, S.E. 2005. Alternative splicing switches the divalent cation selectivity of TRPM3 channels. *J Biol Chem*. **280**(23),pp.22540–8.
- O'Donnell, B.V., Tew, D.G., Jones, O.T. and England, P.J. 1993. Studies on the inhibitory mechanism of iodonium compounds with special reference to neutrophil NADPH oxidase. *Biochem J*. **290** (Pt 1),pp.41–9.
- Olah, M.E., Jackson, M.F., Li, H.B., Perez, Y., Sun, H.S., Kiyonaka, S., Mori, Y., Tymianski, M. and MacDonald, J.F. 2009. Ca²⁺-dependent induction of TRPM2 currents in hippocampal neurons. *Journal of Physiology-London*. **587**(5),pp.965–979.
- Ong, A.C. 2000. Polycystin expression in the kidney and other tissues: complexity, consensus and controversy. *Exp Nephrol*. **8**(4–5),pp.208–14.
- Onohara, N., Nishida, M., Inoue, R., Kobayashi, H., Sumimoto, H., Sato, Y., Mori, Y., Nagao, T. and Kurose, H. 2006. TRPC3 and TRPC6 are essential for angiotensin II-induced cardiac hypertrophy. *The EMBO Journal*. **25**(22),pp.5305–5316.
- Orfanelli, U., Jachetti, E., Chiacchiera, F., Grioni, M., Brambilla, P., Briganti, A., Freschi, M., Martinelli-Boneschi, F., Doglioni, C., Montorsi, F., Bellone, M., Casari, G., Pasini, D. and Lavorgna, G. 2015. Antisense transcription at the TRPM2 locus as a novel prognostic marker and therapeutic target in prostate cancer. *Oncogene*. **34**(16),pp.2094–102.
- Orfanelli, U., Wenke, A.K., Doglioni, C., Russo, V., Bosserhoff, A.K. and Lavorgna, G. 2008. Identification of novel sense and antisense transcription at the TRPM2 locus in cancer. *Cell Res*. **18**(11),pp.1128–40.
- Orts-Del'Immagine, A., Kastner, A., Tillement, V., Tardivel, C., Trouslard, J. and Wanaverbecq, N. 2014. Morphology, Distribution and Phenotype of Polycystin

Kidney Disease 2-like 1-Positive Cerebrospinal Fluid Contacting Neurons in The Brainstem of Adult Mice. *Plos One*. [Online]. **9**(2). Available from: ://WOS:000330631800067.

Ostapchenko, V.G., Chen, M.A., Guzman, M.S., Xie, Y.F., Lavine, N., Fan, J., Beraldo, F.H., Martyn, A.C., Belrose, J.C., Mori, Y., MacDonald, J.F., Prado, V.F., Prado, M.A.M. and Jackson, M.F. 2015. The Transient Receptor Potential Melastatin 2 (TRPM2) Channel Contributes to beta-Amyloid Oligomer-Related Neurotoxicity and Memory Impairment. *Journal of Neuroscience*. **35**(45),pp.15157–15169.

Osyczka, A., Moser, C.C. and Dutton, P.L. 2005. Fixing the Q cycle. *Trends in Biochemical Sciences*. **30**(4),pp.176–182.

Ouchi, Y., Yoshikawa, E., Sekine, Y., Futatsubashi, M., Kanno, T., Oguisu, T. and Torizuka, T. 2005. Microglial activation and dopamine terminal loss in early Parkinson's disease. *Ann Neurol*. **57**(2),pp.168–75.

Ouyang, L., Shi, Z., Zhao, S., Wang, F.T., Zhou, T.T., Liu, B. and Bao, J.K. 2012. Programmed cell death pathways in cancer: a review of apoptosis, autophagy and programmed necrosis. *Cell Prolif*. **45**(6),pp.487–98.

Owsianik, G., Talavera, K., Voets, T. and Nilius, B. 2006. Permeation and selectivity of TRP channels. *Annu Rev Physiol*. **68**,pp.685–717.

Paclet, M.H., Coleman, A.W., Vergnaud, S. and Morel, F. 2000. P67-phox-mediated NADPH oxidase assembly: imaging of cytochrome b558 liposomes by atomic force microscopy. *Biochemistry*. **39**(31),pp.9302–10.

Paolicelli, R.C., Bolasco, G., Pagani, F., Maggi, L., Scianni, M., Panzanelli, P., Giustetto, M., Ferreira, T.A., Guiducci, E., Dumas, L., Ragozzino, D. and Gross, C.T. 2011. Synaptic pruning by microglia is necessary for normal brain development. *Science*. **333**(6048),pp.1456–8.

Paouri, E., Tzara, O., Kartalou, G.-I., Zenelak, S. and Georgopoulos, S. 2017. Peripheral Tumor Necrosis Factor-Alpha (TNF- α) Modulates Amyloid Pathology by Regulating Blood-Derived Immune Cells and Glial Response in the Brain of AD/TNF Transgenic Mice. *The Journal of Neuroscience: The Official Journal of the Society for Neuroscience*. **37**(20),pp.5155–5171.

Papaharalambus, C.A. and Griendling, K.K. 2007. Basic mechanisms of oxidative stress and reactive oxygen species in cardiovascular injury. *Trends Cardiovasc Med*. **17**(2),pp.48–54.

Park, E.S., Gao, X., Chung, J.M. and Chung, K. 2006. Levels of mitochondrial reactive oxygen species increase in rat neuropathic spinal dorsal horn neurons. *Neurosci Lett*. **391**(3),pp.108–11.

Park, L., Wang, G., Moore, J., Girouard, H., Zhou, P., Anrather, J. and Iadecola, C. 2014. The key role of transient receptor potential melastatin-2 channels in amyloid-beta-induced neurovascular dysfunction. *Nature Communications*. [Online]. **5**. Available from: ://WOS:000344061800004.

- Partida-Sánchez, S., Gasser, A., Fliegert, R., Siebrands, C.C., Dammermann, W., Shi, G., Mousseau, B.J., Sumoza-Toledo, A., Bhagat, H., Walseth, T.F., Guse, A.H. and Lund, F.E. 2007. Chemotaxis of mouse bone marrow neutrophils and dendritic cells is controlled by adp-ribose, the major product generated by the CD38 enzyme reaction. *Journal of Immunology (Baltimore, Md.: 1950)*. **179**(11),pp.7827–7839.
- Partida-Sánchez, S., Randall, T.D. and Lund, F.E. 2003. Innate immunity is regulated by CD38, an ecto-enzyme with ADP-ribosyl cyclase activity. *Microbes and Infection*. **5**(1),pp.49–58.
- Patapoutian, A., Peier, A.M., Story, G.M. and Viswanath, V. 2003. Thermotrp channels and beyond: Mechanisms of temperature sensation. *Nature Reviews Neuroscience*. **4**(7),pp.529–539.
- Patel, A., Sharif-Naeini, R., Folgering, J.R., Bichet, D., Duprat, F. and Honore, E. 2010. Canonical TRP channels and mechanotransduction: from physiology to disease states. *Pflugers Arch.* **460**(3),pp.571–81.
- Pedersen, S.F., Owsianik, G. and Nilius, B. 2005. TRP channels: an overview. *Cell Calcium*. **38**(3–4),pp.233–52.
- Peier, A.M., Moqrich, A., Hergarden, A.C., Reeve, A.J., Andersson, D.A., Story, G.M., Earley, T.J., Dragoni, I., McIntyre, P., Bevan, S. and Patapoutian, A. 2002. A TRP channel that senses cold stimuli and menthol. *Cell*. **108**(5),pp.705–15.
- Peier, A.M., Reeve, A.J., Andersson, D.A., Moqrich, A., Earley, T.J., Hergarden, A.C., Story, G.M., Colley, S., Hogenesch, J.B., McIntyre, P., Bevan, S. and Patapoutian, A. 2002. A heat-sensitive TRP channel expressed in keratinocytes. *Science*. **296**(5575),pp.2046–2049.
- Pennekamp, P., Karcher, C., Fischer, A., Schweickert, A., Skryabin, B., Horst, J., Blum, M. and Dworniczak, B. 2002. The ion channel polycystin-2 is required for left-right axis determination in mice. *Current Biology*. **12**(11),pp.938–943.
- Pérez, C.A., Huang, L., Rong, M., Kozak, J.A., Preuss, A.K., Zhang, H., Max, M. and Margolskee, R.F. 2002. A transient receptor potential channel expressed in taste receptor cells. *Nature Neuroscience*. **5**(11),pp.1169–1176.
- Perraud, A.L., Fleig, A., Dunn, C.A., Bagley, L.A., Launay, P., Schmitz, C., Stokes, A.J., Zhu, Q.Q., Bessman, M.J., Penner, R., Kinet, J.P. and Scharenberg, A.M. 2001. ADP-ribose gating of the calcium-permeable LTRPC2 channel revealed by Nudix motif homology. *Nature*. **411**(6837),pp.595–599.
- Perraud, A.-L., Shen, B., Dunn, C.A., Rippe, K., Smith, M.K., Bessman, M.J., Stoddard, B.L. and Scharenberg, A.M. 2003. NUDT9, a member of the Nudix hydrolase family, is an evolutionarily conserved mitochondrial ADP-ribose pyrophosphatase. *The Journal of Biological Chemistry*. **278**(3),pp.1794–1801.
- Perraud, A.L., Takanishi, C.L., Shen, B., Kang, S., Smith, M.K., Schmitz, C., Knowles, H.M., Ferraris, D., Li, W.X., Zhang, J., Stoddard, B.L. and Scharenberg, A.M. 2005. Accumulation of free ADP-ribose from mitochondria mediates oxidative stress-induced gating of TRPM2 cation channels. *Journal of Biological Chemistry*. **280**(7),pp.6138–6148.

- Perry, V.H., Cunningham, C. and Holmes, C. 2007. Systemic infections and inflammation affect chronic neurodegeneration. *Nat Rev Immunol.* **7**(2),pp.161–7.
- Phelps, C.B., Huang, R.J., Lishko, P.V., Wang, R.R. and Gaudet, R. 2008. Structural analyses of the ankyrin repeat domain of TRPV6 and related TRPV ion channels. *Biochemistry.* **47**(8),pp.2476–84.
- Philipp, S., Hambrecht, J., Braslavski, L., Schroth, G., Freichel, M., Murakami, M., Cavalie, A. and Flockerzi, V. 1998. A novel capacitative calcium entry channel expressed in excitable cells. *EMBO J.* **17**(15),pp.4274–82.
- Philipp, S., Strauss, B., Hirnet, D., Wissenbach, U., Mery, L., Flockerzi, V. and Hoth, M. 2003. TRPC3 mediates T-cell receptor-dependent calcium entry in human T-lymphocytes. *The Journal of Biological Chemistry.* **278**(29),pp.26629–26638.
- Phillips, A.M., Bull, A. and Kelly, L.E. 1992. Identification of a *Drosophila* gene encoding a calmodulin-binding protein with homology to the trp phototransduction gene. *Neuron.* **8**(4),pp.631–42.
- Piper, R.C. and Luzio, J.P. 2004. CUPpling calcium to lysosomal biogenesis. *Trends in Cell Biology.* **14**(9),pp.471–473.
- Pourrut, B., Perchet, G., Silvestre, J., Cecchi, M., Guiresse, M. and Pinelli, E. 2008. Potential role of NADPH-oxidase in early steps of lead-induced oxidative burst in *Vicia faba* roots. *Journal of Plant Physiology.* **165**(6),pp.571–579.
- Qian, F. and Noben-Trauth, K. 2005. Cellular and molecular function of mucolipins (TRPML) and polycystin 2 (TRPP2). *Pflugers Archiv: European Journal of Physiology.* **451**(1),pp.277–285.
- Qian, L., Flood, P.M. and Hong, J.S. 2010. Neuroinflammation is a key player in Parkinson's disease and a prime target for therapy. *J Neural Transm (Vienna).* **117**(8),pp.971–9.
- Qian, X.W., Numata, T., Zhang, K., Li, C.X., Hou, J.C., Mori, Y. and Fang, X.M. 2014. Transient Receptor Potential Melastatin 2 Protects Mice against Polymicrobial Sepsis by Enhancing Bacterial Clearance. *Anesthesiology.* **121**(2),pp.336–351.
- Qin, L., Liu, Y., Wang, T., Wei, S.-J., Block, M.L., Wilson, B., Liu, B. and Hong, J.-S. 2004. NADPH Oxidase Mediates Lipopolysaccharide-induced Neurotoxicity and Proinflammatory Gene Expression in Activated Microglia. *Journal of Biological Chemistry.* **279**(2),pp.1415–1421.
- Qin, L., Wu, X., Block, M.L., Liu, Y., Breese, G.R., Hong, J.-S., Knapp, D.J. and Crews, F.T. 2007. Systemic LPS causes chronic neuroinflammation and progressive neurodegeneration. *Glia.* **55**(5),pp.453–462.
- Qiu, L.L., Ji, M.H., Zhang, H., Yang, J.J., Sun, X.R., Tang, H., Wang, J., Liu, W.X. and Yang, J.J. 2016. NADPH oxidase 2-derived reactive oxygen species in the hippocampus might contribute to microglial activation in postoperative cognitive dysfunction in aged mice. *Brain Behavior and Immunity.* **51**,pp.109–118.

- Raad, H., Paclet, M.-H., Boussetta, T., Kroviarski, Y., Morel, F., Quinn, M.T., Gougerot-Pocidalo, M.-A., Dang, P.M.-C. and El-Benna, J. 2009. Regulation of the phagocyte NADPH oxidase activity: phosphorylation of gp91phox/NOX2 by protein kinase C enhances its diaphorase activity and binding to Rac2, p67phox, and p47phox. *The FASEB Journal.* **23**(4),pp.1011–1022.
- Radak, Z., Zhao, Z.F., Goto, S. and Koltai, E. 2011. Age-associated neurodegeneration and oxidative damage to lipids, proteins and DNA. *Molecular Aspects of Medicine.* **32**(4–6),pp.305–315.
- Radeke, H.H., Meier, B., Topley, N., Flöge, J., Habermehl, G.G. and Resch, K. 1990. Interleukin 1-alpha and tumor necrosis factor-alpha induce oxygen radical production in mesangial cells. *Kidney International.* **37**(2),pp.767–775.
- Rah, S.Y., Kwak, J.Y., Chung, Y.J. and Kim, U.H. 2015. ADP-ribose/TRPM2-mediated Ca²⁺ signaling is essential for cytolytic degranulation and antitumor activity of natural killer cells. *Sci Rep.* **5**,p.9482.
- Raha, S. and Robinson, B.H. 2000. Mitochondria, oxygen free radicals, disease and ageing. *Trends Biochem Sci.* **25**(10),pp.502–8.
- Ramsey, I.S., Delling, M. and Clapham, D.E. 2006. An introduction to TRP channels. *Annu Rev Physiol.* **68**,pp.619–47.
- Reeves, E.P., Dekker, L.V., Forbes, L.V., Wientjes, F.B., Grogan, A., Pappin, D.J.C. and Segal, A.W. 1999. Direct interaction between p47(phox) and protein kinase C: evidence for targeting of protein kinase C by p47(phox) in neutrophils. *Biochemical Journal.* **344**,pp.859–866.
- Regen, F., Hellmann-Regen, J., Costantini, E. and Reale, M. 2017. Neuroinflammation and Alzheimer's Disease: Implications for Microglial Activation. *Current Alzheimer Research.*
- Rezaie, P. 2003. Microglia in the Human Nervous System during Development. *Neuroembryology.* **2**(1),pp.18–31.
- Roberge, S., Roussel, J., Andersson, D.C., Meli, A.C., Vidal, B., Blandel, F., Lanner, J.T., Le Guennec, J.Y., Katz, A., Westerblad, H., Lacampagne, A. and Fauconnier, J. 2014. TNF-alpha-mediated caspase-8 activation induces ROS production and TRPM2 activation in adult ventricular myocytes. *Cardiovasc Res.* **103**(1),pp.90–9.
- Rodriguez-Oroz, M.C., Jahanshahi, M., Krack, P., Litvan, I., Macias, R., Bezard, E. and Obeso, J.A. 2009. Initial clinical manifestations of Parkinson's disease: features and pathophysiological mechanisms. *Lancet Neurol.* **8**(12),pp.1128–39.
- Rogers, J., Strohmeyer, R., Kovelowski, C.J. and Li, R. 2002. Microglia and inflammatory mechanisms in the clearance of amyloid beta peptide. *Glia.* **40**(2),pp.260–9.
- Rolon-Reyes, K., Kucheryavykh, Y.V., Cubano, L.A., Inyushin, M., Skatchkov, S.N., Eaton, M.J., Harrison, J.K. and Kucheryavykh, L.Y. 2015. Microglia Activate Migration of Glioma Cells through a Pyk2 Intracellular Pathway. *Plos One.* [Online]. **10**(6). Available from: ://WOS:000356835800139.

- Rossi, F. and Zatti, M. 1964. Biochemical aspects of phagocytosis in polymorphonuclear leucocytes. NADH and NADPH oxidation by the granules of resting and phagocytizing cells. *Experientia*. **20**(1),pp.21–3.
- Runnels, L.W., Yue, L.X. and Capham, D.E. 2001. TRP-PLIK, a bifunctional protein with kinase and ion channel activities. *Science*. **291**(5506),pp.1043–1047.
- Rustin, P. and Rötig, A. 2002. Inborn errors of complex II--unusual human mitochondrial diseases. *Biochimica Et Biophysica Acta*. **1553**(1–2),pp.117–122.
- Ryazanova, L.V., Dorovkov, M.V., Ansari, A. and Ryazanov, A.G. 2004. Characterization of the protein kinase activity of TRPM7/ChaK1, a protein kinase fused to the transient receptor potential ion channel. *J Biol Chem*. **279**(5),pp.3708–16.
- Samie, M.A., Grimm, C., Evans, J.A., Curcio-Morelli, C., Heller, S., Slaugenhaupt, S.A. and Cuajungco, M.P. 2009. The tissue-specific expression of TRPML2 (MCOLN-2) gene is influenced by the presence of TRPML1. *Pflugers Arch*. **459**(1),pp.79–91.
- Sano, Y., Inamura, K., Miyake, A., Mochizuki, S., Yokoi, H., Matsushime, H. and Furuichi, K. 2001. Immunocyte Ca²⁺ influx system mediated by LTRPC2. *Science*. **293**(5533),pp.1327–1330.
- Santos, C.X.C., Raza, S. and Shah, A.M. 2016. Redox signaling in the cardiomyocyte: From physiology to failure. *International Journal of Biochemistry & Cell Biology*. **74**,pp.145–151.
- Sasaki, A., Yamaguchi, H., Ogawa, A., Sugihara, S. and Nakazato, Y. 1997. Microglial activation in early stages of amyloid beta protein deposition. *Acta Neuropathologica*. **94**(4),pp.316–322.
- Sawada, Y., Hosokawa, H., Hori, A., Matsumura, K. and Kobayashi, S. 2007. Cold sensitivity of recombinant TRPA1 channels. *Brain Res*. **1160**,pp.39–46.
- Sazonov, L.A. 2007. Respiratory complex I: mechanistic and structural insights provided by the crystal structure of the hydrophilic domain. *Biochemistry*. **46**(9),pp.2275–2288.
- Schafer, D.P., Lehrman, E.K., Kautzman, A.G., Koyama, R., Mardinly, A.R., Yamasaki, R., Ransohoff, R.M., Greenberg, M.E., Barres, B.A. and Stevens, B. 2012. Microglia sculpt postnatal neural circuits in an activity and complement-dependent manner. *Neuron*. **74**(4),pp.691–705.
- Schapira, A.H., Cooper, J.M., Dexter, D., Jenner, P., Clark, J.B. and Marsden, C.D. 1989. Mitochondrial complex I deficiency in Parkinson's disease. *Lancet*. **1**(8649),p.1269.
- Scheltens, P., Blennow, K., Breteler, M.M., de Strooper, B., Frisoni, G.B., Salloway, S. and Van der Flier, W.M. 2016. Alzheimer's disease. *Lancet*. **388**(10043),pp.505–17.
- Schieber, M. and Chandel, N.S. 2014. ROS Function in Redox Signaling and Oxidative Stress. *Current Biology*. **24**(10),pp.R453–R462.

- Segal, A.W., West, I., Wientjes, F., Nugent, J.H., Chavan, A.J., Haley, B., Garcia, R.C., Rosen, H. and Scrace, G. 1992. Cytochrome b-245 is a flavocytochrome containing FAD and the NADPH-binding site of the microbicidal oxidase of phagocytes. *The Biochemical Journal.* **284** (Pt 3), pp.781–788.
- Selkoe, D.J. and Hardy, J. 2016. The amyloid hypothesis of Alzheimer's disease at 25 years. *EMBO Mol Med.* **8**(6), pp.595–608.
- Seo, S.R., Chong, S.A., Lee, S.I., Sung, J.Y., Ahn, Y.S., Chung, K.C. and Seo, J.T. 2001. Zn²⁺-induced ERK activation mediated by reactive oxygen species causes cell death in differentiated PC12 cells. *Journal of Neurochemistry.* **78**(3), pp.600–610.
- Shen, B.W., Perraud, A.L., Scharenberg, A. and Stoddard, B.L. 2003. The crystal structure and mutational analysis of human NUDT9. *Journal of Molecular Biology.* **332**(2), pp.385–398.
- Shen, S.C., Wu, M.S., Lin, H.Y., Yang, L.Y., Chen, Y.H. and Chen, Y.C. 2014. Reactive Oxygen Species-Dependent Nitric Oxide Production in Reciprocal Interactions of Glioma and Microglial Cells. *Journal of Cellular Physiology.* **229**(12), pp.2015–2026.
- Shen, Y., Heimel, J.A., Kamermans, M., Peachey, N.S., Gregg, R.G. and Nawy, S. 2009. A Transient Receptor Potential-Like Channel Mediates Synaptic Transmission in Rod Bipolar Cells. *Journal of Neuroscience.* **29**(19), pp.6088–6093.
- Sheppard, F.R., Kelher, M.R., Moore, E.E., McLaughlin, N.J.D., Banerjee, A. and Silliman, C.C. 2005. Structural organization of the neutrophil NADPH oxidase: phosphorylation and translocation during priming and activation. *Journal of Leukocyte Biology.* **78**(5), pp.1025–1042.
- Shi, J.-Q., Shen, W., Chen, J., Wang, B.-R., Zhong, L.-L., Zhu, Y.-W., Zhu, H.-Q., Zhang, Q.-Q., Zhang, Y.-D. and Xu, J. 2011. Anti-TNF- α reduces amyloid plaques and tau phosphorylation and induces CD11c-positive dendritic-like cell in the APP/PS1 transgenic mouse brains. *Brain Research.* **1368**, pp.239–247.
- Shi, X., Zheng, Z., Li, J., Xiao, Z., Qi, W., Zhang, A., Wu, Q. and Fang, Y. 2015. Curcumin inhibits A β -induced microglial inflammatory responses in vitro: Involvement of ERK1/2 and p38 signaling pathways. *Neuroscience Letters.* **594**, pp.105–110.
- Shimizu, T., Janssens, A., Voets, T. and Nilius, B. 2009. Regulation of the murine TRPP3 channel by voltage, pH, and changes in cell volume. *Pflugers Arch.* **457**(4), pp.795–807.
- Shimosato, G., Amaya, F., Ueda, M., Tanaka, Y., Decosterd, I. and Tanaka, M. 2005. Peripheral inflammation induces up-regulation of TRPV2 expression in rat DRG. *Pain.* **119**(1–3), pp.225–232.
- Shiose, A., Kuroda, J., Tsuruya, K., Hirai, M., Hirakata, H., Naito, S., Hattori, M., Sakaki, Y. and Sumimoto, H. 2001. A novel superoxide-producing NAD(P)H oxidase in kidney. *J Biol Chem.* **276**(2), pp.1417–23.

- Shiose, A. and Sumimoto, H. 2000. Arachidonic acid and phosphorylation synergistically induce a conformational change of p47phox to activate the phagocyte NADPH oxidase. *J Biol Chem.* **275**(18),pp.13793–801.
- Shirakawa, H., Sakimoto, S., Nakagawa, T. and Kaneko, S. 2014. [Pathophysiology of immune cells during the progression of cerebral ischemic injury - involvement of TRPM2-mediated induction of iNOS in microglia/macrophage]. *Nihon Yakurigaku Zasshi. Folia Pharmacologica Japonica.* **144**(3),pp.104–109.
- Sloviter, R.S. 1985. A SELECTIVE LOSS OF HIPPOCAMPAL MOSSY FIBER TIMM STAIN ACCOMPANIES GRANULE CELL SEIZURE ACTIVITY INDUCED BY PERFORANT PATH STIMULATION. *Brain Res.* **330**(1),pp.150–153.
- Smith, G.D., Gunthorpe, J., Kellsell, R.E., Hayes, P.D., Reilly, P., Facer, P., Wright, J.E., Jerman, J.C., Walhin, J.P., Ooi, L., Egerton, J., Charles, K.J., Smart, D., Randall, A.D., Anand, P. and Davis, J.B. 2002. TRPV3 is a temperature-sensitive vanilloid receptor-like protein. *Nature.* **418**(6894),pp.186–190.
- So, K., Haraguchi, K., Asakura, K., Isami, K., Sakimoto, S., Shirakawa, H., Mori, Y., Nakagawa, T. and Kaneko, S. 2015. Involvement of TRPM2 in a wide range of inflammatory and neuropathic pain mouse models. *J Pharmacol Sci.* **127**(3),pp.237–43.
- Soboloff, J., Spassova, M., Xu, W., He, L.-P., Cuesta, N. and Gill, D.L. 2005. Role of endogenous TRPC6 channels in Ca²⁺ signal generation in A7r5 smooth muscle cells. *The Journal of Biological Chemistry.* **280**(48),pp.39786–39794.
- Sohal, R.S., Mockett, R.J. and Orr, W.C. 2002. Mechanisms of aging: An appraisal of the oxidative stress hypothesis. *Free Radical Biology and Medicine.* **33**(5),pp.575–586.
- Soltys, Z., Ziaja, M., Pawlński, R., Setkowicz, Z. and Janeczko, K. 2001. Morphology of reactive microglia in the injured cerebral cortex. Fractal analysis and complementary quantitative methods. *Journal of Neuroscience Research.* **63**(1),pp.90–97.
- Someya, A., Nunoi, H., Hasebe, T. and Nagaoka, I. 1999. Phosphorylation of p40-phox during activation of neutrophil NADPH oxidase. *Journal of Leukocyte Biology.* **66**(5),pp.851–857.
- Sondag, C.M., Dhawan, G. and Combs, C.K. 2009. Beta amyloid oligomers and fibrils stimulate differential activation of primary microglia. *J Neuroinflammation.* **6**,p.1.
- Song, K., Wang, H., Kamm, G.B., Pohle, J., Reis, F.D., Heppenstall, P., Wende, H. and Siemens, J. 2016. The TRPM2 channel is a hypothalamic heat sensor that limits fever and can drive hypothermia. *Science.* **353**(6306),pp.1393–1398.
- Song, Y., Driessens, N., Costa, M., De Deken, X., Detours, V., Corvilain, B., Maenhaut, C., Miot, F., Van Sande, J., Many, M.-C. and Dumont, J.E. 2007. Roles of hydrogen peroxide in thyroid physiology and disease. *The Journal of Clinical Endocrinology and Metabolism.* **92**(10),pp.3764–3773.

- Sriram, K., Matheson, J.M., Benkovic, S.A., Miller, D.B., Luster, M.I. and O'Callaghan, J.P. 2002. Mice deficient in TNF receptors are protected against dopaminergic neurotoxicity: implications for Parkinson's disease. *FASEB J.* **16**(11),pp.1474–6.
- Stahelin, R.V., Burian, A., Bruzik, K.S., Murray, D. and Cho, W. 2003. Membrane binding mechanisms of the PX domains of NADPH oxidase p40phox and p47phox. *J Biol Chem.* **278**(16),pp.14469–79.
- Starkov, A.A. and Fiskum, G. 2001. Myxothiazol induces H(2)O(2) production from mitochondrial respiratory chain. *Biochem Biophys Res Commun.* **281**(3),pp.645–50.
- Starkov, A.A., Fiskum, G., Chinopoulos, C., Lorenzo, B.J., Browne, S.E., Patel, M.S. and Beal, M.F. 2004. Mitochondrial alpha-ketoglutarate dehydrogenase complex generates reactive oxygen species. *J Neurosci.* **24**(36),pp.7779–88.
- Starkus, J., Beck, A., Fleig, A. and Penner, R. 2007. Regulation of TRPM2 by extra- and intracellular calcium. *The Journal of General Physiology.* **130**(4),pp.427–440.
- Stielow, C., Catar, R.A., Muller, G., Wingler, K., Scheurer, P., Schmidt, H.H. and Morawietz, H. 2006. Novel Nox inhibitor of oxLDL-induced reactive oxygen species formation in human endothelial cells. *Biochem Biophys Res Commun.* **344**(1),pp.200–5.
- Stoica, B.A., Loane, D.J., Zhao, Z., Kabadi, S.V., Hanscom, M., Byrnes, K.R. and Faden, A.I. 2014. PARP-1 inhibition attenuates neuronal loss, microglia activation and neurological deficits after traumatic brain injury. *Journal of Neurotrauma.* **31**(8),pp.758–772.
- Stolk, J., Hiltermann, T.J., Dijkman, J.H. and Verhoeven, A.J. 1994. Characteristics of the inhibition of NADPH oxidase activation in neutrophils by apocynin, a methoxy-substituted catechol. *Am J Respir Cell Mol Biol.* **11**(1),pp.95–102.
- Story, G.M., Peier, A.M., Reeve, A.J., Eid, S.R., Mosbacher, J., Hricik, T.R., Earley, T.J., Hergarden, A.C., Andersson, D.A., Hwang, S.W., McIntyre, P., Jegla, T., Bevan, S. and Patapoutian, A. 2003. ANKTM1, a TRP-like channel expressed in nociceptive neurons, is activated by cold temperatures. *Cell.* **112**(6),pp.819–829.
- Stowers, L., Holy, T.E., Meister, M., Dulac, C. and Koentges, G. 2002. Loss of sex discrimination and male-male aggression in mice deficient for TRP2. *Science.* **295**(5559),pp.1493–500.
- Straub, I., Krugel, U., Mohr, F., Teichert, J., Rizun, O., Konrad, M., Oberwinkler, J. and Schaefer, M. 2013. Flavanones that selectively inhibit TRPM3 attenuate thermal nociception in vivo. *Mol Pharmacol.* **84**(5),pp.736–50.
- Strotmann, R., Harteneck, C., Nunnenmacher, K., Schultz, G. and Plant, T.D. 2000. OTRPC4, a nonselective cation channel that confers sensitivity to extracellular osmolarity. *Nature Cell Biology.* **2**(10),pp.695–702.
- Stuehr, D.J., Fasehun, O.A., Kwon, N.S., Gross, S.S., Gonzalez, J.A., Levi, R. and Nathan, C.F. 1991. INHIBITION OF MACROPHAGE AND ENDOTHELIAL-

CELL NITRIC-OXIDE SYNTHASE BY DIPHENYLENEIODONIUM AND ITS ANALOGS. *Faseb Journal*. **5**(1),pp.98–103.

- Su, L.-T., Agapito, M.A., Li, M., Simonson, W.T.N., Huttenlocher, A., Habas, R., Yue, L. and Runnels, L.W. 2006. TRPM7 regulates cell adhesion by controlling the calcium-dependent protease calpain. *The Journal of Biological Chemistry*. **281**(16),pp.11260–11270.
- Suh, S.W., Aoyama, K., Alano, C.C., Anderson, C.M., Hamby, A.M. and Swanson, R.A. 2007. Zinc inhibits astrocyte glutamate uptake by activation of poly(ADP-ribose) polymerase-1. *Molecular Medicine*. **13**(7–8),pp.344–349.
- Suh, Y.A., Arnold, R.S., Lassegue, B., Shi, J., Xu, X., Sorescu, D., Chung, A.B., Griendling, K.K. and Lambeth, J.D. 1999. Cell transformation by the superoxide-generating oxidase Mox1. *Nature*. **401**(6748),pp.79–82.
- Sumoza-Toledo, A., Lange, I., Cortado, H., Bhagat, H., Mori, Y., Fleig, A., Penner, R. and Partida-Sanchez, S. 2011. Dendritic cell maturation and chemotaxis is regulated by TRPM2-mediated lysosomal Ca²⁺ release. *Faseb Journal*. **25**(10),pp.3529–3542.
- Sumoza-Toledo, A. and Penner, R. 2011. TRPM2: a multifunctional ion channel for calcium signalling. *J Physiol*. **589**(Pt 7),pp.1515–25.
- Sun, M., Goldin, E., Stahl, S., Falardeau, J.L., Kennedy, J.C., Acierno, J.S., Bove, C., Kaneski, C.R., Nagle, J., Bromley, M.C., Colman, M., Schiffmann, R. and Slaugenhoupt, S.A. 2000. Mucolipidosis type IV is caused by mutations in a gene encoding a novel transient receptor potential channel. *Human Molecular Genetics*. **9**(17),pp.2471–2478.
- Sun, Y., Sukumaran, P., Selvaraj, S., Cilz, N.I., Schaar, A., Lei, S. and Singh, B.B. 2016. TRPM2 Promotes Neurotoxin MPP+/MPTP-Induced Cell Death. *Mol Neurobiol*. [Online]. Available from: <http://www.ncbi.nlm.nih.gov/pubmed/27957685>.
- Sweeney, M., Yu, Y., Platoshyn, O., Zhang, S., McDaniel, S.S. and Yuan, J.X. 2002. Inhibition of endogenous TRP1 decreases capacitative Ca²⁺ entry and attenuates pulmonary artery smooth muscle cell proliferation. *Am J Physiol Lung Cell Mol Physiol*. **283**(1),pp.L144–55.
- Szalay, G., Martinecz, B., Lenart, N., Kornyei, Z., Orsolits, B., Judak, L., Csaszar, E., Fekete, R., West, B.L., Katona, G., Rozsa, B. and Denes, A. 2016. Microglia protect against brain injury and their selective elimination dysregulates neuronal network activity after stroke. *Nature Communications*. [Online]. **7**. Available from: ://WOS:000375223600001.
- Szanto, I., Rubbia-Brandt, L., Kiss, P., Steger, K., Banfi, B., Kovari, E., Herrmann, F., Hadengue, A. and Krause, K.H. 2005. Expression of NOX1, a superoxide-generating NADPH oxidase, in colon cancer and inflammatory bowel disease. *J Pathol*. **207**(2),pp.164–76.
- Tai, Y.F., Pavese, N., Gerhard, A., Tabrizi, S.J., Barker, R.A., Brooks, D.J. and Piccini, P. 2007. Microglial activation in presymptomatic Huntington's disease gene carriers. *Brain: A Journal of Neurology*. **130**(Pt 7),pp.1759–1766.

- Takezawa, R., Schmitz, C., Demeuse, P., Scharenberg, A.M., Penner, R. and Fleig, A. 2004. Receptor-mediated regulation of the TRPM7 channel through its endogenous protein kinase domain. *Proc Natl Acad Sci U S A.* **101**(16),pp.6009–14.
- Talavera, K., Yasumatsu, K., Voets, T., Droogmans, G., Shigemura, N., Ninomiya, Y., Margolskee, R.F. and Nilius, B. 2005. Heat activation of TRPM5 underlies thermal sensitivity of sweet taste. *Nature.* **438**(7070),pp.1022–1025.
- Tan, C.H. and McNaughton, P.A. 2016. The TRPM2 ion channel is required for sensitivity to warmth. *Nature.* **536**(7617),p.460–+.
- Tanaka, S., Ide, M., Shibutani, T., Ohtaki, H., Numazawa, S., Shioda, S. and Yoshida, T. 2006. Lipopolysaccharide-induced microglial activation induces learning and memory deficits without neuronal cell death in rats. *J Neurosci Res.* **83**(4),pp.557–66.
- Tateishi, Y., Sasabe, E., Ueta, E. and Yamamoto, T. 2008. Ionizing irradiation induces apoptotic damage of salivary gland acinar cells via NADPH oxidase 1-dependent superoxide generation. *Biochemical and Biophysical Research Communications.* **366**(2),pp.301–307.
- Tian, L., Karimi, M., Loftin, S.K., Brown, C.A., Xia, H., Xu, J., Mach, R.H. and Perlmutter, J.S. 2012. No differential regulation of dopamine transporter (DAT) and vesicular monoamine transporter 2 (VMAT2) binding in a primate model of Parkinson disease. *Plos One.* **7**(2),p.e31439.
- Tiruppathi, C., Freichel, M., Vogel, S.M., Paria, B.C., Mehta, D., Flockerzi, V. and Malik, A.B. 2002. Impairment of store-operated Ca²⁺ entry in TRPC4(-/-) mice interferes with increase in lung microvascular permeability. *Circ Res.* **91**(1),pp.70–6.
- Togashi, K., Hara, Y., Tominaga, T., Higashi, T., Konishi, Y., Mori, Y. and Tominaga, M. 2006. TRPM2 activation by cyclic ADP-ribose at body temperature is involved in insulin secretion. *Embo Journal.* **25**(9),pp.1804–1815.
- Togashi, K., Inada, H. and Tominaga, M. 2008. Inhibition of the transient receptor potential cation channel TRPM2 by 2-aminoethoxydiphenyl borate (2-APB). *Br J Pharmacol.* **153**(6),pp.1324–30.
- Tong, L. and Denu, J.M. 2010. Function and metabolism of sirtuin metabolite O-acetyl-ADP-ribose. *Biochimica Et Biophysica Acta.* **1804**(8),pp.1617–1625.
- Tönnies, E. and Trushina, E. 2017. Oxidative Stress, Synaptic Dysfunction, and Alzheimer's Disease. *Journal of Alzheimer's Disease.* **57**(4),pp.1105–1121.
- Torihashi, S., Fujimoto, T., Trost, C. and Nakayama, S. 2002. Calcium oscillation linked to pacemaking of interstitial cells of Cajal: requirement of calcium influx and localization of TRP4 in caveolae. *J Biol Chem.* **277**(21),pp.19191–7.
- Toth, B. and Csanady, L. 2010. Identification of Direct and Indirect Effectors of the Transient Receptor Potential Melastatin 2 (TRPM2) Cation Channel. *Journal of Biological Chemistry.* **285**(39),pp.30091–30102.

- Toth, B., Iordanov, I. and Csanady, L. 2014. Putative chanzyme activity of TRPM2 cation channel is unrelated to pore gating. *Proc Natl Acad Sci U S A.* **111**(47),pp.16949–16954.
- Toth, B., Iordanov, I. and Csanady, L. 2015. Ruling out pyridine dinucleotides as true TRPM2 channel activators reveals novel direct agonist ADP-ribose-2'-phosphate. *Journal of General Physiology.* **145**(5),pp.419–430.
- Tsavalier, L., Shapero, M.H., Morkowski, S. and Laus, R. 2001. Trp-p8, a novel prostate-specific gene, is up-regulated in prostate cancer and other malignancies and shares high homology with transient receptor potential calcium channel proteins. *Cancer Research.* **61**(9),pp.3760–3769.
- Turrens, J.F. 2003. Mitochondrial formation of reactive oxygen species. *J Physiol.* **552**(Pt 2),pp.335–44.
- Turrens, J.F., Alexandre, A. and Lehninger, A.L. 1985. Ubisemiquinone is the electron donor for superoxide formation by complex III of heart mitochondria. *Arch Biochem Biophys.* **237**(2),pp.408–14.
- Turrens, J.F. and Boveris, A. 1980. Generation of superoxide anion by the NADH dehydrogenase of bovine heart mitochondria. *Biochem J.* **191**(2),pp.421–7.
- Tynan, R.J., Naicker, S., Hinwood, M., Nalivaiko, E., Buller, K.M., Pow, D.V., Day, T.A. and Walker, F.R. 2010. Chronic stress alters the density and morphology of microglia in a subset of stress-responsive brain regions. *Brain Behav Immun.* **24**(7),pp.1058–68.
- Uchida, K. and Tominaga, M. 2011. TRPM2 modulates insulin secretion in pancreatic beta-cells. *Islets.* **3**(4),pp.209–211.
- Ueda, T., Ugawa, S., Yamamura, H., Imaizumi, Y. and Shimada, S. 2003. Functional interaction between T2R taste receptors and G-protein alpha subunits expressed in taste receptor cells. *The Journal of Neuroscience: The Official Journal of the Society for Neuroscience.* **23**(19),pp.7376–7380.
- Uemura, T., Kudoh, J., Noda, S., Kanba, S. and Shimizu, N. 2005. Characterization of human and mouse TRPM2 genes: Identification of a novel N-terminal truncated protein specifically expressed in human striatum. *Biochemical and Biophysical Research Communications.* **328**(4),pp.1232–1243.
- Unger, B.S. and Patil, B.M. 2009. Apocynin improves endothelial function and prevents the development of hypertension in fructose fed rat. *Indian J Pharmacol.* **41**(5),pp.208–12.
- Uttara, B., Singh, A.V., Zamboni, P. and Mahajan, R.T. 2009. Oxidative Stress and Neurodegenerative Diseases: A Review of Upstream and Downstream Antioxidant Therapeutic Options. *Current Neuropharmacology.* **7**(1),pp.65–74.
- Valente, P., García-Sanz, N., Gomis, A., Fernández-Carvajal, A., Fernández-Ballester, G., Viana, F., Belmonte, C. and Ferrer-Montiel, A. 2008. Identification of molecular determinants of channel gating in the transient receptor potential box of vanilloid receptor I. *FASEB journal: official publication of the Federation of American Societies for Experimental Biology.* **22**(9),pp.3298–3309.

- Van Deventer, S.J. 1997. Tumour necrosis factor and Crohn's disease. *Gut.* **40**(4),pp.443–448.
- Vanden Berghe, T., Linkermann, A., Jouan-Lanhouet, S., Walczak, H. and Vandenabeele, P. 2014. Regulated necrosis: the expanding network of non-apoptotic cell death pathways. *Nat Rev Mol Cell Biol.* **15**(2),pp.135–47.
- Vandewauw, I., Owsianik, G. and Voets, T. 2013. Systematic and quantitative mRNA expression analysis of TRP channel genes at the single trigeminal and dorsal root ganglion level in mouse. *Bmc Neuroscience.* [Online]. **14**. Available from: ://WOS:000315190900001.
- Vannier, B., Peyton, M., Boulay, G., Brown, D., Qin, N., Jiang, M., Zhu, X. and Birnbaumer, L. 1999. Mouse trp2, the homologue of the human trpc2 pseudogene, encodes mTrp2, a store depletion-activated capacitative Ca²⁺ entry channel. *Proc Natl Acad Sci U S A.* **96**(5),pp.2060–4.
- Venkatachalam, K. and Montell, C. 2007. TRP channels. *Annu Rev Biochem.* **76**,pp.387–417.
- Venkatachalam, K., van Rossum, D.B., Patterson, R.L., Ma, H.T. and Gill, D.L. 2002. The cellular and molecular basis of store-operated calcium entry. *Nature Cell Biology.* **4**(11),pp.E263–E272.
- Vincenti, J.E., Murphy, L., Grabert, K., McColl, B.W., Cancellotti, E., Freeman, T.C. and Manson, J.C. 2016. Defining the Microglia Response during the Time Course of Chronic Neurodegeneration. *Journal of Virology.* **90**(6),pp.3003–3017.
- Vinten-Johansen, J. 2004. Involvement of neutrophils in the pathogenesis of lethal myocardial reperfusion injury. *Cardiovascular Research.* **61**(3),pp.481–497.
- Voets, T., Nilius, B., Hoefs, S., van der Kemp, A., Droogmans, G., Bindels, R.J.M. and Hoenderop, J.G.J. 2004. TRPM6 forms the Mg²⁺ influx channel involved in intestinal and renal Mg²⁺ absorption. *Journal of Biological Chemistry.* **279**(1),pp.19–25.
- Voets, T., Talavera, K., Owsianik, G. and Nilius, B. 2005. Sensing with TRP channels. *Nature Chemical Biology.* **1**(2),pp.85–92.
- Volk, T., Schwoerer, A.P., Thiessen, S., Schultz, J.H. and Ehmke, H. 2003. A polycystin-2-like large conductance cation channel in rat left ventricular myocytes. *Cardiovasc Res.* **58**(1),pp.76–88.
- Vriens, J., Owsianik, G., Hofmann, T., Philipp, S.E., Stab, J., Chen, X.D., Benoit, M., Xue, F.Q., Janssens, A., Kerselaers, S., Oberwinkler, J., Vennekens, R., Gudermann, T., Nilius, B. and Voets, T. 2011. TRPM3 Is a Nociceptor Channel Involved in the Detection of Noxious Heat. *Neuron.* **70**(3),pp.482–494.
- Wagner, T.F., Drews, A., Loch, S., Mohr, F., Philipp, S.E., Lambert, S. and Oberwinkler, J. 2010. TRPM3 channels provide a regulated influx pathway for zinc in pancreatic beta cells. *Pflugers Arch.* **460**(4),pp.755–65.

- Wagner, T.F.J., Loch, S., Lambert, S., Straub, I., Mannebach, S., Mathar, I., Dufer, M., Lis, A., Flockerzi, V., Philipp, S.E. and Oberwinkler, J. 2008. Transient receptor potential M3 channels are ionotropic steroid receptors in pancreatic beta cells. *Nature Cell Biology*. **10**(12),pp.1421-U103.
- Walker, R.L., Koh, S.D., Sergeant, G.P., Sanders, K.M. and Horowitz, B. 2002. TRPC4 currents have properties similar to the pacemaker current in interstitial cells of Cajal. *Am J Physiol Cell Physiol*. **283**(6),pp.C1637-45.
- Wang, S.W., Zhang, H. and Xu, Y. 2016. Crosstalk between microglia and T cells contributes to brain damage and recovery after ischemic stroke. *Neurological Research*. **38**(6),pp.495–503.
- Wang, X., Feuerstein, G.Z., Xu, L., Wang, H., Schumacher, W.A., Ogletree, M.L., Taub, R., Duan, J.J., Decicco, C.P. and Liu, R.Q. 2004. Inhibition of tumor necrosis factor-alpha-converting enzyme by a selective antagonist protects brain from focal ischemic injury in rats. *Mol Pharmacol*. **65**(4),pp.890–6.
- Wang, X., Miyares, R.L. and Ahern, G.P. 2005. Oleoylethanolamide excites vagal sensory neurones, induces visceral pain and reduces short-term food intake in mice via capsaicin receptor TRPV1: OEA activates vagal capsaicin receptors. *The Journal of Physiology*. **564**(2),pp.541–547.
- Wang, X.J., Ye, M., Zhang, Y.H. and Chen, S.D. 2007. CD200-CD200R regulation of microglia activation in the pathogenesis of Parkinson's disease. *J Neuroimmune Pharmacol*. **2**(3),pp.259–64.
- Wang, Z.Q., Porreca, F., Cuzzocrea, S., Galen, K., Lightfoot, R., Masini, E., Muscoli, C., Mollace, V., Ndengele, M., Ischiropoulos, H. and Salvemini, D. 2004. A newly identified role for superoxide in inflammatory pain. *J Pharmacol Exp Ther*. **309**(3),pp.869–78.
- Warnat, J., Philipp, S., Zimmer, S., Flockerzi, V. and Cavalie, A. 1999. Phenotype of a recombinant store-operated channel: highly selective permeation of Ca²⁺. *J Physiol*. **518** (Pt 3),pp.631–8.
- Wehage, E., Eisfeld, J., Heiner, I., Jüngling, E., Zitt, C. and Lückhoff, A. 2002. Activation of the cation channel long transient receptor potential channel 2 (LTRPC2) by hydrogen peroxide. A splice variant reveals a mode of activation independent of ADP-ribose. *The Journal of Biological Chemistry*. **277**(26),pp.23150–23156.
- Wehrhahn, J., Kraft, R., Harteneck, C. and Hauschmidt, S. 2010. Transient Receptor Potential Melastatin 2 Is Required for Lipopolysaccharide-Induced Cytokine Production in Human Monocytes. *Journal of Immunology*. **184**(5),pp.2386–2393.
- Weinstein, J.R., Koerner, I.P. and Möller, T. 2010. Microglia in ischemic brain injury. *Future Neurology*. **5**(2),pp.227–246.
- Weisiger, R.A. and Fridovich, I. 1973. Superoxide dismutase. Organelle specificity. *J Biol Chem*. **248**(10),pp.3582–92.

- Weissmann, N., Dietrich, A., Fuchs, B., Kalwa, H., Ay, M., Dumitrescu, R., Olschewski, A., Storch, U., Mederos y Schnitzler, M., Ghofrani, H.A., Schermuly, R.T., Pinkenburg, O., Seeger, W., Grimminger, F. and Gudermann, T. 2006. Classical transient receptor potential channel 6 (TRPC6) is essential for hypoxic pulmonary vasoconstriction and alveolar gas exchange. *Proc Natl Acad Sci U S A.* **103**(50),pp.19093–8.
- Welser-Alves, J.V. and Milner, R. 2013. Microglia are the major source of TNF-alpha and TGF-beta1 in postnatal glial cultures; regulation by cytokines, lipopolysaccharide, and vitronectin. *Neurochem Int.* **63**(1),pp.47–53.
- Wes, P.D., Chevesich, J., Jeromin, A., Rosenberg, C., Stetten, G. and Montell, C. 1995. TRPC1, A HUMAN HOMOLOG OF A DROSOPHILA STORE-OPERATED CHANNEL. *Proc Natl Acad Sci U S A.* **92**(21),pp.9652–9656.
- Wes, P.D., Holtman, I.R., Boddeke, E., Moller, T. and Eggen, B.J.L. 2016. Next Generation Transcriptomics and Genomics Elucidate Biological Complexity of Microglia in Health and Disease. *Glia.* **64**(2),pp.197–213.
- Whittemore, E.R., Loo, D.T. and Cotman, C.W. 1994. Exposure to hydrogen peroxide induces cell death via apoptosis in cultured rat cortical neurons. *Neuroreport.* **5**(12),pp.1485–8.
- Wind, S., Beuerlein, K., Armitage, M.E., Taye, A., Kumar, A.H., Janowitz, D., Neff, C., Shah, A.M., Wingler, K. and Schmidt, H.H. 2010. Oxidative stress and endothelial dysfunction in aortas of aged spontaneously hypertensive rats by NOX1/2 is reversed by NADPH oxidase inhibition. *Hypertension.* **56**(3),pp.490–7.
- Wind, S., Beuerlein, K., Eucker, T., Muller, H., Scheurer, P., Armitage, M.E., Ho, H., Schmidt, H.H. and Wingler, K. 2010. Comparative pharmacology of chemically distinct NADPH oxidase inhibitors. *Br J Pharmacol.* **161**(4),pp.885–98.
- Wohleb, E.S., Hanke, M.L., Corona, A.W., Powell, N.D., Stiner, L.M., Bailey, M.T., Nelson, R.J., Godbout, J.P. and Sheridan, J.F. 2011. beta-Adrenergic receptor antagonism prevents anxiety-like behavior and microglial reactivity induced by repeated social defeat. *J Neurosci.* **31**(17),pp.6277–88.
- Wolf, S.A., Boddeke, H.W.G.M. and Kettenmann, H. 2017. Microglia in Physiology and Disease. *Annual Review of Physiology.* **79**,pp.619–643.
- Wong, J.L., Créton, R. and Wessel, G.M. 2004. The oxidative burst at fertilization is dependent upon activation of the dual oxidase Udx1. *Developmental Cell.* **7**(6),pp.801–814.
- Wong, P., Pineault, J., Lakins, J., Taillefer, D., Leger, J., Wang, C. and Tenniswood, M. 1993. Genomic organization and expression of the rat TRPM-2 (clusterin) gene, a gene implicated in apoptosis. *J Biol Chem.* **268**(7),pp.5021–31.
- Wu, L.-J., Wu, G., Sharif, M.R.A., Baker, A., Jia, Y., Fahey, F.H., Luo, H.R., Feener, E.P. and Clapham, D.E. 2012. The voltage-gated proton channel Hv1 enhances brain damage from ischemic stroke. *Nature Neuroscience.* **15**(4),pp.565–573.

- Wu, X., Indzhykulian, A.A., Niksch, P.D., Webber, R.M., Garcia-Gonzalez, M., Watnick, T., Zhou, J., Vollrath, M.A. and Corey, D.P. 2016. Hair-Cell Mechanotransduction Persists in TRP Channel Knockout Mice. *Plos One*. **11**(5),p.e0155577.
- Wyss-Coray, T. and Rogers, J. 2012. Inflammation in Alzheimer disease-a brief review of the basic science and clinical literature. *Cold Spring Harb Perspect Med*. **2**(1),p.a006346.
- Xia, R., Mei, Z.Z., Mao, H.J., Yang, W., Dong, L., Bradley, H., Beech, D.J. and Jiang, L.H. 2008. Identification of pore residues engaged in determining divalent cationic permeation in transient receptor potential melastatin subtype channel. *Journal of Biological Chemistry*. **283**(41),pp.27426–27432.
- Xiang, Z., Haroutunian, V., Ho, L., Purohit, D. and Pasinetti, G.M. 2006. Microglia activation in the brain as inflammatory biomarker of Alzheimer's disease neuropathology and clinical dementia. *Dis Markers*. **22**(1–2),pp.95–102.
- Xiao, Y., Lv, X.Y., Cao, G., Bian, G.H., Duan, J.J., Ai, J.Z., Sun, H., Li, Q.W., Yang, Q.T., Chen, T.L., Zhao, D.H., Tan, R.Z., Liu, Y.H., Wang, Y.D., Zhang, Z., Yang, Y., Wei, Y.Q. and Zhou, Q. 2010. Overexpression of Trpp5 contributes to cell proliferation and apoptosis probably through involving calcium homeostasis. *Molecular and Cellular Biochemistry*. **339**(1–2),pp.155–161.
- Xu, H., Delling, M., Li, L., Dong, X. and Clapham, D.E. 2007. Activating mutation in a mucolipin transient receptor potential channel leads to melanocyte loss in varitint-waddler mice. *Proc Natl Acad Sci U S A*. **104**(46),pp.18321–6.
- Xu, H., Ramsey, I.S., Kotecha, S.A., Moran, M.M., Chong, J.A., Lawson, D., Ge, P., Lilly, J., Silos-Santiago, I., Xie, Y., DiStefano, P.S., Curtis, R. and Clapham, D.E. 2002. TRPV3 is a calcium-permeable temperature-sensitive cation channel. *Nature*. **418**(6894),pp.181–6.
- Xu, S.-Z., Muraki, K., Zeng, F., Li, J., Sukumar, P., Shah, S., Dedman, A.M., Flemming, P.K., McHugh, D., Naylor, J., Cheong, A., Bateson, A.N., Munsch, C.M., Porter, K.E. and Beech, D.J. 2006. A sphingosine-1-phosphate-activated calcium channel controlling vascular smooth muscle cell motility. *Circulation Research*. **98**(11),pp.1381–1389.
- Xu, S.Z., Zeng, F., Boulay, G., Grimm, C., Harteneck, C. and Beech, D.J. 2005. Block of TRPC5 channels by 2-aminoethoxydiphenyl borate: a differential, extracellular and voltage-dependent effect. *Br J Pharmacol*. **145**(4),pp.405–14.
- Xu, X.Z., Chien, F., Butler, A., Salkoff, L. and Montell, C. 2000. TRPgammadelta, a drosophila TRP-related subunit, forms a regulated cation channel with TRPL. *Neuron*. **26**(3),pp.647–57.
- Xu, X.Z., Li, H.S., Guggino, W.B. and Montell, C. 1997. Coassembly of TRP and TRPL produces a distinct store-operated conductance. *Cell*. **89**(7),pp.1155–64.
- Xu, X.Z.S., Moebius, F., Gill, D.L. and Montell, C. 2001. Regulation of melastatin, a TRP-related protein, through interaction with a cytoplasmic isoform. *Proc Natl Acad Sci U S A*. **98**(19),pp.10692–10697.

- Yamamoto, S., Shimizu, S., Kiyonaka, S., Takahashi, N., Wajima, T., Hara, Y., Negoro, T., Hiroi, T., Kiuchi, Y., Okada, T., Kaneko, S., Lange, I., Fleig, A., Penner, R., Nishi, M., Takeshima, H. and Mori, Y. 2008. TRPM2-mediated Ca²⁺ influx induces chemokine production in monocytes that aggravates inflammatory neutrophil infiltration. *Nat Med.* **14**(7),pp.738–47.
- Yamamoto, S., Wajima, T., Hara, Y., Nishida, M. and Mori, Y. 2007. Transient receptor potential channels in Alzheimer's disease. *Biochim Biophys Acta.* **1772**(8),pp.958–67.
- Yang, K.T., Chang, W.L., Yang, P.C., Chien, C.L., Lai, M.S., Su, M.J. and Wu, M.L. 2006. Activation of the transient receptor potential M2 channel and poly(ADP-ribose) polymerase is involved in oxidative stress-induced cardiomyocyte death. *Cell Death and Differentiation.* **13**(10),pp.1815–1826.
- Yang, W., Manna, P.T., Zou, J.E., Luo, J.H., Beech, D.J., Sivaprasadarao, A. and Jiang, L.H. 2011. Zinc Inactivates Melastatin Transient Receptor Potential 2 Channels via the Outer Pore. *Journal of Biological Chemistry.* **286**(27),pp.23789–23798.
- Yao, H., Peng, F., Fan, Y., Zhu, X., Hu, G. and Buch, S.J. 2009. TRPC channel-mediated neuroprotection by PDGF involves Pyk2/ERK/CREB pathway. *Cell Death and Differentiation.* **16**(12),pp.1681–1693.
- Ye, M., Yang, W., Ainscough, J.F., Hu, X.P., Li, X., Sedo, A., Zhang, X.H., Zhang, X., Chen, Z., Li, X.M., Beech, D.J., Sivaprasadarao, A., Luo, J.H. and Jiang, L.H. 2014. TRPM2 channel deficiency prevents delayed cytosolic Zn²⁺ accumulation and CA1 pyramidal neuronal death after transient global ischemia. *Cell Death & Disease.* [Online]. **5**. Available from: ://WOS:000345643900035.
- Yee, N.S. 2015. Roles of TRPM8 Ion Channels in Cancer: Proliferation, Survival, and Invasion. *Cancers (Basel).* **7**(4),pp.2134–46.
- Yee, N.S., Zhou, W.Q. and Liang, I.C. 2011. Transient receptor potential ion channel Trpm7 regulates exocrine pancreatic epithelial proliferation by Mg²⁺-sensitive Socs3a signaling in development and cancer. *Disease Models & Mechanisms.* **4**(2),pp.240-U128.
- Yeh, C.M., Chien, P.S. and Huang, H.J. 2007. Distinct signalling pathways for induction of MAP kinase activities by cadmium and copper in rice roots. *Journal of Experimental Botany.* **58**(3),pp.659–671.
- Yip, H., Chan, W.-Y., Leung, P.-C., Kwan, H.-Y., Liu, C., Huang, Y., Michel, V., Yew, D.T.-W. and Yao, X. 2004. Expression of TRPC homologs in endothelial cells and smooth muscle layers of human arteries. *Histochemistry and Cell Biology.* **122**(6),pp.553–561.
- Yoder, B.K., Hou, X. and Guay-Woodford, L.M. 2002. The polycystic kidney disease proteins, polycystin-1, polycystin-2, polaris, and cystin, are co-localized in renal cilia. *J Am Soc Nephrol.* **13**(10),pp.2508–16.
- Yosida, M., Dezaki, K., Uchida, K., Kodera, S., Lam, N.V., Ito, K., Rita, R.S., Yamada, H., Shimomura, K., Ishikawa, S., Sugawara, H., Kawakami, M., Tominaga, M., Yada, T. and Kakei, M. 2014. Involvement of cAMP/EPAC/TRPM2 activation

- in glucose- and incretin-induced insulin secretion. *Diabetes*. **63**(10),pp.3394–3403.
- Yowtak, J., Lee, K.Y., Kim, H.Y., Wang, J., Kim, H.K., Chung, K. and Chung, J.M. 2011. Reactive oxygen species contribute to neuropathic pain by reducing spinal GABA release. *Pain*. **152**(4),pp.844–52.
- Zagranichnaya, T.K., Wu, X. and Villereal, M.L. 2005. Endogenous TRPC1, TRPC3, and TRPC7 proteins combine to form native store-operated channels in HEK-293 cells. *J Biol Chem*. **280**(33),pp.29559–69.
- Zanier, E.R., Fumagalli, S., Perego, C., Pischiutta, F. and De Simoni, M.-G. 2015. Shape descriptors of the ‘never resting’ microglia in three different acute brain injury models in mice. *Intensive Care Medicine Experimental*. **3**(1),p.39.
- Zeevi, D.A., Frumkin, A. and Bach, G. 2007. TRPML and lysosomal function. *Biochim Biophys Acta*. **1772**(8),pp.851–8.
- Zeng, X., Sikka, S.C., Huang, L., Sun, C., Xu, C., Jia, D., Abdel-Mageed, A.B., Pottle, J.E., Taylor, J.T. and Li, M. 2010. Novel role for the transient receptor potential channel TRPM2 in prostate cancer cell proliferation. *Prostate Cancer Prostatic Dis.* **13**(2),pp.195–201.
- Zhan, K., Yu, P., Liu, C., Luo, J. and Yang, W. 2016. Detrimental or beneficial: the role of TRPM2 in ischemia/reperfusion injury. *Acta Pharmacologica Sinica*. **37**(1),pp.4–12.
- Zhan, Y., Virbasius, J.V., Song, X., Pomerleau, D.P. and Zhou, G.W. 2002. The p40phox and p47phox PX domains of NADPH oxidase target cell membranes via direct and indirect recruitment by phosphoinositides. *J Biol Chem*. **277**(6),pp.4512–8.
- Zhang, F. and Li, P.L. 2007. Reconstitution and characterization of a nicotinic acid adenine dinucleotide phosphate (NAADP)-sensitive Ca²⁺ release channel from liver Lysosomes of rats. *Journal of Biological Chemistry*. **282**(35),pp.25259–25269.
- Zhang, H., Osyczka, A., Dutton, P.L. and Moser, C.C. 2007. Exposing the complex III Qo semiquinone radical. *Biochimica Et Biophysica Acta*. **1767**(7),pp.883–887.
- Zhang, L. and Barritt, G.J. 2004. Evidence that TRPM8 is an androgen-dependent Ca²⁺ channel required for the survival of prostate cancer cells. *Cancer Research*. **64**(22),pp.8365–8373.
- Zhang, W., Chu, X., Tong, Q., Cheung, J.Y., Conrad, K., Masker, K. and Miller, B.A. 2003. A novel TRPM2 isoform inhibits calcium influx and susceptibility to cell death. *Journal of Biological Chemistry*. **278**(18),pp.16222–16229.
- Zhang, W., Hirschler-Laszkiewicz, I., Tong, Q., Conrad, K., Sun, S.C., Penn, L., Barber, D.L., Stahl, R., Carey, D.J., Cheung, J.Y. and Miller, B.A. 2006. TRPM2 is an ion channel that modulates hematopoietic cell death through activation of caspases and PARP cleavage. *Am J Physiol Cell Physiol*. **290**(4),pp.C1146-59.

- Zhang, Y.M., Wang, H., Li, J.R., Dong, L., Xu, P., Chen, W.Z., Neve, R.L., Volpe, J.J. and Rosenberg, P.A. 2006. Intracellular zinc release and ERK phosphorylation are required upstream of 12-lipoxygenase activation in peroxynitrite toxicity to mature rat oligodendrocytes. *Journal of Biological Chemistry*. **281**(14),pp.9460–9470.
- Zhao, L.Y., Xu, W.L., Xu, Z.Q., Qi, C., Li, Y., Cheng, J., Liu, L.K., Wu, Y.N., Gao, J. and Ye, J.H. 2016. The overexpressed functional transient receptor potential channel TRPM2 in oral squamous cell carcinoma. *Scientific Reports*. [Online]. **6**. Available from: ://WOS:000390368600001.
- Zhao, Q.D., Viswanadhapalli, S., Williams, P., Shi, Q., Tan, C., Yi, X., Bhandari, B. and Abboud, H.E. 2015. NADPH oxidase 4 induces cardiac fibrosis and hypertrophy through activating Akt/mTOR and NFkappaB signaling pathways. *Circulation*. **131**(7),pp.643–55.
- Zhao, T. and Bokoch, G.M. 2005. Critical role of proline-rich tyrosine kinase 2 in reversion of the adhesion-mediated suppression of reactive oxygen species generation by human neutrophils. *J Immunol*. **174**(12),pp.8049–55.
- Zholos, A. 2010. Pharmacology of transient receptor potential melastatin channels in the vasculature. *Br J Pharmacol*. **159**(8),pp.1559–71.
- Zhong, Z.Y., Zhai, Y.G., Liang, S., Mori, Y., Han, R.Z., Sutterwala, F. and Qiao, L. 2013. TRPM2 links oxidative stress to the NLRP3 inflammasome activation. *Journal of Immunology*. [Online]. **190**. Available from: ://WOS:000322987101017.
- Zhou, C., Huang, Y. and Przedborski, S. 2008. Oxidative Stress in Parkinson's Disease A Mechanism of Pathogenic and Therapeutic Significance In: G. E. Gibson, R. R. Ratan and M. F. Beal, eds. *Mitochondria and Oxidative Stress in Neurodegenerative Disorders* [Online]. Annals of the New York Academy of Sciences., pp. 93–104. Available from: ://WOS:000262397800010.
- Zhu, X., Chu, P.B., Peyton, M. and Birnbaumer, L. 1995. MOLECULAR-CLONING OF A WIDELY EXPRESSED HUMAN HOMOLOG FOR THE DROSOPHILA TRP GENE. *Fews Letters*. **373**(3),pp.193–198.
- Zou, J., Ainscough, J.F., Yang, W., Sedo, A., Yu, S.P., Mei, Z.Z., Sivaprasadarao, A., Beech, D.J. and Jiang, L.H. 2013. A differential role of macrophage TRPM2 channels in Ca²⁺ signaling and cell death in early responses to H₂O₂. *American Journal of Physiology-Cell Physiology*. **305**(1),pp.C61–C69.
- Zubcevic, L., Herzik, M.A., Chung, B.C., Liu, Z.R., Lander, G.C. and Lee, S.Y. 2016. Cryo-electron microscopy structure of the TRPV2 ion channel. *Nature Structural & Molecular Biology*. **23**(2),p.180–.
- Zurborg, S., Yurgionas, B., Jira, J.A., Caspani, O. and Heppenstall, P.A. 2007. Direct activation of the ion channel TRPA1 by Ca²⁺. *Nat Neurosci*. **10**(3),pp.277–9.